Brain-to-Language Decoding: Tasks, Signals, Methods, Evaluation, Practical Use and Beyond

Yiqian Yang[1,*], Yiqun Duan[1,*], Chenyu Liu[1], Yiqi Wang[1], Xinliang Zhou[1],
Chin-Teng Lin[2] and Yu Zhang[3]

[1]Uploading Inc
[2]Human-centric Artificial Intelligence Centre, University of Technology Sydney
[3]Stanford Institute for Human-Centered Artificial Intelligence (HAI), Stanford University

yiqian@uploading.tech chenyu@uploading.tech yiqiwang@uploading.tech xinliang@uploading.tech
[2]chin-teng.lin@uts.edu.au [3]yzhangsu@stanford.edu
[*]Equal contribution. Correspondence: yiqunduan@uploading.tech

arXiv:2609.27650v1 [cs.CL] 23 Sep 2026

Abstract

Brain-to-language decoding translates neural activity associated with language production, internal speech and perception into linguistic or expressive outputs. It offers a route to restoring communication after speech loss and a means of studying how the brain represents language. Advances in neural recording and representation learning have expanded the field from constrained recognition and acoustic reconstruction to text generation, streaming personalised speech and facial animation. This survey synthesises these developments across invasive and non-invasive measurements, drawing on a search without a lower year limit and source-led updates through September 2026. We connect Articulated, Inner and Perceived tasks to the neural populations they engage, the representations available to decoders and the outputs those representations can support. We examine model development, public resources and the evolution of evaluation, and compare published performance and communication costs within their reported protocols. The synthesis identifies complementary routes to progress: phonetic, acoustic and semantic targets preserve different aspects of a message; shared representations support reuse across recording conditions and tasks; and online communication increasingly depends on calibration, feedback and user control alongside decoding accuracy. Shared benchmarks enable algorithmic comparisons, while longitudinal studies reveal the demands of sustained use. We discuss these developments and their remaining limitations, then outline a prospective five-level trajectory from commands and language to meaning, scenarios and bidirectional cognitive exchange.

1 Introduction

Language allows people to share knowledge, express intentions and participate in social life. Brain-to-language decoding seeks to recover linguistic information directly from neural activity, creating a route to communication when the movements needed for speech are impaired. It also provides a computational approach to studying how sounds, words and meanings are represented during speaking, inner speech, listening and reading. These clinical and scientific aims draw on the same central opportunity: neural recordings contain information about language that can be learned and translated into an observable output.

The field has developed through several connected advances. Reconstruction of speech features from auditory-cortex activity established a route from neural measurements to sound (Pasley et al., 2012). Phoneme-based recognition and articulatory modelling connected speech-production signals to words and synthesised sentences (Herff et al., 2015; Anumanchipalli et al., 2019). Clinical neuroprostheses subsequently enabled sentence-level attempted-speech decoding, large-vocabulary text, personalised voice and facial animation (Moses et al., 2021; Willett et al., 2023; Metzger et al., 2023). Streaming synthesis and prolonged home use are extending this progress from producing an output towards participating in an exchange (Littlejohn et al., 2025; Wairagkar et al., 2025; Card et al., 2026).

Non-invasive research opens complementary paths. EEG and MEG studies learn correspondences between neural activity and heard or read language, supported by shared corpora and pretrained speech and language representations (Hollenstein et al., 2018; Défossez et al., 2023; d' Ascoli et al., 2025). Haemodynamic recordings support semantic reconstruction over longer timescales (Tang et al., 2023).

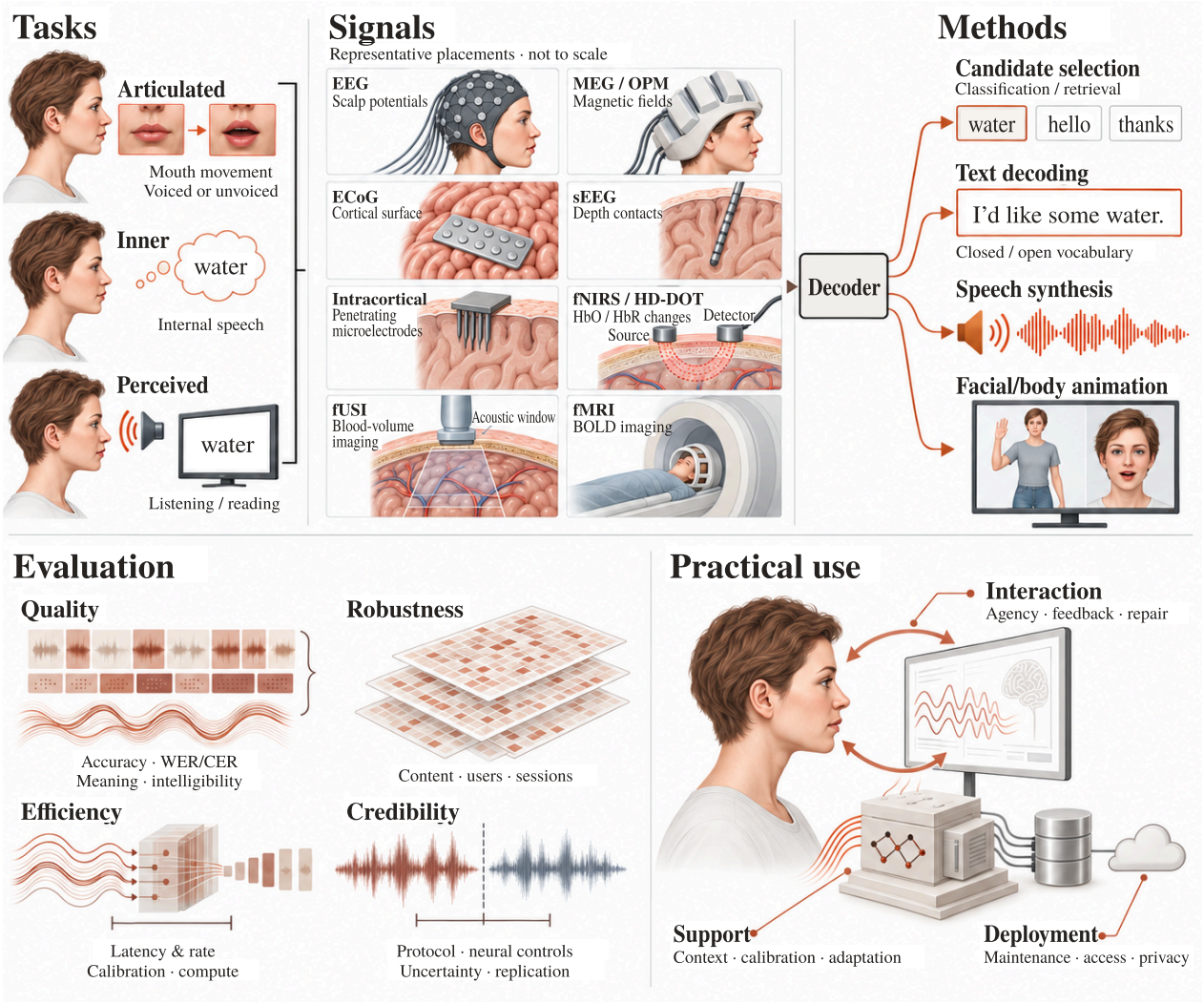


Figure 1. **The survey connects what is decoded with the evidence and mechanisms required for useful communication.** Tasks identifies participant conditions, Signals maps the recording families, and Methods connects neural measurements through a decoder to candidate selection, text decoding, speech synthesis and facial animation. Evaluation separates quality, robustness, efficiency and credibility; Practical use addresses interaction, system support and deployment. These layers distinguish successful output generation from evidence of reliable communication. The sentence pair, event sequence and uncertainty glyph are conceptual examples, not measured results.

Across recording modalities, inner-speech studies investigate internally produced content, ranging from discriminating imagined items to cued large-vocabulary intracortical decoding (Proix et al., 2022; Wandelt et al., 2024; Kunz et al., 2025). Together, these directions reveal a field with several useful objectives: understanding language representations, recovering presented content and enabling a person to express a chosen message.

An organising question connects this diversity: *which aspects of language can different neural measurements recover, and how can those representations support expression?* A phoneme sequence preserves the units needed to compose words; acoustic and articulatory representations provide structured routes to speech synthesis; a semantic representation permits changes in wording while retaining aspects of meaning. These choices interact with the participant's task and the timescale and coverage of the recording. They explain why different methods can share a neural-network architecture yet learn different information and serve different purposes. The task–network–representation map in Figure 5 makes these connections explicit. The decoding routes in Figure 9 explain how the representations become outputs. Section 5 compares published methods and their results within

specified benchmarks; Section 6 explains the evaluation standards and the questions those comparisons can answer.

Existing surveys offer substantial foundations for this synthesis. An early neural-speech review brought the recording modalities together around automatic speech recognition and the promise of silent communication (Herff & Schultz, 2016). Subsequent reviews expanded this foundation as datasets, deep learning and clinical systems developed. EEG speech-imagery reviews organise acquisition, preprocessing, feature extraction and classification methods (Rahman et al., 2024; Zhang et al., 2025; Su & Tian, 2025). Cross-modal imagery reviews connect those pipelines to experimental instructions, calibration and online operation (Tates et al., 2025; Almufareh et al., 2025). EEG-to-text and linguistic-decoding reviews explain the growing role of generative models across perception and production (Murad & Rahimi, 2025; Wang et al., 2025c). Clinical reviews bring cortical mechanisms, recording interfaces and communication restoration together (Silva et al., 2024a; Stavisky, 2025; Belfrouh et al., 2026). More recent frameworks distinguish linguistic target granularity from output pathways, or integrate the intracranial language-BCI pipeline from hardware to clinical deployment (Zhang et al., 2026b; He et al., 2026).

The present survey connects these perspectives across tasks, recording families and output forms. Listening and reading provide paired neural and language observations; overt speech also supplies time-aligned acoustic targets, while attempted and inner speech require alternative labels, alignment or transfer strategies. Comparing them reveals opportunities for shared representations and transfer, as well as the changes in supervision that each transition requires. In parallel, pretrained models increasingly connect neural encoders to text, speech and visual expression. A comprehensive account must therefore explain both how these methods work and how their outputs are evaluated and used. Section 2.2 develops the comparison with earlier reviews in detail.

Our synthesis has three aims. First, it provides a common vocabulary for Articulated, Inner and Perceived tasks and relates their neural signals to the information a decoder can learn. Second, it compares datasets, supervision and decoding mechanisms across candidate selection, text, speech and facial expression, identifying recurring design choices and comparing published results within matched evaluation settings. Third, it connects output quality, generalisation and computational demands to interaction, adaptation and sustained access. This combined view motivates research on transferable representations, self-generated expression and communication interfaces that preserve the user's control over a message.

Section 2 defines the scope and review procedure. Sections 3 and 4 introduce the tasks and neural measurements; Section 5 explains the data and decoding methods. Sections 6 and 7 examine evaluation and practical use. Section 8 synthesises unresolved directions, and Section 9 develops a prospective five-level trajectory from commands and language towards meaning, scenarios and bidirectional cognitive exchange.

2 Review Method and Scope

2.1 Scope and synthesis

The empirical scope is neural recording used to recover language-related content during Articulated, Inner or Perceived tasks. Reading is included as Perceived–Visual language. Clinical attempted-speech studies are retained even when residual articulator movement is not documented; an attempted-speech instruction alone does not assign the condition to Inner speech. We distinguish content decoding from auxiliary state detection, language mapping, representation analysis and dataset reports; adjacent evidence is retained only where it informs acquisition or interpretation. Interfaces based solely on surface electromyography (EMG) or camera-based lipreading, and spelling-by-selection BCIs, fall outside this neural language-decoding scope. Multimodal systems with neural and peripheral inputs retain explicit input labels.

The unit of comparison is an experimental condition: the participant's task, recording, supervision and output together with the tested content, controls and use setting. Multiple conditions within one paper can support different conclusions. This is a critical narrative synthesis with a documented search and selected structured extractions, rather than an exhaustive full-text review of every indexed record. Registry coverage, structured

extraction and claim-level source checking are reported separately.

Comparative approach. Each comparison asks what was demonstrated, which information enabled it and what would have to change for another task or use. Candidate identification, semantic reconstruction and exact transcription require different tests even when all produce text. Scores are therefore interpreted within their participant, task, supervision and evaluation conditions rather than pooled. Missing controls or operating details remain unknown; they establish neither the presence nor the absence of a capability.

2.2 Prior reviews and the synthesis developed here

Existing reviews organise the field around different decisions: how to decode a signal, how to define a linguistic target, or how to restore communication. We compare their organising questions, task and signal scope, treatment of outputs and evaluation, and relation to practical use. These perspectives are complementary: detailed coverage of a pipeline does not by itself specify whether its supervision is available in another task, just as a clinical outcome does not isolate the contribution of each decoder component. Table 1 compares the closest surveys. Appendix D records all 30 directly relevant reviews and 16 contextual sources, with abstract-level, targeted-section or title-only checking stated separately.

From neural speech recognition to language interfaces. Early synthesis connected EEG, MEG, haemodynamic and intracranial recordings through the goal of recognising speech from neural signals (Herff & Schultz, 2016). This established acquisition and linguistic target as joint design choices. Later reviews could build on a wider empirical base: speech imagery added internally generated targets, clinical work added continuous communication, and pretrained models added reusable acoustic and semantic representations. The comparison below follows these extensions, including earlier foundations where they explain a method or evaluation practice.

EEG pipelines and task conditions. EEG-focused reviews provide detailed accounts of preprocessing, features, models and datasets (Rahman et al., 2024; Zhang et al., 2025; Su & Tian, 2025; Estrella-Ibarra et al., 2026). A recent PRISMA review extends deep-learning speech classification and decoding to EEG and intracranial EEG studies from 2018–2025 (Sbaih et al., 2026). These methodological maps identify the tools available for a target. Their applicability also depends on actual articulation versus internal simulation, supplied versus self-generated content, and matched versus transferred supervision. Architecture specifies the computation; task conditions specify the information that computation can use.

Imagined-speech targets and participant behaviour. Cross-modal speech-imagery reviews connect task instructions and processing routes with information-transfer rates, online use and calibration (Tates et al., 2025; Almufareh et al., 2025). A task-oriented review further separates semantic or intent targets, phonemes or syllables, words and sentences from output-space constraints and pathways (Zhang et al., 2026b). This separation is essential: linguistic granularity, vocabulary size and output form do not specify what the participant did. Articulated, Inner and Perceived conditions provide that behavioural distinction. A reading task and an inner-speech task can consequently share a text target while testing different capacities for voluntary expression.

Text generation and neural attribution. The EEG-to-text review follows acquisition, signal processing and text-generation pipelines (Murad & Rahimi, 2025), while the linguistic-decoding review spans perception and production and considers deep models and language-model assistance (Wang et al., 2025c). Generative and foundation-model reviews further connect neural representations, pretraining, alignment and synthesis (Mai et al., 2025; Kuruppu et al., 2026; Sümer-Arpak et al., 2026). Their convergence raises an attribution question: what target information is available during training and testing, and which controls isolate the contribution of neural input from language, prompt, candidate-set or peripheral information? Fluency, exact wording and semantic fidelity require distinct evidence; none alone establishes recovery of an unconstrained intended message.

Clinical performance and operating requirements. Speech-neuroprosthesis reviews relate cortical mechanisms and recording interfaces to text, voice and communication restoration (Silva et al., 2024a; Stavisky, 2025;

Jhilal et al., 2025). A paralysis-focused systematic review appraises acquisition and AI methods across studies available through 18 September 2025 (Belfrouh et al., 2026). Reviews of outcomes, recalibration and user control explain why decoder accuracy captures only part of that clinical objective (Dohle et al., 2025; Swanson et al., 2026; van Stuijvenberg et al., 2024b). Accuracy and stability are properties to evaluate; correction, adaptation and assistance are mechanisms through which users obtain them. Keeping these distinct makes it possible to ask whether an apparent performance gain reduces the burden of communication.

An integrated comparison. The intracranial-language BCI review provides a close account spanning mechanisms, recording choices, experimental design, decoding, evaluation and clinical pathways (He et al., 2026). The present synthesis brings this integrated perspective into dialogue with non-invasive language decoding, speech imagery and generative modelling. Tasks explain how linguistic activity is elicited; signals explain what can be measured; methods explain how representations are learned and expressed. Evaluation and practical use then connect these capabilities to reliable communication. The resulting comparison highlights reusable representations, complementary output routes and the interaction mechanisms needed to turn technical advances into usable expression.

Table 1. How the present synthesis builds on the closest review perspectives. The third column identifies an additional comparison developed here, not a claim that the preceding review never discusses it. Dates are publication dates unless an evidence window is explicitly stated. The full inventory and checking depth are retained in Appendix D.

Review perspective and sources	What the review organises	Additional comparison developed here
EEG speech-imagery pipelines (2024–2026) (Rahman et al., 2024; Zhang et al., 2025; Su & Tian, 2025; Estrella-Ibarra et al., 2026)	Acquisition, preprocessing, representations, learning methods and datasets	Compare how task conditions and available supervision shape intermediate representations and output forms across signal families.
Cross-modal imagery and inner speech (2025) (Tates et al., 2025; Almufareh et al., 2025)	Internal tasks, recording modalities, decoding pipelines, calibration and use constraints	Apply the same task descriptors to Articulated, Inner and Perceived conditions, keeping cues and execution explicit.
Task-oriented imagined speech (2026) (Zhang et al., 2026b)	Linguistic target level, output-space property and output pathway	Separate those target axes from participant behaviour and distinguish reading or listening from self-generated expression.
EEG-to-text and linguistic decoding (2025) (Murad & Rahimi, 2025; Wang et al., 2025c)	Neural-to-text pipelines; language perception and production; deep and language-model methods	Connect candidate selection, sequence generation and meaning-level reconstruction to alignment, pretrained representations and test-time inputs.
Speech restoration (2024–2025) (Silva et al., 2024a; Stavisky, 2025; Jhilal et al., 2025)	Cortical speech representations, clinical outputs, patient conditions and translation	Relate text, streaming voice and facial expression to calibration, feedback, user control and sustained communication.
Paralysis-focused AI review (2026; evidence: 2019–18 Sep 2025) (Belfrouh et al., 2026)	Acquisition, preprocessing, AI methods, clinical applicability and methodological appraisal	Connect clinical and non-invasive approaches through shared questions of supervision, transfer, output quality and operating burden.
Deep-learning speech review (2026 online; 2027 issue; evidence: 2018–2025) (Sbaih et al., 2026)	EEG/iEEG speech classification and decoding through a PRISMA-organised synthesis	Compare classification with text, speech and semantic reconstruction; relate newer systems to transfer and interaction requirements.
Integrated intracranial language BCI (2026 preprint) (He et al., 2026)	Neural mechanisms, hardware, algorithms, evaluation and clinical deployment	Connect the same design chain across recording families to task transfer, neural attribution and operating burden.
Generative and foundation models (2025–2026) (Mai et al., 2025; Kuruppu et al., 2026; Sümer-Arpak et al., 2026)	Multimodal synthesis, neural pretraining, transferable representations and adaptation	Separate three roles of pretraining: reusable neural encoders, acoustic/linguistic alignment targets and output generators.
Present synthesis	Articulated, Inner and Perceived language; invasive and non-invasive recordings; text, speech and other language-related outputs	Condition-level evidence linking Tasks, Signals, Methods, Evaluation and Practical Use; proposed future interface capabilities in Beyond.

Coverage and dates. The search has no lower publication-year limit. The database retrieval used a first-publication cut-off of 15 September 2026; subsequent source-led additions and the registry were updated through 21 September 2026. Earlier foundational studies and reviews are included when they explain a relevant mechanism, recording choice or evaluation practice. The current registry spans 2008–2026; this range describes its retrieved contents rather than an eligibility restriction. The scope spans Articulated, Inner and Perceived tasks and invasive and non-invasive recordings. Of 920 canonical registry entries, 246 have selected structured extractions. Registry size describes retrieval breadth, not the number of full-text studies included in a systematic synthesis.

2.3 Search and study selection

Retrieval. Our search reporting is informed by PRISMA-S (Rethlefsen et al., 2021) and the PRISMA 2020 distinction between records, reports and studies (Page et al., 2021), while making no claim of preregistration or dual independent full-text screening. Twelve Europe PMC query groups and four OpenAlex query groups crossed signal synonyms with speech, phoneme, vowel, word and language terms and with decode, recognise, classify, synthesise, reconstruct and neuroprosthesis terms; separate queries targeted *unspoken*, *attempted*, *watched* and *functional ultrasound*. All queries were paginated to exhaustion with no start-year restriction and a first-publication cut-off of 15 September 2026. Forward citation tracking was run from 16 seed reviews and key papers; backward tracking used the reference lists of existing surveys and of the fUSI primary literature, with DOIs completed through Crossref. A recall check confirmed that all 44 studies of a prior in-house survey were retrieved.

Screening and coding. Database queries retrieved 28,515 records including cross-query duplicates; the initial query hit counts sum to 28,489, with pagination-time updates accounting for the difference in the retrieval log. Citation tracking and DOI/title matching produced a combined set of 20,335 records. Rule-assisted screening retained 774 entries. Author tracing added three records (777 in total), and a reading-route supplement added 36 (813 stable IDs). Both supplements retained the original first-publication cut-off. Linking 18 duplicate reports and publication versions yielded the original 795 canonical entries. The source-led supplement subsequently added 125 eligible report/resource entries, bringing the updated registry to 920 entries. The original search, supplements and version links are documented in Appendix C; archived aliases preserve their notes. Canonical entries need not represent independent participant cohorts.

Recent-review supplement. A separate search on 18 September 2026 targeted reviews available from 2024 onwards, combining review terms with language tasks, speech neuroprostheses and recording modalities. Three fully paginated Europe PMC queries returned 3,970 hits and 3,942 unique records; fifteen Crossref queries, limited to their top 75 results, yielded 921 unique DOIs. Publisher and repository searches and backward tracking supplemented discovery. Screening titles, abstracts and targeted sections produced a 73-entry inventory: 30 directly relevant reviews, 37 adjacent reviews, two chapters, two perspectives and two candidates. The comparison cites the 30 direct reviews and 16 contextual sources (Appendix D). These review-only records do not increase the primary-study counts. Exact queries, source links, publication status and checking depth are retained in the supplement.

Thematic primary-source supplement. On 19–21 September 2026, source-led searches examined all 47 subsections and subsubsections from Tasks through Limitations, together with the five prospective Beyond targets. Three research agents covered tasks/signals, methods, and evaluation/use; each recorded topic-specific discovery and focused follow-up queries, source locations and reading depth. Backward and forward source-led searches sought foundational work, independent approaches and recent developments and updated the synthesis through 21 September 2026. Overlapping reports and publication versions were reconciled before integration. The first thematic pass added 48 cited sources; subsequent dataset, method and evaluation searches extended this set. Sources include neural-language reports and resources as well as methodological foundations and contextual BCI research. A source-led update on 20 September added targeted searches for neural language representations, generative MEG-to-text, shared decoding benchmarks and reported communication costs. Eligible reports and

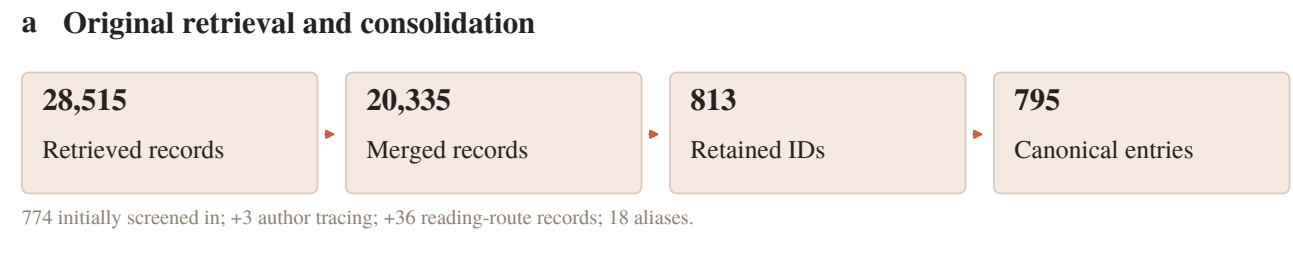


Figure 2. **Literature retrieval, the updated registry and manuscript citation coverage.** (a) The original retrieval and supplements produced 813 retained IDs and 795 canonical entries after publication-version consolidation. (b) Source-led additions bring the registry to 920 report/resource entries, including 246 with selected structured fields. (c) The active manuscript cites 448 distinct references: 317 in the main text and 131 only in appendices; 354 are linked to registry entries and 94 provide contextual reviews, foundations or adjacent evidence. The footer counts citations in the 8 Methods comparison figures separately from the communication-cost result rows. References, reports, resources, experimental conditions and participants are different counting units. Publication versions are linked; companion data releases and articles can describe the same acquisition.

citable resources have been backfilled into the registry, with source locations and coding provenance preserved. Reviews, generic metrics and contextual user studies remain references rather than additions to the primary report/resource census. A unified citation ledger links each active reference to its registry identity where applicable (Figure 2). Quantitative comparison tables retain the original paper, test condition, metric and source location; their figures reproduce reported results without new decoder experiments. Targeted citation tracking supplements the database search but is not dual independent human screening.

2.4 Evidence extraction and source verification

Structured extraction. The 246 selected entries contain task, recording, output or resource fields used in the synthesis. Their recorded provenance comprises 10 full-text checks, 65 abstract checks, 39 inherited extractions with metadata rechecked, and 132 targeted source-field checks. Targeted checks cover both newly added sources and previously indexed reports examined in greater detail. These categories describe the recorded depth of source use; checking selected fields does not amount to a whole-paper risk-of-bias appraisal. The remaining 674 entries retain bibliographic and available label information. Selection was neither random nor a prespecified risk-of-bias stratum.

Claim-level use and remaining gaps. Abstract-derived descriptions are treated as author-reported claims. The source-check table in Table 25 separately states source locations and supporting evidence for selected conclusions; checking one claim does not verify every result in its paper or its complete methodological description.

Cohort links are retained where known, with missing links treated as unknown rather than as proof of independent participants. The completed database retrieval used Europe PMC and OpenAlex, complemented by publisher, preprint and conference sources and source-led citation tracking. Native-platform access attempts on 20 September did not produce exportable Scopus, Web of Science, IEEE Xplore or ACM DL search results; the access outcomes are recorded with the queries. These platforms are therefore not counted as completed searches. Non-English coverage and citation tracking are incomplete. The documented search supports a broad critical synthesis, without establishing exhaustive retrieval.

2.5 Corpus coverage

Corpus shape. The registry updated through 21 September 2026 contains 920 canonical report/resource entries and 18 archived publication aliases, which are excluded from corpus totals. The update adds 125 entries to the original 795-entry collection. Of the current entries, 246 have selected structured fields: 10 from the earlier full-text checks, 65 from abstract checks, 39 from inherited extractions with metadata rechecked and 132 from subsequent targeted source checks. The remaining 674 entries retain bibliographic and available label information. These provenance labels describe source checking, not a risk-of-bias rating or a ranking of decoder performance. The registry preserves original task labels for traceability; these are not assignments to the three operational groups in this survey. A total of 747 entries carry at least one of the eight grouped signal labels. The multi-label signal counts are EEG 503, MEG 67, ECoG 65, intracortical/spikes 31, sEEG 26, fMRI 51, fUSI 19 and fNIRS/HD-DOT 24. The registry spans 2008–2026, with no lower-year eligibility limit: 409 entries precede 2024 and 511 date from 2024–2026. A paper and a separately citable data deposit can describe the same acquisition; neither report counts nor resource counts imply independent cohorts. These are counts within a selectively assembled index with incomplete labels, not prevalence estimates of the field. The distributions in Figure 3 combine publication-year coverage, signal labels, output scopes and source-checking provenance. Labels are multi-valued: a report can use several signals or study more than one output. Unassigned fields therefore remain distinct from negative findings. The companion registry preserves the original task labels and links later source-field checks to the reports or resources they describe.

Data availability. The accompanying workbook and study exports contain the search queries, screening decisions, study descriptions and linked publication versions. The exports also identify where each study is discussed in the manuscript. The artifact index links the current workbook, citation ledger, source-value tables and search records. The reference list gives the cited works, and Appendix C summarises the search and targeted supplements.

3 Tasks

3.1 Intended users and communication needs

Brain-to-language tasks investigate how people produce, internally formulate and perceive language. In communication restoration, the goal is to convey a person's chosen message through an alternative to audible speech. In perception research, the presented speech or text supplies a known target for studying neural representations and training decoders (Moses et al., 2021; Willett et al., 2023; Tang et al., 2023; Hollenstein et al., 2018). These aims create different experimental opportunities: production connects decoding to voluntary expression, whereas controlled presentation makes language content and timing available for systematic comparison.

Prospective users help determine which tasks matter. Interviews with people with locked-in syndrome identified communication, computer access and environmental control as desired applications, alongside preferences for active control; surveys of people with amyotrophic lateral sclerosis examined setup, training and interface requirements (Branco et al., 2021; Huggins et al., 2011). These findings make initiation, message choice and manageable operating effort central design considerations. Requirements vary across populations and available movements, so an experimental vocabulary should be chosen in relation to a communication goal.

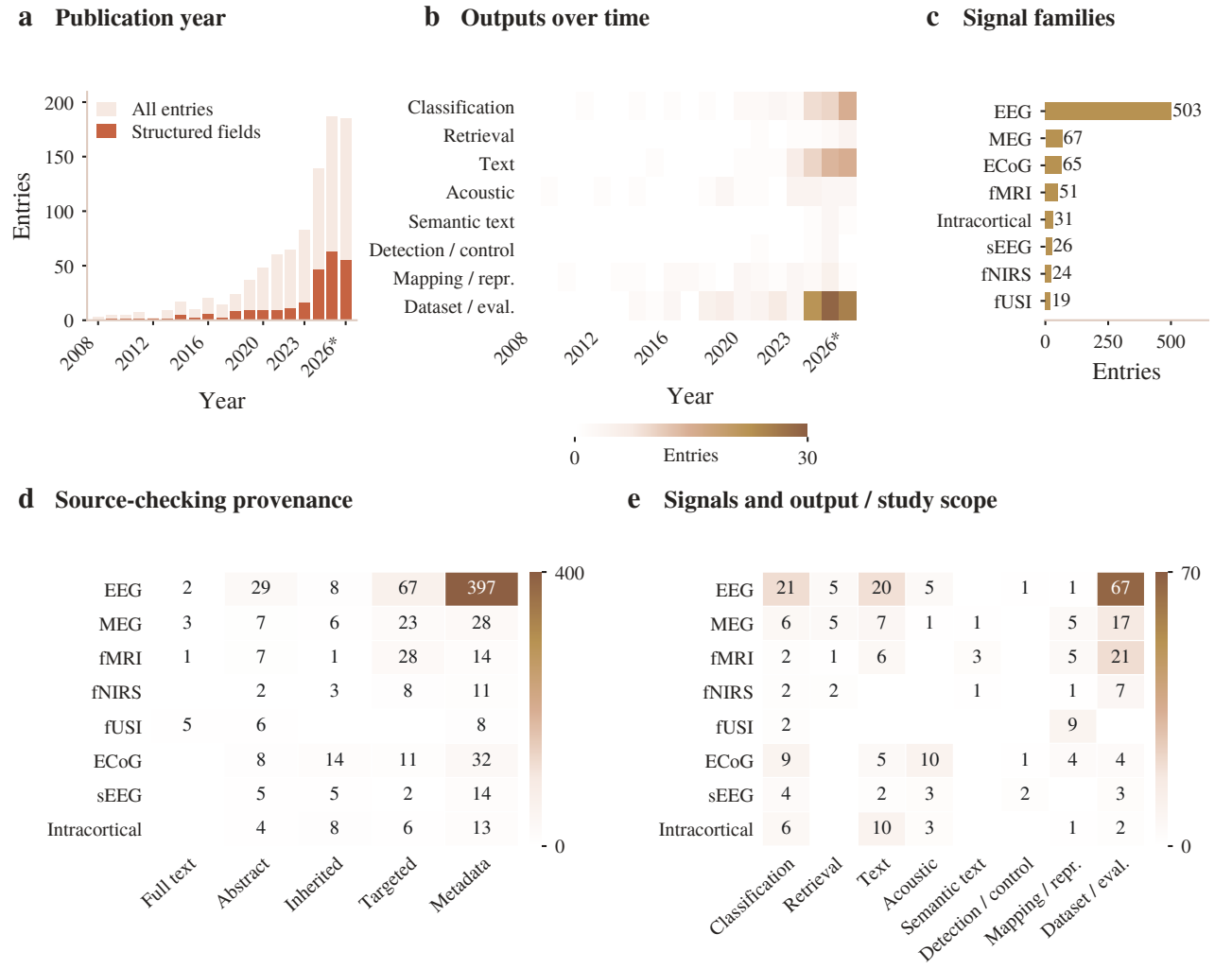


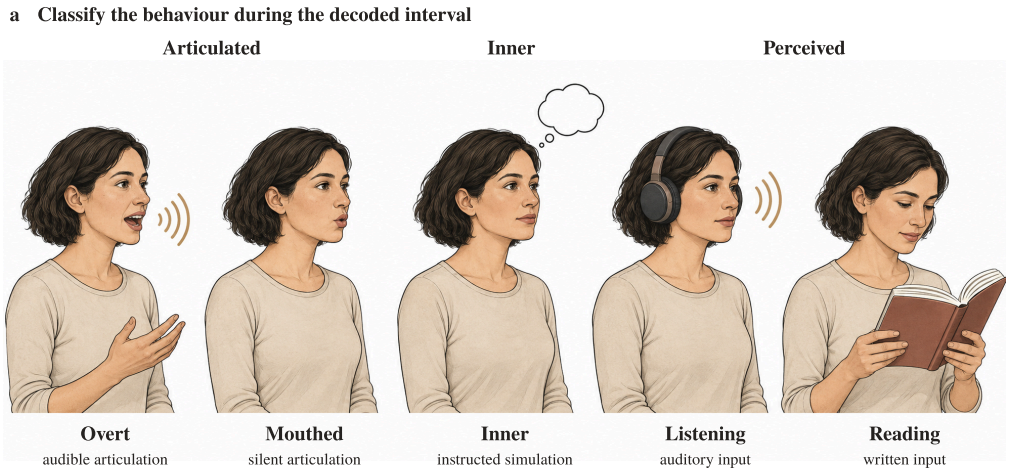
Figure 3. **Publication years, signal families and output coverage in the updated registry.** (a) Annual counts of canonical report/resource entries, with structured fields highlighted. (b) Output and study-scope labels by year among the extracted entries. (c) Signal-family counts across the registry; ECoG includes micro-ECoG, fNIRS includes HD-DOT, and intracortical includes spike recordings. (d) Source-checking provenance by signal: full-text, abstract, inherited extraction, targeted source-field checks and bibliographic metadata. (e) Signal–output and signal–study-scope pairs among the extracted entries. The registry is updated through 21 September 2026; the asterisk marks a partial year. Heatmaps use separate count scales and blank cells denote zero assigned pairs. Labels overlap, and companion articles or data deposits may share acquisitions. These distributions describe the indexed collection, including adjacent evidence, rather than independent cohorts or field-wide success rates.

Articulated, Inner and Perceived conditions distinguish actual articulation, internal speech production or simulation, and perception of externally presented language. The distinction matters because the same target word can be heard, read, imagined or attempted, with different sources of supervision and feedback. These are operational definitions for conditions, not classifications of diseases, devices or model architectures. A participant or study may contribute several conditions. The groups establish what changes in a task comparison; they do not assume that the underlying neural representations are disjoint. Clinical attempts without established residual movement remain in scope under the explicit descriptor *attempted speech*; they are not automatically assigned to Articulated or Inner.

Table 2. Three task groups and nine subtypes distinguish executed articulation, internal simulation and externally presented language. Limited requires residual articulation; Mixed requires evidence of both imagery strategies.

Group	Subtype	Meaning
Articulated	Overt	Executed articulation with audible speech.
	Mouthed	Executed articulation without audible speech.
	Limited	Impaired speech attempts with actual residual articulation; voicing may remain.
Inner	Articulatory	Internal simulation of speaking movements or sensations, without attempted execution.
	Auditory	Internal simulation of speech sounds.
	Mixed	Explicit combination of articulatory and auditory imagery.
Perceived	Auditory	Perception of externally presented speech sounds.
	Visual	Perception of written language (Reading) or visible articulation (Lipreading).
	Audiovisual	Joint auditory and visual language perception.

Clinical attempted speech specifies a motor intention. Residual movement determines confirmed Articulated membership; a movement-free motor attempt is retained explicitly as attempted speech, not reassigned to Inner imagery.



b Task groups differ in execution and the source of language

	Articulation	External language	Language source
Articulated Overt / Mouthed / Limited	present or limited	not required	executed production
Inner Articulatory / Auditory / Mixed	not instructed	not required	internal simulation
Perceived Auditory / Visual / Audiovisual	not required	defines the task	presented language

Visual includes reading and lipreading. A written cue does not make a later imagery interval Reading.

Attempted speech without confirmed articulation remains a separate boundary case; it is not automatically Inner.

Figure 4. **Task conditions distinguish producing language, simulating speech and perceiving a linguistic input.** Overt and Mouthed involve executed articulation; Inner involves instructed internal simulation; listening and reading provide external language. The lower panel compares the three groups by execution and content source. Clinical attempts without confirmed residual articulation remain explicitly qualified. Instructions alone do not establish absence of muscle activity; a written cue before imagery does not make that later interval a Reading task.

3.2 Articulated: Overt, Mouthed and Limited

Articulated. This group requires actual speech-articulator movement. *Overt* denotes audible speech with executed articulation; *Mouthed* denotes executed articulation without audible speech; *Limited* denotes attempted speech with documented residual articulation under motor impairment. Limited describes residual execution, not vocabulary size or decoding accuracy. For impaired attempts with residual articulation, Limited describes the motor condition and voicing is specified separately. Attempted speech is a source task description, not an automatic synonym for Limited. Attempts without observable articulation, or with insufficient behavioural reporting, remain explicitly qualified boundary cases outside confirmed Articulated membership. Absence of observable movement does not turn a motor attempt into Inner speech (Kunz et al., 2025; Jude et al., 2026).

Execution, supervision and transfer. Overt production can supply a participant's acoustic target for learning and alignment; Mouthed retains execution while removing audible speech. Limited can retain movement without intelligible production, as in clinical attempted-speech decoding (Willett et al., 2023). Transfer across these conditions must therefore account for differences in target availability and sensory feedback, alongside residual execution. Audible whispering is recorded as Overt with absent voicing: acoustic audibility and vocal-fold voicing are separate descriptors. Evidence from long-standing anarthria motivates studying retained articulation, but participant comparisons also differ in neural coverage, training and disease history (Jude et al., 2026). Those comparisons cannot isolate the effect of movement by themselves. The clinical reports in Table 10 retain the source term attempted when residual movement is not established for that condition.

Direct comparisons help explain the relationship between these modes. Intracranial recordings during overt, mouthed and imagined speech reveal shared but non-equivalent activity and cross-mode speech-activity decoding (Soroush et al., 2023). Overt production also reveals coordinated population representations of the articulators (Bouchard et al., 2013). Shared production structure provides a basis for transfer, while mode-specific timing and sensory feedback explain why transfer is a learning problem in its own right.

3.3 Inner: Articulatory, Auditory and Mixed

Inner. This group comprises internally generated or simulated speech without an attempt to execute speech-articulator movements. *Articulatory* emphasises the imagined movement or feeling of speaking; *Auditory* emphasises imagined speech sounds, including one's own or another person's voice; *Mixed* requires an explicit combination of both strategies. Speech-BCI studies use inner, covert and imagined as overlapping names (Martin et al., 2016; Bhadra et al., 2025; Kunz et al., 2025). Covert conditions involving actual mouthing belong under Articulated. Mixed denotes a reported combination, not an unspecified strategy. Instructions define the task, while electromyography (EMG) or motion monitoring separately assesses compliance and peripheral contributions.

The articulatory–auditory distinction has an experimental basis. MEG studies separately instructed participants to imagine pronouncing a syllable and to imagine hearing a voice; subsequent fMRI work examined motor-simulation and memory-retrieval routes to perceptual reactivation (Tian & Poeppel, 2010; Tian et al., 2016). These routes can lead to related auditory experiences through different internal strategies.

Internal production and content choice. Inner speech offers a way to express content without executing articulation. Real-time intracortical decoding of cued inner sentences enabled self-paced production in severely dysarthric participants, who reported less physical effort; shared but distinguishable attempted- and inner-speech representations supported cross-task learning (Kunz et al., 2025). This result links an internal linguistic process to an observable communication channel. Extending the channel to independently chosen messages adds a further challenge: the intended content is no longer supplied by the experimental prompt, so both reference collection and decoder training must accommodate it.

Relation to wider inner-speech terminology. Articulatory and auditory imagery describe how an inner utterance is generated. Inner experience also varies in condensation, dialogality, intentionality and prosody, so

rehearsing an expanded prompted sentence samples only part of this broader capacity (Grandchamp et al., 2019; Dahò & Monzani, 2025; Alexander & Stark, 2024; Kreiner & Eviatar, 2024). Speech-imagery reviews document heterogeneous elicitation and recording protocols (Tates et al., 2025; Almufareh et al., 2025). Retaining the instruction, content source and behavioural monitoring alongside the subtype connects these cognitive dimensions to reproducible decoding tasks.

3.4 Perceived: Auditory, Visual and Audiovisual

Perceived concerns externally presented language. Auditory denotes heard speech; Visual includes written-language Reading and visible-articulation Lip-reading; Audiovisual combines auditory and visual language input. Reading and Lip-reading are task descriptors within Visual, not additional top-level groups. ZuCo reading EEG therefore belongs to Perceived–Visual (Hollenstein et al., 2018; 2020). Reading may engage inner speech, but the presence of printed language alone does not establish an instructed Inner condition. Conversely, a written cue followed by an instructed speech attempt or imagery interval does not make that later interval a reading-decoding task.

Imagining a voice belongs to Inner–Auditory. Visible objects or silent scenes without a linguistic target remain outside Perceived–Visual; movie-based matching is language decoding only when the evaluated target is language. Audiovisual speech representation, for example, includes the interaction of heard phonemes and visible articulation (Li et al., 2026c). These distinctions preserve the difference between input modality and output meaning.

Perceived tasks also reveal transformations across sensory inputs. During silent lipreading, MEG responses carry information about unheard acoustic features beyond that explained by visible lip trajectories, while fMRI and intracranial recordings distinguish lipread word identities in auditory cortex (Bröhl et al., 2022; Karthik et al., 2024). Visual therefore names the presented input, not a restriction to visual brain regions. Feature tracking and word discrimination illuminate this shared representation at different levels.

A resource for learning and testing transfer. Presented language provides a known target and timing, making Perceived tasks useful for studying neural representations and learning decoder components. The value can extend beyond stimulus reconstruction: an fMRI decoder trained during listening was also evaluated during imagined storytelling, with semantic agreement assessed against separately recorded accounts (Tang et al., 2023). That result motivates cross-task learning while locating the achievement at the tested semantic target and protocol. Shared information between tasks is a resource for transfer; the fidelity and user control required for a communication interface still need to be established in its intended task.

3.5 Task instructions, cues and behavioural verification

Independent task descriptors. Content may be externally specified or self-generated; internal speech may be instructed or spontaneously occurring; items may be produced once or repeatedly. These dimensions can combine and are not additional subtypes. Cue modality, preparation intervals, residual sound and movement supply additional context; peripheral monitoring tests compliance with the instruction. A pre-articulatory window preceding an overt utterance is not automatically Inner or clinical attempted speech (Dash et al., 2020; 2024). Figure 4 shows the task ingredients implied by the definitions, not measured neural strengths.

Auxiliary recordings help characterise how a participant performs the task. A preregistered experiment found that facial EMG distinguished phonetic classes during overt speech but did not establish comparable group-level discrimination during instructed inner speech; increased activity relative to rest was not itself specific to speech content (Nalborczyk et al., 2020). The useful analysis therefore relates peripheral activity to the instruction and linguistic target. Exact cue sequences, imagery instructions and control channels allow later studies to reproduce that comparison.

What a task-transfer claim should test. Task transfer can change the neural activity being decoded, the source of the message, or both. Each change requires its own test. To distinguish a cue-dependent result from decoding

of a later attempt or imagery interval, useful tests vary the cue–target mapping and evaluate the later interval separately. Temporal separation should reflect the signal's physiological response and any carry-over from the cue; separating epochs alone does not establish independence (Sections 4 and 6). A claim of self-generated expression additionally requires user-chosen content that is unavailable to the decoder, together with a means of checking whether the output conveys the intended message. Such tests target the dependency being removed, rather than treating a change of task name as evidence of transfer.

4 Signals

Neural recording provides complementary views of language processing. Electrical and magnetic measurements resolve rapid population dynamics; haemodynamic measurements capture spatially structured vascular responses over longer intervals. Within each family, placement and coverage determine which linguistic processes are most accessible. Choosing a signal therefore connects a scientific target—such as articulatory movement, speech sounds or contextual meaning—to a feasible recording configuration and timescale.

Table 3. Temporal and spatial scales in representative neural-recording configurations. Values describe the cited studies, rather than universal family limits. Sampling intervals, feature windows and vascular response dynamics describe different stages; contact pitch and voxel size specify sampling geometry, rather than independently measured functional localisation.

Family and example	Temporal sampling or analysis	Response being measured	Spatial sampling and coverage
EEG (Nieto et al., 2022)	1,024-Hz acquisition (0.98-ms interval)	Scalp potentials; analysis depends on the frequency band and time window	128 scalp electrodes; cortical localisation additionally depends on the head and source models.
MEG (Gwilliams et al., 2023)	1,000-Hz acquisition (1-ms interval)	Magnetic fields from neural currents; temporal filtering shapes the features	208 axial gradiometers around the head; sensor spacing is not cortical localisation accuracy.
fMRI (Tang et al., 2023)	Volume repetition time, TR $= 2$ s	BOLD vascular response; TR is not the response duration	2.6-mm isotropic voxels; distributed brain coverage, with voxel sampling distinct from functional specificity.
fNIRS / HD-DOT (Schroeder et al., 2023)	Analysis resampled to 1 Hz after low-pass filtering	Haemoglobin changes mediated by vascular dynamics	Overlapping optical paths over superficial cortex; 13-mm nearest-neighbour spacing is optode geometry, not image resolution.
fUSI (Soloukey et al., 2020)	500–667-Hz compounded frames; 3.6–4.8-Hz live Doppler images	Blood-volume-sensitive Doppler power; neural activity is related through vascular coupling	Reported 300-μm imaging scale; plane and acoustic window determine coverage.
ECoG / μECoG (Duraivel et al., 2023)	Field-potential features depend on band selection and temporal averaging	Local cortical-surface electrical activity	Example μECoG array: 200-μm contacts, 1.33-mm pitch; coverage follows the implanted surface array.
sEEG (Verwoert et al., 2025)	1,024- or 2,048-Hz acquisition; analysed at 1,024 Hz	Field potentials near depth contacts	Sparse sampling along clinically selected depth trajectories; access to deep sites does not imply dense whole-brain coverage.
Intracortical (Wairagkar et al., 2025)	30-kHz voltages; 1-ms feature extraction; 10-ms feature bins	Threshold crossings and spike-band power	256 microelectrodes in ventral precentral cortex; local coverage rather than whole-cortex sampling.

4.1 Neural representations of language

Language tasks recruit overlapping systems while placing different demands on them: producing a word requires a plan for its form and articulation, hearing it requires interpreting an acoustic event, and reading it requires identifying a visual form. Across these tasks, words acquire meaning through their relationships to surrounding words and the broader situation. The useful unit for neural decoding is therefore a task-dependent representation in a sampled population, rather than a fixed correspondence between one brain region and one linguistic function. Figure 5 connects representative observations to the output interfaces developed from them.

From linguistic plans to articulation. Speech production combines the construction of an utterance with coordination of the vocal tract. Cortical-surface recordings over ventral sensorimotor cortex reveal overlapping representations of the lips, tongue, jaw and larynx; their population activity changes as these articulators combine into speech sounds (Bouchard et al., 2013). This organization provides a basis for predicting articulatory or acoustic trajectories from neural activity. Planning also carries structure before a movement or sound occurs. Acute single-neuron recordings in the language-dominant posterior middle frontal gyrus distinguish the phonetic composition, order and syllabification of upcoming words (Khanna et al., 2024). More extensive frontotemporal recordings resolve grammatical relationships, phrase structure and contextual semantic information before word utterance (Cai et al., 2026). These studies distinguish the information needed to construct a word sequence from the information needed to execute its articulation, while showing that both involve distributed, mixed population codes. Accordingly, recording placement influences whether a decoder has direct access to phonetic planning, articulatory dynamics or higher-level sentence organization.

From speech sounds to contextual meaning. During listening, superior temporal gyrus responses distinguish acoustic–phonetic features through sensitivity to spectrotemporal cues in continuous speech (Mesgarani et al., 2014). Such responses motivate acoustic reconstruction and speech-feature alignment, because the predicted target preserves aspects of the sound that elicited the activity. Comprehension additionally represents what a word means in context. Voxelwise models of narrative-listening fMRI reveal semantic selectivity across bilateral temporal, parietal and prefrontal territories (Huth et al., 2016). At a different scale, single neurons in left posterior middle frontal cortex respond to word meanings in ways that change with the sentence context, rather than simply following phonetic form (Jamali et al., 2024). Thus, contextual semantic information is accessible both in local spiking and in distributed haemodynamic measurements; it is not a property exclusive to one recording family. Conversely, a shared recording region need not imply identical task codes: the posterior frontal neurons selective for heard phonetic content were largely distinct from those selective during speech planning in a within-study task comparison (Khanna et al., 2024).

Reading links visual forms to language composition. Reading begins with a visual input whose orthographic structure must be connected to lexical and sentence information. Intracranial recordings in left midfusiform cortex distinguish an early representation organized by orthographic similarity from later word-specific activity. Electrical stimulation at the tested sites, and resection in one participant, impaired visual word or letter perception, providing evidence for a causal contribution to these reading operations (Hirshorn et al., 2016). Sentence understanding extends beyond recognition of individual forms: high-gamma responses across frontal and temporal sites build up as meaningful sentences unfold, with different response profiles for word lists, nonword lists and syntactically structured nonwords (Fedorenko et al., 2016). The contrasts link this build-up to the construction of sentence meaning. Recent natural-reading MEG with eye tracking further identifies parafoveal orthographic similarity in left ventral occipitotemporal cortex and semantic similarity in left inferior frontal cortex before the target word is fixated (Wang et al., 2025b). These source-localised associations show why a fixation-aligned neural segment can contain information about neighbouring words and context as well as the currently fixated word. A reading decoder consequently samples a mixture of visual recognition, linguistic integration and, depending on the reader's strategy, internal verbal activity (Kunz et al., 2025).

Inner and attempted speech share content but differ in state. Internally saying a word, imagining its sound and attempting its articulation provide related routes to linguistic content. Their overlap creates opportunities for transfer, while their differences determine which supervision remains appropriate. Microelectrode recordings from supramarginal gyrus support classification of internally and overtly produced words and pseudowords in two participants; shared representations with word reading and vocalized speech were demonstrated in one participant (Wandelt et al., 2024). Motor-cortex recordings in four participants subsequently showed correlated word-pattern geometry across attempted, inner and perceived speech. Inner speech was more weakly modulated, and a population dimension associated with motor intention helped distinguish inner from attempted speech (Kunz et al., 2025). This combination is useful for an interface: content information can be shared while the intended mode of communication remains distinguishable. It also explains why an absence of visible movement does not by itself identify the neural task. Transfer between listening, attempted and inner speech depends on the particular population, instructions and representation, rather than on a shared word label alone.

Matching the representation to the measurement and output. Cross-task reuse also extends to longer linguistic context. Models fitted to fMRI responses during matched reading and listening narratives reveal similar cortical organization of language-context timescales across temporal, parietal and prefrontal regions (Chen et al., 2024a). This supports a common substrate for integration beyond the modality-specific input, without requiring identical fine-scale dynamics. Measurement scale still matters: the linguistic selectivity of individual neurons can differ from that of field potentials at the same recording sites (Cai et al., 2026). Broad coverage and local precision therefore answer complementary questions about accessible information.

The decoding target selects which of these properties the interface preserves. Acoustic representations can support reconstruction of heard speech (Pasley et al., 2012); phoneme sequences can connect attempted speech to text (Willett et al., 2023); contextual representations can constrain a generated description of perceived or imagined language (Tang et al., 2023). A single speech-cortex recording can also feed text, speech synthesis and audio-linked facial animation through different prediction targets (Metzger et al., 2023). These are many-to-many relationships between neural information and output forms. Representation studies explain why a target is plausible; held-out and online decoding establish how effectively a particular system can recover it.

Table 4. Representative measurements and evidence for the region–task map in Figure 5. Labels identify groups of observations rather than exclusive anatomical functions.

Group	Representative measurement	Representative primary evidence
A	Sensorimotor surface / array recordings	Articulator organization and cross-task word patterns (Bouchard et al., 2013; Kunz et al., 2025).
B	Posterior frontal single neurons	Planned phonetic sequences and heard contextual meanings (Khanna et al., 2024; Jamali et al., 2024).
C	Temporal surface recordings	Heard acoustic–phonetic features in STG (Mesgarani et al., 2014).
D	Supramarginal single-neuron arrays	Vocalised and internal words in two participants; auditory-cue listening, written-cue reading and cross-task comparisons in participant 1 (source Figure 6 and auditory/written cue tasks) (Wandelt et al., 2024).
E	Frontotemporal cells / ECoG; distributed fMRI	Sentence composition, contextual meaning and reading–listening timescales (Fedorenko et al., 2016; Huth et al., 2016; Chen et al., 2024a; Cai et al., 2026).
F	Ventral temporal iEEG / source-localised MEG	Orthographic identity, local stimulation effects and parafoveal processing (Hirshorn et al., 2016; Wang et al., 2025b).

4.2 Electrophysiological signals

Electroencephalography (EEG) measures scalp potentials arising from the combined electrical activity of neuronal populations; around-ear placement is one recording configuration. Magnetoencephalography (MEG), in-

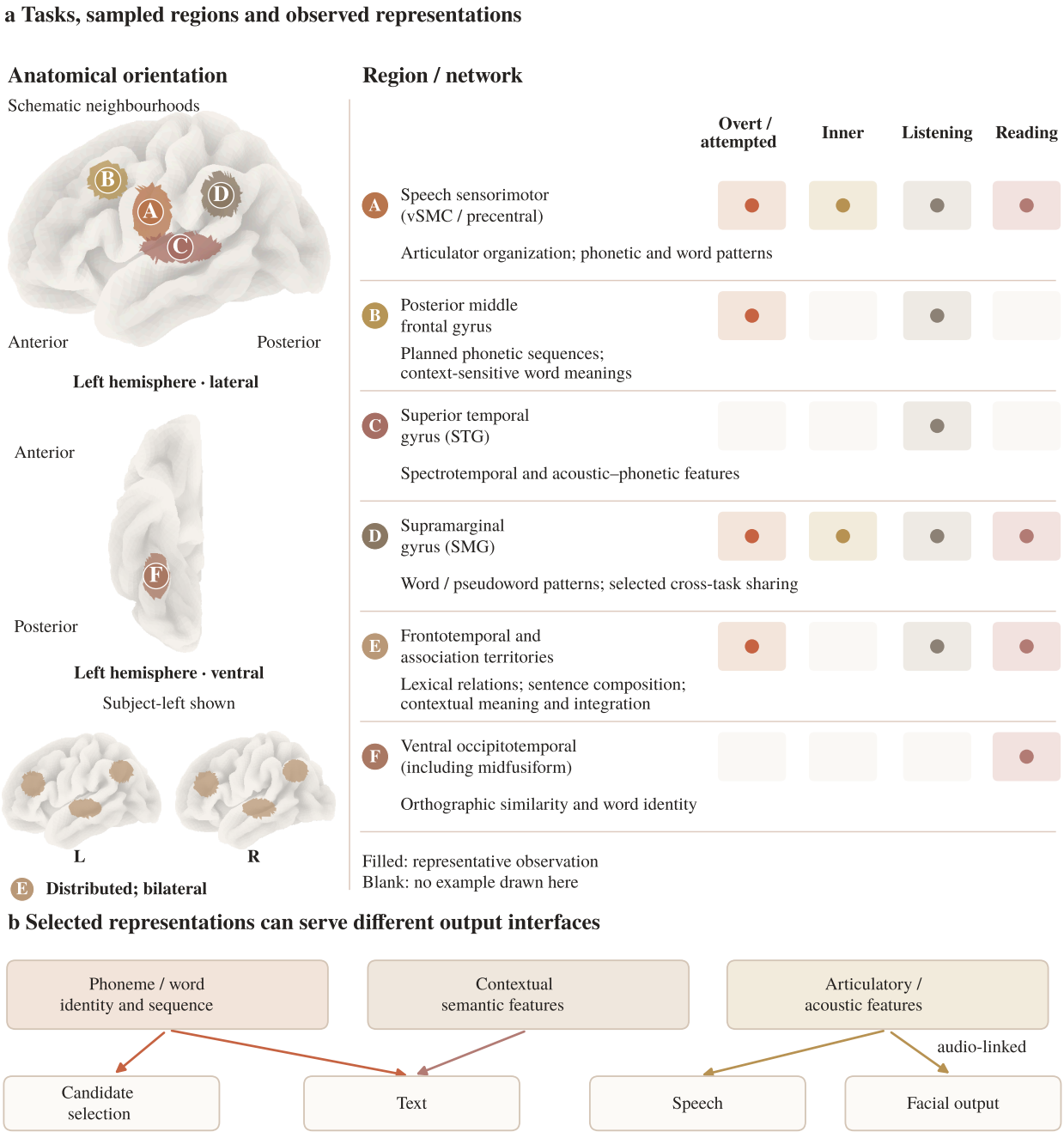


Figure 5. **Neural representations across language tasks and their decoding targets.** (a) Lateral and ventral fsaverage5 surfaces provide anatomical orientation (Fischl et al., 1999); coloured neighbourhoods are schematic, not electrode coordinates or functional boundaries. E represents bilateral distributed territories. Filled cells show representative observations; blank cells indicate no example drawn here. Overt and attempted speech remain distinct tasks despite sharing a column. The corresponding measurements and primary studies are given in Table 4. (b) Arrows identify selected decoding interfaces for word selection, text, voice and audio-linked facial output (Wandelt et al., 2024; Willett et al., 2023; Metzger et al., 2023; Tang et al., 2023; Landau et al., 2026). They are model connections, not anatomical tracts or one-region–one-function assignments.

cluding conventional systems and optically pumped magnetometers (OPMs), measures magnetic fields associated with neural activity. Invasive recordings include cortical-surface electrocorticography (ECoG) and its high-density or micro-ECoG configurations, stereoelectroencephalography (sEEG) depth macro-contacts, intracortical arrays and acute Neuropixels probes. Intracranial EEG (iEEG) encompasses ECoG and sEEG. Extracellular field potentials reflect pooled local activity, whereas spikes and threshold crossings provide features associated with neuronal firing. Intracortical decoders use these alongside spike-band power and local field potentials. These families differ in spatial coverage and signal access; a common model architecture does not make their neural inputs equivalent (Herff & Schultz, 2016; Duraivel et al., 2023; Khanna et al., 2024; Willett et al., 2023).

These measurements offer different forms of information access. Scalp and ear EEG can track features of attended external speech, and source-localised MEG can characterise auditory and visual speech information over time (Geirnaert et al., 2025b; Bröhl et al., 2022). Cortical-surface recordings resolve local population activity with articulatory and acoustic-phonetic organisation (Bouchard et al., 2013; Mesgarani et al., 2014). Intracortical arrays add features derived from neuronal spiking and local fields, which have supported large-vocabulary speech decoding (Willett et al., 2023). Thus, the feature representation and recording location explain a decoder's input more precisely than the device name alone.

Beyond content reconstruction, distributed sEEG recordings support speech-state detection and identification of intent-related contacts (Verwoert et al., 2025; Prakash et al., 2025). These targets help identify when and where language-related activity can be read out.

4.3 Haemodynamic signals

Functional magnetic resonance imaging (fMRI), functional near-infrared spectroscopy (fNIRS), high-density diffuse optical tomography (HD-DOT) and functional ultrasound imaging (fUSI) measure vascular responses associated with neural processing. BOLD fMRI uses magnetic-resonance contrast sensitive to blood oxygenation; fNIRS estimates haemoglobin changes optically, with dense sampling and reconstruction in HD-DOT; fUSI uses Doppler measurements sensitive to microvascular blood-volume changes. Simultaneous electrophysiological and fMRI experiments in nonhuman primates provided an empirical basis for interpreting this relationship (Logothetis et al., 2001). Optical reconstruction and Doppler acquisition provide different views of vascular activity (Schroeder et al., 2023; Soloukey et al., 2020). The response integrates activity over time, making temporal alignment and target duration important parts of a language-decoding model.

Language applications illustrate the range of targets available through this response. fNIRS has supported concept discrimination from responses to paired pictures and spoken labels, while fMRI decoders reconstruct the gist of extended language and high-density fNIRS systems investigate cue-conditioned sentence generation (Cao et al., 2021; Tang et al., 2023; Zhang et al., 2024b). HD-DOT combines dense optical sampling with reconstruction to map tasks such as silent reading, silent verb generation and overt production, and to retrieve stimulus segments (Schroeder et al., 2023; Tripathy et al., 2025). These approaches exploit information integrated over longer intervals. Faster sampling can improve the measurement, but the vascular response must still be included when interpreting output latency.

4.3.1 Functional ultrasound: mapping and decoding boundaries

An ultrasound array sends acoustic pulses into tissue and records returning echoes. Rapid image sequences allow tissue motion to be suppressed and echoes from moving blood cells to be retained; power-Doppler processing then yields a measurement sensitive to local blood volume. Neural activity is related to this vascular signal through neurovascular coupling, so image acquisition speed and the underlying physiological response are different timescales (Soloukey et al., 2020; Rabut et al., 2024). Figure 6 follows this measurement from pulse transmission to task-linked readout.

Functional ultrasound imaging offers sub-millimetre vascular measurements in selected configurations. Its potential for language interfaces depends on joining three advances that currently address different problems:

localising language-related activity, predicting content from single trials and maintaining recording access (Table 15).

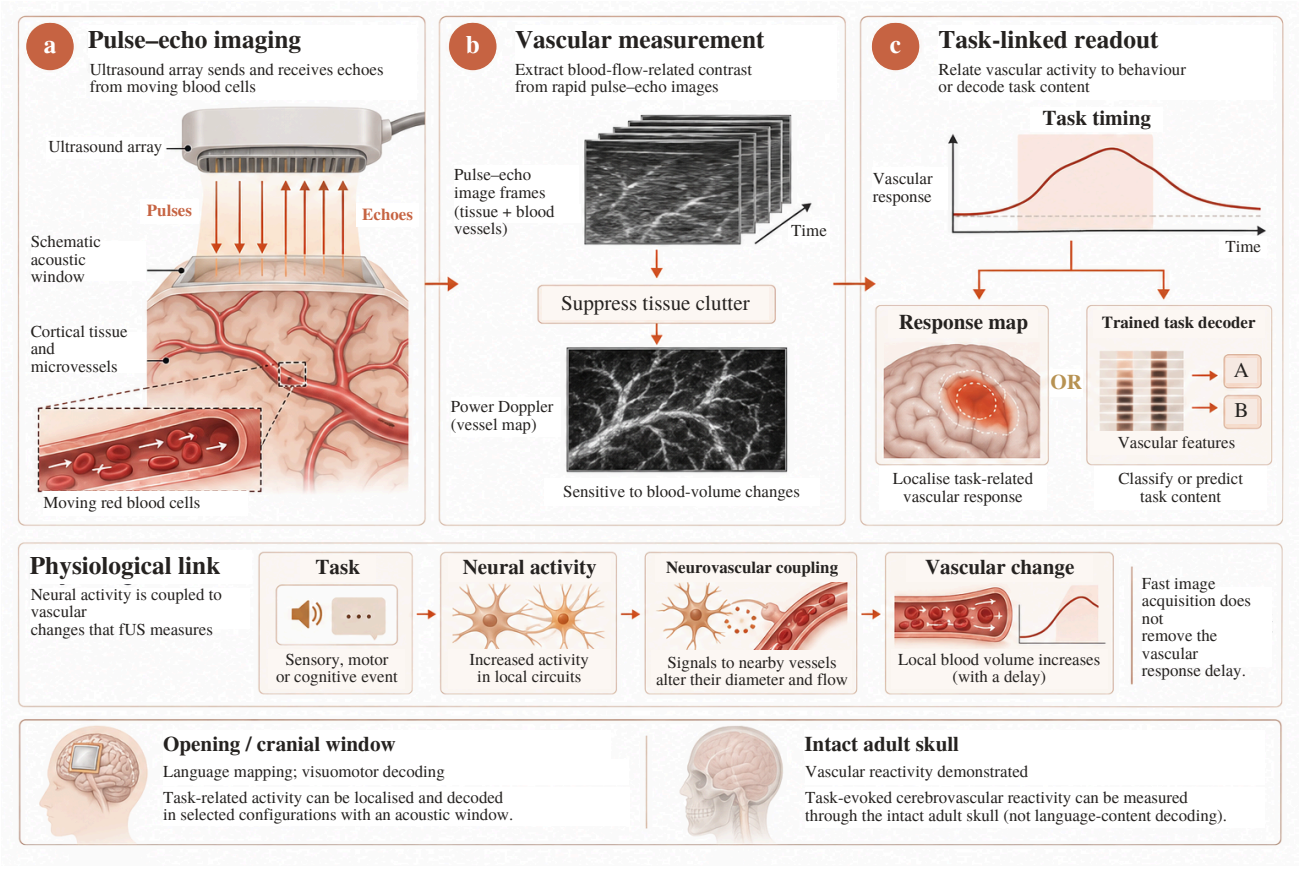


Figure 6. **How functional ultrasound imaging (fUSI) relates neural activity to a vascular measurement.** (a) An array transmits pulses and receives echoes, including those scattered by moving blood cells. (b) Tissue-clutter suppression and power-Doppler processing yield a blood-volume-sensitive image sequence. (c) Task-linked vascular changes support response mapping or a trained decoder. Neurovascular coupling provides the physiological link; rapid acquisition does not remove the vascular response delay. Intra-operative language mapping and window-based visuomotor decoding have been reported (Soloukey et al., 2020; Rabut et al., 2024). The cited intact-skull study instead measured breath-hold vascular reactivity (Vienneau et al., 2026). All anatomy, vessel images and traces are schematic. The figure depicts imaging, not ultrasound stimulation or direct spike measurement.

Localising a response is the first step. Intra-operative fUSI establishes that task-related haemodynamics can be measured in awake patients (Imbault et al., 2017). Language evidence includes aloud and source-labelled covert repetition in a ten-patient series with 18 language measurements, with both responses shown for one patient (Soloukey et al., 2020), and overlap with fMRI and electrical stimulation mapping (ESM) (Soloukey et al., 2023). Agreement between maps supports localisation of a task response. It leaves open whether that response distinguishes the words or sentences within the task.

Decodability and sustained access are separate advances. Human single-trial finger and effector decoding across sessions demonstrates usable motor information through acoustically transparent cranial windows (Rabut et al., 2024; Lin et al., 2026). Natural-behaviour imaging over more than 20 months and miniaturised four-dimensional systems address access and recording practicality (Soloukey et al., 2025; Verhoef et al., 2025). Neither establishes language-content recovery: imagined lip licking in the former study is non-speech motor imagery, outside Inner. Non-human primate evidence progresses from propagation of task-related activity to

movement-intention decoding and closed-loop ultrasonic brain–machine interfaces (Dizeux et al., 2019; Norman et al., 2021; Griggs et al., 2024).

The access route limits extrapolation. Intact-skull human fUSI measured breath-hold vascular reactivity without contrast agents in 13 participants (Vienneau et al., 2026); ex-vivo human-skull acoustic transparency is additional feasibility evidence (Wang et al., 2025e). These findings show that a cranial window is not universally required, but the motor-decoding results obtained through windows cannot simply be assigned to transcranial acquisition. Auditory-response work in ferret, crow and marmoset, and click responses in comatose patients, similarly establishes sensitivity to stimulation rather than language identity (Bimbard et al., 2018; Landemard et al., 2025; Liao et al., 2025; Takahashi et al., 2021; Chen et al., 2025d). Cross-species comparisons and mouse temporal-resolution measurements help explain the signal while retaining their species and modality boundaries (Landemard et al., 2021; Bian et al., 2026).

Together, human studies link language-related vascular mapping, single-trial motor decoding and repeated recording access (Soloukey et al., 2020; Lin et al., 2026; Soloukey et al., 2025). They motivate testing linguistic distinctions under a specified access route, with the target duration matched to the vascular response.

4.4 Sensors, placement and recording configurations

Density, coverage and alignment solve different problems. Denser sampling can recover distinctions lost when nearby signals are pooled: 128- and 256-contact intra-operative μECoG improved decoding of non-words built from nine phonemes in four participants (Duraivel et al., 2023). Across patients, the challenge changes because the sampled populations differ; shared latent dynamics improve decoding with μECoG and sparse sEEG (Spalding et al., 2026; Singh et al., 2025). Temporal modelling is another design choice: recurrent and Transformer models outperformed linear regression for sEEG speech reconstruction, with no significant difference detected between the two deep-learning methods in that study (Wu et al., 2024c). These examples support improving spatial sampling, representational alignment and temporal modelling for different reasons; none shows that model choice compensates for missing coverage. Acute Neuropixels findings resolve articulatory planning, phonemes and sequences at single-neuron scale (Khanna et al., 2024), but do not establish the same information access in a chronic communication system.

Placement determines which tissue and neural populations are observed. Scalp, cortical-surface, depth and intracortical configurations therefore differ in coverage as well as access requirements (Table 3). Source localisation and cross-participant latent alignment can reduce mismatch between recordings, but cannot create direct measurements of populations that were not sampled. The clinical configurations in Table 10 illustrate why implant choice and participant condition must be considered together.

Simultaneous recording allows configurations to be compared under the same behavioural conditions. Scalp, around-ear and in-ear EEG recorded during one auditory-attention task showed that recording configuration and reference choice affect decoding (Geirnaert et al., 2025b). Complementary intraoperative work demonstrated speech decoding with a dense cortical-surface microelectrode interface (Lehner et al., 2026). The first comparison informs sensor placement and referencing; the second establishes feasibility for an acute cortical recording route.

Comparing recording routes. Signal selection couples a linguistic target to an access and supervision requirement. Reviews of imagined-speech reconstruction and EEG–fNIRS acquisition explain the range of non-invasive options (Tang et al., 2024; Motaqi et al., 2026); implantable-speech reviews relate cortical access to patient selection and training (Jhilal et al., 2025). Hybrid sensing adds another design choice: peripheral information may improve communication even when it contributes no neural evidence. Broader silent-speech sensing reviews include these peripheral routes (Tang et al., 2026). Channel-specific comparisons are needed to determine what combining them with neural recording actually adds.

Choosing acquisition around the target. Three questions narrow a recording choice before model selection: does the configuration sample the relevant population, does its temporal support match the target, and can that access be sustained in the intended setting? A phoneme-timed speech output and a semantic account of a long

passage require different temporal information. Greater spatial coverage can aid representation learning while introducing setup and access costs; denser sampling of one region cannot substitute for sampling the relevant process. The conditional trade-offs in Table 5 therefore concern configurations and objectives, not a global ordering of signal families.

Table 5. Acquisition choices change the learning and use problem. The trade-offs synthesise the cited configurations; they are not controlled estimates of modality superiority.

Configuration	Useful information access	Main trade-off	Consequence for a language system
Intracortical / cortical-surface recording	Local speech-related activity with fast temporal features (Willett et al., 2023; Metzger et al., 2023)	Surgical access and participant-specific coverage; chronic and acute data are distinct	Test calibration and stability for the actual implant and user, rather than extrapolating from acute decoding.
Scalp EEG	Time-resolved potentials; reading data with eye tracking (Hollenstein et al., 2018)	Distributed mixtures, electrode contact and peripheral activity	Pair neural decoding with eye/muscle controls and calibration under the intended behaviour.
MEG	Time-resolved magnetic responses; reusable listening recordings (Défossez et al., 2023; Özdogan et al., 2025)	Sensor geometry, head movement and system-specific magnetic environment	Test content and participant transfer with the acquisition setup explicitly specified.
fMRI	Distributed BOLD patterns carrying contextual language information (Tang et al., 2023)	Delayed response and scanner-constrained acquisition	Match targets to response support; distinguish semantic fidelity from feedback latency.
Optical haemodynamics	Cortical haemoglobin responses through fNIRS / HD-DOT (Zhang et al., 2024b; Schroeder et al., 2023)	Optical coverage, motion and delayed vascular response	Separate cue-conditioned language information from reference inputs and operating delay.
Functional ultrasound	Selected human language mapping and motor-decoding configurations (Soloukey et al., 2020; Rabut et al., 2024)	Access differs between cranial-window recording and intact-skull feasibility	First establish held-out language-content decoding for the proposed access route.

4.5 Signal quality and acquisition constraints

Confounds depend on both task and acquisition. Articulated conditions introduce movement, muscle activity and possible acoustic contamination; Reading adds gaze and fixation timing. Inner instructions reduce intended movement but do not measure compliance. Auxiliary EOG, EMG or motion channels can test these explanations, while deliberate EEG–EMG fusion uses peripheral activity as part of the communication signal (Nieto et al., 2022; Hollenstein et al., 2018; Inoue et al., 2026). The same channel can thus serve as a control or a useful input, depending on the claim. Neural specificity requires separating these roles.

Acquisition controls are most informative when they follow the physical measurement. Multicentre analyses and recording-chain experiments show that sound-related vibration can introduce speech-correlated components into invasive signals during production or sound perception (Roussel et al., 2020; Bush et al., 2022). Synchronous sound and movement measurements, frequency-specific analyses and hardware controls help separate these components from physiology. Optical measurements require a different separation: short-separation channels can estimate superficial physiological activity, and controlled comparisons show how optode density, noise regres-

sion and image reconstruction affect decoding (Fischer et al., 2026). These adjacent methodological results guide signal preparation without serving as language-performance estimates.

Implications for method choice. A model must accommodate both the information in the recording and the timescale on which it arrives. Electrophysiological decoders in the reviewed systems use time-varying features for phoneme, acoustic or sequence targets, whereas haemodynamic decoding must account for the delayed vascular response when aligning language and measurements (Willett et al., 2023; Anumanchipalli et al., 2019; Tang et al., 2023). Recording coverage and access also shape the available supervision: clinical production systems, naturalistic listening corpora and reading datasets provide different paired observations. A useful decoder must therefore match its target representation and training supervision to the information and timing of the chosen recording.

The supplementary mechanism map (Figure 24) distinguishes physiological response and access constraints that the sampling configurations in Table 3 alone cannot express.

5 Methods

Decoding methods distribute the reconstruction problem between neural measurements, paired training data and a model of plausible outputs. Their central design choice is which information the neural representation must preserve: distinctions among candidates, a linguistic sequence, a voice trajectory or a semantic relationship. Supervision determines which of these mappings can be learned, and the model prior supplies structure that the recordings do not fully specify. Shared benchmarks now support comparisons across successive methods in clinical text decoding, non-invasive retrieval and generation, speech synthesis and neural pretraining. These comparisons reveal which design choices improve a common task, while differences in test inputs and training resources explain why the same method can perform differently across settings.

5.1 Data and supervision

5.1.1 Experimental protocols and datasets

Datasets supply both the examples from which a decoder learns and the experimental contrasts through which its behaviour can be understood (Table 6). Multi-session recordings support study of day-to-day variation; matched overt conditions supply acoustic or linguistic supervision; peripheral EOG/EMG channels help characterise task execution (Nieto et al., 2022). Recording vocalised, mouthed and internal production of the same items adds a direct basis for cross-task learning (Ma et al., 2026b; He et al., 2025b). These contrasts depend on the elicited behaviour: silent articulation includes attempted articulatory movement, whereas imagined speech need not. SS-EEG, for example, instructs articulation attempts without sound (Zhou et al., 2025a).

Perceived tasks provide stimulus transcripts, acoustic timing or visible text. Listening corpora and repeated reading datasets support reusable benchmarks, whereas clinical production data may require participant-specific collection. ZuCo combines EEG with eye tracking; LibriBrain pairs one participant's MEG with 52.32 hours of listening stimuli (Hollenstein et al., 2018; 2020; Özdogan et al., 2025). Across signal families, task-related recording totals and paired-material coverage span several orders of magnitude (Figure 7). Repeated presentations and additional participants increase the available neural observations without necessarily introducing new linguistic material. Material coverage therefore complements recording hours and participant counts when assessing the resources available for learning. The inventory in Table 27 provides the task designs, recording scopes and access conditions.

Recording depth and participant breadth support different kinds of learning. LibriBrain100 extends listening-MEG data along both dimensions, enabling prolonged within-person training and comparison across listeners (Mantegna et al., 2026b). Protocol diversity adds another resource: post-imagery overt responses can help check task compliance, while repeated reading and recall sessions allow stability to be studied with familiar content (Aguilera-Rodríguez et al., 2025; Zhang et al., 2026e). These resources support complementary research questions. Long recordings from one person support fitting a detailed personal mapping; many participants support

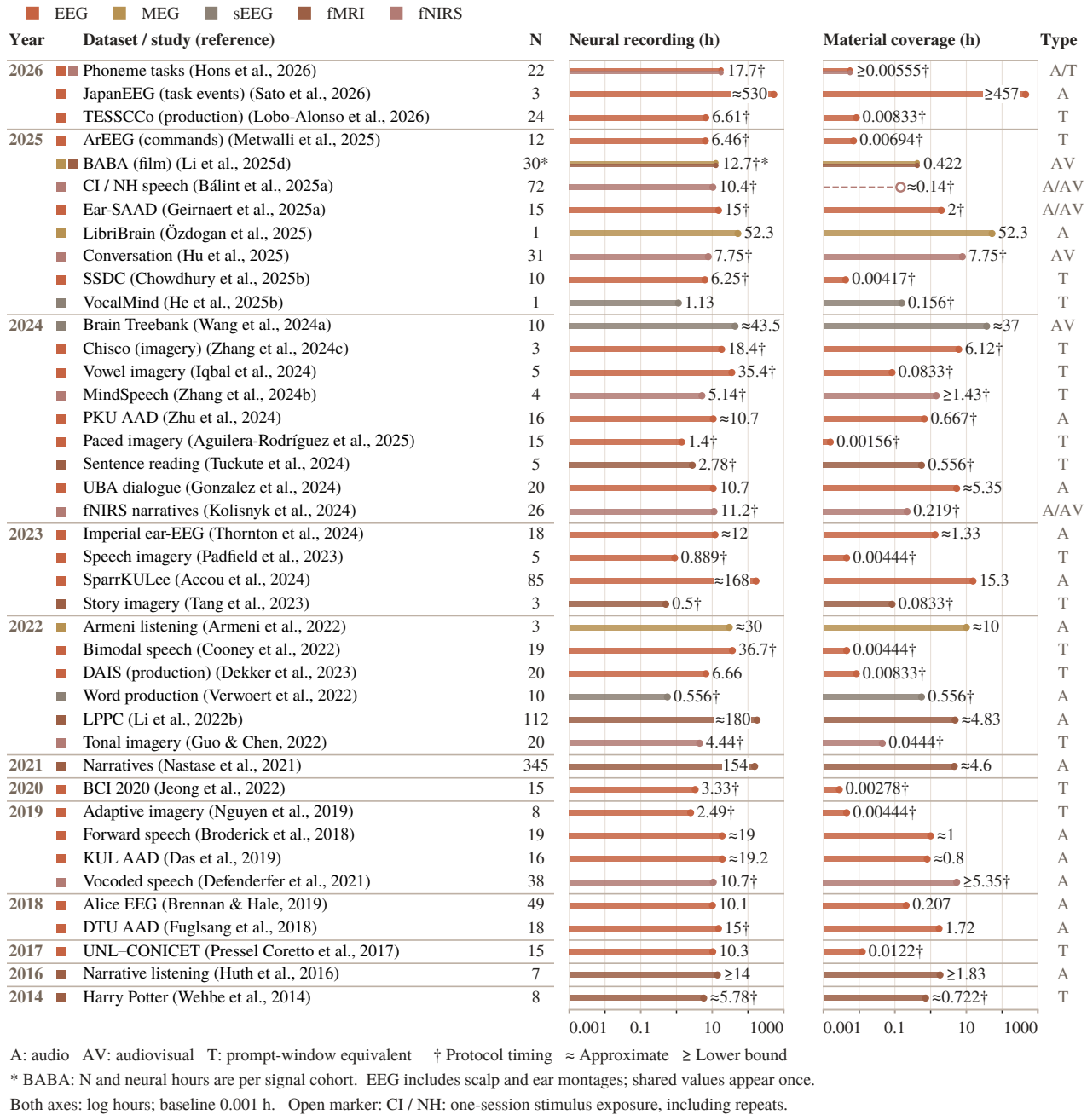


Figure 7. **Task-related neural recordings and paired-material coverage across datasets.** Each dataset or study occupies one row, ordered by release year (or report year); N describes the shown neural cohort. Left: task intervals summed across participants and repetitions. Right: filled markers show material coverage, counting each source once; text is duration-equivalent coverage using the stated window per distinct prompt, rather than measured stimulus-audio duration. The open CI/NH marker estimates one-session stimulus exposure (about 0.14 h), including repeated sentences; it is not unique-source duration. Coloured squares denote signals; multiple colours share a row without summing their durations. BABA has separate MEG and fMRI cohorts: N and neural hours are stated per cohort. Both axes use identical logarithmic hour scales. Lower bounds can represent a verified component; audio includes aligned task windows. Shared material across participants and simultaneous modalities is not additive. The full resource inventory appears in Table 27.

Table 6. Selected datasets provide complementary task contrasts and forms of supervision. Counts refer to the cited releases; the two Moreira experiments and two ZuCo releases are listed separately. Task conditions, auxiliary measurements and annotations determine which comparisons each resource supports. The complete inventory appears in Table 27.

Resource	N	Task contrasts, auxiliary measurements and supervision
Thinking Out Loud (Nieto et al., 2022)	10	EEG with EOG and lip EMG; overt speech, imagined speech and visualised-direction trials share four direction classes, allowing task contrasts and movement checks.
Chisco (Zhang et al., 2024c)	3	High-density EEG during reading followed by imagined production of the same Chinese text; paired phases and 39 semantic categories connect comprehension with prompted production.
Moreira articulation corpus (Moreira et al., 2025)	8; 16	Two 64-channel EEG experiments use phonemes, syllable pairs, real words and pseudowords, with perception/production tasks and control versus transcranial magnetic stimulation conditions.
3M-CPSEED (Ma et al., 2026b)	20	EEG for the same ten Pinyin items during overt, mouthed and imagined production; shared class labels support comparisons across articulatory conditions.
Aguilera paradigm comparison (Aguilera-Rodríguez et al., 2025)	15	EEG during the same four imagined commands under conventional cues and a maze-game protocol; user-experience and affect questionnaires characterise the elicitation context.
VocalMind (He et al., 2025b)	1	sEEG from Mandarin words and sentences in vocalised, mimed and imagined conditions; overt speech supplies an acoustic reference for cross-condition decoding.
LibriBrain (Özdogan et al., 2025)	1	Multi-session MEG during audiobook listening, with aligned audio, word and phoneme annotations and session-based training, validation and test partitions.
ZuCo 1.0 / 2.0 (Hollenstein et al., 2018; 2020)	12 / 18	Simultaneous EEG and eye tracking during natural and task-directed English sentence reading; fixations link neural responses to the presented words.
SS-EEG (Zhou et al., 2025a)	12	EEG during instructed silent articulation of 24 English words in six semantic groups; 16 sessions per participant support word/semantic classification and cross-session evaluation.

testing shared representations; repeated sessions expose recording drift; distinct stories or sentences support tests of new content. Repetitions improve estimation of a response but add less linguistic diversity than new material. For transfer, the availability of matched tasks and languages can consequently matter as much as total hours.

5.1.2 Target labels and temporal alignment

Overt audio provides acoustic and phonetic targets, although alignment remains an explicit processing step. Mouthed and Inner conditions do not provide the same simultaneous audible reference; reviewed systems use prompted content, paired Overt recordings or transferred models (Anumanchipalli et al., 2019; Angrick et al., 2021; Lee et al., 2023). In Reading, fixation markers can define word-aligned inputs, while marker-free methods pose a different segmentation problem (Duan et al., 2023). An expected prompt identifies the requested content; it does not prove that every trial followed it.

Alignment can be learned during model fitting. Iterative alignment discovery uses dynamic time warping within neural voice-activity training to accommodate uncertain response onset and duration (Rabbani et al., 2024). This offers a constructive way to learn from imperfectly timed labels. Because the alignment is part of training, it need not supply a reference waveform for the test utterance; reference-dependent test alignment has a different information requirement.

Training supervision must be distinguished from information required during testing. Overt-reference temporal alignment in silent-reading reconstruction (Martin et al., 2014) and DTW reference alignment in EEG synthesis

(Xiong et al., 2025) constrain conclusions about autonomous operation. Haemodynamic models must additionally account for the relation between stimulus time and measured response (Tang et al., 2023). The reported test protocol should state which boundaries, alignments and transcripts are supplied to the decoder.

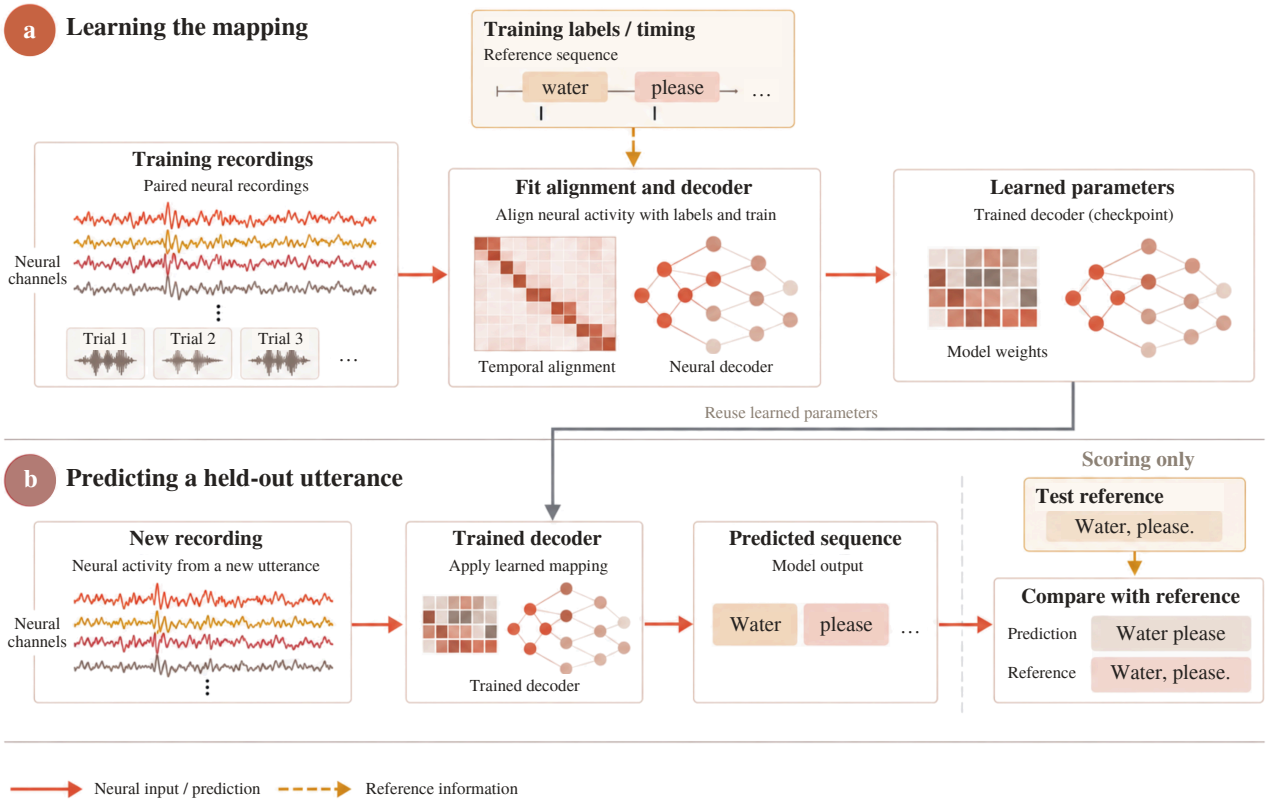


Figure 8. **Training supervision and test information occupy different paths.** (a) Training recordings and reference information fit an alignment and decoder; learned parameters are then reused. (b) A new recording produces a sequence, while the held-out reference enters only the scoring step. Iterative alignment discovery illustrates training-time alignment learning (Rabbani et al., 2024). Reference-dependent alignment during testing, as in silent-reading reconstruction with an Overt reference, supplies additional information (Martin et al., 2014). The illustrated test path excludes that input. Traces, weights and utterances are schematic; protocols must state any test-time references or boundaries.

5.1.3 Preprocessing and artifact handling

Filtering, referencing, epoching and artifact handling define the input available to a model, rather than being interchangeable implementation details. EEG reviews describe heterogeneous feature and preprocessing pipelines (Panachakel & Ramakrishnan, 2021; Lopez-Bernal et al., 2022); the selected invasive and MEG systems likewise use different neural features and temporal windows (Willett et al., 2023; Défossez et al., 2023). The appropriate pipeline follows the signal physiology, the target timescale and the information permitted during inference.

Preprocessing determines which regularities reach the learner. A multiverse analysis of EEG event-related-potential experiments showed that artifact correction could lower classification accuracy, consistent with models exploiting structured non-neural variation (Kessler et al., 2025). This explains why signal cleaning and prediction performance should be assessed together: the best pipeline for a neural interpretation may differ from the one that most easily separates the recorded conditions. Speech-specific recording-chain controls address acoustic contamination through a separate physical mechanism (Roussel et al., 2020).

A reproducible comparison specifies filter causality and temporal support, referencing or channel selection, rejection criteria, auxiliary channels and normalization. Learned transforms and feature selection should be fitted within the training partition. Artifact removal should be accompanied by residual-confound controls, rather than treated as proof of neural origin. A pipeline using future samples or reference-dependent alignment may remain useful offline, but its latency and information access differ from a causal communication system.

5.1.4 Data partitioning and leakage prevention

Data partitioning specifies the kind of reuse a model is expected to support. Within-person fitting, transfer across sessions and prediction for a new user are distinct learning settings. Cross-validation and hyperparameter selection can be organised around the corresponding independent unit, keeping validation separate from the final test (Varoquaux et al., 2017). This makes a performance estimate answer a useful deployment or scientific question.

Partitions should be defined before overlapping windows, repeated items or learned preprocessing can link training and test observations. The split unit follows the claim: trial-held-out tests assess new observations, stimulus-held-out tests assess new material, and session- or participant-held-out tests assess transfer to those conditions. The examined reading split audit identifies sentence overlap across nominal participant partitions (Yin et al., 2025). The MEG attribution audit additionally shows why fixed-duration windows and stimulus-identity separation matter when input structure can reveal the candidate (Zhang et al., 2026c). Each split removes a different source of familiarity, so the split unit is part of the generalisation claim (Section 6).

Preprocessing, supervision and architecture interact: a model can exploit differences introduced by the pipeline before it learns a linguistic distinction. EEG and end-to-end reviews accordingly connect features, task design and neural assumptions with model choice (Rahman et al., 2024; Zhang et al., 2025; Jin et al., 2025; Divya Keerthana et al., 2026; Yang et al., 2025; Estrella-Ibarra et al., 2026). Extending this perspective from imagery classification to language generation requires identifying what each output route asks the neural representation to preserve (Qiu et al., 2025; Yu et al., 2025).

5.2 Output types and decoding objectives

Four presentation forms organise the content outputs: candidate selection, text sequences, audible speech and facial animation. Classification and retrieval select from explicit alternatives. Text may aim at verbatim transcription or a semantic paraphrase; open vocabulary is a property of the decoding task, not a separate output medium. Spectrograms, phoneme posteriors and semantic embeddings can be intermediate targets. Facial animation is a visual expression channel, distinct from reconstructing arbitrary images. A system can combine several forms (Metzger et al., 2023).

Output, validation and use remain separate axes. Strongly controlled classification may establish neural information more convincingly than poorly controlled generation. Conversely, a generated waveform remains an acoustic output even when intelligibility is limited. State detection supports interaction; language mapping, representation studies and dataset reports describe study scope.

5.3 Neural features and learned representations

Three routes describe recurring intermediate representations across content decoders (Figure 9). The *text route* maps neural features to phoneme or character posteriors and lets a language model resolve them into words (Herff et al., 2015; Willett et al., 2023; Metzger et al., 2023). The *voice route* predicts an articulatory or acoustic intermediate and renders audio with a vocoder, increasingly in streaming form (Anumanchipalli et al., 2019; Littlejohn et al., 2025; Wairagkar et al., 2025). The *meaning route* predicts semantic embeddings to rank supplied candidates or guide a language model that generates gist (Tang et al., 2023; d' Ascoli et al., 2025; Zhang et al., 2024b). These are interfaces between measurements and output constraints, not successive stages of technical maturity. A method can share an architecture with another route while solving a different reconstruction problem (Table 8).

Table 7. Content-output forms and associated evaluation questions. Auxiliary control and study scope are recorded separately.

Form	Objective	Interpretation details
Candidate selection	classification or retrieval	class/candidate count, chance, top-k, repeated observations
Text decoding	character, word or sentence sequences	WER/CER; vocabulary and content limits; verbatim versus semantic target
Speech synthesis	audible speech, via acoustic or articulatory targets	intelligibility, listener protocol, naturalness, prosody and latency
Facial animation	speech-related visual expression	separate visual and audiovisual assessment; not text accuracy

Speech-state detection and device control are auxiliary outputs. Mapping, representation analysis, dataset release and methodological audits describe study scope, not content-output forms.

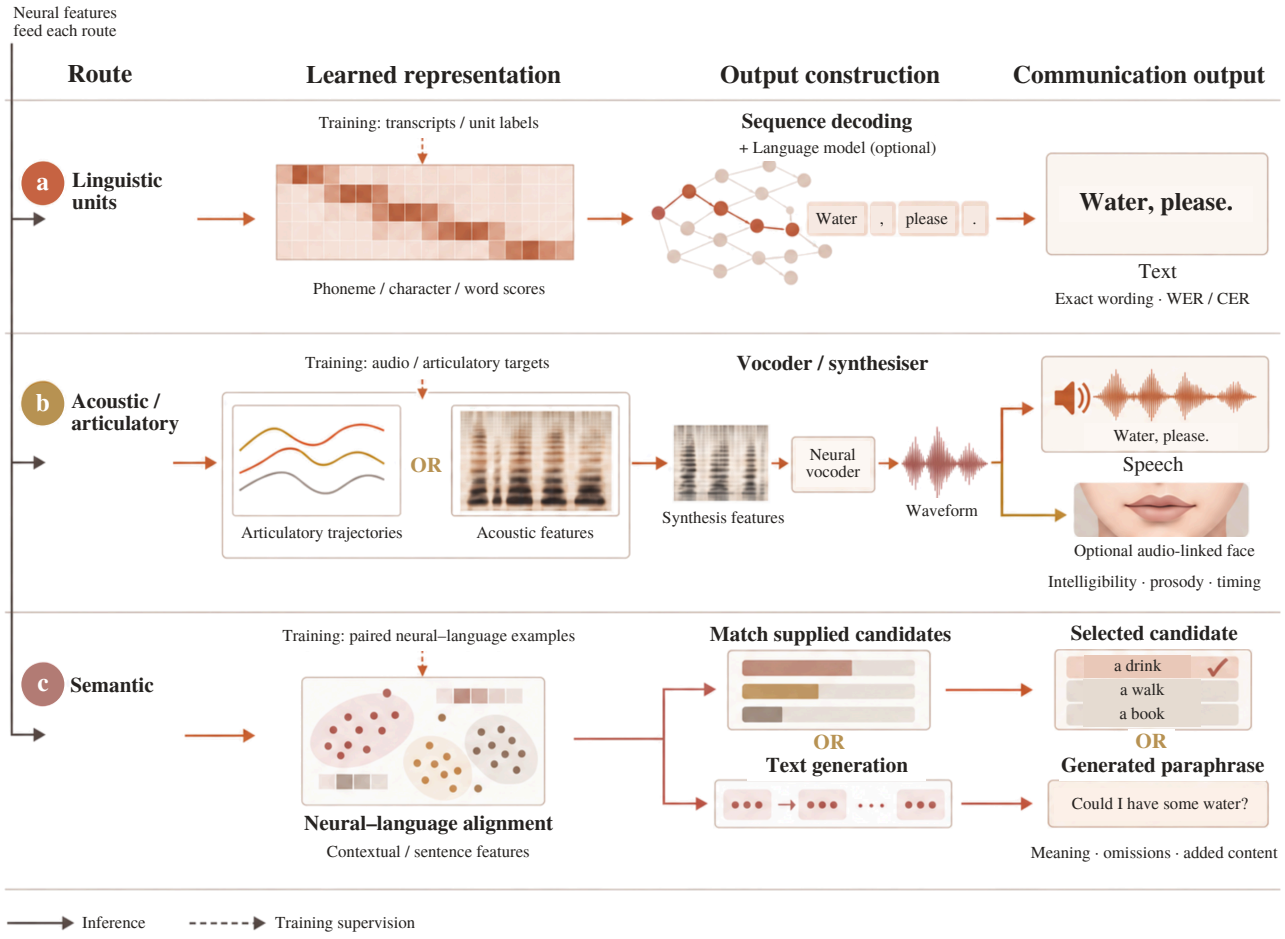


Figure 9. **Three intermediate-representation routes connect neural features to communication outputs.** (a) Linguistic-unit scores support sequence decoding and word or character fidelity (Willett et al., 2023). (b) Articulatory or acoustic features support speech synthesis and optional audio-linked facial output (Anumanchipalli et al., 2019; Metzger et al., 2023). (c) Semantic alignment supports matching supplied candidates or generating text that can differ in wording while preserving meaning (Tang et al., 2023). Solid arrows indicate inference; dashed arrows mark training supervision, not test-time reference inputs. Patterns, trajectories, scores and messages are illustrations, not reported results. The evaluation terms identify distinct output qualities; routes can be combined.

Intermediate targets also connect model design to physiology. Population recordings reveal articulator organisation and coordinated articulatory trajectories, while phoneme classifiers expose distinctions that can be composed into words (Bouchard et al., 2013; Chartier et al., 2018; Mugler et al., 2014). These findings motivate production-related targets for learning. When an articulatory trajectory is inferred from audio, it remains model-derived supervision rather than a direct measurement of the participant's movement.

Pretrained models supply useful structure at these interfaces. Speech representations such as wav2vec 2.0 provide alignment targets for MEG/EEG, whereas sequence decoders supply linguistic structure for Perceived–Auditory text generation (Défossez et al., 2023; Wang et al., 2026a; Yang et al., 2026b; 2024a). This can reduce what must be learned from scarce paired neural data. It also makes two outcomes separable: a better completed output and a more informative neural representation. Shared latent spaces align neural populations across patients, whereas long recordings within one participant provide repeated observations for learning temporal structure (Spalding et al., 2026; Singh et al., 2025; Özdogan et al., 2025; Zhang et al., 2024c). These approaches address different sources of data scarcity: variation in the neural populations sampled and limited coverage of linguistic experience.

The task-dependent representations in Figure 5 provide the physiological basis for these computational interfaces. Local motor recordings can supply fast articulatory or phonemic structure; auditory recordings can align with the presented speech; distributed and slower responses can constrain meaning over longer context. The decoding objective selects which part of that information must survive the mapping to an output.

What the intermediate representation buys. A phoneme or character interface makes lexical errors inspectable and allows a language model to combine neural evidence into new sequences. It also requires a linguistic target and an account of how the prior changes the decoded message (Willett et al., 2023; Metzger et al., 2023). An acoustic or articulatory interface instead preserves a route to voice characteristics and temporally evolving expression; paired audio and a vocoder supply information that is harder to obtain during silent production (Anumanchipalli et al., 2019; Wairagkar et al., 2025). Semantic alignment can relax exact wording and exploit longer-context representations, but an output can preserve gist while losing a negation, name or intended action (Tang et al., 2023). Route selection therefore fixes both the information that must be learned and the errors that matter to the user.

Selection and generation solve different bottlenecks. Retrieval makes the alternative set explicit and can be useful when only a small number of decisions is needed; its success is conditional on that set. Generation permits combinations beyond a supplied candidate list, but shifts part of the prediction problem into a learned prior. Moving from retrieval accuracy to generated text is consequently a change of task, not just a stronger score on the same task. A useful comparison holds the intended content and test information fixed, then asks whether the extra output freedom preserves the user's distinctions.

5.4 Classification and retrieval

Which distinction is being decoded? Classification is useful when a small set of alternatives matches the intended decision. It also tests whether a representation contains a particular distinction: selected ECoG electrodes separate internally articulated vowels, and low- and cross-frequency ECoG features carry Inner item or attribute information (Ikeda et al., 2014; Proix et al., 2022). The strength of that evidence is condition- and participant-specific. Eight-class cued Inner decoding from supramarginal single neurons reached online accuracies of 79% and 23% in two participants (Wandelt et al., 2024); pairwise ECoG inner-word decoding averaged 58% against 50% chance across five participants, despite a best value of 88% (Martin et al., 2016). A population code demonstrated in one configuration therefore does not establish uniformly usable control.

Spatial structure offers another architectural choice for classification. BrainStack combines seven regional convolutional experts with a global convolution–Transformer expert, using learned routing and global-to-local distillation to coordinate their predictions (Zhao et al., 2026). This makes regional specialisation and cross-region integration explicit within one model. Its EEG word-decoding task selects among predefined classes, so

Table 8. Intermediate representations distribute the learning problem differently. The same neural architecture can serve several routes; the useful comparison is what structure it learns, which supervision it needs and how the output is constructed. Clinical attempted remains a source-task description.

Mechanism / route	Structure made available	Supervision and principal trade-off	Representative conditions and systems
Linguistic-unit decoding	Phones, phonemes or characters connect neural dynamics to a compositional lexicon.	Transcripts and sequence alignment; the language model resolves uncertainty but can alter wording.	Overt / clinical attempted ECoG and intracortical text (Herff et al., 2015; Moses et al., 2021; Willett et al., 2023; Card et al., 2024; 2026); cued Inner (Kunz et al., 2025).
Sequence-to-sequence text	Learned temporal encoding connects recordings directly to linguistic sequences.	Paired sequences; learned alignment reduces hand specification while placing greater demands on data and partition design.	Overt ECoG / sEEG (Makin et al., 2020; Zhang et al., 2024a; Feng et al., 2025); pretrained MEG sequence interfaces (Yang et al., 2026b; 2024c;a).
Articulatory / acoustic synthesis	Movement trajectories, spectra or acoustic tokens retain a route to voice and expression.	Audio or articulatory targets, often supplied by Overt training; transfer must bridge missing audible targets.	Articulatory synthesis (Anumanchipalli et al., 2019; Chen et al., 2024b); spectral/vocoder routes (Kwon et al., 2024; Lee et al., 2023; Xiong et al., 2025; Angrick et al., 2021).
Streaming voice	Causal sequence models couple ongoing neural input to incremental audio.	Paired participant recordings and synthesis targets; temporal context trades off against responsive feedback.	Clinical ECoG / intracortical synthesis (Littlejohn et al., 2025; Wairagkar et al., 2025; 2026).
Acoustic / semantic alignment	Shared embeddings support candidate matching or constrain a language generator.	Paired stimuli or messages; the target embedding and candidate inventory determine which distinctions are preserved.	Speech-representation alignment (Défossez et al., 2023; Wang et al., 2026a); embedding retrieval (d' Ascoli et al., 2025); semantic generation (Tang et al., 2023; Ye et al., 2025; Zhang et al., 2024b; Rastogi et al., 2025).
Discriminative features	Covariance, spatial filters, learned temporal features or neural populations distinguish a finite inventory.	Class labels; simpler objectives can suit small datasets but fix the target distinctions in advance.	Riemannian / SVM (Nguyen et al., 2018; Hons et al., 2026; Ikeda et al., 2014); CNN (Dash et al., 2020; Cooney et al., 2022; Ko et al., 2025); regional tokens (Jiang et al., 2026); population decoding (Wandelt et al., 2024; Khanna et al., 2024).

the relevant contribution concerns how those alternatives are discriminated.

Task contrasts are more informative than isolated peaks. Reading versus Inner, preparation versus execution, and neural-only versus fused inputs test different explanations of a score. A five-word EEG/MEG comparison decoded silent reading more successfully than its mostly near-chance Inner conditions (Csaky et al., 2025). MEG preparation-window results, including 93% for five phrases and 67.2% for self-paced yes/no compared with 90.4% during overt production, remain tied to forthcoming speech (Dash et al., 2020; 2024). Repeated-word EEG windows must additionally separate content from cues and overlapping observations (Jiang et al., 2026). For EEG–fNIRS, group means of 34.3% and 77.3% in different four-class studies are not a controlled improvement; the latter study's within-protocol finding of no fusion benefit over EEG alone answers a narrower, more useful acquisition question (Cooney et al., 2022; Hons et al., 2026).

Non-invasive classification can likewise probe a specific target without establishing sequence reconstruction. A 7-T fMRI study classified pairs of spoken phonemes at 53% against 33% chance in 15 participants (Vitória et al., 2024), while an OPM-MEG/EEG comparison examined time-resolved decoding of six Mandarin vowels in

ten participants (Xu et al., 2026). Their value lies in testing access to these distinctions and their timing; sentence generation requires additional evidence about how distinctions compose.

Retrieval exposes the granularity of the target. Contrastive speech alignment can identify a multi-second segment without resolving its individual words. Across four datasets and 175 participants, MEG/EEG alignment retrieved the correct 3-second segment among more than 1,000 candidates with top-1 accuracy of 41% in the best MEG setting (Défossez et al., 2023). Word-level retrieval in a larger pooled corpus of 723 participants, nine datasets, three languages and five million words reached top-10 of 37% among 250 candidates against 4% chance, including words absent from training (d' Ascoli et al., 2025). MEG, silent reading and test-time averaging were generally easier under that protocol. Hierarchical alignment to spectrograms, wav2vec2 and GPT-2 further tests representations at several linguistic or acoustic levels, with reported top-1 of 35.6% for MEG and 20.0% for EEG on SMN4Lang and SparrKULee (Wang et al., 2026a). These studies broaden representation learning, but their candidate units and observation budgets remain part of the result: neither a larger candidate pool nor a higher top-k score alone establishes finer content recovery. HD-DOT movie-segment retrieval provides an adjacent example (Tripathy et al., 2025); without a speech-specific target, movie identification is not Perceived–Audiovisual speech decoding.

Long-context pretraining extends the retrieval route by reconstructing masked neural tokens from extended surrounding context, before the encoder is adapted to predict contextual word embeddings. MEG-XL uses this strategy for nearest-neighbour word selection with supplied word onsets and fixed candidate vocabularies (Jayalath & Parker Jones, 2026). Its contribution is improved data efficiency and contextual representation learning within retrieval. This illustrates how a broader temporal context can improve a neural encoder without changing the output task into sentence generation. The shared LibriBrain comparison in Figure 10 shows the resulting data-efficiency difference: MEG-XL reaches 57.3% top-10 balanced accuracy with 13% of the training data and 63.0% at the full budget, where BrainOmni also reaches 63.0%. These results favour long-context pretraining at the smaller budget while showing that the ordering can change as more paired data become available.

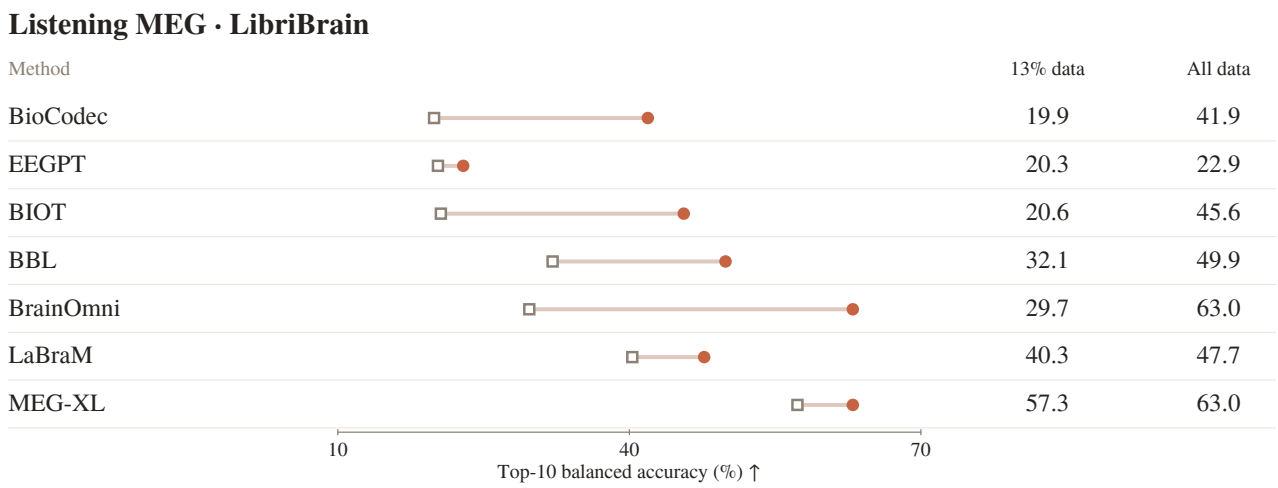


Figure 10. **Listening-MEG word retrieval under two training-data budgets.** Pairs connect the 13% and full-data conditions in MEG-XL's 50-word LibriBrain benchmark (Jayalath & Parker Jones, 2026); squares and circles denote these conditions, respectively. Method references are BioCodec (Avramidis et al., 2025), EEGPT (Wang et al., 2024b), BIOT (Yang et al., 2023a), BBL (Jayalath et al., 2025b), BrainOmni (Xiao et al., 2025), LaBraM (Jiang et al., 2024) and MEG-XL (Jayalath & Parker Jones, 2026). Word onsets are supplied; pretraining resources and context lengths differ. Top-10 chance is 20%. Exact values are printed beside each pair; three-seed SEMs appear in Table 18.

Negative evidence. A leakage-audited benchmark of cross-subject auditory-evoked EEG vowel perception in 16 participants found a best balanced accuracy of 21.5% against 20% chance, with no implementation significant

after correction (Li & Tao, 2026). For MEG-to-audio retrieval, a source-attribution audit showed that signal-blind noise reaches Rank@1 66.3% under variable-length decoding and collapses to chance once fixed-duration windows and stimulus-identity splits are enforced, after which a smaller but real stimulus-locked signal remains (Zhang et al., 2026c).

Visual language separates tracking a representation from identifying content. Cortical tracking of inferred acoustic features during unfamiliar silent lip-reading supports a link between visual input and acoustic representations (Bourguignon et al., 2020). Word-identity decoding in MEG (Keitel et al., 2020) and syllable or consonant decoding in auditory cortex, using fMRI in 64 participants and iEEG in 14 (Karthik et al., 2024), additionally test discrimination among linguistic alternatives. Their convergence motivates asking which representation carries the content; different target sets and recording conditions preclude a common accuracy comparison. These lip-reading tests also remain distinct from decoding written language.

5.5 Text decoding

Text decoding composes neural evidence into linguistic sequences. One family predicts phonemes or characters and uses a language model to assemble them into words; another learns an encoder–decoder mapping from recordings to a text sequence. Early chronic phoneme discrimination and a 50-word clinical ECoG system established useful building blocks and a sentence-level application, respectively (Brumberg et al., 2011; Moses et al., 2021). Larger-vocabulary systems combine these building blocks with richer sequence models. The distinction between an explicit linguistic intermediate and an end-to-end text objective helps explain their supervision and generalisation behaviour.

Composing text from neural units. ECoG phone representations combined with an automatic speech recognition (ASR) back-end and language model enabled continuous phrase-to-text decoding in seven participants (Herff et al., 2015). Encoder–decoder learning subsequently treated neural-to-text mapping as a sequence-translation problem, reaching a best WER of 3% in a four-participant study with repeated sentences (Makin et al., 2020). Self-supervised pretraining on separate unlabelled overt ECoG recordings further improved decoding in a repeated 30–50-sentence setting (Yuan & Makin, 2024). These developments improve representation and sequence learning under a controlled inventory; held-out repetitions, unseen sentences and new participants remain distinct generalisation tests.

Language changes the useful intermediate. A representation that separates articulatory units must also preserve distinctions that change lexical identity in the target language. Mandarin illustrates the resulting choice of targets: sEEG in two speakers classified seven places of articulation at 86.5% from superior temporal gyrus and four lexical tones at 58.3% from thalamus (Wu et al., 2024a). These local classifications identify potentially useful features, whereas a five-participant iEEG study tested sentence recovery, decoding ten Mandarin sentences composed of 40 characters at 21% WER with 93% tone classification (Zhang et al., 2024a). Acoustic-inspired sentence decoders further connect speech features with logosyllabic text (Feng et al., 2025; Liu et al., 2023). The design implication is to test both the relevant linguistic distinction and composed text: tone accuracy cannot substitute for word accuracy, and a closed sentence inventory does not establish new-sentence composition.

Clinical text systems connect sequence decoding to communication without normal audible production. Phoneme-based models have expanded from constrained lexicons to large vocabularies, while rapid calibration makes participant-specific fitting more practical (Table 10). Multi-user intracortical models address a complementary objective: reusing a decoder across people by learning user-specific projections and calibrating it for held-out users (Fogg et al., 2026). This shift from fitting each model in isolation to sharing linguistic structure is a concrete route towards reducing initial training requirements.

What shared attempted-speech benchmarks reveal. Brain-to-Text '24 comparisons on a common private test set separate algorithmic gains from differences in participant recordings (Figure 11). The retrospective attributes the strongest gains to complementary decoder predictions and language-model rescoring, alongside improved training and phonemic objectives (Willett et al., 2024). A later time-masked Transformer ensemble reports 5.68%

Table 9. Inner research develops content discrimination, cross-condition output generation and reusable protocols. Rows are grouped by contribution; task instructions, participant counts and chance levels define the tested condition. Study N can exceed condition N. Quantities are author-reported under heterogeneous protocols and are not a common ranking.

Study	Signal	N	Task and output	Reported result and its boundary
Content discrimination				
(Martin et al., 2016)	ECoG	5	six words, pairwise classification	Inner mean 58% (best 88%) vs. Overt 86% and Perceived–Auditory 89%; chance 50%
(Nguyen et al., 2018)	EEG (64 ch)	15	Inner vowels and words; Riemannian features	up to 70% for three-word and 95% for two-word classification; task-specific maxima, not group means
(Dash et al., 2020)	MEG (306 ch)	8	five phrases; cue → prepare → speak; CNN	93% in the source-labelled imagery/preparation window and 96% in Overt; preparation limits an Inner interpretation; chance 20%
(Proix et al., 2022)	ECoG (3 datasets)	13	Inner word-feature discrimination; decoding subset N=8	median binary accuracy 60% across 12 significant participant–representation pairs using cross-frequency features; chance 50%
(Cooney et al., 2022)	EEG + fNIRS	19	four-class Overt and Inner; bimodal CNN	group mean Overt 46.3%, Inner 34.3% (chance 25%); best individual 87.2% / 53%
(Hons et al., 2026)	EEG + fNIRS	22	Inner and Perceived /a, i, b, k/; SVM	Inner 77.3%, perceived 76.1% (chance 25%); fusion not better than EEG alone
Cross-condition generation and auxiliary detection				
(Angrick et al., 2021)	sEEG (119 contacts)	1	overt-trained (100 words) synthesis transferred online to whispered and Inner	real-time audio produced but explicitly not yet intelligible; $r = 0.62 \pm 0.15$ is overt cross-validation
(Lee et al., 2023)	EEG (64 ch)	6	NeuroTalk: 12 words/phrases; GAN + vocoder; one unseen word	Inner CER 68.3%, MOS 2.78; unseen-word CER 83.1%
(Zhang et al., 2024b)	HD-fNIRS	4	MindSpeech: word-cloud-cued sentences; text-prefix-conditioned continuation	BLEU-1 26.5 / 30.8 / 19.1 / 23.0 versus shuffled-brain 22.4 / 25.3 / 18.9 / 20.6 (P1–P4; 0–100); significant in 3 of 4
(Rastogi et al., 2025)	EEG (64 ch)	56	30 Spanish sentences, listen then imagine; masked autoencoder + BERT	48.9% is training masked-token accuracy; validation 27.3%; not test-set sentence accuracy
(Xiong et al., 2025)	EEG (45 of 64 ch)	13	four Mandarin disyllables; overt bridging; DTW alignment	4-alternative listener accuracy 91.2%, MOS 3.50; closed-set, not open-vocabulary intelligibility
(Ko et al., 2025)	EEG	19/6	Inner versus idle detection; word/sentence datasets	mean offline accuracy 79.9% / 81.3%, macro-F1 0.754 / 0.770; additional pseudo-online tests, not word decoding
Paired resources, protocol comparison and replication				
(He et al., 2025b)	sEEG	1	VocalMind: Mandarin words/sentences; Overt, Mouthed, Inner	Inner mel correlation 0.358 / 0.608 (words/sentences), rising to 0.785 / 0.793 after DTW; six-fold CV with overt acoustic references
(Ma et al., 2026b)	EEG	20	3M-CPSEED: pinyin in Overt, Mouthed, Inner	80 raw EEG recordings; cross-mode comparison
(Aguilera-Rodríguez et al., 2025)	EEG	15	paradigm-design comparison dataset	attention, fatigue and engagement effects
(Tates et al., 2026)	EEG	9–16	replication across four Inner datasets (9, 15, 10 and 16 participants)	36.1% of participants reach significance at 99% confidence, averaged across datasets; replicated scores 2–39 percentage points below original reports

WER, and BIT lowers the cascaded ensemble result to 5.10% after cross-task and cross-species encoder pretraining (Feghhi et al., 2025; Zhang et al., 2026d). BIT's end-to-end ensemble reaches 10.22%, compared with 24.69% for the earlier end-to-end system in its comparison. A stronger pretrained encoder therefore helps both frameworks, but the cascaded language-decoding stage remains advantageous on this benchmark. LightBeam

Table 10. Clinical speech interfaces expand from compositional text to audible, expressive and sustained communication. Rows are grouped by contribution, retaining the source term attempted where residual articulation is unconfirmed. N is study- or condition-specific. T15 recurs across Card and Wairagkar reports, and BRAVO3 across Metzger and Littlejohn; rows cannot be summed as independent cohorts. Vocabulary, WER and word accuracy refer to the stated tasks.

Study	Signal	N	Task and output	Reported result and its boundary
Compositional text and language access				
(Moses et al., 2021)	ECoG	1	attempted words → text; 50-word vocabulary	15.2 words/min, WER 25.6%; anarthria after brainstem stroke
(Metzger et al., 2022)	ECoG	1	attempted phonetic code-words → spelling	29.4 characters/min, median CER 6.13% with a 1,152-word vocabulary; online spelling
(Willett et al., 2023)	intracortical (4 arrays)	1	phonemes → LM → text	125,000-word WER 23.8% at 62 words/min; 50-word WER 9.1%; source-reported unvoiced attempts 24.7% at 125,000 words
(Silva et al., 2024b)	ECoG	1	bilingual attempted speech → text; 178-word vocabulary	median online WER 25.0% overall (Spanish 26.7%, English 22.2%); language classification 87.5%
(Card et al., 2024)	intracortical	1	rapidly calibrating large-vocabulary text	97.5% word accuracy (WER 2.5%) after further training; sustained about 8 months
(Jude et al., 2026)	intracortical	1	long-standing anarthria, locked-in, ventilated	online WER 22% (50 words, second session); best unconstrained-vocabulary block 48%; offline WER 39% on day 68
Audible output and expressive control				
(Guenther et al., 2009)	neurotrophic electrode	1	online formant control; vowel synthesis	first direct audio feedback; output space limited to vowels
(Angrick et al., 2024)	ECoG	1	online synthesis of six self-chosen keywords	listeners identified 80% of synthesised keywords; participant retained some voicing
(Littlejohn et al., 2025)	high-density ECoG	1	streaming brain-to-voice (RNN transducer, RNN-T)	80 ms decoding increments; increment size is not end-to-end latency
(Wairagkar et al., 2025)	intracortical	1	instantaneous voice synthesis with prosody	median listener-transcription WER 43.75%; six-choice sentence matching 94.34%; real-time emphasis and melody
(Wairagkar et al., 2026)	intracortical	1	Brain2voice 2.0 multitask synthesis	mean listener WER 5.24% (continuous) / 5.65% (tokenized); offline causal benchmark; 10 ms output step; preprint
(Srinivasan et al., 2026)	intracortical	2	mouthed / whispered / normal / loud modes	mode and loudness classification 94% and 89%; not word accuracy
Multimodal expression and sustained use				
(Metzger et al., 2023)	253-ch ECoG	1	text, personalised voice, avatar	78 words/min; 1,024-word WER 25%; audio and avatar evaluated separately
(Brosler et al., 2026)	253-ch ECoG	2	parallel phrase text and preset avatar gestures	Bravo-6: vocalised attempts and imagined gestures, with 70% phrase and 66% gesture accuracy in real-time copy trials; 10 phrases and 10 gestures plus rest; 3 participants in movement mapping
(Card et al., 2026)	intracortical	1	independent home use, speech and cursor	>3,800 h including idle; 1.96 M words; 56 words/min; 99.2% word accuracy on cued copy; 92% conversational ratings at least mostly correct, including user-corrected sentences

subsequently compares the language-decoding stage with the neural encoder held fixed, improving WER across its paired GRU and Transformer settings while changing the language resources (Feghhi et al., 2026). Together, these comparisons locate progress at the interface between neural evidence and sequence inference, rather than attributing every gain to a larger neural encoder.

Perceived–Auditory MEG provides a complementary test of whether these interfaces can work with non-invasive recordings. Phoneme-level sentence reconstruction from ten hours per participant reported phoneme error of 62.2% and sentence CER of 65.8% (Vélez et al., 2026); a joint text-and-acoustic model proposes coupling

a Brain-to-Text '24

Method	WER (%) ↓
RNN baseline	9.76
Linderman	8.00
LISA	8.90
TeamCyber	8.26
DCoND-LIFT	5.77
Time-masked Transformer	5.68
BIT (cascade ensemble)	5.10

b Transformer decoder

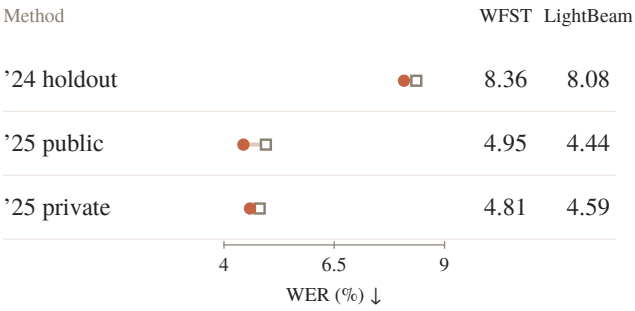


Figure 11. **Attempted-speech comparisons separate complete systems from paired language decoders.** (a) Brain-to-Text '24 private-test WER: the RNN baseline follows BIT's comparison (Zhang et al., 2026d); Linderman, LISA and TeamCyber follow Willett et al. (2024); DCoND-LIFT (Li et al., 2025b), the time-masked Transformer (Feghhi et al., 2025) and BIT (Zhang et al., 2026d) use their strongest reported cascaded ensembles. These systems share 1,200 test sentences but differ in training and language resources. (b) LightBeam (Feghhi et al., 2026) holds a Transformer encoder fixed within each pair: squares use a weighted finite-state transducer (WFST) to combine lexical and language-model constraints; circles use LightBeam. Language resources change from 5-gram/OPT to 4-gram/Llama, with benchmark-text adaptation; public and private partitions remain separate. Values are means across ten encoder seeds.

two output targets (Jin et al., 2026). These approaches make the intermediate linguistic or acoustic constraint explicit. Generative sequence models additionally learn how to complete linguistic content, making held-out text and matched input controls central to the comparison.

Generative MEG-to-text. Generative MEG models connect a neural encoder to a language or speech generator through three main interfaces: continuous neural features, discrete neural tokens, or predicted linguistic representations. The last route can operate on individual words or whole sentences. These choices determine how much timing information the decoder needs and whether its output is primarily constrained by lexical evidence or sentence meaning (Figure 12).

Direct sequence models adapt an existing generator to neural input. NeuSpeech uses a Whisper-style decoder and reports BLEU-1 of 60.30 on Gwilliams without test-time teacher forcing (Yang et al., 2024b). This sentence–recording-pair split permits familiar stimulus sentences across partitions; holding out an entire story asks the model to recover new linguistic content. Under story holdout, MAD aligns neural and speech features and reports BLEU-1 of 6.86 and CER of 89.82% (Yang et al., 2024c). NeuGPT instead compresses the recording into discrete neural tokens and incorporates these tokens into a Qwen2 language model. Its MEG-MASC comparison reports BLEU-1 of 12.92 and ROUGE-1F of 13.06, compared with 5.49 and 8.43 for NeuSpeech in the same table (Yang et al., 2024a). NeuGPT's CER is 99.8%, showing that the gain in overlapping words does not translate into correspondingly accurate character sequences. The choice of neural interface and the held-out linguistic content therefore matter alongside the generator's capacity.

A word-level interface makes the lexical constraints on generation explicit. The Oxford system predicts contextual word embeddings from onset-aligned MEG, converts their vocabulary similarities into word probabilities, and rescores candidate sequences with a language model (Jayalath et al., 2025a). Its comparison extends the NeuGPT benchmark on the same held-out-story split, placing NeuSpeech, MAD, NeuGPT and word-based generation together (Figure 12a). The rounded BLEU-1 scores rise from 5 and 7 for NeuSpeech and MAD to 13 for NeuGPT and 18 for Oxford beam-and-fill decoding; CER falls from NeuGPT's 100% to 71%. Earlier baseline scores are quoted, whereas Oxford evaluates its own models with supplied word onsets and out-of-vocabulary

positions. Pooling additional LibriBrain and Armeni training data retains BLEU-1 of 18 but changes CER to 72%, so more training data does not improve every measure. On LibriBrain, a separate comparison replaces supplied out-of-vocabulary positions with a learned detector: BLEU-1 rises from 19 for greedy decoding to 22 after beam rescoring and 24 after in-filling, while CER falls from 77% to 76% and 69%. Together, these results show how composing uncertain lexical predictions can improve text reconstruction, while making the timing and vocabulary information supporting that improvement explicit.

A sentence-level interface changes the target from individual words to their combined meaning. Brain2 Semantics2Text maps MEG through a temporal encoder and attention pooling into a sentence-embedding space, then inverts the predicted vector into text (Landau et al., 2026). This later Oxford study compares three methods on the same 172 held-out LibriBrain sentences from one participant (Figure 12b). Brain2Semantics2Text and BrainECHO retain sentence boundaries but remove word-level alignment, reaching BERTScores of 0.830 and 0.828, respectively; their matched noise controls score 0.819 and 0.825. A word-aligned implementation of d'Ascoli's method reaches 0.820, versus 0.794 with noise. WER orders the methods differently: 192.5%, 101.8% and 87.1%, respectively. The semantic route's longer reconstructions contribute to its higher WER. These descriptive scores suggest a trade-off between sentence-level similarity and control of exact wording and length; the word-aligned route benefits from a more explicit lexical constraint. Both semantic quality and the improvement over matched input controls are needed to understand this trade-off.

a MEG-MASC · held-out story

Method	CER (%) ↓	BLEU-1 ↑	ROUGE-1 F ↑	BERTScore ↑
NeuSpeech	77	5	8	84
MAD	90	7	7	83
NeuGPT	100	13	13	84
Oxford pooled + fill	72	18	19	78

b LibriBrain · held-out sessions

Method	WER (%) ↓	BLEU-1 ↑	ROUGE-1 ↑	BERTScore ↑
Brain2Semantics2Text	192.5	10.0	13.2	83.0
BrainECHO	101.8	6.1	9.1	82.8
d'Ascoli · word-aligned	87.1	19.0	17.2	82.0

Figure 12. **MEG-to-text methods share benchmark lineages but use different linguistic interfaces.** (a) NeuSpeech (Yang et al., 2024b), MAD (Yang et al., 2024c), NeuGPT (Yang et al., 2024a) and Oxford (Jayalath et al., 2025a) follow Oxford's held-out-story comparison. Earlier scores are quoted by that paper; Oxford's pooled beam-and-fill configuration adds LibriBrain/Armeni training data and uses supplied word onsets and out-of-vocabulary positions. (b) Brain2Semantics2Text (Landau et al., 2026), BrainECHO (Li et al., 2025c) and d'Ascoli's word-aligned method (d' Ascoli et al., 2025) follow the later LibriBrain comparison (Landau et al., 2026). All receive sentence boundaries; the last also receives word timing. Metrics are displayed on a 0–100 scale, with WER allowed above 100. Each row uses one configuration. Matched noise results and SDs are in Table 19.

Acoustic intermediates across listening benchmarks. BrainECHO inserts a vector-quantised spectrogram reconstruction between the neural encoder and Whisper, comparing this route with EEG-to-Text, NeuSpeech and MAD under shared evaluations (Li et al., 2025c). On Brennan EEG with held-out participants, the four implementations yield BLEU-1 scores of 8.82, 85.31, 80.34 and 89.78; the corresponding WERs are 233.99%, 16.97%, 42.14% and 11.72% (Figure 13). On shuffled Gwilliams MEG recording pairs, BrainECHO reaches BLEU-1 of 73.35 and WER of 31.44%, compared with 50.49 and 71.17% for the authors' NeuSpeech implemen-

tation. The acoustic intermediate thus improves both lexical overlap and edit accuracy in these comparisons. The story-held-out Oxford benchmark asks a different generalisation question: participant or recording-pair holdout can retain familiar stimulus text, whereas story holdout removes that source of linguistic familiarity. Its lower absolute scores cannot isolate the effect of this split because the models, implementations and supplied timing information also differ.

a Brennan EEG · held-out participants

Method	BLEU-1 ↑	BLEU-4 ↑	ROUGE-1 F ↑	WER (%) ↓
EEG-to-Text	8.82	1.44	13.12	233.99
NeuSpeech	85.31	83.75	82.64	16.97
MAD	80.34	78.15	83.79	42.14
BrainECHO	89.78	88.55	87.13	11.72

b Gwilliams MEG · recording-pair split

Method	BLEU-1 ↑	BLEU-4 ↑	ROUGE-1 F ↑	WER (%) ↓
EEG-to-Text	9.21	0.14	11.38	118.25
NeuSpeech	50.49	42.55	47.10	71.17
MAD	3.93	0.00	7.26	105.33
BrainECHO	73.35	72.42	69.73	31.44

Figure 13. **Listening benchmarks compare lexical overlap and edit errors within each recording split.** BrainECHO's published comparison (Li et al., 2025c) evaluates EEG-to-Text (Wang & Ji, 2022), NeuSpeech (Yang et al., 2024b), MAD (Yang et al., 2024c) and BrainECHO (Li et al., 2025c). (a) Brennan EEG uses participant holdout; (b) Gwilliams MEG uses shuffled recording-pair splits. Values are the comparison authors' implementations, including their NeuSpeech rerun. Familiar stimulus texts can occur across participants or recordings, unlike the story holdout in Figure 12a. Each row reports a single configuration, on the source's 0–100 scale.

5.5.1 Perceived–Visual: Reading EEG-to-text

Reading-based decoding targets text that the participant sees, rather than speech that they hear or intend to produce. Visual stimulation, eye movements and language processing can all contribute to the recordings. Much EEG-to-text research relies on ZuCo, which combines EEG and eye tracking during English reading: 12 participants and 1,107 sentences in ZuCo 1.0 (Hollenstein et al., 2018), and 18 participants and 739 sentences in ZuCo 2.0 (Hollenstein et al., 2020). Fixation-based segmentation supplies word-aligned features in some pipelines; other methods process continuous segments without fixation markers. Reuse of these corpora across algorithm papers does not provide new participant cohorts.

Where the methods differ. Methods address three recurring mismatches between EEG and a pretrained text generator (Table 11). First, neural recordings and linguistic tokens have different structure: contrastive learning, discrete encoders, masked autoencoding, cross-modal codebooks and byte-pair alignment seek a more usable interface (Feng et al., 2023; Duan et al., 2023; Wang et al., 2024c; Tao et al., 2025; Zhou et al., 2024a). Second, recordings vary across people and datasets; participant-dependent representations and EEG pretraining address this learning problem, while shared fMRI/EEG architectures and Chinese reading data broaden the settings examined (Amrani et al., 2026; Liu et al., 2024; Xi et al., 2023; Lu et al., 2025a). Third, the language generator completes information missing from the neural representation. BART-based decoding and GPT-4 refinement illustrate that dependence on a text prior (Wang & Ji, 2022; Amrani et al., 2026). Each intervention changes a different part of the information chain: improved text overlap alone cannot show which mismatch has been

resolved.

Shared benchmarks and successive improvements. Repeated use of ZuCo makes several method families directly traceable through published comparisons (Figure 14a). In the 10,710-training-sample comparison reported by CET-MAE, BLEU-4 rises from 6.80 for EEG-to-Text to 8.22 for DeWave and 8.99 for E2T-PTR (Wang et al., 2024c). Broader representation learning and decoder adaptation extend this lineage: the reported multi-view EEG2Text result is 14.10, and BELT-2 with a T5 decoder reports 17.95 (Liu et al., 2024; Zhou et al., 2024a). The earlier teacher-forced results are shown separately in Figure 14a; SEE and BELT-2 retain their original reporting conditions in Table 11. Their differing training pools, test-prefix policies and output processing determine the strength of cross-paper comparisons. For example, C-SCL removes consecutive repeated generated words before scoring, whereas the original EEG-to-Text pipeline retains them (Feng et al., 2023; Wang et al., 2024c).

Autonomous generation and neural contribution. Supplying correct previous tokens during testing changes autonomous generation into prediction conditional on a correct prefix. A ZuCo evaluation compared BART-, Pegasus- and T5-based pipelines with real and noise inputs, both with and without test-time teacher forcing (Jo et al., 2026). Comparable EEG/noise performance in the tested configurations shows why text overlap alone cannot establish a neural contribution. Separately, sentence overlap in inspected cross-participant splits leaves linguistic familiarity available even when the participant changes (Yin et al., 2025). These are distinct shortcuts: removing correct prefixes does not remove repeated content, and holding out participants does not necessarily hold out text.

From token overlap to semantic recovery. GLIM combines language modeling with contrastive alignment and multiple textual variants to learn representations that support autoregressive generation (Liu et al., 2025a). SemKey adds explicit semantic attributes and evaluates this progression against EEG-to-Text under a unique-text split (Wang et al., 2026d). In that common comparison, original-reference BLEU-1 is 11.90, 7.84 and 8.98 for EEG-to-Text, GLIM and SemKey, respectively; generated-text 24-way identification is 4.17%, 10.74% and 16.24% (Figure 14b). The strongest n-gram baseline is therefore at chance on the semantic identification task. Higher overlap with a reference and better discrimination of its meaning are distinct forms of progress, and both are needed to interpret these methods.

A complementary line explicitly recovers semantic anchors before reconstructing a sentence. Guiding LLMs aligns EEG and language representations; Brain-CLIPLM then uses ordered keyword anchors, language-model reasoning and a task-specific sentence corpus (Zheng et al., 2026; Yang et al., 2026a). Brain-CLIPLM's published comparison reports BLEU-1 of 17.0, 21.3 and 22.4 for EEG-to-Text, Guiding LLMs and Brain-CLIPLM, alongside ROUGE-1 F of 17.8, 20.3 and 22.9 (Figure 14c). The progression motivates intermediate semantic targets, while the corpus-assisted reconstruction condition remains central to interpreting what the neural signal supplies.

COFETT additionally re-evaluates reading decoders without correct test prefixes. On its ZuCo 1+2 comparison, BrainBART, BELT and DeWave produce BLEU-1 values of 13.75, 15.55 and 14.36, with WER above 108% in all three cases; EEGNet, EEGConformer and EEGPT adaptations extend the same comparison to distinct neural encoders (Figure 14d) (Zhang et al., 2026e). Discrete diffusion offers another output model: DELTA raises BLEU-1 from 13.69 for its autoregressive BART baseline to 21.93 under the same residual-vector-quantisation interface, while WER remains 110.03% (Jeon & Kim, 2025). Improvements in local overlap have thus outpaced reliable sentence reconstruction in these autonomous tests.

A related but different task is COFETT's cued recall after reading: its central comparison measures Pearson correlation between EEG-derived and text embeddings across sessions with repeated sentences and noise controls (Zhang et al., 2026e). This tests cross-session representation alignment on repeated content; it does not establish autonomous generation of novel sentences. The distinction connects reading benchmarks to internal recall without treating them as the same behavioural task.

a ZuCo · teacher-forced reports

Method	BLEU-1 ↑	BLEU-2 ↑	BLEU-4 ↑
EEG-to-Text	40.10	23.10	6.80
DeWave	41.35	24.15	8.22
C-SCL †	35.91	25.91	18.89
Participant-dependent BART	42.75	25.90	9.56
CET-MAE	42.09	25.13	8.99
EEG2Text	45.20	29.10	14.10

b Unique-text holdout · autoregressive generation

Method	BLEU-1 ↑	BLEU-2 ↑	24-way acc. ↑
EEG-to-Text (no TF)	11.90	1.58	4.17
GLIM	7.84	1.28	10.74
SemKey	8.98	1.42	16.24

c Semantic-anchor comparison

Method	BLEU-1 ↑	ROUGE-1 F ↑	BERTScore ↑
EEG-to-Text	17.0	17.8	83.3
Guiding LLMs	21.3	20.3	84.8
Brain-CLIPLM	22.4	22.9	86.2

d ZuCo 1+2 · shared autoregressive reevaluation

Method	BLEU-1 ↑	ROUGE-1 F ↑	WER (%) ↓
BrainBART	13.75	11.84	108.24
BELT	15.55	13.75	110.09
DeWave	14.36	12.83	109.88
EEGNet	7.30	0.08	120.06
EEGConformer	12.54	10.11	105.01
EEGPT	16.34	14.92	109.85

Figure 14. **Reading EEG-to-text comparisons distinguish supplied prefixes from autonomous generation.** (a) Teacher-forced reports: EEG-to-Text (Wang & Ji, 2022), DeWave (Duan et al., 2023), C-SCL (Feng et al., 2023), participant-dependent BART (Amrani et al., 2026), CET-MAE (Wang et al., 2024c) and EEG2Text (Liu et al., 2024). Training pools differ; the dagger marks C-SCL's removal of consecutive repeated output words. (b) EEG-to-Text, GLIM (Liu et al., 2025a) and SemKey (Wang et al., 2026d) use SemKey's unique-text autoregressive benchmark. Identification compares generated text with its target and 23 distractors; chance is 4.17%. (c) Guiding LLMs (Zheng et al., 2026) and Brain-CLIPLM (Yang et al., 2026a) extend EEG-to-Text under the latter paper's semantic-anchor comparison, which quotes earlier values. (d) COFETT's autoregressive reruns (Zhang et al., 2026e) compare BrainBART/EEG-to-Text, BELT (Zhou et al., 2024b), DeWave, EEGNet (Lawhern et al., 2018), EEGConformer (Song et al., 2023) and EEGPT (Wang et al., 2024b). All scores use a 0–100 scale; panels are separate evaluation settings.

Testing the learned representation. A useful comparison holds the generator, segmentation information and inference protocol fixed, then tests whether neural inputs improve decoding of held-out text over matched uninformative inputs. Participant or session holdout tests whether that advantage survives recording changes. Together with controls for visual, ocular and other task-related signals, these comparisons provide stronger evidence that the representation carries transferable linguistic information.

5.5.2 Semantic targets and generated text

Cued text generation. Cue-conditioned generation combines a neural representation with content supplied by the experiment. An EEG masked-autoencoder/BERT system reported masked-token accuracy of 48.9% in train-

Table 11. Reading EEG-to-text methods, grouped by the interface between neural representations and language. Results retain the stated input and inference conditions; shared benchmark comparisons appear in Figure 14. BLEU, ROUGE and BERTScore values are on a 0–100 scale. TF denotes test-time teacher forcing (correct previous tokens). Classification, EEG-embedding retrieval and semantic identification of generated text are distinct evaluation tasks.

Study	Input / task	Intermediate / mechanism	Learning / inference conditions	Selected result
Sequence decoders and output-model adaptation				
(Wang & Ji, 2022)	ZuCo EEG / text	Transformer EEG encoder → pretrained BART	Fixation-aligned word features; original evaluation uses TF	BLEU-1 40.1
(Xi et al., 2023)	ZuCo EEG / text	UniCoRN: snapshot and sequence reconstruction → text decoder	Two-stage representation pretraining; architecture also evaluated separately on listening fMRI	BLEU-1 57.68; BLEU-4 37.04
(Amrani et al., 2026)	ZuCo 1+2 EEG / text	Participant-dependent encoder → BART; optional GPT-4 refinement	Learned participant embeddings; sentence-based split; reported scores before GPT-4 refinement	BLEU-1 42.75; BERTScore-F 53.86
(Lu et al., 2025a)	ChineseEEG / text	Character-level EEG encoder with MiniLM	Autoregressive character decoding; known sentence start and fixed-length input	BLEU-1 6.38
Contrastive and masked representation learning				
(Feng et al., 2023)	ZuCo EEG / text	C-SCL: curriculum contrastive alignment	BrainBART-Large variant; semantic curriculum across participants	BLEU-1 35.91; WER 68.48%
(Liu et al., 2024)	ZuCo EEG / text	EEG2Text: regional and global transformers → BART	EEG pretraining on ZuCo and Image-EEG; v1 multi-view result	BLEU-1 45.2; BLEU-4 14.1
(Wang et al., 2024c)	ZuCo EEG / text	CET-MAE: contrastive EEG–text masked autoencoder → BART	Paired-modality reconstruction and alignment; 10,710 training samples; TF	BLEU-1 42.09; BLEU-4 8.99
(Zhou et al., 2024c)	ZuCo EEG / word classification; retrieval	ETER: masked contrastive encoder; keyword-based sentence retrieval	Word encoder predicts a 100-word vocabulary; training-free sentence search	Top-20 word accuracy 55.15%
Discrete, token-level and semantic alignment				
(Duan et al., 2023)	ZuCo EEG / text	DeWave: vector-quantised EEG codebook → BART	Reconstruction pretraining; fixation-aligned features or raw waves; both evaluated with TF	BLEU-1 41.35 / 20.51, respectively
(Tao et al., 2025)	ZuCo EEG / text	SEE: cross-modal codebook and semantic matching	Text-encoder similarities provide soft targets; joint semantic-matching and generation losses	BLEU-4 7.7; ROUGE-1-F 31.1
(Zhou et al., 2024a)	ZuCo EEG / text	BELT-2: byte-pair alignment and Q-Conformer → LLM	Multi-task representation learning; T5 decoder with learned prefix tuning (Table 1)	BLEU-1 52.38; BLEU-4 17.95
Autoregressive semantic guidance and anchor-based reconstruction				
(Liu et al., 2025a)	ZuCo EEG / text	GLIM: contrastive alignment, language modeling and multiple text variants	Autoregressive; original-reference scoring and generated-text identification (Wang et al., 2026d)	BLEU-1 7.84; 24-way accuracy 10.74%
(Wang et al., 2026d)	ZuCo EEG / text	SemKey: semantic-attribute heads and EEG key–value embeddings	Autoregressive; unique-text split; generated-text semantic identification (v3)	BLEU-1 8.98; 24-way accuracy 16.24%
(Zheng et al., 2026)	ZuCo EEG / text	Guiding LLMs: EEG–language semantic alignment	Published benchmark values quoted by Brain-CLIPLM (Yang et al., 2026a)	BLEU-1 21.3; ROUGE-1 F 20.3
(Yang et al., 2026a)	ZuCo EEG / sentence reconstruction	Brain-CLIPLM: ordered keyword anchors → LLM reasoning and retrieval	Semantic-anchor recovery; reconstruction supported by a task-specific sentence corpus	BLEU-1 22.4; ROUGE-1 F 22.9

ing and 27.3% in validation (Rastogi et al., 2025), illustrating the gap between learning a token representation and predicting held-out content. MindSpeech uses HD-fNIRS from word-cloud-cued internal sentence production to prompt-tune Llama-2 for text-prefix-conditioned continuation, reporting BLEU-1 and BERT-precision improvements in three of four participants (Zhang et al., 2024b). Cue words and the language prior already constrain plausible sentences. Prompt-only and matched shuffled-signal comparisons are therefore needed to measure the

additional content supplied by the neural recording.

Semantic reconstruction. fMRI-based language decoding with a language-model prior reconstructed the gist of continuous heard stories in three participants and transferred to internally narrated stories and silent videos (Tang et al., 2023); the target is semantic content rather than verbatim wording. In the imagined-speech experiment, the decoder generated text for five one-minute stories; evaluation compared these sequences with separately recorded retellings using semantic similarity and five-story identification. This demonstrates generative transfer under that protocol, while leaving unrestricted self-generated communication unestablished. Autoregressive generation reconstructed ten minutes of language stimulus (Ye et al., 2025), and language-free movies have been used for cross-participant alignment (Tang & Huth, 2025). These extensions test whether a shared semantic representation can support transfer when the source and target stimuli differ.

Semantic reconstruction describes the target relationship between input and output, rather than a medium alongside text and audio. An embedding-retrieval model and a text generator can both recover semantic information but produce different outputs. Prompt-conditioned HD-fNIRS generation similarly requires separating neural evidence from cue and language-model constraints (Zhang et al., 2024b).

Semantic models also differ in how brain-derived information conditions language generation. PredFT introduces a predictive representation from selected brain regions alongside a primary fMRI language-decoding network (Yin et al., 2026). Multimodal alignment models instead route among text-, image- and audio-related semantic features (Ye et al., 2026). These alternatives extend semantic conditioning beyond a single fixed embedding. Their evaluation still depends on the task and dataset; use of a shared architecture across modalities is not itself transfer of a fitted decoder between them.

Comparing fMRI language decoders. The Narratives benchmark connects these representational choices to reconstruction over longer context windows. CogReader compares UniCoRN, an fMRI-adapted EEG-to-Text model, BP-GPT, PredFT and its own incremental-and-wrap-up architecture on story-disjoint data (Lu et al., 2025b). Across 20, 40 and 60 repetition-time (TR) windows, CogReader's BLEU-1 rises from 25.4 to 31.2 and 36.2, whereas PredFT rises from 24.3 to 25.9 and 26.4; UniCoRN decreases from 22.9 to 18.0. The 60-TR comparison appears in Figure 15a. CogReader's BERTScore F1 also increases, from 46.3 to 53.5 on the source's 0–100 scale. These contrasting window-length trends are consistent with differences in context use, although the comparison does not isolate which architectural component causes them. A second comparison on Huth recordings tests Tang's decoder, BrainLLM and multimodal routing without a supplied text prompt: BLEU-1 is 9.67, 13.56 and 14.72, respectively, while WER decreases from 97.00% to 95.41% and 95.03% (Ye et al., 2026). The multimodal route scores higher on these text metrics, although exact word recovery remains much weaker than the fluency of generated sentences might suggest (Figure 15b). Narratives and Huth form separate benchmark lineages; their absolute scores depend on different recordings and decoding windows.

5.6 Speech synthesis

Choosing what the neural decoder predicts. Speech synthesis separates prediction from rendering: the neural model estimates a representation and a synthesiser turns it into sound. Unit selection can reuse the participant's voice, as demonstrated from motor, premotor and inferior frontal ECoG (Herff et al., 2019). Articulatory-kinematic targets instead impose a production-related structure, enabling ECoG sentence synthesis and transfer to mouthed production in a five-participant study (Anumanchipalli et al., 2019); its listener tests used a limited candidate word pool. Interpretable speech parameters paired with a differentiable synthesiser were studied in a 48-participant ECoG cohort (Chen et al., 2024b), although each condition need not contain all 48 participants. Direct reconstruction from sensorimotor ECoG during overt speech provides another production-based route, evaluated with complementary acoustic and perceptual measures (Berezutskaya et al., 2023). These alternatives change the supervision needed and the aspects of voice accessible to the decoder.

What successful rendering establishes. Heard-speech reconstruction has a measured acoustic reference: auditory-cortex ECoG recovered spectrotemporal structure of words and sentences with average correlation

a Narratives · 60-TR windows

Method	BLEU-1 ↑	BLEU-4 ↑	ROUGE-1 F ↑	BERTScore F ↑
UniCoRN	18.0	0.4	16.5	43.2
EEG-Text	22.1	1.6	28.1	47.7
BP-GPT	19.3	0.6	19.4	41.6
PREDFT	26.4	0.6	28.1	48.1
CogReader	36.2	12.1	36.2	53.5

b Huth · no text prompt

Method	BLEU-1 ↑	ROUGE-1 ↑	ROUGE-L ↑	WER (%) ↓
Tang decoder	9.67	8.18	7.88	97.00
BrainLLM	13.56	11.60	10.99	95.41
Multimodal routing	14.72	11.79	11.31	95.03

Figure 15. **fMRI language decoding has complementary Narratives and Huth benchmarks.** (a) CogReader's 60-TR comparison (Lu et al., 2025b) includes UniCoRN (Xi et al., 2023), an fMRI-adapted EEG-Text encoder (Wang & Ji, 2022), BP-GPT (Chen et al., 2025c), PREDFT (Yin et al., 2026) and CogReader (Lu et al., 2025b); train, validation and test stories differ. (b) Multimodal routing (Ye et al., 2026) is compared with Tang's decoder (Tang et al., 2023) and BrainLLM (Ye et al., 2025) without a supplied text prompt. The two datasets and decoding protocols remain separate. All metrics use a 0–100 scale; 20/40-TR and text-prompt conditions appear in Tables 20 and 21.

$r = 0.28$ in 15 participants (Pasley et al., 2012). Predicting vocoder parameters from iEEG supported 75% digit recognition in a five-participant, ten-alternative listening test (Akbari et al., 2019). The latter adds perceptual evidence to acoustic similarity, but still leaves open whether listeners can recover sentences without supplied alternatives. Evaluation must follow the information the output is intended to convey.

Interactive control is a further test, even within a small output space. A single-participant sEEG system controlled two synthesised vowels after Overt training, with 85% first-round success (Tankus et al., 2025). This tests whether a user can act through audible feedback; it does not resolve the larger representational problem of composing intelligible sentences. Output diversity and closed-loop controllability should therefore be varied and measured separately.

Inner synthesis and perceptual tests. The voice route of Figure 9 is also applied to Inner conditions. Real-time synthesis transferred from overt training to whispered and Inner speech in one sEEG participant, but the authors state the audio is not yet intelligible, and the $r = 0.62$ often quoted is overt cross-validation (Angrick et al., 2021). NeuroTalk reported inner-speech character error rate (CER) of 68.3% with a mean opinion score (MOS) of 2.78 on twelve words and CER 83.1% on the single held-out word (Lee et al., 2023). An EEG synthesis study (Xiong et al., 2025) reports 91.2% listener accuracy for "intelligible utterances" from EEG, but the test is a four-alternative choice among known Mandarin disyllables with overt bridging and dynamic-time-warping (DTW) reference alignment, and the train/test independence is not fully documented.

The synthesis route predicts acoustic features or articulatory parameters and renders audio. Overt training offers paired signals, whereas Mouthed and Inner transfer must cope with missing or altered acoustic supervision. Some ten-participant ECoG conditions yielded recognisable online Overt or Mouthed synthesis without intelligible Inner synthesis (Meng et al., 2023). Clinical streaming systems extend the objective to timely audible feedback (Littlejohn et al., 2025; Wairagkar et al., 2025; 2026). Generated audio, perceptual intelligibility and an interactive speaking experience therefore require separate evidence.

Non-invasive overt decoding. Non-invasive overt results are smaller in scale and must be checked for orofacial EMG, head motion, eye movement and acoustic cross-talk. Early EEG-to-acoustics regression with recurrent networks in four participants predicted acoustic features, evaluated by mel-cepstral distortion and cepstral reconstruction error (Krishna et al., 2020). These acoustic errors do not measure whether a listener can recover the words. MEG-to-mel synthesis with a Squeezeformer and BigVGAN vocoder reported a spectral correlation of $r = 0.954 \pm 0.014$ for five repeated phrases in four participants (Kwon et al., 2024); this is a within-participant, closed-phrase correlation, not word accuracy.

Perceived-auditory reconstruction. Listening supplies a measured acoustic target for non-invasive synthesis. FESDE connects EEG and speech latent modules to generate the listened waveform directly, providing an alternative to a separately predicted spectrogram (Lee et al., 2024). Together with the production-based systems above, this illustrates how waveform rendering can be learned through different intermediate representations.

Comparing synthesis routes on shared recordings. Brain2Speech-Net compares text-mediated synthesis, direct speech units and a phoneme-bottleneck generator on a common attempted-speech corpus (Chandra et al., 2026). On 880 unseen utterances, the LLM-rescored text cascade attains ASR WER of 20.6%, compared with 105.4% for direct speech units and 47.2% for Brain2Speech-Net (Figure 16). Their reported real-time factors are 1.962, 0.060 and 0.532, respectively. Text mediation preserves lexical content most accurately in this comparison, while direct units render fastest; Brain2Speech-Net occupies an intermediate position. These are implementations with a shared neural content encoder, evaluated against synthetic reference speech, rather than the original systems' clinical outcomes. ASR WER measures machine recognition of the rendered output, and real-time factor measures rendering cost relative to audio duration; listener intelligibility and interactive onset latency remain separate outcomes. For non-invasive recordings, NeuroSonic compares EEG-conditioned adaptations of mean-flow, GAN and diffusion generators on held-out participants in CineBrain and EAV (Gao et al., 2026). Its EAV result reduces Fréchet audio distance from 15.87 for the diffusion baseline to 11.64 and increases predicted overall audio quality from 2.29 to 2.59; on CineBrain, the corresponding values change from 72.56 to 39.06 and from 1.07 to 1.44. CineBrain includes environmental sound, whereas EAV contains conversation. These comparisons extend acoustic generation beyond clinical speech corpora, but neither audio-distribution similarity nor a predicted quality score measures how accurately a listener can recover linguistic content.

5.7 Facial and body animation

Facial animation adds a visual channel to neural communication. An ECoG neuroprosthesis combines decoded text, personalised speech and an avatar (Metzger et al., 2023). Its real-time avatar is driven by decoded audio, while direct neural prediction of facial motion was evaluated offline. These two designs place visual rendering at different points in the pipeline: one inherits speech timing from the synthesiser, and the other estimates movement from neural features. Visual evaluation includes sentence identification and lip/jaw trajectories, complementing the text and acoustic outcomes.

Parallel speech and gesture decoding extends expressive control beyond the face. Each of two participants used a 253-channel ECoG array for concurrent phrase-to-text and gesture decoding, within a three-participant movement-mapping study (Brosler et al., 2026). In Bravo-6, who attempted speech with vocalisation and imagined the gestures, 200 simultaneous real-time copy trials yielded phrase accuracy of 70% and gesture accuracy of 66%, using ten phrases and ten gestures plus rest. Decoded gestures triggered preset full-body avatar animations. Training on both isolated and simultaneous attempts improved performance across contexts, showing that combining output channels also requires learning their concurrent neural activity. The contribution is coordinated verbal and nonverbal control within this repertoire, with phrase selection and gesture classification measured separately.

a Attempted speech · unseen utterances

Method	ASR WER (%) ↓	PER (%) ↓	MCD (dB) ↓	RTF ↓
NTS-Cascade (+ LLM)	20.6	18.8	4.894	1.962
Direct speech units	105.4	78.5	6.181	0.060
Brain2Speech-Net	47.2	37.3	5.522	0.532

b CineBrain EEG · held-out participants

Method	FAD ↓	LSD ↓	SC ↓	DNSMOS ↑	Time (s) ↓
Mean flow	173.65	69.78	1.34	1.10	0.04
GAN	57.12	15.13	1.25	1.14	0.02
Diffusion	72.56	22.08	1.12	1.07	2.00
NeuroSonic	39.06	14.24	0.64	1.44	0.86

c EAV EEG · held-out participants

Method	FAD ↓	LSD ↓	SC ↓	DNSMOS ↑	Time (s) ↓
Mean flow	85.27	29.25	1.49	1.08	0.04
GAN	39.47	15.71	1.00	1.45	0.02
Diffusion	15.87	19.47	1.25	2.29	2.08
NeuroSonic	11.64	12.98	0.28	2.59	1.40

Figure 16. **Synthesis benchmarks compare lexical fidelity, acoustic quality and computation.** (a) Brain2Speech-Net (Chandra et al., 2026) reimplements an LLM-rescored text cascade (Willett et al., 2024) and direct speech units (Metzger et al., 2023) with a common neural encoder on 880 unseen attempted-speech utterances. ASR WER and phoneme error rate (PER) score generated audio; mel-cepstral distortion (MCD) uses synthetic VITS references. RTF is computation time divided by audio duration. (b,c) NeuroSonic's held-out-participant comparisons (Gao et al., 2026) adapt MeanFlow (Geng et al., 2025), HiFi-GAN (Kong et al., 2020) and Moûsai diffusion (Schneider et al., 2023) to EEG. CineBrain includes environmental sound; EAV contains conversation. FAD is Fréchet audio distance, LSD log-spectral distance and SC spectral convergence. DNSMOS predicts overall audio quality; it is not a listener intelligibility score. Seconds report the source's inference time, not clinical feedback latency. Values are source means; each dataset forms its own comparison.

5.8 Pretraining, transfer and personal calibration

Three roles for pretrained models. Pretraining can supply a neural encoder, an acoustic or linguistic alignment target, or an output generator. These roles address different shortages in paired neural-language data (Mai et al., 2025; Wang et al., 2025d). Contrastive EEG pretraining in BENDR and masked intracranial representation learning in BrainBERT illustrate reusable encoders (Kostas et al., 2021; Wang et al., 2023). Speech-specific work applies self-supervised learning to overt ECoG, heterogeneous MEG data and long-context word retrieval (Yuan & Makin, 2024; Jayalath et al., 2025b; Jayalath & Parker Jones, 2026). Speech and language models provide the other two roles: a structured target to which neural features can align, and a prior for rendering those features as an output.

Shared benchmarks for pretrained neural encoders. Imagined-speech classification supplies a language-related downstream test for general EEG models. REVE's BCIC2020-3 comparison brings together eleven methods, from task-trained EEGNet and Conformer models to BIOT, LaBraM and CBraMod (El Ouahidi et al., 2025). Five-class balanced accuracy increases from 44.13% for EEGNet to 49.20% for BIOT, 50.60% for LaBraM, 53.73% for CBraMod and 56.35% for REVE (Figure 18a). Earlier scores are quoted from prior reports under the trial split, and each complete downstream procedure includes its own model and tuning choices. CodeBrain extends this trial-split comparison to 61.01% balanced accuracy, a Cohen's κ of 0.513 and weighted F1 of 0.610; its BENDR and EEGPT baselines remain near 25% accuracy under the same reported split (Ma et al., 2026a). The

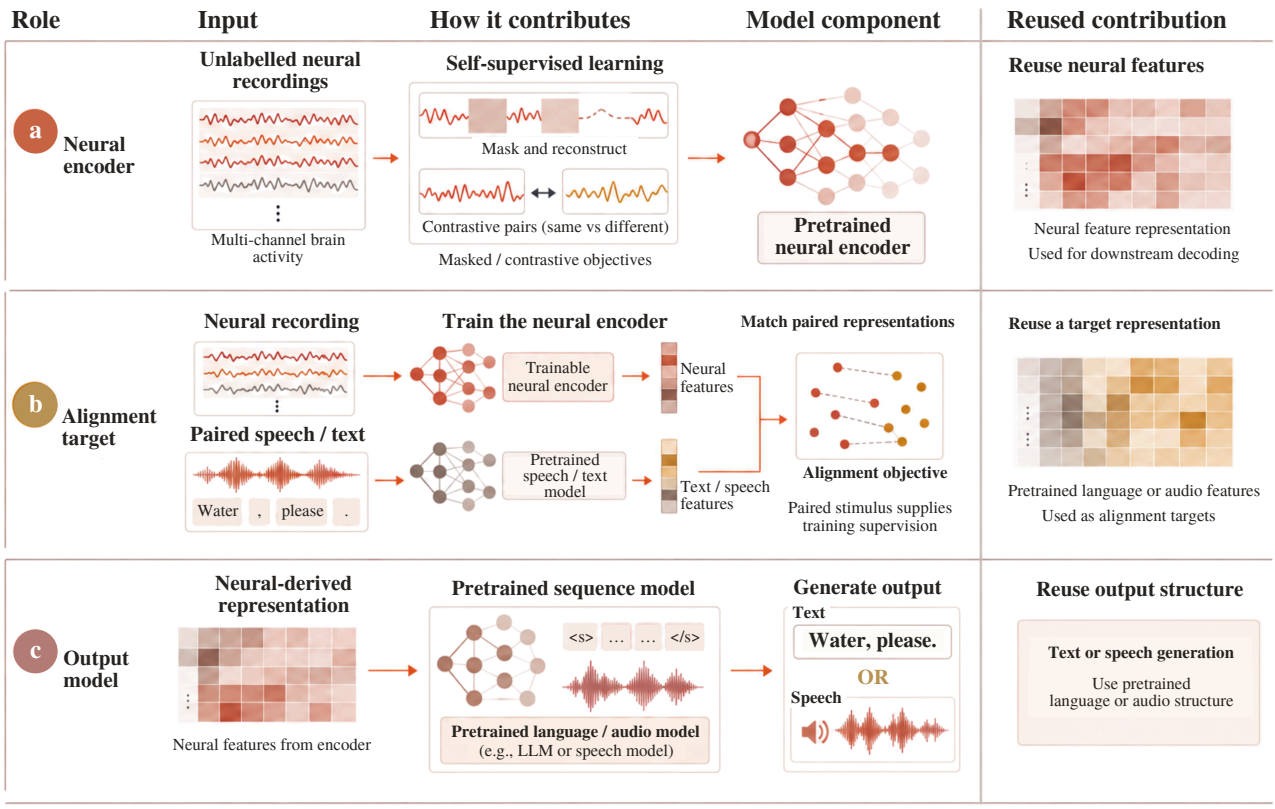


Figure 17. **Pretraining contributes at three different interfaces.** (a) Neural self-supervision learns reusable recording structure, as in BENDR and BrainBERT (Kostas et al., 2021; Wang et al., 2023). (b) A pretrained speech or text model provides targets for aligning a neural encoder (Défossez et al., 2023). The paired stimulus supplies training supervision. (c) An output model provides structure for constructing text or speech from neural evidence, as in language-guided semantic reconstruction (Tang et al., 2023). These roles can be combined without requiring the same training data or transfer setting. Feature patterns and messages are illustrative; the right column summarises the contribution being reused.

spread across encoders is therefore larger than the incremental gains among recent leaders. Model architecture, source data and the downstream tuning recipe jointly determine the quality of adaptation.

Transfer to new participants changes this picture. OmniEEG-Bench evaluates ten foundation models on the separate five-class BCI-Speech dataset using a subject-disjoint split and common adaptation procedures (Lu et al., 2026). Frozen linear probes and full fine-tuning produce different rankings (Figure 18b): CBraMod scores 28.9% and 26.2%, BIOT 20.4% and 26.7%, and REVE 22.3% and 20.8%, respectively, against 20% chance. Fine-tuning helps some representations but does not consistently improve all models on unseen participants. A separate BCIC2020-T3 comparison also finds lower scores when a participant is excluded from training: its five methods span 25.7–30.2% within participant and 18.9–20.2% in leave-one-participant-out evaluation (Khanday et al., 2026). That study evaluates official validation trials, so its absolute values should be kept separate from REVE's test split. Trial-split performance and cross-participant transfer answer complementary questions: how well an encoder can fit a target task, and how much of its learned structure survives a change of user.

Transfer can bridge tasks, participants or recording sessions; these are different learning problems. Overt-trained synthesis transferred to Mouthed production in ECoG (Anumanchipalli et al., 2019). Overt or Perceived–Auditory training also improved Inner word classification in a ten-participant low-density ECoG study; four participants exceeded chance on Inner only after such transfer (de Borman et al., 2026). Silent-reading reconstruction using Overt reference alignment remains a different Perceived–Visual test (Martin et al., 2014). Transfer is useful

a BCIC2020-3 · trial split

Method	Acc. % ↑	κ ↑	F1 ↑
EEGNet	44.13	0.302	0.441
EEGConformer	45.06	0.313	0.449
SPaRCNet	44.26	0.303	0.442
ContraWR	42.57	0.308	0.441
CNN-Transformer	45.33	0.317	0.451
FFCL	46.78	0.330	0.469
ST-Transformer	41.26	0.294	0.425
BIOT	49.20	0.365	0.492
LaBraM-Base	50.60	0.380	0.505
CBraMod	53.73	0.422	0.538
REVE-Base	56.35	0.454	0.563
BENDR	24.85	0.061	0.238
EEGPT	24.53	0.057	0.244
CodeBrain	61.01	0.513	0.610

b BCI-Speech · subject split

Method	Probe	Tune
BrainOmni	22.5	19.9
CBraMod	28.9	26.2
REVE	22.3	20.8
FEMBA	21.0	24.9
BIOT	20.4	26.7
LaBraM	20.3	22.5
NeuroLM	21.1	20.7
Neuro-GPT	21.2	21.0
EEGMamba	19.7	20.0
BENDR	20.0	20.0

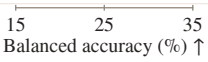


Figure 18. **Pretrained encoders differ in task adaptation and transfer across participants.** (a) Official BCIC2020-3 trial-split results combine REVE's comparison (El Ouahidi et al., 2025) with BENDR, EEGPT and CodeBrain values from Ma et al. (2026a); downstream tuning remains paper-specific. (b) OmniEEG-Bench (Lu et al., 2026) uses subject-disjoint BCI-Speech data: squares are frozen probes and circles full fine-tuning. The two panels use separate datasets. Method references: EEGNet (Lawhern et al., 2018), EEGConformer (Song et al., 2023), SPaRCNet (Jing et al., 2023), ContraWR (Yang et al., 2023b), CNN-Transformer (Peh et al., 2022), FFCL (Li et al., 2022a), ST-Transformer (Song et al., 2021), BIOT (Yang et al., 2023a), LaBraM (Jiang et al., 2024), CBraMod (Wang et al., 2025a), REVE (El Ouahidi et al., 2025), BENDR (Kostas et al., 2021), EEGPT (Wang et al., 2024b), CodeBrain (Ma et al., 2026a), BrainOmni (Xiao et al., 2025), FEMBA (Tegon et al., 2025), NeuroLM (Jiang et al., 2025), Neuro-GPT (Cui et al., 2024) and EEGMamba (Gui et al., 2024). Accuracy is balanced; F1 is weighted; κ is Cohen's agreement. Source SDs appear in Tables 22 and 23.

to the extent that the target task retains the learned representation without requiring an unavailable reference.

Transfer outcomes depend on the source and target task. Articulated EEG did not improve speaker-independent imagined-vowel classification in one study (Bras et al., 2024), whereas other multi-condition EEG work investigates how overt, whispered and imagined modes can be combined (Alonso-Vázquez et al., 2025). Such comparisons identify when shared production structure is useful and when the change in task outweighs it. They also motivate reporting learning curves over target-task labels, rather than only the final accuracy of a pretrained model.

Intracortical Inner decoding used attempted-speech pretraining and up to an hour of Inner data. Cued online decoding reached a 50-word vocabulary in three participants and 125,000 words in two, with large-vocabulary WERs of 26% and 54%; the full study enrolled four participants (Kunz et al., 2025). Articulatory and Auditory instructions, prompted sentences and the partial free-recall or counting results remain distinct conditions. The large-vocabulary result thus concerns instructed linguistic production; spontaneous content and unrestricted message choice pose additional tests.

Across participants, shared latent dynamics and position-aware models address differences in the populations sampled by micro-ECoG, surface and depth electrodes (Spalding et al., 2026; Singh et al., 2025; Chen et al., 2025a). Calibrated multi-user intracortical models reuse phoneme structure while fitting a new user's projection (Fogg et al., 2026). Across sessions, ALIGN uses semi-supervised adversarial alignment to reduce session-specific variation while retaining phoneme information (Zhang et al., 2026f). Source-task transfer, new-user

fitting and longitudinal adaptation thus solve different forms of mismatch; the relevant comparison keeps the target-data budget and output task explicit.

Additional indexed directions are documented in Appendix E.1; the main comparisons here retain their task and source boundaries.

What can be shared, and what remains personal? These studies share a design question: which learned structure can be reused, and which mapping must be adapted to the target recordings? The reusable component may be neural temporal structure, acoustic or linguistic targets, or decoder dynamics. Adaptation may use labelled target-task examples, a fitted user projection or session-domain alignment, depending on the method (de Borman et al., 2026; Kunz et al., 2025; Fogg et al., 2026; Zhang et al., 2026f). Their value is measured by performance at an explicit target-data budget.

Evaluation connects these design choices to their outcomes: which learned representation or prior improves performance, which intended distinctions are preserved, and under what conditions the gain remains useful.

6 Evaluation

Evaluation has expanded with the outputs that neural decoders can produce. Early classification and retrieval studies measured whether a recording distinguished specified alternatives. Sentence decoders adopted transcription and language-generation metrics; speech synthesis added listener judgements; online neuroprostheses added speed, feedback and sustained operation. Established BCI frameworks had already separated decoder performance, interface performance and the benefit to the user (Thompson et al., 2013; 2014). That distinction remains useful as language outputs become less constrained.

Shared benchmarks now make some algorithmic comparisons possible. Brain-to-Text '24 fixed a private attempted-speech test set, allowing different decoding pipelines to be compared by word error rate (Willett et al., 2024). The PNPL series introduced standardised listening-MEG tasks and data conditions, progressing from speech detection and phoneme classification to word classification and adaptation with limited target-user data (Landau et al., 2025; Mantegna et al., 2026a). In parallel, independent evaluations of EEG-to-text have examined how inference settings and language priors affect the interpretation of text scores (Jo et al., 2026; Zhang et al., 2026e). The development is therefore both quantitative and methodological: better outputs are being accompanied by clearer definitions of what was predicted and what information was available.

Four dimensions organise the following synthesis: *Quality*, *Robustness*, *Efficiency* and *Credibility* (Figure 19). They summarise related measurement traditions rather than a settled universal standard. Published results can be compared where their task, data and scoring conditions match; broader clinical progress can be described across studies while retaining differences in participants and use settings. Method-specific benchmark results accompany their decoding routes in Section 5; the following discussion traces the measurement standards and their interpretation. Reported timing examples retain their original definitions and use settings.

6.1 Quality

From item recognition to sequences. Classification and retrieval remain useful when the scientific question concerns a specific linguistic distinction or an interface offers a defined set of alternatives. Accuracy, classwise scores and confusion matrices describe recoverable contrasts; top-k accuracy or rank describes retrieval among supplied candidates. Candidate size and class frequency matter because a system that favours common words can achieve high aggregate accuracy while rarely recovering less frequent content. Balanced measures and explicit vocabularies make that behaviour visible. Finite-sample significance additionally depends on the number and dependence of observations, not only the nominal chance probability (Combrisson & Jerbi, 2015). The PNPL 2026 design retains explicit word vocabularies and discusses vocabulary coverage alongside performance, reflecting the difficulty of comparing retrieval tasks whose candidate sets differ (Mantegna et al., 2026a).

Sequence outputs require accounting for insertions and deletions as well as wrong choices. Phoneme, character and word error rates measure edit operations against a reference; WER is $(S+D+I)/N$, where S, D and I count

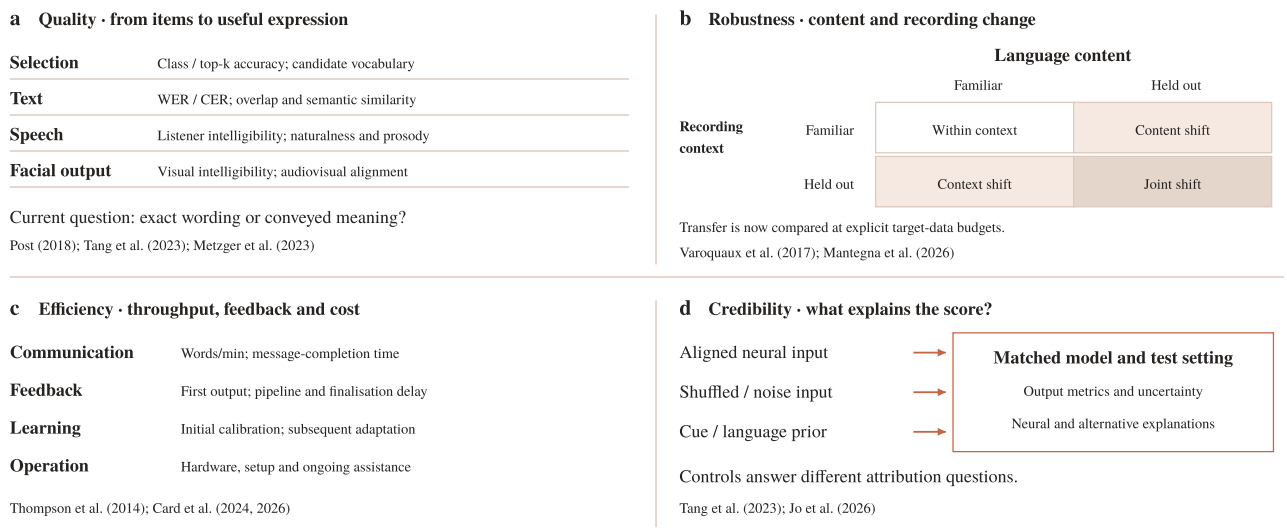


Figure 19. **Evaluation practices have broadened from decoding scores to transfer, communication costs and source attribution.** Each panel connects a measurement question to methods used in the literature and an active point of discussion (Thompson et al., 2014; Post, 2018; Willett et al., 2024; Jo et al., 2026; Mantegna et al., 2026a). The four dimensions organise the review; they do not define a new composite score or a universal evaluation protocol. WER and CER denote word and character error rates.

substitutions, deletions and insertions, and N is the number of reference words. Clinical text studies and shared attempted-speech benchmarks use WER to compare decoded messages with prompted transcripts (Willett et al., 2023; Metzger et al., 2023; Willett et al., 2024). This supports interpretable within-protocol comparison while retaining an important distinction between the neural-unit decoder and the language-assisted final transcript.

From exact wording to conveyed meaning. BLEU and ROUGE entered neural text generation through machine translation and summarisation, while contextual similarity measures such as BERTScore allow agreement beyond exact lexical overlap (Papineni et al., 2002; Zhang et al., 2020). These metrics answer different questions: BLEU-1 measures unigram overlap, not word accuracy, and semantic similarity may reward a paraphrase despite changes in a name, relation or negation. Tokenisation and implementation also change the resulting score (Post, 2018). For semantic reconstruction, information understood by a recipient supplies a complementary endpoint. Independent readers answered questions about a heard story after reading its fMRI-decoded reconstruction (Tang et al., 2023). This links generation to comprehension while leaving verbatim transcription as a separate objective.

The current debate concerns both the metric and the evidence that produced it. Jo and colleagues compared EEG-to-text models under the same decoding settings with real and noise inputs, showing that overlap scores can remain similar in the tested configurations (Jo et al., 2026). COFETT instead emphasises sentence-level embedding alignment across repeated reading/recall conditions and recording sessions (Zhang et al., 2026e). These studies broaden the available tests, but embedding alignment, repeated-content recognition and autonomous generation of new sentences remain different endpoints. For text intended as exact communication, edit errors and meaning-sensitive assessment therefore provide complementary information; for a semantic target, recipient understanding directly addresses the purpose of the representation.

From an acoustic match to intelligible expression. Speech synthesis has moved from correlation with recorded acoustic features towards testing what listeners can understand and how they perceive the voice. Objective measures such as STOI were developed for particular distortions of audible speech (Taal et al., 2011); subjective assessment separately measures intelligibility and perceived quality (International Telecommunication Union, 1994). Neural speech studies use both constrained identification and less constrained transcription. Ten-alternative digit recognition and four-alternative disyllable identification establish recoverable distinctions within

those inventories (Akbari et al., 2019; Xiong et al., 2025); open transcription asks whether a listener can recover an utterance without being offered the answer set. Naturalness, prosody and voice identity describe further gains that a transcription score alone would miss. Avatar neuroprostheses add sentence identification and facial-trajectory measurements for visual expression (Metzger et al., 2023). Consequently, a useful assessment pairs content recovery with the expressive property that the system aims to preserve.

What makes a benchmark comparison interpretable. A shared test set supports a method comparison when the target, scoring implementation and permitted inference information are fixed. Training-data budgets, external language resources and candidate vocabularies remain part of that comparison. The route-specific results in Figures 10 to 12 and 14 illustrate these choices in Methods. Across routes, the reusable standard is the declared evaluation contract: what is held out, what information is supplied and which output property is scored. It does not require pooling different tasks into one ranking.

6.2 Robustness

Generalisation follows the available datasets. Repeated-item recordings made within-person decoding and held-out repetitions early practical evaluation settings. Larger natural-language corpora subsequently enabled tests of new sentences or stories, while pooled recordings enabled session and participant transfer. These splits change different parts of the prediction problem: new content challenges linguistic generalisation, a new day changes the recording, and a new participant changes anatomy, coverage and the learned neural mapping. Cross-validation methodology formalises the corresponding separation between training, model selection and testing (Varoquaux et al., 2017). The settings are complementary, rather than successive grades on one robustness scale.

This distinction explains several apparently conflicting results. A decoder can recover another recording of a familiar sentence yet perform poorly on unfamiliar text. Repeated-sentence ECoG results, reading split analyses and repeated-cue EEG studies show why the unit held out matters (Makin et al., 2020; Yin et al., 2025; Jiang et al., 2026). In listening-MEG generation, story holdout changes the task from recovering familiar material to composing text for new linguistic content (Section 5). Common data and fixed holdouts make these differences explicit and allow subsequent studies to improve the same prediction setting.

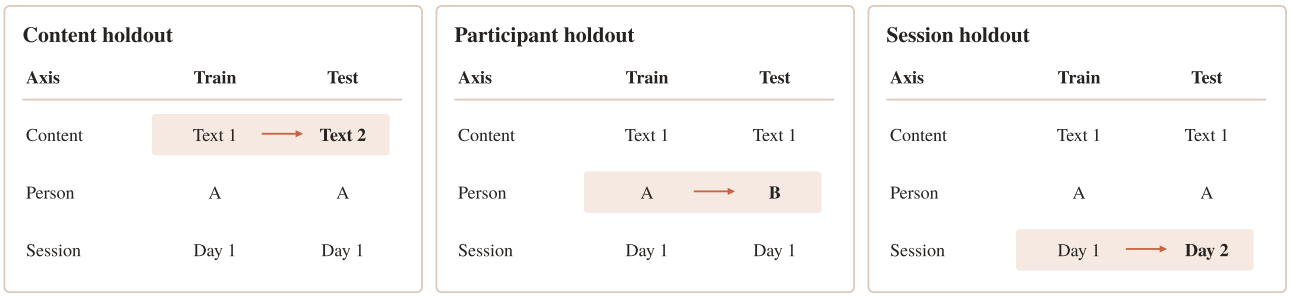


Figure 20. **A held-out unit defines the generalisation question.** Illustrative train/test pairs vary content, participant or session while keeping the other attributes familiar. Session indices are local to each participant; holding out person B does not establish future-session transfer. Jointly new participants and text require both forms of separation. Reading split analyses show why participant separation alone can retain familiar sentences (Yin et al., 2025); cross-validation must preserve the independent unit relevant to the intended use (Varoquaux et al., 2017). These are different prediction settings rather than stages on a single robustness scale.

From personal fitting to measured transfer. Shared representations across distributed intracranial recordings demonstrate that data from other people can improve a target decoder (Singh et al., 2025). Multi-user models, shared MEG encoders and session-domain alignment extend this approach through different reusable components (Fogg et al., 2026; Jayalath & Parker Jones, 2026; Zhang et al., 2026f). The important comparison is performance at a stated amount of target data: zero-shot prediction asks what transfers without fitting, whereas calibrated

prediction asks how efficiently prior learning supports a new recording. High accuracy after extensive personal fitting answers a different question from effective adaptation with a few minutes of data.

Benchmark design is beginning to make this cost explicit. The PNPL 2025 tasks separated standard and extended data conditions; PNPL 2026 introduced deep within-person learning and a broad cross-person track with progressively reduced target-user training budgets (Landau et al., 2025; Mantegna et al., 2026a). At the review date, the latter describes an ongoing competition, not a completed leaderboard. Its design illustrates a methodological shift from reporting a single transfer score to comparing performance across available calibration data.

Stability during continued use. Longitudinal operation adds changes that static data partitions only approximate. Initial calibration, updates with newly confirmed messages and recovery after a recording change affect the mapping over time (Card et al., 2024; 2026). User learning adds another source of change: a controlled, repeated-day feedback study found improved binary syllable-imagery control with practice and substantial individual variation (Bhadra et al., 2025). Thus stability may be maintained by a fixed decoder, algorithmic adaptation, user adaptation or their combination. The emerging practical question is how much ongoing supervision and interruption each approach requires; Section 7 explains the corresponding support mechanisms.

6.3 Efficiency

Efficiency concerns four related costs: producing a message, receiving feedback, learning the user's neural mapping and maintaining the running system. Classical BCI work formalised the distinction between the rate of neural selections and the communication enabled by an interface (Thompson et al., 2013; 2014). Selection-based information-transfer rates assume a defined alternative set and error model; they do not transfer unchanged to variable-length language generation. Speech neuroprostheses therefore commonly report words per minute alongside decoding errors, while calibration and processing measurements describe different demands on the user and equipment.

Communication rate and message fidelity. Early online sentence decoding combined a 50-word vocabulary with a median rate of 15.2 words per minute and median WER of 25.6%; the same study separately reported correctly decoded throughput of 12.5 words per minute (Moses et al., 2021). Later work expanded vocabulary and pace, including a study-wide mean of 62 words per minute in attempted-speech text decoding (Willett et al., 2023) and a median of 78.3 words per minute with median WER of 25.5% in a 1,024-word ECoG condition (Metzger et al., 2023). Card and colleagues paired a mean of 31.6 words per minute with aggregate WER of 2.5% over their final five copy-task sessions using a 125,000-word vocabulary (Card et al., 2024). These results show complementary gains in vocabulary, speed and fidelity across different participants and protocols. Reporting rate together with errors makes this progress interpretable: rapid output can still impose substantial correction time, whereas lower error can make a slower stream more useful.

From initial learning to maintenance. Calibration reporting has moved beyond total training-corpus size towards the time needed to begin and continue using a decoder. In the 2023 intracortical study, daily training-data collection averaged 41 minutes, while preparation including breaks and model training averaged 140 minutes (Willett et al., 2023). A later participant achieved 0.44% WER on a 50-word copy task after 30 minutes of first-day copy-task data, then 9.8% WER with a 125,000-word vocabulary after an additional 1.4 hours on day two (Card et al., 2024). The increase in error accompanied a much larger vocabulary, illustrating why calibration time must be reported with the capability it enables. The 2026 home-use follow-up combined background updating with optional daily prompted sentences (Card et al., 2026). Together with transfer benchmarks that vary target-data budgets, these studies make adaptation cost an outcome in its own right rather than an unreported preliminary step.

Vocabulary coverage and transmitted information. Recent work extends information-based evaluation from accuracy within a decoder's vocabulary to the fraction of a user's language that vocabulary can express. Open-

vocabulary mutual information (OVMI) weights information conveyed among supported words by their coverage of an explicit reference language distribution (Jayalath et al., 2026). It therefore distinguishes a highly accurate small-vocabulary interface from a broader but less accurate decoder, and makes the intended communication domain part of the evaluation. The proposal complements shared benchmarks: a common reference distribution supports a common lexical-information scale, whereas a benchmark controls the neural task and test data. OVMI estimates from scalar accuracy or WER still depend on assumptions about errors and the reference distribution; they do not make attempted-speech and listening experiments clinically equivalent. This direction broadens the discussion from correctly decoded words to the range of messages a system could support.

From completed utterances to streaming feedback. Streaming synthesis reduces the amount of output that must be accumulated before feedback. Littlejohn and colleagues generated audio in 80 ms increments; Wairagkar and colleagues generated 10 ms frames (Littlejohn et al., 2025; Wairagkar et al., 2025). The latter also measured acquisition through speech-sample synthesis at less than 10 ms using an RTX A6000, with audio-driver playback measured separately. Frame duration specifies how often output advances, while acquisition-to-synthesis time measures the processing that produces it. A GO-cue-to-audio measurement additionally includes the participant's response timing. These distinct endpoints explain how feedback becomes more continuous without equating the output step with the total time from intention to audible speech.

Incremental feedback and final output. Text systems can display a provisional sequence before completing a more expensive sentence-level pass. The long-term home system estimates incremental feedback at 160–240 ms and reports median finalisation processing of 2,657 ms for its RNN route and 1,791 ms for its Transformer route (Card et al., 2026). These medians concern the reported utterances rather than a matched-length test of decoder speed. The measurements locate two opportunities for improvement: quick feedback supports ongoing interaction, while faster finalisation shortens the wait for a revised final sentence. Neither includes every action required to repair an incorrect message, so communication utility remains broader than either component delay.

Computational cost and the remaining comparison gap. Some recent papers report hardware-specific component times. An offline causal voice model evaluated on earlier T15 recordings reports mean neural-model inference times of 1.47 ms and 2.11 ms for continuous and tokenised output heads on an RTX 5090, with an additional reported 1.2 ms for vocoding (Wairagkar et al., 2026). These source measurements describe computational feasibility, not a new online clinical trial. Comparable end-to-end energy, memory and maintenance measurements are still too sparse among the selected reports for a common cost ranking. The emerging pattern is more specific: as text accuracy and raw output rate improve, feedback, finalisation, correction and calibration become increasingly consequential parts of the remaining communication time. For other tasks, especially transfer to new users, collecting enough target data remains a major cost.

6.4 Credibility

Credibility concerns the inference supported by an experiment. Prediction conditions determine what information the model could use; controls distinguish possible sources of its performance; statistical analysis describes variation and uncertainty. Reproducible protocols and independent replication connect these questions across studies.

6.4.1 Information available during testing

Offline, pseudo-online and live closed-loop evaluation expose a system to different information and interaction conditions (Ko et al., 2025; Card et al., 2026). Published protocols differ in their use of correct prefixes, reference-dependent alignment, known candidates, stimulus boundaries, future samples and repeated observations. These inputs change what the prediction measures. Test-time teacher forcing is one case of privileged information, particularly relevant to autoregressive text; it is not a universal evaluation criterion for classifiers or synthesis systems (Jo et al., 2026). Known boundaries or reference-dependent alignment can simplify decoding even without teacher forcing (Table 25).

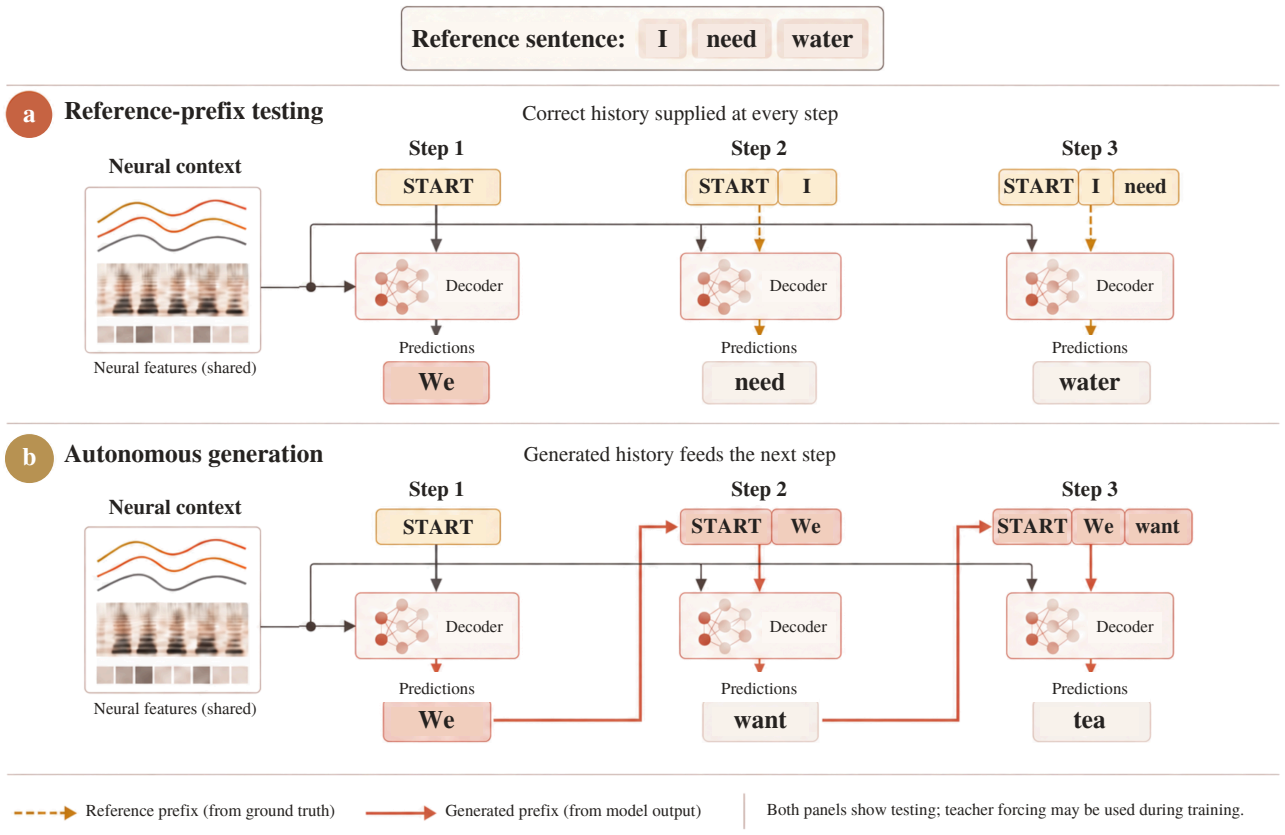


Figure 21. **The source of the preceding tokens changes what a text-generation test measures.** Both conditions receive neural context. (a) Reference-prefix testing supplies correct preceding tokens even after a prediction error. (b) Autonomous generation uses its own generated history. In the illustrative example, the first prediction, "We", enters the next prefix only in (b); subsequent outputs may consequently differ. Teacher forcing may be used during training in either case. The distinction is explicit in the ZuCo noise comparison and the split audit's with/without-teacher-forcing results (Jo et al., 2026; Yin et al., 2025). It concerns autoregressive generation, not every classifier or speech synthesiser.

6.4.2 Neural contribution and controls

Behaviour. The first control concerns what the participant actually did. Mouthing retains articulatory activity, and preparation windows remain contiguous with forthcoming speech (Willett et al., 2023; Anumanchipalli et al., 2019; Dash et al., 2020; 2024). Reading versus Inner task contrasts and comparisons involving loss of residual articulation show why removing sound does not hold the behavioural source constant (Csaky et al., 2025; Jude et al., 2026). In an around-ear EEG–EMG system, peripheral activity can be a useful communication input while limiting a neural-only interpretation (Inoue et al., 2026). The appropriate question is not whether all movement should be excluded from a useful device, but whether the reported contribution matches the claimed source. Channel-specific comparisons separate the benefit of fused inputs, while peripheral recordings address residual movement in internally produced speech.

Priors. A prior can improve communication while the neural input remains necessary. Attempted-speech systems report phoneme error separately from the WER obtained after language-model decoding (Willett et al., 2023; Metzger et al., 2023). In fMRI semantic reconstruction, replacing brain-based likelihoods with random scores caused decoding to fall to chance, whereas resetting linguistic context produced a transient loss followed by recovery (Tang et al., 2023). That ablation demonstrates ongoing neural constraint in a system that also uses a strong language prior. Prompt-conditioned generation adds cue information that needs its own compari-

son (Zhang et al., 2024b). Conversely, the ZuCo audit compared BART, Pegasus and T5 using real and noise inputs, with and without test-time teacher forcing (Jo et al., 2026). Comparable EEG/noise results limit the neural-decoding interpretation of those Perceived–Visual pipelines; they do not establish a universal impossibility result for Inner, Auditory or later untested generators. The useful question is which information the tested decoder actually requires.

A control is informative only when its preserved and removed information match the alternative explanation. Prior-only or cue-only decoding asks how much can be predicted without a neural measurement. Shuffling the association between recordings and targets tests trial-specific information only if nuisance structure and the permitted timing information are preserved. Replacing inputs with noise tests dependence on the measured values, but an arbitrary replacement can also create an unfamiliar input distribution; failure on that control alone is weak evidence of neural specificity. Conversely, success with signal-blind input exposes an available shortcut, as in the MEG retrieval audit (Zhang et al., 2026c). Peripheral-channel comparisons then ask a different question: which measured source supplies the usable information. No single control resolves all of these explanations, and artifact cleaning cannot replace this analysis.

6.4.3 Statistical support and replication

Theoretical chance is a null expectation, not a finite-sample threshold for reliable decoding (Combrisson & Jerbi, 2015). Permutation tests and uncertainty estimates address sampling variation, with the inferential unit determined by repeated items, sessions and participants. At the group level, the fraction of individually significant participants differs from an estimate of population prevalence; the latter requires its own inferential framework (Allefeld et al., 2016). This distinction matters when many trials are available from only a few people.

Variation across participants. Peak performance can conceal a large difference in who benefits. Eight-class cued Inner decoding reached 79% and 23% in two participants (Wandelt et al., 2024); pairwise inner-word ECoG decoding averaged 58% across five participants despite a best result of 88% (Martin et al., 2016). These distributions are more informative about reproducibility than either peak alone. Repeated clinical reports also require participant links, because additional follow-up does not add independent recruitment (Table 10).

Replication in Inner EEG decoding. A replication audit (Tates et al., 2026) re-implemented published inner-speech pipelines on multiple public and in-house EEG datasets and found a mean fraction of 36.1% statistically significant participants across the tested speech-imagery datasets, below the corresponding motor-imagery fraction, with replicated accuracies below the original reports. This is an average of dataset-level fractions, rather than a pooled participant proportion. This does not bound every Inner method. It does show why the distribution of reliable decoding across the tested participants is a different outcome from the best observed accuracy. Paired cross-mode and paradigm-design datasets can help distinguish failure to transfer a model from changes in task execution or engagement (He et al., 2025b; Ma et al., 2026b; Aguilera-Rodríguez et al., 2025).

These studies expose two levels of reproducibility. Reusing ZuCo or a clinical benchmark tests whether an algorithmic result can be obtained on the same recordings; recruiting additional participants tests whether it extends to another population sample. Repeated reports from T15 or BRAVO3 add longitudinal or functional evidence without adding independent recruitment (Table 10). Participant-level analysis and correction for multiple comparisons also affect conclusions in auditory EEG benchmarking (Li & Tao, 2026). The field therefore has established tools for assessing individual decoding and increasingly explicit protocols for algorithm comparison, while population-level reliability remains less well characterised.

From evidence to use. Output metrics, shared benchmarks, source controls and longitudinal tests answer complementary questions. Their combined development makes some method comparisons increasingly reproducible while exposing remaining differences in task and use conditions. Table 26 collects the details needed to interpret a result. The next section follows the corresponding system mechanisms: initiation, feedback, correction, adaptation and continued access.

7 Practical Use

A practical language interface lets a person initiate, express and complete a communication goal. Decoding contributes the content; feedback, correction and adaptation help turn that content into an exchange. User-centred BCI studies consequently assess effectiveness, workload and satisfaction together, while prospective-user research establishes communication priorities before engineering choices are fixed (Kübler et al., 2014; Huggins et al., 2011; Branco et al., 2021). These priorities connect three parts of the interface: *Interaction* governs expression and user control, *Support* supplies context and decoder updates, and *Deployment* sustains recording access and assistance. Figure 22 shows how they contribute to the same communication loop.

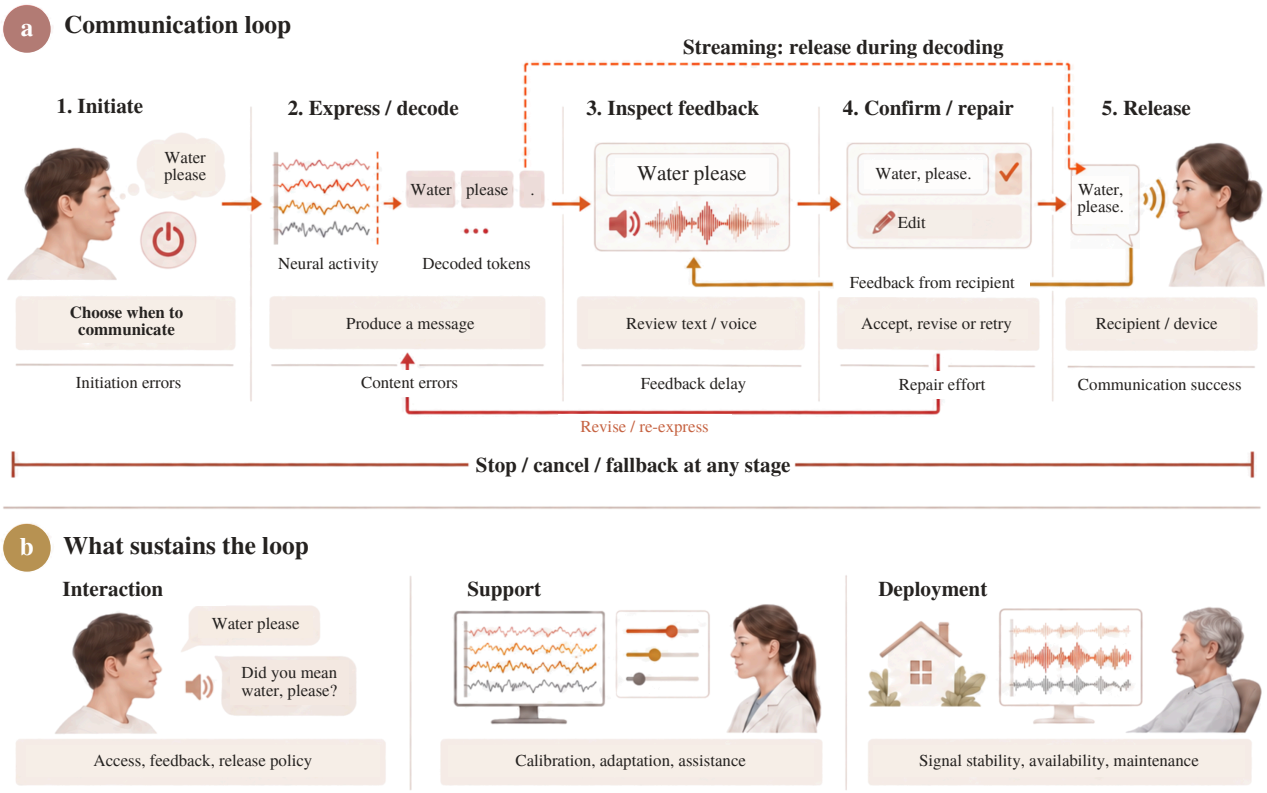


Figure 22. **Communication combines message production, feedback, release and repair under user control.** (a) The solid forward path illustrates confirmation before release; the dashed branch illustrates provisional streaming to the recipient during decoding. Feedback and revision provide return paths, while initiation errors, content errors, delay and repair effort locate different sources of communication cost. (b) Interaction design, calibration and assistance, and sustained recording access support the loop. The people and messages are illustrative. Interfaces may combine these functions differently, including their release policy and available stopping or fallback controls.

7.1 Interaction

Interaction determines when decoded content becomes a message and how the user responds to an error. The distinction between executory control over releasing speech and guidance control over its expression helps separate initiation or cancellation from linguistic correction (van Stuijvenberg et al., 2024b). Different interfaces distribute these decisions between automatic detection, explicit user actions and continuous feedback. A confirmation step can prevent an unwanted utterance, but it also consumes time and can interrupt a conversational turn.

7.1.1 Speech onset, stopping and unintended activation

Speech-state classification, onset detection and idle-state modelling allow a decoder to operate between utterances as well as during them (de Borman et al., 2025; Ko et al., 2025; Padfield et al., 2025). In Card's clinical text system, conversation mode detects speech automatically and finalises an utterance after six seconds without detected speech or an eye-tracker button action (Card et al., 2024). Automatic segmentation reduces the need to issue a separate command for every turn; the button provides a direct way to finish early. A later Inner-speech system demonstrates real-time keyword gating in one participant, adding a deliberate internally produced action before message output (Kunz et al., 2025).

These mechanisms address different use conditions. Automatic detection supports natural turn-taking, whereas a deliberate gate can help separate communication from other verbal activity. Long-term home use also exposes states uncommon in cued testing: occasional false detections produced nonsensical output when the participant was nominally asleep (Card et al., 2026). The available activation action, sensitivity to idle behaviour and means of stopping output therefore jointly shape dependable access, especially when fatigue or another control channel changes.

7.1.2 Feedback, confirmation and error correction

Feedback has developed from audible formant control to multimodal and streaming speech interfaces (Guenther et al., 2009; Brumberg et al., 2018; Littlejohn et al., 2025; Wairagkar et al., 2025). Streaming synthesis lets the user hear output while an utterance is being produced. Sentence-level text interfaces instead provide a point at which a complete message can be reviewed before further use. These policies distribute delay and repair differently: early audio supports ongoing adjustment, while an already spoken error may require a clarification to the recipient.

Auxiliary controls can make repair part of routine use. Eye-tracker confirmation in Card's 2024 system identifies correctly decoded sentences for online fine-tuning; the later home system supports correction through gaze or a neural cursor (Card et al., 2024; 2026). A correction channel thus serves two roles, improving the current message and supplying information for later adaptation. Feedback can also change the user's control strategy: in a five-day binary syllable-imagery study, continuous feedback supported learning, with substantial individual differences and a discontinuous-feedback comparison (Bhadra et al., 2025). This constrained task provides evidence for user learning alongside decoder learning, without equating that gain with conversational proficiency.

7.1.3 Communication benefit and user experience

Useful communication includes choice of language, voice and expression. Bilingual decoding extends language choice, while personalised speech, facial animation and expressive voice restore additional aspects of identity and delivery (Silva et al., 2024b; Metzger et al., 2023; Wairagkar et al., 2025). Loudness or mode control and parallel gestures add further dimensions (Srinivasan et al., 2026; Brosler et al., 2026). Their benefit depends on the person's goals and the effort required to control them; attention, fatigue and engagement consequently matter alongside output quality (Aguilera-Rodríguez et al., 2025).

Long-term conversational reports capture both decoding and the user's contribution to a successful message. In the home-use system, sentence ratings include immediately correct, user-corrected and mostly correct output, whereas cued-copy testing provides a known reference transcript (Card et al., 2026). The former describes achieved communication with the interface; the latter more directly isolates word recovery. Effectiveness, workload and satisfaction complement these outcomes (Kübler et al., 2014). The Communicative Participation Item Bank supplies a patient-reported construct for speaking situations, whose applicability to a particular neural communication aid still requires appropriate validation (Baylor et al., 2013). Together, these measures connect the quality and timing endpoints in Section 6 to the experience of completing an exchange.

Table 12. Demonstrated features and operating conditions of selected communication interfaces. The rows describe different tasks and stages of use, rather than a common performance test. The two Card reports follow the same participant.

Study / setting	Demonstrated feature	Operating support	Implication for use
(Card et al., 2024); T15, longitudinal clinical use	Rapid initial fitting followed by text conversation over an eight-month study	Prompted calibration; eye-tracker confirmation of accepted sentences	Starting quickly and refining the decoder during use address different parts of learning.
(Littlejohn et al., 2025); BRAVO3, online speech	Continuous voice output in 80 ms increments	Participant-specific neural training and a streaming speech synthesiser	The user can hear output during production; cadence and onset delay describe different experience costs.
(Kunz et al., 2025); T15/T16, large-vocabulary condition	Cued online Inner-speech text decoding	Attempted-speech pretraining, Inner data and participant-specific updates	Shared representations provide a route to an alternative instructed mode of expression.
(Card et al., 2026); T15, home follow-up	More than 3,800 h of logged operation, including idle time; speech and cursor access	Background recalibration, gaze/neural correction and daily caregiver setup	Self-directed message production becomes available within an ongoing support arrangement.
Longitudinal selection/control interfaces: complementary experience with communication access			
(Wolpaw et al., 2018); multisite EEG BCI	Home communication with continued use and availability tracked	User/caregiver training and technical support	Service availability and user burden influence sustained access.
(Vansteensel et al., 2024); implanted BCI	Seven-year follow-up of communication control	Longitudinal signal access and assistance as needs change	Long service life involves adaptation of both the interface and its support.

7.2 Support

Support mechanisms work at different points in learning and use. Context helps interpret the current neural evidence; personal calibration fits a new recording; continued adaptation maintains the mapping as signals and user behaviour change. Their practical effects differ accordingly, from fewer corrections within a sentence to fewer interruptions between sessions.

7.2.1 Inference-time assistance

Language models help convert uncertain phoneme evidence into words, while a preceding question narrows the likely answer (Willett et al., 2023; Moses et al., 2019). Semantic beam search uses contextual representations to guide sentence generation, and the home-use text system rescores candidate sequences at finalisation (Tang et al., 2023; Card et al., 2026). These mechanisms place linguistic constraints around the neural prediction. They extend an established principle in BCI spelling, where probabilistic language context improves the conversion of noisy selections into text (Speier et al., 2015).

The resulting fluency is useful when contextual expectations agree with the intended message. Names, negation and unusual expressions create a different demand: the interface needs to retain a low-probability choice that matters to the user. Direct editing and confirmation offer ways to resolve that conflict. The relevant practical gain is the reduction in total correction effort while preserving intended distinctions; the matched model and control comparisons in Section 6 address how much of the improvement comes from neural evidence and inference support.

7.2.2 Long-term stability and recalibration

Initial fitting and continued adaptation have already changed the cost of using clinical speech interfaces. Card's 2024 report began with 30 minutes of calibration for a 50-word task, added 1.4 hours on the second day before

large-vocabulary testing, and improved further with accumulated data (Card et al., 2024). These stages explain how an interface can become useful early while continuing to learn. Later home operation employed background recalibration to maintain performance during extended use (Card et al., 2026). The cued Inner study followed another route, combining attempted-speech pretraining with Inner data and participant-specific online updates (Kunz et al., 2025).

The source of update labels distinguishes these mechanisms. Prompted sentences supply known targets; T16's large-vocabulary Inner protocol incorporates each cued sentence after decoding it. User-confirmed conversational output can supply accepted targets during communication (Kunz et al., 2025; Card et al., 2024). The former offers direct supervision, while the latter can reduce separate calibration but depends on reliable confirmation. Recalibration consequently has costs in time, labels and assistance even when it preserves accuracy (Swanson et al., 2026).

Related control BCIs illustrate two further approaches. Aligning low-dimensional neural activity recovered cursor control after recording changes in nonhuman primates; sustained user–decoder adaptation enabled stable human ECoG control (Degenhart et al., 2020; Silversmith et al., 2021). These are algorithmic stabilisation and coadaptation precedents, respectively. Their relevance to language is the prospect of maintaining a useful representation with fewer interruptions, while preserving the linguistic distinctions and temporal structure that communication requires.

7.3 Deployment

Deployment joins the decoder to the equipment and people that keep it available. Recording access, preparation, maintenance and recovery determine when a successful laboratory capability becomes a dependable communication option.

7.3.1 Setup, portability and maintenance

The prolonged home-use report makes this operating arrangement concrete. One participant used a wired, multicomputer system for more than 3,800 hours, including idle time, with about 20 minutes of daily caregiver setup (Card et al., 2026). Once set up, speech, cursor control and correction supported self-directed use without a researcher present. Assistance at the start of a day and independent message production during the day therefore describe complementary parts of the same achievement.

Longitudinal selection/control studies add experience with service availability. A multisite EEG communication study tracked home use, unavailable days, attrition and user–caregiver benefit and burden (Wolpaw et al., 2018); an implanted communication interface was followed for seven years in one person with ALS (Vansteensel et al., 2024). These systems differ from direct language-content decoding, but they show how access evolves with health, support and recording conditions. Caregiver contributions include preparation, maintenance and troubleshooting (Wohns et al., 2024). Smaller sensors and automatic calibration can reduce particular tasks within this arrangement; their contribution to autonomy depends on which remaining tasks the user or caregiver still performs.

7.3.2 Privacy and user control

Privacy controls operate at several stages of an interface. Cooperation affected successful semantic reconstruction in the fMRI study; keyword gating in the Inner study supplied a deliberate activation action; a privacy mode in the home-use system disabled data logging (Tang et al., 2023; Kunz et al., 2025; Card et al., 2026). Activation, message release and data retention are therefore separate design decisions with different technical mechanisms. Disabling storage, for example, changes the retained record rather than the decoder's output policy.

Access to the input also matters. Stimulus-based EEG probing demonstrated information leakage under a defined adversary and observation protocol (Martinovic et al., 2012), while developer interviews identify responsibilities around autonomy and maintenance (van Stuijvenberg et al., 2024a). These findings connect control of recordings to control of inferred content and released messages. A usable language interface combines such con-

trols with feedback and repair, so that the user can express a message and manage its consequences throughout an exchange.

8 Limitations

Brain-to-language decoding has progressed through complementary advances: richer representations, more reusable training data, efficient personal fitting and interfaces that operate during conversation. The remaining limitations arise where these advances meet. A representation learned from externally supplied language may change during self-generated expression; a shared model still encounters new recording geometry; a fast decoder can leave substantial correction or setup work. Four connected questions organise these challenges (Table 13).

Table 13. Remaining limitations and the approaches that provide a basis for addressing them. Each direction concerns a capability needed across learning, decoding and use.

Challenge	Source of difficulty	Existing progress	Remaining capability
Self-generated expression	Intended content has no externally supplied transcript or reliable acoustic reference.	Cued Inner decoding and listening-to-imagery transfer (Kunz et al., 2025; Tang et al., 2023).	Flexible expression of user-chosen content with a dependable account of message fidelity.
Signal access and supervision	Coverage, task and labels differ between large corpora and intended users.	Pooled perception data and shared intracranial representations (Défossez et al., 2023; d' Ascoli et al., 2025; Singh et al., 2025).	Source representations that reduce target-task learning costs under feasible recording conditions.
Transfer and stability	New content, people and sessions change different parts of the learned mapping.	Calibrated multi-user models, session alignment and continued adaptation (Fogg et al., 2026; Zhang et al., 2026f; Card et al., 2026).	Predictable performance across users with manageable personal fitting and recovery.
Sustained communication	Expression, correction and support compete for the user's time and effort.	Streaming voice, home operation and user-centred assessment (Littlejohn et al., 2025; Card et al., 2026; Kübler et al., 2014).	Improved participation and complete exchanges with affordable maintenance and assistance.

8.1 Task coverage and self-generated expression

Perceived-language tasks offer reusable recordings and precise targets, while clinical attempted-speech systems demonstrate voluntary communication under a different acquisition and supervision setting (Tang et al., 2023; Card et al., 2026). Inner research connects these settings through constrained classification, feedback-driven learning and overt-bridged synthesis (Bhadra et al., 2025; Lee et al., 2023). Intracortical work further combines attempted-speech pretraining with instructed Inner decoding (Kunz et al., 2025). The open question is which parts of these learned representations remain useful when a person chooses new content without an external stimulus or audible reference.

The neural state matters as much as the word label. Motor attempt, internal articulation and auditory imagery can share content-related structure while differing in intention and execution. Results from users without residual articulation, together with paired-task and peripheral-monitoring studies, make these differences accessible to investigation (Jude et al., 2026; Nieto et al., 2022; Ma et al., 2026b; Inoue et al., 2026). Their value is to identify transferable linguistic structure while separating it from cue processing and correlated movement. Linking controlled tasks to user-chosen messages also changes the reference: a known prompt provides exact labels, whereas confirmation and independent accounts of intended meaning become central to judging self-generated

expression. Better learning from these complementary forms of supervision is a route towards less constrained communication.

8.2 Signal access and supervision

Large pooled perception corpora and long within-person recordings have made representation learning possible at a scale that is difficult to reproduce for clinical attempted or Inner speech (Défossez et al., 2023; d' Ascoli et al., 2025; Özdogan et al., 2025). General EEG and intracranial pretraining provide reusable encoders, while speech-specific latent alignment and multi-user models bring source information closer to a target decoder (Kostas et al., 2021; Wang et al., 2023; Singh et al., 2025; Fogg et al., 2026). The limitation is the mismatch between available supervision and intended use. More source data help when they preserve distinctions the target task needs; differences in task, sensor coverage or labels can reduce that benefit. Target-data learning curves consequently offer a more informative account of reuse than source hours alone.

Recording advances can change this balance by improving access to relevant populations or making acquisition easier. Around-ear EEG–EMG resources, distributed intracranial recordings and emerging magnetic or optical configurations broaden the available design choices (Inoue et al., 2026; Spalding et al., 2026; Xu et al., 2026; Tripathy et al., 2025). Their demonstrated targets currently differ: OPM-MEG includes overt-vowel classification, HD-DOT includes language mapping and audiovisual-segment retrieval, and human fUSI language work primarily provides task maps (Section 4). These achievements establish different starting points. Extending a new configuration towards communication depends on obtaining sufficient content-specific information under the target behaviour, together with a practicable supply of training labels.

8.3 Transfer across content, people and time

Shared representations and session alignment have begun to reduce the dependence on a separately trained decoder for every recording (Singh et al., 2025; Zhang et al., 2026f). Their benefits address different changes: new content challenges linguistic composition, a new participant changes anatomy and sampled populations, and a later session changes the recording within a person. Calibrated multi-user models and continued adaptation provide evidence that reuse and personal fitting can work together (Fogg et al., 2026; Card et al., 2026). The unresolved issue is how reliably the gains persist across users and how much target supervision each change requires.

Common datasets support repeated method comparisons, while longitudinal and independent-cohort studies extend the range of conditions represented. Split analyses and controlled replications have shown that familiar stimuli and output priors can account for part of apparent transfer in the tested configurations (Yin et al., 2025; Jo et al., 2026; Tates et al., 2026; Li & Tao, 2026). These findings identify specific obstacles to learning robust neural-to-language mappings. Assessing performance across content novelty, recording shift and calibration budgets can reveal whether a model reuses linguistic structure or remains tied to its original setting. Variation between participants, including unsuccessful users, remains consequential for estimating how broadly a reported capability applies (Allefeld et al., 2016).

8.4 Sustained communication and operating burden

Streaming synthesis, expressive control, facial animation and prolonged home use have moved neural language interfaces closer to everyday exchange (Littlejohn et al., 2025; Wairagkar et al., 2025; Metzger et al., 2023; Card et al., 2026). These developments improve different parts of communication: immediate feedback supports ongoing production, additional output dimensions carry expression, and background adaptation maintains access. Each also changes the work required of the user or support network. A richer output may need additional control, and continued learning depends on labels and recovery when the mapping changes.

User-centred and longitudinal BCI studies already connect effectiveness to workload, availability and assistance (Kübler et al., 2014; Wolpaw et al., 2018; Vansteensel et al., 2024). For direct speech interfaces, the remaining challenge is to sustain gains over complete exchanges and changing needs, including correction and

unavailable time. Comparisons with a person's existing communication aid can identify whether an advance reduces effort, improves participation or transfers work to setup and maintenance. This connects the technical directions above to clinical translation: useful representations and efficient models matter through the communication they keep available (Stavisky, 2025; Dohle et al., 2025; Swanson et al., 2026).

9 Beyond

Future interfaces could expand both what a person communicates and how information returns to them. We propose five levels organised by the *depth of cognitive interfacing* (Figure 23). L1–L4 progress from a selected action to formulated language, intended meaning and an unfolding scenario. L5 adds a neural return channel through which meaningful content enters the person's cognitive process. These are prospective functional targets, not an established standard or a ranking of current systems. A river-crossing story illustrates the added capability at each transition; throughout, the user retains authority to initiate, reject and revise the exchange.

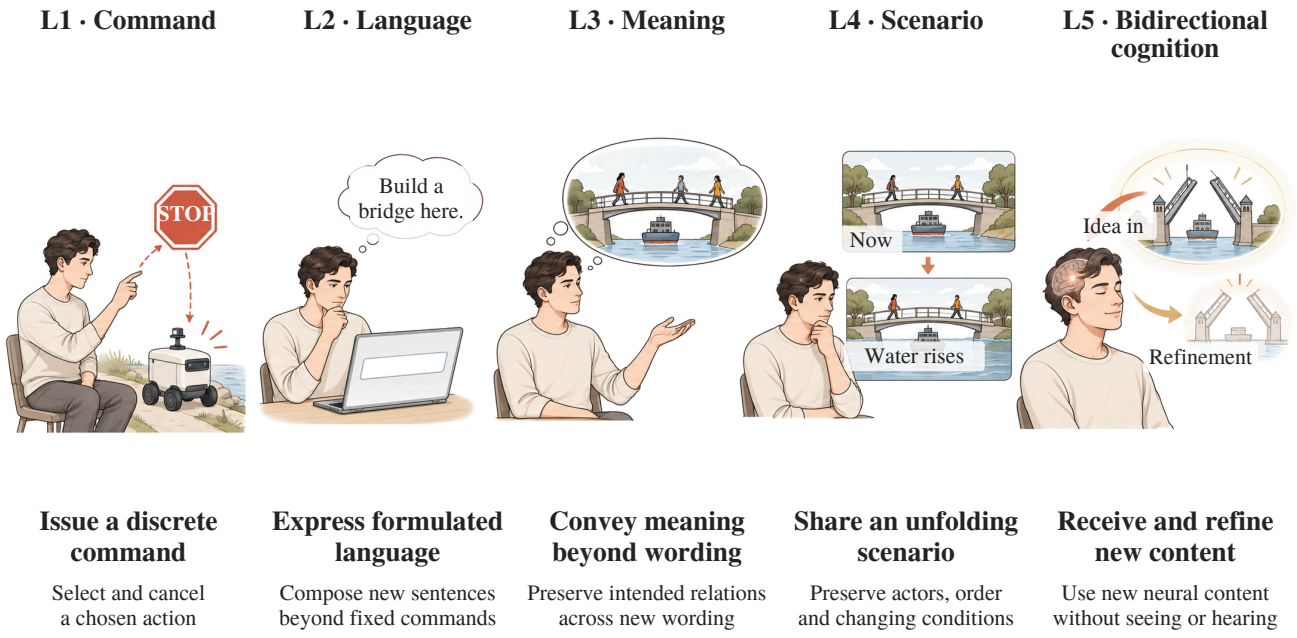


Figure 23. **The proposed progression expands what a person can convey, then adds direct neural receipt of meaningful content.** The river-crossing story distinguishes commands (L1), formulated language (L2), intention independent of wording (L3), actors and relations in an unfolding scenario (L4), and direct neural receipt and refinement of a concept (L5). The upper labels identify the added function; the smaller lower labels state tests for that transition. L4 conveys the user's scenario; L5 requires incoming content to inform understanding without audiovisual presentation. These are proposed research targets, not maturity grades or a ranking of existing systems. L3 remains a frontier and L4–L5 are prospective. The vignettes illustrate hypothetical functions rather than measured results.

L1: Command interface—issue a discrete instruction. A person intends one action from a finite set, and the interface selects the corresponding command. In the story, the user mentally selects "move" or "stop" to position a delivery robot beside a river. Establishing L1 requires evidence of intentional selection, including the ability to withhold or cancel an action; task-correlated activity alone is insufficient.

L2: Language interface—express formulated words. The person composes a sentence internally—"Build a bridge here"—and the interface recovers it as text or speech without requiring an audible utterance. The transition from L1 is composition beyond a fixed command inventory. Large-vocabulary speech neuroprostheses provide

relevant foundations (Willett et al., 2023; Metzger et al., 2023). To establish the transition, the user should convey new combinations of words beyond learned command associations. The relevant advance is composing a new intended message, beyond selecting or repeating a familiar command.

L3: Meaning interface—convey an intention before choosing wording. The person intends that villagers should cross the river while boats remain able to pass, without needing to formulate a particular sentence. The interface helps express that meaning. The transition from L2 is abstraction from wording: different expressions can preserve the same intended distinctions. Semantic reconstruction and the perspective of moving from speech to language BCIs motivate this frontier (Tang et al., 2023; Li et al., 2026b); neither establishes voluntary meaning-level communication on its own.

The defining capability is preservation of intended relations across wording: allowing a boat to pass and blocking its passage share the same topic but express opposite requirements. An interface at this level would preserve that distinction and the user's revisions without requiring a fixed verbal formulation. Paraphrase accuracy alone cannot establish this transition: evidence must also distinguish intended meaning from covertly formulated words, for example through nonverbal elicitation and transfer to new formulations.

L4: Scenario interface—share an unfolding situation. The person imagines villagers walking across a bridge, a cargo boat approaching below, and rising water reducing the space available for passage. The interface externalises the scenario's actors, goals, relationships and changes. The transition from L3 is contextualisation: an intention is situated within a structured, evolving situation that supports predictions about what may happen. A scenario can be conveyed through language, diagrams or other representations. Multimodal brain-encoding/decoding surveys broaden the representations available for investigation (Oota et al., 2024), without establishing voluntary scenario communication.

Shared event-specific neural patterns during perception and verbal recall provide a basis for investigating scenario structure (Chen et al., 2017). They suggest that an account of an event can retain organisation across experience and recollection. Turning such representations into voluntary transmission of a new scenario remains a prospective interface objective.

The defining capability is relational and temporal structure: who acts, in what order and under which changing conditions. Changing the arrival time of the boat would change the consequences conveyed by the interface. This can be expressed in language or a diagram; a realistic image or three-dimensional object alone need not contain that scenario structure. The additional evidence concerns new combinations of actors, relations and temporal changes beyond rehearsed narratives; an output description alone does not identify the cognitive representation that produced it.

L5: Bidirectional cognitive interface—receive and develop concepts directly. The AI proposes an opening bridge and conveys that concept through a neural return channel. In this hypothetical endpoint, the person acquires meaningful content without first viewing a picture or hearing an explanation, considers it, and returns a refinement such as waiting areas on the two banks. The transition from L4 is reciprocity: content can enter as well as leave the person's cognitive process, with the user able to understand, assess, reject and revise it. Reviews of stimulation-induced speech perception address possible neural return channels (Hong et al., 2024); perceptual stimulation remains a different target from this proposed concept-level exchange.

Existing brain-to-brain demonstrations provide limited signalling precursors: EEG-derived decisions have been transmitted through distinguishable stimulation events (Grau et al., 2014; Jiang et al., 2019). These learned codes establish communication through a neural input channel at a much narrower level than the proposed direct receipt of a new concept.

L5 would require the recipient to use neurally delivered content in a new judgement and return a meaningful revision, with the content absent from audiovisual channels. Distinguishing a learned stimulation code is an important precursor; generalisable receipt of concepts remains an open long-term hypothesis. A convincing transition would require transfer to untrained content and new judgements beyond a memorised stimulation–response code.

The direction is increasing depth of exchange under the user's control: selecting an action, composing language, conveying meaning, sharing a scenario and receiving meaningful neural input. Utility remains separate from level. A reliable command interface may serve a person better than an unreliable scenario interface; the purpose of the progression is to define what additional capacity and evidence each new form of exchange requires.

10 Conclusion

Brain-to-language decoding connects neural measurements to several forms of linguistic expression. Speaking and attempting speech reveal planning and articulatory activity; listening and reading provide sensory, lexical and contextual information; inner speech shares some of these representations while retaining task-dependent differences. Across these settings, the recoverable information depends jointly on behaviour, the sampled neural populations and the measurement timescale. This relationship explains the complementary roles of recording modalities and the value of choosing a decoding target that matches the information available.

Phonetic and lexical representations support word-sequence construction, acoustic and articulatory trajectories support voice, and contextual representations support recovery of meaning across changes in wording. Pretraining and multimodal supervision increasingly connect these routes, while shared benchmarks make particular learning and inference choices directly comparable. Progress also extends beyond offline prediction: streaming feedback, adaptation and sustained use connect decoder performance to communication. Accuracy, generalisation, calibration and interaction therefore describe complementary achievements; their significance depends on the task and the conditions under which a person uses the system.

The next stage is to make these capabilities more transferable and useful for self-chosen expression. Learning from broader neural and language experience can reduce calibration, but interfaces must preserve the distinctions a user intends and make errors easy to recognise and repair. The five-level outlook extends this direction from commands and formulated language towards meaning, scenarios and a prospective neural return channel. Richer exchange will require evidence of the added capability at each transition, together with the user's ability to initiate, understand and control the communication.

Impact Statement

Speech neuroprostheses can restore communication functions for people who have lost speech. Advances in inner-speech decoding also raise questions about mental privacy, consent and the interpretation of generated content. Distinguishing cued from self-generated messages, and neural evidence from language-model assistance, is necessary for accurate public understanding of these capabilities. User authority over activation, message release and data retention should remain explicit as interfaces become more capable. Fluent output alone should not be interpreted as unrestricted access to thought.

Illustration provenance. Figures 1, 4 and 23 include conceptual artwork generated with OpenAI's image-generation tool in Codex and independently typeset labels. Anatomy, device schematics and scientific meaning were reviewed against the cited sources. These illustrations contain no participant photographs or measured data.

References

Accou, B., Bollens, L., Gillis, M., Verheijen, W., Van hamme, H., and Francart, T. SparrKULee: A Speech-Evoked Auditory Response Repository from KU Leuven, Containing the EEG of 85 Participants. *Data*, 9(8): 94, 2024. doi: 10.3390/data9080094. URL `https://doi.org/10.3390/data9080094`.

Aguilera-Rodríguez, E., Cuevas-Romero, A., Mendoza-Franco, S., Wornovitzky-Green, J., Rivera-Cerros, E., Villanueva-Cazares, D., Muñoz-Ubando, L. A., Ibarra-Zárate, D., and Alonso-Valerdi, L. M. An EEG-based imagined speech database for comparing paradigm designs. *Scientific Data*, 12(1):1644, 2025. doi: 10.1038/s41597-025-05926-5.

Akbari, H., Khalighinejad, B., Herrero, J. L., Mehta, A. D., and Mesgarani, N. Towards reconstructing intelligible speech from the human auditory cortex. *Scientific Reports*, 9(1):874, 2019. doi: 10.1038/s41598-018-37359-z.

Aldhaheri, T. A., Kulkarni, S. B., Bhise, P. R., and Tawfik, M. Utilizing machine and deep learning algorithms to identify learning-related features in electroencephalography data during second language acquisition. *Cogent Arts & Humanities*, 12(1):2485696, 2025. doi: 10.1080/23311983.2025.2485696. URL https://doi.org/10.1080/23311983.2025.2485696.

Aldhaheri, T. A., Kulkarni, S. B., and Al-Zidi, N. M. Optimizing machine learning models with multi feature selection for EEG analysis in second language acquisition research. *Discover Artificial Intelligence*, 6(1):99, 2026a. doi: 10.1007/s44163-025-00801-z. URL https://doi.org/10.1007/s44163-025-00801-z.

Aldhaheri, T. A., Tawfik, M., and Kulkarni, S. B. EEG Dataset for Second Language Acquisition Arbic and Hindi. Mendeley Data data release, 2026b. doi: 10.17632/7cdyp2r5cz.1. URL https://data.mendeley.com/datasets/7cdyp2r5cz/1.

Alexander, J. M. and Stark, B. C. Interdisciplinary approaches to understanding the inner speech, with emphasis on the role of incorporating clinical data. *European Journal of Neuroscience*, 60(5):4785–4797, 2024. doi: 10.1111/ejn.16470. URL https://doi.org/10.1111/ejn.16470.

Aliko, S., Huang, J., Gheorghiu, F., Meliss, S., and Skipper, J. I. A naturalistic neuroimaging database for understanding the brain using ecological stimuli. *Scientific Data*, 7(1), 2020. doi: 10.1038/s41597-020-00680-2. URL https://doi.org/10.1038/s41597-020-00680-2.

Allefeld, C., Görgen, K., and Haynes, J.-D. Valid population inference for information-based imaging: From the second-level t -test to prevalence inference. *NeuroImage*, 2016. doi: 10.1016/j.neuroimage.2016.07.040.

Almalah, A., Darwish, H., Al Jallad, K., and Ghneim, N. ArEEG_Chars. Mendeley Data, 2024. doi: 10.17632/f2bgr7tdtt.1. URL https://data.mendeley.com/datasets/f2bgr7tdtt/1. Version 1, published 1 November 2024.

Almufareh, M. F., Kausar, S., Humayun, M., Tehsin, S., and Farooq, A. Inner Speech Decoding: A Comprehensive Review. *WIREs Cognitive Science*, 16(6):e70016, 2025. doi: 10.1002/wcs.70016. URL https://doi.org/10.1002/wcs.70016.

Alonso-Vázquez, D., Mendoza-Montoya, O., Caraza, R., Martinez, H. R., and Antelis, J. M. From pronounced to imagined: improving speech decoding with multi-condition EEG data. *Frontiers in Neuroinformatics*, 19:1583428, 2025. doi: 10.3389/fninf.2025.1583428.

Alzahrani, S., Banjar, H., and Mirza, R. Systematic review of EEG-Based imagined speech classification methods. *Sensors*, 24(24):8168, 2024. doi: 10.3390/s24248168.

Amrani, H., Micucci, D., and Napoletano, P. Deep representation learning for open vocabulary Electroencephalography-to-Text decoding. *IEEE Journal of Biomedical and Health Informatics*, 30(4):3593–3600, 2026. doi: 10.1109/jbhi.2024.3416066.

Angrick, M., Herff, C., Mugler, E., Tate, M. C., Slutzky, M. W., Krusienski, D. J., and Schultz, T. Speech synthesis from ECoG using densely connected 3d convolutional neural networks. *Journal of Neural Engineering*, 16(3):036019, 2019. doi: 10.1088/1741-2552/ab0c59.

Angrick, M., Ottenhoff, M. C., Diener, L., Ivucic, D., Ivucic, G., Goulis, S., Saal, J., Colon, A. J., Wagner, L., Krusienski, D. J., Kubben, P. L., Schultz, T., and Herff, C. Real-time synthesis of imagined speech processes from minimally invasive recordings of neural activity. *Communications Biology*, 4(1):1055, 2021. doi: 10.1038/s42003-021-02578-0.

Angrick, M., Luo, S., Rabbani, Q., Candrea, D. N., Shah, S., Milsap, G. W., Anderson, W. S., Gordon, C. R., Rosenblatt, K. R., Clawson, L., Tippett, D. C., Maragakis, N., Tenore, F. V., Fifer, M. S., Hermansky, H., Ramsey, N. F., and Crone, N. E. Online speech synthesis using a chronically implanted brain–computer interface in an individual with ALS. *Scientific Reports*, 14(1):9617, 2024. doi: 10.1038/s41598-024-60277-2.

Anumanchipalli, G. K., Chartier, J., and Chang, E. F. Speech synthesis from neural decoding of spoken sentences. *Nature*, 568(7753):493–498, 2019. doi: 10.1038/s41586-019-1119-1.

Armeni, K., Güçlü, U., van Gerven, M., and Schoffelen, J.-M. A 10-hour within-participant magnetoencephalography narrative dataset to test models of language comprehension. *Scientific Data*, 9(1), 2022. doi: 10.1038/s41597-022-01382-7. URL https://doi.org/10.1038/s41597-022-01382-7.

Avramidis, K., Feng, T., Jeong, W., Lee, J., Cui, W., Leahy, R. M., and Narayanan, S. Neural codecs as biosignal tokenizers, 2025. doi: 10.48550/arXiv.2510.09095. URL https://arxiv.org/abs/2510.09095.

Baylor, C., Yorkston, K., Eadie, T., Kim, J., Chung, H., and Amtmann, D. The communicative participation item bank (cpib): Item bank calibration and development of a disorder-generic short form. *Journal of Speech, Language, and Hearing Research*, 2013. doi: 10.1044/1092-4388(2012/12-0140). URL https://pmc.ncbi.nlm.nih.gov/articles/PMC4377222/.

Bel, C., Bonnaire, J., King, J.-R., and Pallier, C. LittlePrince_MEG_French_Read_Pallier2025. OpenNeuro dataset release, 2026a. URL https://github.com/OpenNeuroDatasets/ds007524. Year follows the public dataset repository history, not the year embedded in its dataset name.

Bel, C., Bonnaire, J., Pallier, C., and King, J.-R. LittlePrince_MEG_French_Listen_Pallier2025. OpenNeuro dataset release, 2026b. URL https://github.com/OpenNeuroDatasets/ds007523. Year follows the public dataset repository history, not the year embedded in its dataset name.

Belfrouh, S., Salmam, F. Z., Errattahi, R., Hanine, M., Obidallah, W. J., and Alhulayyil, H. Artificial intelligence for brain-to-speech decoding in paralysis: a systematic review. *BMC Medical Informatics and Decision Making*, 26(1):272, 2026. doi: 10.1186/s12911-026-03552-8. URL https://doi.org/10.1186/s12911-026-03552-8.

Berezutskaya, J., Vansteensel, M. J., Aarnoutse, E. J., Freudenburg, Z. V., Piantoni, G., Branco, M. P., and Ramsey, N. F. Open multimodal iEEG-fMRI dataset from naturalistic stimulation with a short audiovisual film. *Scientific Data*, 9(1), 2022. doi: 10.1038/s41597-022-01173-0. URL https://doi.org/10.1038/s41597-022-01173-0.

Berezutskaya, J., Freudenburg, Z. V., Vansteensel, M. J., Aarnoutse, E. J., Ramsey, N. F., and van Gerven, M. A. J. Direct speech reconstruction from sensorimotor brain activity with optimized deep learning models. *Journal of Neural Engineering*, 20(5):056010, 2023. doi: 10.1088/1741-2552/ace8be.

Bhadra, K., Giraud, A.-L., and Marchesotti, S. Learning to operate an imagined speech Brain-Computer interface involves the spatial and frequency tuning of neural activity. *Communications Biology*, 8(1):271, 2025. doi: 10.1038/s42003-025-07464-7.

Bian, C., Yang, J., Xie, M., He, J., Sun, Y. H. S., Zhao, J., Chen, Z., Lai, H.-Y., Yuan, Z., Wang, Y., and Qiu, Z. Characterizing the spatiotemporal boundaries of functional ultrasound for brain decoding, 2026. doi: 10.64898/2026.08.30.748086. Preprint.

Bimbard, C., Demene, C., Girard, C., Radtke-Schuller, S., Shamma, S., Tanter, M., and Boubenec, Y. Multi-scale mapping along the auditory hierarchy using high-resolution functional UltraSound in the awake ferret. *eLife*, 7:e35028, 2018. doi: 10.7554/elife.35028.

Blakely, T., Miller, K. J., Rao, R. P., Holmes, M. D., and Ojemann, J. G. Localization and classification of phonemes using high spatial resolution electrocorticography (ECoG) grids. In *2008 30th Annual International Conference of the IEEE Engineering in Medicine and Biology Society*, pp. 4964–4967. IEEE, 2008. doi: 10.1109/iembs.2008.4650328.

Boddapu, L., Likhitha, C., S, P. S., Sunil, N., Sumitra, S., and BS, M. IIST BCI Dataset-8 for Selected Common Telugu words. Preprint, 2024. doi: 10.36227/techrxiv.172417996.61924642/v1. URL https://doi.org/10.36227/techrxiv.172417996.61924642/v1.

Boddapu, L., Sumitra, S., and BS, M. IIST BCI Dataset-10 for Telugu Vowels and Consonants. Preprint, 2025. doi: 10.36227/techrxiv.174612068.80718242/v1. URL https://doi.org/10.36227/techrxiv.174612068.80718242/v1.

Bouchard, K. E., Mesgarani, N., Johnson, K., and Chang, E. F. Functional organization of human sensorimotor cortex for speech articulation. *Nature*, 2013. doi: 10.1038/nature11911. URL https://doi.org/10.1038/nature11911.

Bourguignon, M., Baart, M., Kapnoula, E. C., and Molinaro, N. Lip-reading enables the brain to synthesize auditory features of unknown silent speech. *The Journal of Neuroscience*, 40(5):1053–1065, 2020. doi: 10.1523/jneurosci.1101-19.2019.

Branco, M. P., Pels, E. G. M., Sars, R. H., Aarnoutse, E. J., Ramsey, N. F., Vansteensel, M. J., and Nijboer, F. Brain-Computer Interfaces for Communication: Preferences of Individuals With Locked-in Syndrome. *Neurorehabilitation and Neural Repair*, 2021. doi: 10.1177/1545968321989331. URL https://doi.org/10.1177/1545968321989331.

Bras, C., Patel, T., and Scharenborg, O. Using articulated speech EEG signals for imagined speech decoding. In *Interspeech 2024*, pp. 407–411. ISCA, 2024. doi: 10.21437/interspeech.2024-1289.

Brennan, J. R. and Hale, J. T. Hierarchical structure guides rapid linguistic predictions during naturalistic listening. *PLOS ONE*, 14(1):e0207741, 2019. doi: 10.1371/journal.pone.0207741. URL https://doi.org/10.1371/journal.pone.0207741.

Broderick, M. P., Anderson, A. J., Di Liberto, G. M., Crosse, M. J., and Lalor, E. C. Electrophysiological Correlates of Semantic Dissimilarity Reflect the Comprehension of Natural, Narrative Speech. *Current Biology*, 28(5):803–809.e3, 2018. doi: 10.1016/j.cub.2018.01.080. URL https://doi.org/10.1016/j.cub.2018.01.080.

Brosler, S. C., Liu, J. R., Silva, A. B., Hallinan, I. P., Kurtz-Miott, C. M., Dunkel Wilker, J. F. B., Tu-Chan, A., Ganguly, K., and Chang, E. F. Simultaneous speech and gesture decoding for multimodal communication in paralysis. *Nature Neuroscience*, September 2026. doi: 10.1038/s41593-026-02446-2. URL https://www.nature.com/articles/s41593-026-02446-2. Published online 14 September 2026.

Brumberg, J. S., Wright, E. J., Andreasen, D. S., Guenther, F. H., and Kennedy, P. R. Classification of intended phoneme production from chronic intracortical microelectrode recordings in speech-motor cortex. *Frontiers in Neuroscience*, 5, 2011. doi: 10.3389/fnins.2011.00065.

Brumberg, J. S., Pitt, K. M., and Burnison, J. D. A noninvasive Brain-Computer interface for Real-Time speech synthesis: The importance of multimodal feedback. *IEEE Transactions on Neural Systems and Rehabilitation Engineering*, 26(4):874–881, 2018. doi: 10.1109/tnsre.2018.2808425.

Bröhl, F., Keitel, A., and Kayser, C. MEG Activity in Visual and Auditory Cortices Represents Acoustic Speech-Related Information during Silent Lip Reading. *eNeuro*, 2022. doi: 10.1523/ENEURO.0209-22.2022. URL https://doi.org/10.1523/ENEURO.0209-22.2022.

Bush, A., Chrabaszcz, A., Peterson, V., Saravanan, V., Dastolfo-Hromack, C., Lipski, W. J., and Richardson, R. M. Differentiation of speech-induced artifacts from physiological high gamma activity in intracranial recordings. *NeuroImage*, 2022. doi: 10.1016/j.neuroimage.2022.118962. URL https://doi.org/10.1016/j.neuroimage.2022.118962.

Bálint, A., Wimmer, W., Rummel, C., Caversaccio, M., and Weder, S. An fNIRS dataset for multimodal speech comprehension in normal hearing individuals and cochlear implant users. *Scientific Data*, 12(1):1305, 2025a. doi: 10.1038/s41597-025-05654-w. URL https://doi.org/10.1038/s41597-025-05654-w.

Bálint, A., Wimmer, W., Rummel, C., Caversaccio, M., and Weder, S. An fNIRS dataset for multimodal speech comprehension in normal hearing individuals and cochlear implant users. Dryad data release, 2025b. doi: 10.5061/dryad.crjdfn3g9. URL https://datadryad.org/dataset/doi:10.5061/dryad.crjdfn3g9.

Cai, J., Kfir, Y., Jamali, M., Huang, H., Kim, Y. J., Cash, S. S., and Williams, Z. M. Mapping the neuronal building blocks of human language with language models. *Nature*, 656(8127):425–433, 2026. doi: 10.1038/s41586-026-10691-5. URL https://doi.org/10.1038/s41586-026-10691-5.

Cao, L., Huang, D., Zhang, Y., Jiang, X., and Chen, Y. Brain Decoding Using fNIRS. *Proceedings of the AAAI Conference on Artificial Intelligence*, 2021. doi: 10.1609/aaai.v35i14.17493. URL https://doi.org/10.1609/aaai.v35i14.17493.

Card, N., Wairagkar, M., Iacobacci, C., Hou, X., Singer-Clark, T., Willett, F., Kunz, E., Fan, C., Vahdati Nia, M., Deo, D., Srinivasan, A., Choi, E. Y., Glasser, M., Hochberg, L., Henderson, J., Shahlaie, K., Stavisky, S., and Brandman, D. Data for: An accurate and rapidly calibrating speech neuroprosthesis. Dryad data release, version 5, 2025. doi: 10.5061/dryad.dncjsxm85. URL https://datadryad.org/dataset/doi:10.5061/dryad.dncjsxm85. Version published 3 July 2025; includes the T15 neural data used in Brain-to-Text 2025.

Card, N. S., Wairagkar, M., Iacobacci, C., Hou, X., Singer-Clark, T., Willett, F. R., Kunz, E. M., Fan, C., Vahdati Nia, M., Deo, D. R., Srinivasan, A., Choi, E. Y., Glasser, M. F., Hochberg, L. R., Henderson, J. M., Shahlaie, K., Stavisky, S. D., and Brandman, D. M. An accurate and rapidly calibrating speech neuroprosthesis. *New England Journal of Medicine*, 391(7):609–618, 2024. doi: 10.1056/nejmoa2314132.

Card, N. S., Singer-Clark, T., Peracha, H., Iacobacci, C., Hou, X., Wairagkar, M., Fogg, Z., Offenberg, E. C., Hochberg, L. R., Stavisky, S. D., and Brandman, D. M. Long-term independent use of an intracortical brain–computer interface for speech and cursor control. *Nature Medicine*, 32(7):2504–2510, 2026. doi: 10.1038/s41591-026-04414-6.

Carvalho, V. R., Mendes, E. M. A. M., Fallah, A., Sejnowski, T. J., Comstock, L., and Lainscsek, C. Decoding imagined speech with delay differential analysis. *Frontiers in Human Neuroscience*, 18:1398065, 2024. doi: 10.3389/fnhum.2024.1398065.

Chandra, S. S., Cai, Z., Tsao, Y., King, S., and Sisman, B. Brain2speech-net: Intelligible, Real-Time Brain-to-Speech synthesis without text decoding, 2026. doi: 10.48550/ARXIV.2609.04455.

Chartier, J., Anumanchipalli, G. K., Johnson, K., and Chang, E. F. Encoding of articulatory kinematic trajectories in human speech sensorimotor cortex. *Neuron*, 98(5):1042–1054.e4, 2018. doi: 10.1016/j.neuron.2018.04.031. URL https://pubmed.ncbi.nlm.nih.gov/29779940/.

Chen, C., Dupré la Tour, T., Gallant, J. L., Klein, D., and Deniz, F. The cortical representation of language timescales is shared between reading and listening. *Communications Biology*, 7:284, 2024a. doi: 10.1038/s42003-024-05909-z. URL https://doi.org/10.1038/s42003-024-05909-z.

Chen, J., Leong, Y. C., Honey, C. J., Yong, C. H., Norman, K. A., and Hasson, U. Shared memories reveal shared structure in neural activity across individuals. *Nature Neuroscience*, 2017. doi: 10.1038/nn.4450. URL https://www.nature.com/articles/nn.4450.

Chen, J., Chen, X., Wang, R., Le, C., Khalilian-Gourtani, A., Jensen, E., Dugan, P., Doyle, W., Devinsky, O., Friedman, D., Flinker, A., and Wang, Y. Transformer-based neural speech decoding from surface and depth electrode signals. *Journal of Neural Engineering*, 22(1):016017, 2025a. doi: 10.1088/1741-2552/adab21.

Chen, S., Li, B., He, C., Li, D., Wu, M., Shen, X., Wang, S., Wei, X., Wang, X., Wu, H., and Liu, Q. An EEG Dataset for Multimodal Semantic Alignment and Neural Decoding during Reading and Listening. *Scientific Data*, 13(1), 2025b. doi: 10.1038/s41597-025-06466-8. URL https://doi.org/10.1038/s41597-025-06466-8.

Chen, X., Wang, R., Khalilian-Gourtani, A., Yu, L., Dugan, P., Friedman, D., Doyle, W., Devinsky, O., Wang, Y., and Flinker, A. A neural speech decoding framework leveraging deep learning and speech synthesis. *Nature Machine Intelligence*, 6(4):467–480, 2024b. doi: 10.1038/s42256-024-00824-8.

Chen, X., Du, C., Liu, C., Wang, Y., and He, H. BP-GPT: Auditory neural decoding using fMRI-prompted LLM, 2025c. doi: 10.48550/arXiv.2502.15172. URL https://arxiv.org/abs/2502.15172.

Chen, Y.-P., Schmidt, F., Keitel, A., Rösch, S., Hauswald, A., and Weisz, N. Speech intelligibility changes the temporal evolution of neural speech tracking. *NeuroImage*, 268:119894, 2023. doi: 10.1016/j.neuroimage.2023.119894. URL https://doi.org/10.1016/j.neuroimage.2023.119894.

Chen, Y.-P., Schmidt, F., Keitel, A., Rösch, S., Hauswald, A., and Weisz, N. MEG dataset of continuous speech with five-level noise vocoding. Austrian NeuroCloud data release, 2026. doi: 10.60817/v2fd-cq35. URL https://doi.org/10.60817/v2fd-cq35.

Chen, Z., Li, N., Xi, C., He, J., Zhu, J., Wu, G., Xia, J., Fei, C., Sun, L., Xu, H., and Qiu, Z. Functional ultrasound imaging of auditory responses in comatose patients. *Research*, 8:0709, 2025d. doi: 10.34133/research.0709.

Chowdhury, A. T., Hassanein, A., Al Shibli, A. N., Khanafer, Y., AbuHaweeleh, M. N., Pedersen, S., and Chowdhury, M. E. H. Neural signals, machine learning, and the future of inner speech recognition. *Frontiers in Human Neuroscience*, 19:1637174, 2025a. doi: 10.3389/fnhum.2025.1637174. URL https://doi.org/10.3389/fnhum.2025.1637174.

Chowdhury, M. E. H., Sarmun, R., Bushnaq, D., Chabbouh, M., Aljindi, R., Pedersen, S., Faisal, M. A. A., Nahid, N., Hassan, I., and Garcia, C. Summary of the Silent Speech Decoding Challenge Using EEG Data for Arabic Inner Speech Recognition. *International Journal of Activity and Behavior Computing*, 2025(2): 1–21, 2025b. doi: 10.60401/ijabc.104. URL https://www.jstage.jst.go.jp/article/ijabc/2025/2/2025_104/_article.

Collautti, E., Mao, X., Tonin, L., Tortora, S., and Puthusserypady, S. Rag-based EEG-to-Text translation using deep learning and LLMs, 2026. doi: 10.48550/ARXIV.2605.17503.

Combrisson, E. and Jerbi, K. Exceeding chance level by chance: The caveat of theoretical chance levels in brain signal classification and statistical assessment of decoding accuracy. *Journal of Neuroscience Methods*, 2015. doi: 10.1016/j.jneumeth.2015.01.010. URL https://www.sciencedirect.com/science/article/pii/S0165027015000114.

Cooney, C., Folli, R., and Coyle, D. A bimodal deep learning architecture for EEG-fNIRS decoding of overt and imagined speech. *IEEE Transactions on Biomedical Engineering*, 69(6):1983–1994, 2022. doi: 10.1109/tbme.2021.3132861.

Craik, A., Dial, H., and L Contreras-Vidal, J. Continuous and discrete decoding of overt speech with scalp electroencephalography (EEG). *Journal of Neural Engineering*, 22(2):026017, 2025. doi: 10.1088/1741-2552/ad8d0a.

Csaky, R., van Es, M. W., Jones, O. P., and Woolrich, M. Towards decoding inner speech from EEG and MEG, 2025. doi: 10.1101/2025.10.13.682161. Preprint.

Cui, W., Jeong, W., Thölke, P., Medani, T., Jerbi, K., Joshi, A. A., and Leahy, R. M. Neuro-GPT: Towards a foundation model for EEG. In *2024 IEEE International Symposium on Biomedical Imaging (ISBI)*, 2024. URL https://arxiv.org/abs/2311.03764v4.

Dahò, M. and Monzani, D. The multifaceted nature of inner speech: Phenomenology, neural correlates, and implications for aphasia and psychopathology. *Cognitive Neuropsychology*, 42(1-2):1–21, 2025. doi: 10.1080/02643294.2025.2527983. URL https://doi.org/10.1080/02643294.2025.2527983.

Darwish, H., Almalah, A., Al Jallad, K., and Ghneim, N. ArEEG_Words. Mendeley Data, 2024a. doi: 10.17632/7m472ykkx7.1. URL https://data.mendeley.com/datasets/7m472ykkx7/1. Version 1, published 2 December 2024.

Darwish, H., Malah, A. A., Jallad, K. A., and Ghneim, N. Areeg_chars: Dataset for envisioned speech recognition using EEG for Arabic characters, 2024b. doi: 10.48550/ARXIV.2402.15733.

Darwish, H., Malah, A. A., Jallad, K. A., and Ghneim, N. Areeg_words: Dataset for envisioned speech recognition using EEG for Arabic words, 2024c. doi: 10.48550/ARXIV.2411.18888.

Das, N., Francart, T., and Bertrand, A. Auditory Attention Detection Dataset KULeuven. Zenodo data release, 2019. doi: 10.5281/zenodo.4004271. URL https://zenodo.org/doi/10.5281/zenodo.4004271.

DaSalla, C. S., Kambara, H., Sato, M., and Koike, Y. Single-trial classification of vowel speech imagery using common spatial patterns. *Neural Networks*, 22(9):1334–1339, 2009. doi: 10.1016/j.neunet.2009.05.008.

Dash, D., Ferrari, P., and Wang, J. Decoding imagined and spoken phrases from non-invasive neural (MEG) signals. *Frontiers in Neuroscience*, 14:290, 2020. doi: 10.3389/fnins.2020.00290.

Dash, D., Ferrari, P., and Wang, J. Neural decoding of spontaneous overt and intended speech. *Journal of Speech, Language, and Hearing Research*, 67(11):4216–4225, 2024. doi: 10.1044/2024_jslhr-24-00046.

de Borman, A., Wittevrongel, B., Dauwe, I., Carrette, E., Meurs, A., Van Roost, D., Boon, P., and Van Hulle, M. M. Imagined speech event detection from electrocorticography and its transfer between speech modes and subjects. *Communications Biology*, 7(1):818, 2024. doi: 10.1038/s42003-024-06518-6.

de Borman, A., Wittevrongel, B., Van Dyck, B., Van Rooy, K., Carrette, E., Meurs, A., Van Roost, D., and Van Hulle, M. M. Speech mode classification from electrocorticography: transfer between electrodes and participants. *Journal of Neural Engineering*, 22(4):046033, 2025. doi: 10.1088/1741-2552/adf2de.

de Borman, A., Dyck, B. V., Rooy, K. V., Carrette, E., Meurs, A., Roost, D. V., and Van Hulle, M. M. Word classification across speech modes from low-density electrocorticography signals. *Journal of Neural Engineering*, 23(1):016016, 2026. doi: 10.1088/1741-2552/ae3a1b.

Defenderfer, J. Defenderfer 2019; fNIRS data files for event-related vocoding/background noise study. Mendeley data release, 2019. doi: 10.17632/4cjgvyg5p2.1. URL https://data.mendeley.com/datasets/4cjgvyg5p2/1.

Defenderfer, J., Forbes, S., Wijeakumar, S., Hedrick, M., Plyler, P., and Buss, A. T. Frontotemporal activation differs between perception of simulated cochlear implant speech and speech in background noise: An image-based fNIRS study. *NeuroImage*, 240:118385, 2021. doi: 10.1016/j.neuroimage.2021.118385. URL https://doi.org/10.1016/j.neuroimage.2021.118385.

Degenhart, A. D., Bishop, W. E., Oby, E. R., Tyler-Kabara, E. C., Chase, S. M., Batista, A. P., and Yu, B. M. Stabilization of a brain–computer interface via the alignment of low-dimensional spaces of neural activity. *Nature Biomedical Engineering*, 2020. doi: 10.1038/s41551-020-0542-9. URL https://www.nature.com/articles/s41551-020-0542-9.

Dekker, B., Schouten, A. C., and Scharenborg, O. Dais: The delft database of EEG recordings of Dutch articulated and imagined speech. In *ICASSP 2023 - 2023 IEEE International Conference on Acoustics, Speech and Signal Processing (ICASSP)*, pp. 1–5. IEEE, 2023. doi: 10.1109/icassp49357.2023.10096145.

Deng, S., Srinivasan, R., Lappas, T., and D' Zmura, M. Eeg classification of imagined syllable rhythm using Hilbert spectrum methods. *Journal of Neural Engineering*, 7(4):046006, 2010. doi: 10.1088/1741-2560/7/4/046006.

Derakhshesh, A., Dehghanian, Z., Ebrahimpour, R., and Rabiee, H. R. Cueless EEG imagined speech for subject identification: dataset and benchmarks. arXiv preprint, 2025. doi: 10.48550/arxiv.2501.09700. URL https://arxiv.org/abs/2501.09700.

Divya Keerthana, K., Ramakrishnan, S., Abraham, G. K., Vandana, V. P., Agrawal, N., Raghavendra, K., and Rao, M. Decoding of imagined speech using EEG: An overview of techniques, applications, and challenges. *IEEE Access*, 14:102454–102472, 2026. doi: 10.1109/access.2026.3708197.

Dizeux, A., Gesnik, M., Ahnine, H., Blaize, K., Arcizet, F., Picaud, S., Sahel, J.-A., Deffieux, T., Pouget, P., and Tanter, M. Functional ultrasound imaging of the brain reveals propagation of task-related brain activity in behaving primates. *Nature Communications*, 10(1):1400, 2019. doi: 10.1038/s41467-019-09349-w.

Doda, D. Y., He, R., Pang, M., Sun, Y., Li, C., Anwar, F., Yasi, A., Jiang, R., Wang, W., Ming, D., and Liu, X. Speech brain–computer interfaces for communication rehabilitation: State-of-the-art decoding models, clinical applications, and ethical challenges. *Journal of Intelligent Medicine*, 2(3):122–133, 2025. doi: 10.1002/jim4.70012. URL https://doi.org/10.1002/jim4.70012.

Dohle, E., Swanson, E., Jovanovic, L., Yusuf, S., Thompson, L., Horsfall, H. L., Muirhead, W., Bashford, L., and Brannigan, J. Toward the Clinical Translation of Implantable Brain–Computer Interfaces for Motor Impairment: Research Trends and Outcome Measures. *Advanced Science*, 12(32):e01912, 2025. doi: 10.1002/advs.202501912. URL https://doi.org/10.1002/advs.202501912.

Duan, Y., Zhou, J., Wang, Z., Wang, Y.-K., and Lin, C.-T. DeWave: Discrete encoding of EEG waves for EEG to text translation. In *Advances in Neural Information Processing Systems 36*, pp. 9907–9918. Neural Information Processing Systems Foundation, Inc. (NeurIPS), 2023. doi: 10.52202/075280-0432.

Duhair, H. T. M., Ibrahim, M. B. M., Farid, M., Alsayaydeh, J. A. J., and Herawan, S. G. EEG-Based Imagined-Speech Decoding: A Review. *International Journal of Advanced Computer Science and Applications*, 17(1), 2026. doi: 10.14569/IJACSA.2026.0170136. URL https://doi.org/10.14569/IJACSA.2026.0170136.

Duraivel, S., Rahimpour, S., Chiang, C.-H., Trumpis, M., Wang, C., Barth, K., Harward, S. C., Lad, S. P., Friedman, A. H., Southwell, D. G., Sinha, S. R., Viventi, J., and Cogan, G. B. High-resolution neural recordings improve the accuracy of speech decoding. *Nature Communications*, 14(1):6938, 2023. doi: 10.1038/s41467-023-42555-1.

Défossez, A., Caucheteux, C., Rapin, J., Kabeli, O., and King, J.-R. Decoding speech perception from non-invasive brain recordings. *Nature Machine Intelligence*, 5(10):1097–1107, 2023. doi: 10.1038/s42256-023-00714-5.

d' Ascoli, S., Bel, C., Rapin, J., Banville, H., Benchetrit, Y., Pallier, C., and King, J.-R. Towards decoding individual words from non-invasive brain recordings. *Nature Communications*, 16(1):10521, 2025. doi: 10.1038/s41467-025-65499-0.

El Ouahidi, Y., Lys, J., Thölke, P., Farrugia, N., Pasdeloup, B., Gripon, V., Jerbi, K., and Lioi, G. REVE: A foundation model for EEG – adapting to any setup with large-scale pretraining on 25,000 subjects. In *Advances in Neural Information Processing Systems*, volume 38, 2025. doi: 10.52202/085713-0760. URL https://papers.neurips.cc/paper_files/paper/2025/hash/20a917f77773ac0fa8bea2bdd6606b66-Abstract-Conference.html.

Estrella-Ibarra, L. F., García-Noguez, L. R., Pedraza-Ortega, J. C., Ramos-Arreguín, J. M., and Tovar-Arriaga, S. Lost in Thought: An End-to-End Systematic Review on Imagined Speech Decoding Through Electroencephalographic Readings. *AI*, 7(2):75, 2026. doi: 10.3390/ai7020075. URL https://doi.org/10.3390/ai7020075.

Fedorenko, E., Scott, T. L., Brunner, P., Coon, W. G., Pritchett, B., Schalk, G., and Kanwisher, N. Neural correlate of the construction of sentence meaning. *Proceedings of the National Academy of Sciences*, 113(41), 2016. doi: 10.1073/pnas.1612132113. URL https://doi.org/10.1073/pnas.1612132113.

Feghhi, E., Kaasyap, S., Hadidi, N., and Kao, J. C. Time-masked transformers with lightweight test-time adaptation for neural speech decoding, 2025. doi: 10.48550/arXiv.2507.02800. URL https://arxiv.org/abs/2507.02800v2.

Feghhi, E., Hu, J., Hadidi, N., and Kao, J. C. LightBeam: An accurate and memory-efficient CTC decoder for speech neuroprostheses, 2026. doi: 10.48550/arXiv.2603.14002. URL https://arxiv.org/abs/2603.14002v1. Version 1, 14 March 2026.

Feng, C., Cao, L., Wu, D., Zhang, E., Wang, T., Jiang, X., Chen, J., Wu, H., Lin, S., Hou, Q., Zhu, J., Yang, J., Sawan, M., and Zhang, Y. Acoustic inspired Brain-to-Sentence decoder for logosyllabic language. *Cyborg and Bionic Systems*, 6:0257, 2025. doi: 10.34133/cbsystems.0257.

Feng, X., Feng, X., Qin, B., and Liu, T. Aligning semantic in brain and language: A curriculum contrastive method for Electroencephalography-to-Text generation. *IEEE Transactions on Neural Systems and Rehabilitation Engineering*, 31:3874–3883, 2023. doi: 10.1109/tnsre.2023.3314642.

Fischer, T., Middell, E., Moradi, S., and von Lühmann, A. fNIRS single-trial decoding improves systematically with higher optode density, model-based noise regression, and image reconstruction. *Journal of Neural Engineering*, 2026. doi: 10.1088/1741-2552/ae782f. URL https://doi.org/10.1088/1741-2552/ae782f.

Fischl, B., Sereno, M. I., Tootell, R. B. H., and Dale, A. M. High-resolution intersubject averaging and a coordinate system for the cortical surface. *Human Brain Mapping*, 8(4):272–284, 1999. doi: 10.1002/(SICI)1097-0193(1999)8:4<272::AID-HBM10>3.0.CO;2-4.

Fogg, Z. M., Card, N. S., Wairagkar, M., Srinivasan, A., Singer-Clark, T., Hou, X., Okorokova, E., Peracha, H., Iacobacci, C., Brailow, T., Jude, J., Levi-Aharoni, H., Le, T., Mifsud, D., Deevi, P. I., Nason-Tomaszewski, S. R., Pritchard, A. L., Zhang, Y., Richards, B., Bechefsky, P., Hochberg, L. R., Williams, Z., Shahlaie, K., AuYong, N., Rubin, D. B., Pandarinath, C., Brandman, D. M., and Stavisky, S. D. A generalizable speech neuroprosthesis, 2026. doi: 10.64898/2026.07.23.739430. Preprint.

Friedrichs, D., Vyshnevetska, V., Lancheros, M., Bolt, E., Dellwo, V., and Moran, S. A multimodal speech-production dataset with time-aligned articulography, EEG, audio, and vocal-tract anatomy. *Scientific Data*, 13(1), 2026. doi: 10.1038/s41597-026-07704-3. URL https://doi.org/10.1038/s41597-026-07704-3.

Fuglsang, S. A., Wong, D. D., and Hjortkjær, J. EEG and audio dataset for auditory attention decoding. Zenodo data release, 2018. doi: 10.5281/zenodo.1199011. URL https://zenodo.org/record/1199011.

Gao, T. Decoding the Brain for Communication: A Review of Brain-to-Text, Brain-to-Speech, and Brain-to-Image Interfaces. *BIO Web of Conferences*, 237:03002, 2026. doi: 10.1051/bioconf/202623703002. URL https://doi.org/10.1051/bioconf/202623703002.

Gao, W., Wang, Y., Ma, Y., Yang, C., Li, W., and You, C. NeuroSonic: Conditional flow matching for EEG-to-speech reconstruction. arXiv preprint arXiv:2606.24087, 2026. doi: 10.48550/arXiv.2606.24087. URL https://arxiv.org/abs/2606.24087v1.

Gedawy, M. E., Nabil, O., Mamdouh, O., Nady, M., Adel, N. A., and Fares, A. Bridging brain signals and language: A deep learning approach to EEG-to-Text decoding, 2025. doi: 10.48550/ARXIV.2502.17465.

Geetha, S., Thrisha, M., Gowda, V., and Varsha, K. The Neuro-Linguistic Frontier: A Review of Brain-to-Text Technologies and Their Application in Restoring Communication Aids. In *2025 International Conference on Computational Innovations and Sustainable Technologies (ICCIST)*, pp. 1–6, 2025. doi: 10.1109/ICCIST67338.2025.11438651. URL https://doi.org/10.1109/ICCIST67338.2025.11438651.

Geirnaert, S., Kappel, S. L., and Kidmose, P. Ear-SAAD dataset. Zenodo data release, 2025a. doi: 10.5281/zenodo.16536441. URL https://zenodo.org/doi/10.5281/zenodo.16536441.

Geirnaert, S., Kappel, S. L., and Kidmose, P. A direct comparison of simultaneously recorded scalp, around-ear and in-ear EEG for neural selective auditory attention decoding to speech. *Scientific Reports*, 2025b. doi: 10.1038/s41598-025-25576-2. URL https://doi.org/10.1038/s41598-025-25576-2.

Geng, Z., Deng, M., Bai, X., Kolter, J. Z., and He, K. Mean flows for one-step generative modeling. arXiv preprint arXiv:2505.13447, 2025. doi: 10.48550/arXiv.2505.13447. URL https://arxiv.org/abs/2505.13447.

Gonzalez, J. E., Nieto, N., Brusco, P., Gravano, A., and Kamienkowski, J. E. Speech-induced suppression during natural dialogues. *Communications Biology*, 7(1), 2024. doi: 10.1038/s42003-024-05945-9. URL https://doi.org/10.1038/s42003-024-05945-9.

Grandchamp, R., Rapin, L., Perrone-Bertolotti, M., Pichat, C., Haldin, C., Cousin, E., Lachaux, J.-P., Dohen, M., Perrier, P., Garnier, M., Baciu, M., and Lœvenbruck, H. The ConDialInt Model: Condensation, Dialogality, and Intentionality Dimensions of Inner Speech Within a Hierarchical Predictive Control Framework. *Frontiers in Psychology*, 2019. doi: 10.3389/fpsyg.2019.02019. URL https://doi.org/10.3389/fpsyg.2019.02019.

Grau, C., Ginhoux, R., Riera, A., Nguyen, T. L., Chauvat, H., Berg, M., Amengual, J. L., Pascual-Leone, A., and Ruffini, G. Conscious brain-to-brain communication in humans using non-invasive technologies. *PLoS ONE*, 2014. doi: 10.1371/journal.pone.0105225. URL https://journals.plos.org/plosone/article?id=10.1371/journal.pone.0105225.

Griggs, W. S., Norman, S. L., Deffieux, T., Segura, F., Osmanski, B.-F., Chau, G., Christopoulos, V., Liu, C., Tanter, M., Shapiro, M. G., and Andersen, R. A. Decoding motor plans using a closed-loop ultrasonic brain–machine interface. *Nature Neuroscience*, 27(1):196–207, 2024. doi: 10.1038/s41593-023-01500-7.

Guenther, F. H., Brumberg, J. S., Wright, E. J., Nieto-Castanon, A., Tourville, J. A., Panko, M., Law, R., Siebert, S. A., Bartels, J. L., Andreasen, D. S., Ehirim, P., Mao, H., and Kennedy, P. R. A wireless Brain-Machine interface for Real-Time speech synthesis. *PLoS ONE*, 4(12):e8218, 2009. doi: 10.1371/journal.pone.0008218.

Gui, Y., Chen, M., Su, Y., Luo, G., and Yang, Y. EEGMamba: Bidirectional state space model with mixture of experts for EEG multi-task classification, 2024. doi: 10.48550/arXiv.2407.20254. URL https://arxiv.org/abs/2407.20254.

Guo, Z. and Chen, F. Decoding lexical tones and vowels in imagined tonal monosyllables using fNIRS signals. *Journal of Neural Engineering*, 19(6):066007, 2022. doi: 10.1088/1741-2552/ac9e1d.

Guo, Z., Xu, L., Tan, W., and Chen, F. Impact of generation rate of speech imagery on neural activity and BCI decoding performance: A fNIRS study. *IEEE Transactions on Neural Systems and Rehabilitation Engineering*, 33:1180–1190, 2025. doi: 10.1109/tnsre.2025.3552606.

Gwilliams, L., Flick, G., Marantz, A., Pylkkänen, L., Poeppel, D., and King, J.-R. Introducing MEG-MASC a high-quality magneto-encephalography dataset for evaluating natural speech processing. *Scientific Data*, 10 (1):862, 2023. doi: 10.1038/s41597-023-02752-5.

Habersetzer, T. and Meyer, B. T. MEG-SCANS - A comprehensive magnetoencephalography speech dataset with Stories, Chirps And Noisy Sentences. OpenNeuro data release, version 1.1.2, 2025. doi: 10.18112/openneuro.ds006468.v1.1.2. URL https://openneuro.org/datasets/ds006468/versions/1.1.2.

Habersetzer, T., Steuer, S., Radeloff, A., and Meyer, B. T. Meg-scans - a comprehensive magnetoencephalography speech dataset with stories, chirps and noisy sentences. *Scientific Data*, 12(1):1938, 2025. doi: 10.1038/s41597-025-06397-4.

Hanke, M., Baumgartner, F. J., Ibe, P., Kaule, F. R., Pollmann, S., Speck, O., Zinke, W., and Stadler, J. A high-resolution 7-Tesla fMRI dataset from complex natural stimulation with an audio movie. *Scientific Data*, 1(1), 2014. doi: 10.1038/sdata.2014.3. URL https://doi.org/10.1038/sdata.2014.3.

Hanke, M., Adelhöfer, N., Kaule, F. R., Sengupta, A., Guntupalli, J. S., Häusler, C., Hoffmann, M., Baumgartner, F. J., and Stadler, J. Studyforrest-Data-Phase2: First Public Release. Zenodo data release, 2016. doi: 10.5281/zenodo.48421. URL https://zenodo.org/record/48421.

He, D., Siok, W. T., and Wang, N. Toward Robust, Reproducible, and Widely Accessible Intracranial Language Brain-Computer Interfaces: A Comprehensive Review of Neural Mechanisms, Hardware, Algorithms, Evaluation, Clinical Pathways and Future Directions. arXiv preprint, 2026. URL https://arxiv.org/abs/2603.12279. Version 2, 16 March 2026; not peer reviewed.

He, S., Li, Z., Dang, J., Luo, Y., and Zhang, G. CIRE: A Chinese EEG Dataset for decoding speech intention modulated by prosodic emotion. *Scientific Data*, 12(1), 2025a. doi: 10.1038/s41597-025-05957-y. URL https://doi.org/10.1038/s41597-025-05957-y.

He, T., Wei, M., Wang, R., Wang, R., Du, S., Cai, S., Tao, W., and Li, H. Vocalmind: A stereotactic EEG dataset for vocalized, mimed, and imagined speech in tonal language. *Scientific Data*, 12(1):657, 2025b. doi: 10.1038/s41597-025-04741-2.

Heelan, C., Lee, J., O' Shea, R., Lynch, L., Brandman, D. M., Truccolo, W., and Nurmikko, A. V. Decoding speech from spike-based neural population recordings in secondary auditory cortex of non-human primates. *Communications Biology*, 2(1):466, 2019. doi: 10.1038/s42003-019-0707-9.

Herff, C. and Schultz, T. Automatic speech recognition from neural signals: A focused review. *Frontiers in Neuroscience*, 10, 2016. doi: 10.3389/fnins.2016.00429.

Herff, C., Heger, D., de Pesters, A., Telaar, D., Brunner, P., Schalk, G., and Schultz, T. Brain-to-text: decoding spoken phrases from phone representations in the brain. *Frontiers in Neuroscience*, 9, 2015. doi: 10.3389/fnins.2015.00217.

Herff, C., Johnson, G., Diener, L., Shih, J., Krusienski, D., and Schultz, T. Towards direct speech synthesis from ECoG: A pilot study. In *2016 38th Annual International Conference of the IEEE Engineering in Medicine and Biology Society (EMBC)*, pp. 1540–1543. IEEE, 2016. doi: 10.1109/embc.2016.7591004.

Herff, C., Diener, L., Angrick, M., Mugler, E., Tate, M. C., Goldrick, M. A., Krusienski, D. J., Slutzky, M. W., and Schultz, T. Generating natural, intelligible speech from brain activity in motor, premotor, and inferior frontal cortices. *Frontiers in Neuroscience*, 13:1267, 2019. doi: 10.3389/fnins.2019.01267.

Hirshorn, E. A., Li, Y., Ward, M. J., Richardson, R. M., Fiez, J. A., and Ghuman, A. S. Decoding and disrupting left midfusiform gyrus activity during word reading. *Proceedings of the National Academy of Sciences*, 113(29):8162–8167, 2016. doi: 10.1073/pnas.1604126113. URL https://doi.org/10.1073/pnas.1604126113.

Hollenstein, N., Rotsztejn, J., Troendle, M., Pedroni, A., Zhang, C., and Langer, N. Zuco, a simultaneous EEG and eye-tracking resource for natural sentence reading. *Scientific Data*, 5(1):180291, 2018. doi: 10.1038/sdata.2018.291.

Hollenstein, N., Troendle, M., Zhang, C., and Langer, N. ZuCo 2.0: A dataset of physiological recordings during natural reading and annotation. In Calzolari, N., Béchet, F., Blache, P., Choukri, K., Cieri, C., Declerck, T., Goggi, S., Isahara, H., Maegaard, B., Mariani, J., Mazo, H., Moreno, A., Odijk, J., and Piperidis, S. (eds.), *Proceedings of the Twelfth Language Resources and Evaluation Conference*, pp. 138–146, Marseille, France, may 2020. European Language Resources Association. ISBN 979-10-95546-34-4. URL https://aclanthology.org/2020.lrec-1.18/.

Hong, Y., Ryun, S., and Chung, C. K. Evoking artificial speech perception through invasive brain stimulation for brain-computer interfaces: current challenges and future perspectives. *Frontiers in Neuroscience*, 18: 1428256, 2024. doi: 10.3389/fnins.2024.1428256. URL https://doi.org/10.3389/fnins.2024.1428256.

Hons, M., Kober, S. E., Wriessnegger, S. C., and Wood, G. Hybrid EEG-fNIRS phoneme classification based on imagined and perceived speech. *Frontiers in Neuroergonomics*, 7:1696865, 2026. doi: 10.3389/fnrgo.2026.1696865.

Hu, Y., Liu, Y., Hou, Y., Pan, Y., and Gao, X. Dataset of natural conversations about appearance using fNIRS. *Scientific Data*, 12(1), 2025. doi: 10.1038/s41597-025-05574-9. URL https://doi.org/10.1038/s41597-025-05574-9.

Huggins, J. E., Wren, P. A., and Gruis, K. L. What would brain-computer interface users want? Opinions and priorities of potential users with amyotrophic lateral sclerosis. *Amyotrophic Lateral Sclerosis*, 2011. doi: 10.3109/17482968.2011.572978. URL https://doi.org/10.3109/17482968.2011.572978.

Huth, A. G., de Heer, W. A., Griffiths, T. L., Theunissen, F. E., and Gallant, J. L. Natural speech reveals the semantic maps that tile human cerebral cortex. *Nature*, 532(7600):453–458, 2016. doi: 10.1038/nature17637. URL https://doi.org/10.1038/nature17637.

Ikeda, S., Shibata, T., Nakano, N., Okada, R., Tsuyuguchi, N., Ikeda, K., and Kato, A. Neural decoding of single vowels during covert articulation using electrocorticography. *Frontiers in Human Neuroscience*, 8, 2014. doi: 10.3389/fnhum.2014.00125.

Imbault, M., Chauvet, D., Gennisson, J.-L., Capelle, L., and Tanter, M. Intraoperative functional ultrasound imaging of Human brain activity. *Scientific Reports*, 7(1):7304, 2017. doi: 10.1038/s41598-017-06474-8.

Inoue, M., Hatakeyama, E., Kita, Y., and Sasai, S. Large-scale training data enhances silent speech decoding with around-ear EEG. *Journal of Neural Engineering*, 23(2):026027, 2026. doi: 10.1088/1741-2552/ae54d0.

International Telecommunication Union. A method for subjective performance assessment of the quality of speech voice output devices, 1994. URL https://www.itu.int/rec/T-REC-P.85/en. ITU-T Recommendation P.85 (06/1994).

Iqbal, A., Bhardwaj, A., Suhag, A. K., Diwakar, M., and Bijalwan, A. Analysis of machine learning models using proposed EEG vowel dataset, 2024. doi: 10.21203/rs.3.rs-4008991/v1. Preprint.

Ivucic, D., Bayer, T., Ivucic, G., Ries, S., Shih, J., Krusienski, D. J., and Schultz, T. Speech envelope reconstruction from stereo EEG in a speech production task. In *2025 47th Annual International Conference of the IEEE Engineering in Medicine and Biology Society (EMBC)*, pp. 1–5. IEEE, 2025. doi: 10.1109/embc58623.2025.11253269.

Jamali, M., Grannan, B., Cai, J., Khanna, A. R., Muñoz, W., Caprara, I., Paulk, A. C., Cash, S. S., Fedorenko, E., and Williams, Z. M. Semantic encoding during language comprehension at single-cell resolution. *Nature*, 631(8021):610–616, 2024. doi: 10.1038/s41586-024-07643-2. URL https://doi.org/10.1038/s41586-024-07643-2.

Jayalath, D. and Parker Jones, O. MEG-XL: Data-efficient brain-to-text via long-context pre-training, 2026. doi: 10.48550/arXiv.2602.02494. URL https://arxiv.org/abs/2602.02494. Version 2, 9 May 2026; author record identifies ICML 2026 conference paper.

Jayalath, D., Landau, G., and Parker Jones, O. Unlocking non-invasive brain-to-text, 2025a. doi: 10.48550/arXiv.2505.13446. URL https://arxiv.org/abs/2505.13446. arXiv preprint, version 1.

Jayalath, D., Landau, G., Shillingford, B., Woolrich, M., and Parker Jones, O. The brain's bitter lesson: Scaling speech decoding with self-supervised learning. In Singh, A., Fazel, M., Hsu, D., Lacoste-Julien, S., Berkenkamp, F., Maharaj, T., Wagstaff, K., and Zhu, J. (eds.), *Proceedings of the 42nd International Conference on Machine Learning*, volume 267 of *Proceedings of Machine Learning Research*, pp. 27005–27020. PMLR, July 2025b. URL https://proceedings.mlr.press/v267/jayalath25a.html.

Jayalath, D., Ballyk, B., and Parker Jones, O. A common measure of communication for speech brain-computer interfaces, 2026. doi: 10.48550/arXiv.2609.02887. URL https://arxiv.org/abs/2609.02887v1. arXiv preprint, version 1.

Jeon, M. and Kim, H. Delta: Language diffusion-based EEG-to-Text architecture. In *NeurIPS 2025 Workshop on Foundation Models for the Brain and Body*, 2025. URL https://openreview.net/forum?id=Hw3wWRyLs4. Workshop paper; preprint available as arXiv:2511.21746.

Jeong, J.-H., Cho, J.-H., Lee, Y.-E., Lee, S.-H., Shin, G.-H., Kweon, Y.-S., Millán, J. d. R., Müller, K.-R., and Lee, S.-W. 2020 International brain–computer interface competition: A review. *Frontiers in Human Neuroscience*, 16, 2022. doi: 10.3389/fnhum.2022.898300. URL https://doi.org/10.3389/fnhum.2022.898300.

Jhilal, S., Marchesotti, S., Thirion, B., Soudrie, B., Giraud, A.-L., and Mandonnet, E. Implantable Neural Speech Decoders: Recent Advances, Future Challenges. *Neurorehabilitation and Neural Repair*, 40(2):157–172, 2025. doi: 10.1177/15459683251369468. URL https://doi.org/10.1177/15459683251369468.

Jia, Z., Wang, H., Shen, Y., Hu, F., An, J., Shu, K., and Wu, D. Magnetoencephalography (MEG) based non-invasive Chinese speech decoding. *Journal of Neural Engineering*, 22(6):066014, 2025. doi: 10.1088/1741-2552/ae1ea2.

Jiang, L., Stocco, A., Losey, D. M., Abernethy, J. A., Prat, C. S., and Rao, R. P. N. Brainnet: A multi-person brain-to-brain interface for direct collaboration between brains. *Scientific Reports*, 2019. doi: 10.1038/s41598-019-41895-7. URL https://www.nature.com/articles/s41598-019-41895-7.

Jiang, M., Zhang, W., Ding, Y., Teo, K. A. C., Fong, L., Zhang, S., Guo, Z., Liu, C., Bhuvanakantham, R., Sim, W. K. J., Foo, C. H. V., Chua, R. H. J., Padmanabhan, P., Leong, V., Lu, J., Gulyás, B., and Guan, C. Decoding covert speech from EEG by functional areas Spatio-Temporal Transformer. *IEEE Journal of Biomedical and Health Informatics*, 30(6):4974–4984, 2026. doi: 10.1109/jbhi.2026.3653025.

Jiang, W., Wang, Y., Lu, B.-l., and Li, D. NeuroLM: A universal multi-task foundation model for bridging the gap between language and EEG signals. In *The Thirteenth International Conference on Learning Representations*, 2025. URL https://openreview.net/forum?id=Io9yFt7XH7.

Jiang, W.-B., Zhao, L.-M., and Lu, B.-L. Large brain model for learning generic representations with tremendous EEG data in BCI. In *The Twelfth International Conference on Learning Representations*, 2024. URL https://openreview.net/forum?id=QzTpTRVtrP.

Jin, Z., Li, D., and Huang, S. A systematic review of EEG-based Imagined Speech decoding. *Applied Soft Computing*, 183:113563, 2025. doi: 10.1016/j.asoc.2025.113563. URL https://doi.org/10.1016/j.asoc.2025.113563.

Jin, Z., Li, D., Zhou, Q., and Wang, Z. Neural-vox: NEURal auditory language decoding for voice and text reconstruction. *Neural Networks*, 204:109221, 2026. doi: 10.1016/j.neunet.2026.109221.

Jing, J., Ge, W., Hong, S., Fernandes, M. B., Lin, Z., Yang, C., An, S., Struck, A. F., Herlopian, A., Karakis, I., Halford, J. J., Ng, M. C., Johnson, E. L., Appavu, B. L., Sarkis, R. A., Osman, G., Kaplan, P. W., Dhakar, M. B., Arcot Jayagopal, L., Sheikh, Z., Taraschenko, O., Schmitt, S., Haider, H. A., Kim, J. A., Swisher, C. B., Gaspard, N., Cervenka, M. C., Rodriguez Ruiz, A. A., Lee, J. W., Tabaeizadeh, M., Gilmore, E. J., Nordstrom, K., Yoo, J. Y., Holmes, M. G., Herman, S. T., Williams, J. A., Pathmanathan, J., Nascimento, F. A., Fan, Z., Nasiri, S., Shafi, M. M., Cash, S. S., Hoch, D. B., Cole, A. J., Rosenthal, E. S., Zafar, S. F., Sun, J., and Westover, M. B. Development of expert-level classification of seizures and rhythmic and periodic patterns during EEG interpretation. *Neurology*, 100(17), 2023. doi: 10.1212/wnl.0000000000207127.

Jo, H., Yang, Y., Han, J., Duan, Y., Xiong, H., and Lee, W. H. Evaluating EEG-to-text models through noise-based performance analysis. *Scientific Reports*, 16:350, 2026. doi: 10.1038/s41598-025-29587-x. URL https://www.nature.com/articles/s41598-025-29587-x. Article 350; first published online 1 December 2025.

Jude, J. J., Haro, S., Levi-Aharoni, H., Hashimoto, H., Acosta, A. J., Card, N. S., Wairagkar, M., Brandman, D. M., Stavisky, S. D., Williams, Z. M., Cash, S. S., Simeral, J. D., Hochberg, L. R., and Rubin, D. B. Decoding intended speech with an intracortical brain-computer interface in a person with long-standing anarthria and locked-in syndrome. *Cell Reports*, 45(4):117162, 2026. doi: 10.1016/j.celrep.2026.117162.

K, S. D., S, S. M., Sahoo, S., Sheetal, K. B., Anil, N., Sajeev, N., K, A., T, S. N., Sumitra, S., and S., M. B. IIST BCI Dataset-9: EEG Dataset For Malayalam Vocal and Subvocal Commands with Dialect Variation For Wheelchair Control. Preprint, 2025. doi: 10.36227/techrxiv.174586818.88790131/v1. URL https://doi.org/10.36227/techrxiv.174586818.88790131/v1.

Kamavuako, E. N., Sheikh, U. A., Gilani, S. O., Jamil, M., and Niazi, I. K. Classification of overt and covert speech for Near-Infrared Spectroscopy-Based brain computer interface. *Sensors*, 18(9):2989, 2018. doi: 10.3390/s18092989.

Kaongoen, N., Choi, J., and Jo, S. A novel online BCI system using speech imagery and ear-EEG for home appliances control. *Computer Methods and Programs in Biomedicine*, 224:107022, 2022. doi: 10.1016/j.cmpb.2022.107022.

Kappenman, E. S., Farrens, J. L., Zhang, W., Stewart, A. X., and Luck, S. J. ERP CORE: An open resource for human event-related potential research. *NeuroImage*, 225:117465, 2021. doi: 10.1016/j.neuroimage.2020.117465. URL https://doi.org/10.1016/j.neuroimage.2020.117465.

Karthik, G., Cao, C. Z., Demidenko, M. I., Jahn, A., Stacey, W. C., Wasade, V. S., and Brang, D. Auditory cortex encodes lipreading information through spatially distributed activity. *Current Biology*, 34(17):4021–4032.e5, 2024. doi: 10.1016/j.cub.2024.07.073.

Keitel, A., Gross, J., and Kayser, C. Shared and modality-specific brain regions that mediate auditory and visual word comprehension. *eLife*, 9:e56972, 2020. doi: 10.7554/elife.56972.

Kellis, S., Miller, K., Thomson, K., Brown, R., House, P., and Greger, B. Decoding spoken words using local field potentials recorded from the cortical surface. *Journal of Neural Engineering*, 7(5):056007, 2010. doi: 10.1088/1741-2560/7/5/056007.

Kessler, R., Enge, A., and Skeide, M. A. How EEG preprocessing shapes decoding performance. *Communications Biology*, 8:1039, 2025. doi: 10.1038/s42003-025-08464-3. URL https://www.nature.com/articles/s42003-025-08464-3.

Khan, S., Kallis, L., Mee, H., El Hadwe, S., Barone, D., Hutchinson, P., and Kolias, A. Invasive Brain–Computer Interface for Communication: A Scoping Review. *Brain Sciences*, 15(4):336, 2025. doi: 10.3390/brainsci15040336. URL https://doi.org/10.3390/brainsci15040336.

Khanday, O. M., Ticha, M. B. B., Belfrouh, S., Ouellet, M., and Gonzalez-Lopez, J. A. Do EEG foundation models transfer to speech? a benchmark on overt and imagined speech decoding, 2026. doi: 10.48550/ARXIV.2607.27268.

Khanna, A. R., Muñoz, W., Kim, Y. J., Kfir, Y., Paulk, A. C., Jamali, M., Cai, J., Mustroph, M. L., Caprara, I., Hardstone, R., Mejdell, M., Meszéna, D., Zuckerman, A., Schweitzer, J., Cash, S., and Williams, Z. M. Single-neuronal elements of speech production in humans. *Nature*, 626(7999):603–610, 2024. doi: 10.1038/s41586-023-06982-w.

Khushiyant. Neurocognitive modeling for text generation: Deep learning architecture for EEG data, 2025. doi: 10.48550/ARXIV.2509.07202.

Ko, B.-K., Lee, S.-H., and Lee, S.-W. Imagined speech detection using Multi-Receptive CNN for asynchronous BCI communication and neurorehabilitation. *IEEE Transactions on Neural Systems and Rehabilitation Engineering*, 33:2904–2914, 2025. doi: 10.1109/tnsre.2025.3592312.

Kolisnyk, M., Novi, S., Abdalmalak, A., Ardakani, R. M., Kazazian, K., Laforge, G., Debicki, D. B., and Owen, A. M. Assessing the consistency and sensitivity of the neural correlates of narrative stimuli using functional near-infrared spectroscopy. *Imaging Neuroscience*, 2, 2024. doi: 10.1162/imag_a_00331. URL https://doi.org/10.1162/imag_a_00331.

Komeiji, S., Mitsuhashi, T., Iimura, Y., Suzuki, H., Sugano, H., Shinoda, K., and Tanaka, T. Feasibility of decoding covert speech in ECoG with a Transformer trained on overt speech. *Scientific Reports*, 14(1):11491, 2024. doi: 10.1038/s41598-024-62230-9.

Kong, J., Kim, J., and Bae, J. HiFi-GAN: Generative adversarial networks for efficient and high fidelity speech synthesis. In *Advances in Neural Information Processing Systems*, volume 33, pp. 17022–17033, 2020. URL https://proceedings.neurips.cc/paper/2020/hash/c5d736809766d46260d816d8dbc9eb44-Abstract.html.

Kostas, D., Aroca-Ouellette, S., and Rudzicz, F. BENDR: Using transformers and a contrastive self-supervised learning task to learn from massive amounts of EEG data. *Frontiers in Human Neuroscience*, 15:653659, 2021. doi: 10.3389/fnhum.2021.653659. URL https://www.frontiersin.org/journals/human-neuroscience/articles/10.3389/fnhum.2021.653659/full.

Kostulin, D. V., Shaposhnikov, P. D., Ekizyan, A., Shevchenko, I. G., Shaposhnikov, D. G., Shcherban, I. V., and Kiroy, V. N. EEG-based brain-computer interface (BCI) dataset for directional word recognition. *Scientific Data*, 13(1), 2026. doi: 10.1038/s41597-026-07809-9. URL https://doi.org/10.1038/s41597-026-07809-9.

Kreiner, H. and Eviatar, Z. The sound of thought: Form matters–The prosody of inner speech. *Physics of Life Reviews*, 51:231–242, 2024. doi: 10.1016/j.plrev.2024.10.006. URL https://doi.org/10.1016/j.plrev.2024.10.006.

Krishna, G., Tran, C., Han, Y., Carnahan, M., and Tewfik, A. H. Speech synthesis using EEG. In *ICASSP 2020 - 2020 IEEE International Conference on Acoustics, Speech and Signal Processing (ICASSP)*, pp. 1235–1238. IEEE, 2020. doi: 10.1109/icassp40776.2020.9053340.

Kunz, E. M., Abramovich Krasa, B., Kamdar, F., Avansino, D. T., Hahn, N., Yoon, S., Singh, A., Nason-Tomaszewski, S. R., Card, N. S., Jude, J. J., Jacques, B. G., Bechefsky, P. H., Iacobacci, C., Hochberg, L. R., Rubin, D. B., Williams, Z. M., Brandman, D. M., Stavisky, S. D., AuYong, N., Pandarinath, C., Druckmann, S., Henderson, J. M., and Willett, F. R. Inner speech in motor cortex and implications for speech neuroprostheses. *Cell*, 188(17):4658–4673.e17, 2025. doi: 10.1016/j.cell.2025.06.015.

Kuruppu, G., Wagh, N., Kremen, V., and Varatharajah, Y. EEG foundation models: a critical review of current progress and future directions. *Journal of Neural Engineering*, 23(2):021001, 2026. doi: 10.1088/1741-2552/ae4455. URL https://doi.org/10.1088/1741-2552/ae4455.

Kwon, J., Harwath, D., Dash, D., Ferrari, P., and Wang, J. Direct speech synthesis from Non-Invasive, neuromagnetic signals. In *Interspeech 2024*, pp. 412–416. ISCA, 2024. doi: 10.21437/interspeech.2024-2153.

Kwon, T., Somaiya, P., Elvers, G., Mantegna, F., Camera, A., Braeutigam, S., Woolrich, M., and Parker Jones, O. MegNIST: A Benchmark for Non-Invasive Inner Speech Decoding. Official PNPL dataset release, 2026. URL https://huggingface.co/datasets/pnpl/MegNIST.

Kübler, A., Holz, E. M., Riccio, A., Zickler, C., Kaufmann, T., Kleih, S. C., Staiger-Sälzer, P., Desideri, L., Hoogerwerf, E.-J., and Mattia, D. The user-centered design as novel perspective for evaluating the usability of bci-controlled applications. *PLoS ONE*, 2014. doi: 10.1371/journal.pone.0112392. URL https://journals.plos.org/plosone/article?id=10.1371/journal.pone.0112392.

Lamprou, Z. and Moshfeghi, Y. On creating a Brain-To-Text decoder, 2025. doi: 10.48550/ARXIV.2501.06326.

Lamprou, Z., Tenedios, I., and Moshfeghi, Y. On the role of activation functions in EEG-to-text decoder. In *Machine Learning, Optimization, and Data Science*, pp. 46–60. Springer Nature Switzerland, 2025. doi: 10.1007/978-3-031-82487-6_4.

Landau, G., Özdogan, M., Elvers, G., Mantegna, F., Somaiya, P., Jayalath, D., Kurth, L., Kwon, T., Shillingford, B., Farquhar, G., Jiang, M., Jerbi, K., Abdelhedi, H., Ramos, Y. M., Gulcehre, C., Woolrich, M., Voets, N., and Parker Jones, O. The 2025 PNPL competition: Speech detection and phoneme classification in the LibriBrain dataset, 2025. doi: 10.48550/ARXIV.2506.10165.

Landau, G. D., Jayalath, D., and Parker Jones, O. The semantic bottleneck: Leveraging semantic representations for non-invasive speech decoding, 2026. doi: 10.48550/arXiv.2609.10296. URL https://arxiv.org/abs/2609.10296. arXiv preprint, version 1.

Landemard, A., Bimbard, C., Demené, C., Shamma, S., Norman-Haignere, S., and Boubenec, Y. Distinct higher-order representations of natural sounds in human and ferret auditory cortex. *eLife*, 10:e65566, 2021. doi: 10.7554/elife.65566.

Landemard, A., Bimbard, C., and Boubenec, Y. Hierarchical encoding of natural sound mixtures in ferret auditory cortex. *eLife*, 14:RP106628, 2025. doi: 10.7554/elife.106628.

Lara, E., Takacs, A., and Rodríguez, J. EEGIS - Electroencephalogram Imagined Speech dataset. Mendeley Data data release, 2024. doi: 10.17632/73g4fw884c.1. URL https://data.mendeley.com/datasets/73g4fw884c/1.

Lawhern, V. J., Solon, A. J., Waytowich, N. R., Gordon, S. M., Hung, C. P., and Lance, B. J. EEGNet: A compact convolutional neural network for EEG-based brain–computer interfaces. *Journal of Neural Engineering*, 15 (5):056013, 2018. doi: 10.1088/1741-2552/aace8c.

LeBel, A., Wagner, L., Jain, S., Adhikari-Desai, A., Gupta, B., Morgenthal, A., Tang, J., Xu, L., and Huth, A. G. A natural language fMRI dataset for voxelwise encoding models. *Scientific Data*, 10(1), 2023. doi: 10.1038/s41597-023-02437-z. URL https://doi.org/10.1038/s41597-023-02437-z.

Lee, D.-Y., Lee, M., and Lee, S.-W. Decoding imagined speech based on deep metric learning for intuitive BCI communication. *IEEE Transactions on Neural Systems and Rehabilitation Engineering*, 29:1363–1374, 2021. doi: 10.1109/tnsre.2021.3096874.

Lee, J., Kommineni, A., Feng, T., Avramidis, K., Shi, X., Kadiri, S. R., and Narayanan, S. Toward Fully-End-to-End listened speech decoding from EEG signals. In *Interspeech 2024*, pp. 1500–1504. ISCA, 2024. doi: 10.21437/interspeech.2024-223.

Lee, J., Feng, T., Kommineni, A., Kadiri, S. R., and Narayanan, S. Enhancing listened speech decoding from EEG via parallel phoneme sequence prediction. In *ICASSP 2025 - 2025 IEEE International Conference on Acoustics, Speech and Signal Processing (ICASSP)*, pp. 1–5. IEEE, 2025a. doi: 10.1109/icassp49660.2025.10887915.

Lee, S.-H., Lee, M., and Lee, S.-W. Neural decoding of imagined speech and visual imagery as intuitive paradigms for BCI communication. *IEEE Transactions on Neural Systems and Rehabilitation Engineering*, 28 (12):2647–2659, 2020. doi: 10.1109/tnsre.2020.3040289.

Lee, S.-H., Lee, S.-H., and Lee, S.-W. Eeg-translator: A Cross-Modality framework for Subject-Specific EEG and voice reconstruction from imagined speech. In *2025 47th Annual International Conference of the IEEE Engineering in Medicine and Biology Society (EMBC)*, pp. 1–7. IEEE, 2025b. doi: 10.1109/embc58623.2025.11254826.

Lee, Y.-E., Lee, S.-H., Kim, S.-H., and Lee, S.-W. Towards voice reconstruction from EEG during imagined speech. *Proceedings of the AAAI Conference on Artificial Intelligence*, 37(5):6030–6038, 2023. doi: 10.1609/aaai.v37i5.25745.

Lehner, K. R., Luo, S., Greene, B., Angrick, M., Candrea, D., Husari, K. S., Barth, K., Dister, J., Anushiravani, R., Miller, J. S., Ho, E., Rincon-Torroella, J., Rapoport, B., Comair, Y., and Crone, N. E. Initial experience with the precision neuroscience Layer 7 micro-electrocorticography interface for real-time intraoperative neural decoding. *Neurosurgical Focus*, 2026. doi: 10.3171/2025.11.FOCUS25908. URL https://doi.org/10.3171/2025.11.FOCUS25908.

Li, F., Chao, W., Li, Y., Fu, B., Ji, Y., Wu, H., and Shi, G. Decoding imagined speech from EEG signals using hybrid-scale spatial-temporal dilated convolution network. *Journal of Neural Engineering*, 18(4):0460c4, 2021. doi: 10.1088/1741-2552/ac13c0.

Li, H., Ding, M., Zhang, R., and Xiu, C. Motor imagery EEG classification algorithm based on cnn-lstm feature fusion network. *Biomedical Signal Processing and Control*, 72:103342, 2022a. doi: 10.1016/j.bspc.2021.103342.

Li, J., Bhattasali, S., Zhang, S., Franzluebbers, B., Luh, W.-M., Spreng, R. N., Brennan, J. R., Yang, Y., Pallier, C., and Hale, J. Le Petit Prince multilingual naturalistic fMRI corpus. *Scientific Data*, 9(1), 2022b. doi: 10.1038/s41597-022-01625-7. URL https://doi.org/10.1038/s41597-022-01625-7.

Li, J., Hale, J., and Pallier, C. Le Petit Prince: A multilingual fMRI corpus using ecological stimuli. OpenNeuro data release, version 2.0.7, 2025a. doi: 10.18112/openneuro.ds003643.v2.0.7. URL https://openneuro.org/datasets/ds003643/versions/2.0.7.

Li, J., Le, T., Fan, C., Chen, M., and Shlizerman, E. Brain-to-text decoding with context-aware neural representations and large language models. *Journal of Neural Engineering*, 22(5):056026, 2025b. doi: 10.1088/1741-2552/adfab1.

Li, J., Song, Z., Wang, J., Zhang, M., Liu, H., Zhang, M., and Zhang, Z. BrainECHO: Semantic brain signal decoding through vector-quantized spectrogram reconstruction for Whisper-enhanced text generation. In *Findings of the Association for Computational Linguistics: ACL 2025*, pp. 2762–2778, Vienna, Austria, July 2025c. Association for Computational Linguistics. doi: 10.18653/v1/2025.findings-acl.142. URL https://aclanthology.org/2025.findings-acl.142/.

Li, J., Wang, Q., Wang, Y., Wang, C., Ma, Z., Xu, R., Feng, S., Jiang, X., and Meng, Z. Naturalistic fMRI and MEG recordings during viewing of a reality TV show. *Scientific Data*, 12(1), 2025d. doi: 10.1038/s41597-025-06110-5. URL https://doi.org/10.1038/s41597-025-06110-5.

Li, J., Guo, C., Zhang, C., Chang, E. F., and Li, Y. High-fidelity neural speech reconstruction through an efficient acoustic-linguistic dual-pathway framework. *eLife*, 14:RP109400, 2026a. doi: 10.7554/elife.109400.

Li, J., Singh, A., and Tandon, N. Transitioning from speech to language brain–computer interfaces. *Nature Reviews Bioengineering*, 4(8):702–704, 2026b. doi: 10.1038/s44222-026-00460-4. URL https://doi.org/10.1038/s44222-026-00460-4.

Li, S., Tang, Z., Li, M., Yang, L., and Shang, Z. A survey of neural signal decoding based on domain adaptation. *Neurocomputing*, 657:131653, 2025e. doi: 10.1016/j.neucom.2025.131653. URL https://doi.org/10.1016/j.neucom.2025.131653.

Li, X. and Tao, Z. Leakage-audited benchmarking reveals limited evidence for cross-subject auditory-evoked EEG vowel perception decoding. *Journal of Neural Engineering*, 2026. doi: 10.1088/1741-2552/aea4f7.

Li, Y., DeWitt, I., Brennan, J. R., Wasade, V. S., Stacey, W., and Brang, D. Visual speech enhances phoneme separability in human superior temporal gyrus, 2026c. doi: 10.64898/2026.09.10.750762. Preprint.

Liao, D. A., Schwarzbach, E., and Nieder, A. Exploring neural dynamics in the auditory telencephalon of crows using functional ultrasound imaging. *The Journal of Neuroscience*, 45(29):e0016252025, 2025. doi: 10.1523/jneurosci.0016-25.2025.

Likhitha, C., Tayade, S., S, P. S., Sunil, N., Sahoo, S., Sumitra, S., and Manoj, B. S. IIST BCI Dataset-4 for Selected 100 Telugu words. Preprint, 2024. doi: 10.36227/techrxiv.171387874.40408574/v1. URL https://doi.org/10.36227/techrxiv.171387874.40408574/v1.

Lin, L. J., Callier, T., Heiles, B., Pejsa, K., Liu, C. Y., Shapiro, M. G., and Andersen, R. A. Functional ultrasound imaging through a human cranial window for mesoscopic mapping of motor effector encoding within the sensorimotor cortex, 2026. doi: 10.64898/2026.07.03.735688. Preprint.

Littlejohn, K. T., Cho, C. J., Liu, J. R., Silva, A. B., Yu, B., Anderson, V. R., Kurtz-Miott, C. M., Brosler, S., Kashyap, A. P., Hallinan, I. P., Shah, A., Tu-Chan, A., Ganguly, K., Moses, D. A., Chang, E. F., and Anumanchipalli, G. K. A streaming brain-to-voice neuroprosthesis to restore naturalistic communication. *Nature Neuroscience*, 28(4):902–912, 2025. doi: 10.1038/s41593-025-01905-6.

Liu, H., Hajialigol, D., Antony, B., Han, A., and Wang, X. EEG2Text: Open vocabulary EEG-to-text translation with multi-view Transformer. In *2024 IEEE International Conference on Big Data (BigData)*, pp. 1824–1833. IEEE, 2024. doi: 10.1109/bigdata62323.2024.10825980. Earlier preprint: arXiv:2405.02165; version-specific summaries are identified in the text.

Liu, X., Shen, D., and Liu, X. Learning interpretable representations leads to semantically faithful EEG-to-Text generation, 2025a. doi: 10.48550/ARXIV.2505.17099.

Liu, X., Yang, B., Gan, A., and Zhang, J. [study on speech imagery electroencephalography decoding of chinese words based on the cam-net model]. *Sheng wu yi xue gong cheng xue za zhi = Journal of biomedical engineering = Shengwu yixue gongchengxue zazhi*, 42(3):473–479, 2025b. doi: 10.7507/1001-5515.202503048. URL https://pubmed.ncbi.nlm.nih.gov/40566768/.

Liu, Y., Zhao, Z., Xu, M., Yu, H., Zhu, Y., Zhang, J., Bu, L., Zhang, X., Lu, J., Li, Y., Ming, D., and Wu, J. Decoding and synthesizing tonal language speech from brain activity. *Science Advances*, 9(23):eadh0478, 2023. doi: 10.1126/sciadv.adh0478.

Lobo-Alonso, M., Martín-Fernández, I., Oropesa, I., Barra-Chicote, R., Kontaxakis, G., and San-Segundo, R. A dataset with bilingual TV commands for silent speech interfaces using electroencephalographic signals. *Scientific Data*, 2026. doi: 10.1038/s41597-026-07745-8.

Logothetis, N. K., Pauls, J., Augath, M., Trinath, T., and Oeltermann, A. Neurophysiological investigation of the basis of the fMRI signal. *Nature*, 2001. doi: 10.1038/35084005. URL https://doi.org/10.1038/35084005.

Lopez-Bernal, D., Balderas, D., Ponce, P., and Molina, A. A State-of-the-Art review of EEG-Based imagined speech decoding. *Frontiers in Human Neuroscience*, 16:867281, 2022. doi: 10.3389/fnhum.2022.867281.

Lopez-Bernal, D., Balderas, D., Ponce, P., and Molina, A. Exploring inter-trial coherence for inner speech classification in EEG-based brain–computer interface. *Journal of Neural Engineering*, 21(2):026048, 2024. doi: 10.1088/1741-2552/ad3f50.

Lopopolo, A., Frank, S. L., van den Bosch, A., Nijhof, A., and Willems, R. M. The Narrative Brain Dataset (NBD), an fMRI Dataset for the Study of Natural Language Processing in the Brain. In *Proceedings of LREC 2018 Workshop Linguistic and Neuro-Cognitive Resources (LiNCR)*, pp. 8–11, 2018. URL https://pure.mpg.de/pubman/item/item_3010245.

Lu, J. T.-Y., Chiang, J., Chen, C.-S., Tung, A. N.-Y., Hu, H. W., and Cheng, Y. C. Eeg2text-cn: An exploratory study of Open-Vocabulary Chinese Text-EEG alignment via large language model and contrastive learning on ChineseEEG, 2025a. doi: 10.48550/ARXIV.2506.00854.

Lu, W., Nie, D., Xue, P., Cui, Z., Li, P., Zhang, D., and Wen, X. Brain-inspired fMRI-to-text decoding via incremental and wrap-up language modeling. In *Advances in Neural Information Processing Systems*, volume 38, 2025b. URL https://proceedings.neurips.cc/paper_files/paper/2025/file/dca63f2650fe9e88956c1b68440b8ee9-Paper-Conference.pdf.

Lu, Z., Li, Z., Shen, X., Lou, K., Xin, Y., Chen, X., Wang, S., Chen, X., Fan, J., Huang, C., Xu, X., Hou, Z., Wei, C., and Liu, Q. OmniEEG-Bench: A standardized evaluation benchmark for EEG foundation models, 2026. doi: 10.48550/arXiv.2606.00815. URL https://arxiv.org/abs/2606.00815v1.

Luo, S., Angrick, M., Coogan, C., Candrea, D. N., Wyse-Sookoo, K., Shah, S., Rabbani, Q., Milsap, G. W., Weiss, A. R., Anderson, W. S., Tippett, D. C., Maragakis, N. J., Clawson, L. L., Vansteensel, M. J., Wester, B. A., Tenore, F. V., Hermansky, H., Fifer, M. S., Ramsey, N. F., and Crone, N. E. Stable decoding from a speech BCI enables control for an individual with ALS without recalibration for 3 months. *Advanced Science*, 10(35):2304853, 2023. doi: 10.1002/advs.202304853.

Ma, J., Wu, F., Lin, Q., Xing, Y., Liu, C., Jia, Z., and Feng, M. CodeBrain: Bridging decoupled tokenizer and multi-scale architecture for EEG foundation model. In *The Fourteenth International Conference on Learning Representations*, 2026a. URL https://openreview.net/forum?id=msJgEkjwh5.

Ma, X., Jiang, Y., and Jiang, N. 3m-cpseed, an EEG-based dataset for Chinese Pinyin production in overt, mouthed, and imagined speech. *Scientific Data*, 13(1):34, 2026b. doi: 10.1038/s41597-025-06346-1.

Ma, Z., Wang, N., and Li, J. Le Petit Prince (LPP) Multi-talker: Naturalistic 7T fMRI and EEG Dataset. OpenNeuro data release, 2025. doi: 10.18112/openneuro.ds005345.v1.0.1. URL https://openneuro.org/datasets/ds005345/versions/1.0.1.

MacIntyre, A. D., Gaultier, C., and Goehring, T. Decoding of speech acoustics from EEG: going beyond the amplitude envelope. *Journal of Neural Engineering*, 23(1):016014, 2026. doi: 10.1088/1741-2552/ae3ae1.

Maghsoudi, M. and Shamma, S. Zero-shot imagined speech decoding via Imagined-to-Listened MEG mapping, 2026. doi: 10.48550/ARXIV.2605.08075.

Mai, W., Zhang, J., Fang, P., and Zhang, Z. Brain-Conditional Multimodal Synthesis: A Survey and Taxonomy. *IEEE Transactions on Artificial Intelligence*, 6(5):1080–1099, 2025. doi: 10.1109/TAI.2024.3516698. URL https://doi.org/10.1109/TAI.2024.3516698.

Makin, J. G., Moses, D. A., and Chang, E. F. Machine translation of cortical activity to text with an encoder–decoder framework. *Nature Neuroscience*, 23(4):575–582, 2020. doi: 10.1038/s41593-020-0608-8.

Mantegna, F., Elvers, G., Jayalath, D., Landau, G., Kim, T., Özdogan, M., Kurth, L., Kwon, T., Cho, S., Ballyk, B., Fung, A., Greer, A., Somaiya, P., Herff, C., Ramos, Y. M., Abdelhedi, H., Jerbi, K., Farquhar, G., Shillingford, B., Woolrich, M., and Parker Jones, O. The 2026 PNPL competition: Word classification and efficient cross-subject generalisation in LibriBrain100, 2026a. doi: 10.48550/arXiv.2609.03231. URL https://arxiv.org/abs/2609.03231.

Mantegna, F., Jayalath, D., Elvers, G., Kim, T., Ballyk, B., Fung, A., Cho, S., Kwon, T., Kurth, L., Özdogan, M., Landau, G., Somaiya, P., Voets, N., Woolrich, M., and Parker Jones, O. Libribrain100: One hundred hours of broad and deep MEG data for neural speech decoding at scale, 2026b. doi: 10.48550/ARXIV.2608.25204.

Martin, S., Brunner, P., Holdgraf, C., Heinze, H.-J., Crone, N. E., Rieger, J., Schalk, G., Knight, R. T., and Pasley, B. N. Decoding spectrotemporal features of overt and covert speech from the human cortex. *Frontiers in Neuroengineering*, 7, 2014. doi: 10.3389/fneng.2014.00014.

Martin, S., Brunner, P., Iturrate, I., Millán, J. d. R., Schalk, G., Knight, R. T., and Pasley, B. N. Word pair classification during imagined speech using direct brain recordings. *Scientific Reports*, 6(1):25803, 2016. doi: 10.1038/srep25803.

Martinovic, I., Davies, D., Frank, M., Perito, D., Ros, T., and Song, D. On the feasibility of side-channel attacks with brain-computer interfaces. In *21st USENIX Security Symposium*, pp. 143–158, 2012. URL https://www.usenix.org/conference/usenixsecurity12/technical-sessions/presentation/martinovic.

Masry, M., Amen, M., Elzyat, M., Hamed, M., Magdy, N., and Khaled, M. Ets: Open vocabulary Electroencephalography-To-Text decoding and sentiment classification, 2025. doi: 10.48550/ARXIV.2506.14783.

matin, H., faraji, m., and Ebrahimpour, R. Imagined Speech eeg data. Mendeley Data data release, 2025. doi: 10.17632/v3tbnxpgm8.1. URL https://data.mendeley.com/datasets/v3tbnxpgm8/1.

McGuire, N. and Moshfeghi, Y. Towards brain passage retrieval: An investigation of EEG query representations. In *Proceedings of the 48th International ACM SIGIR Conference on Research and Development in Information Retrieval*, pp. 613–623. ACM, 2025. doi: 10.1145/3726302.3730097.

Meng, K., Goodarzy, F., Kim, E., Park, Y. J., Kim, J. S., Cook, M. J., Chung, C. K., and Grayden, D. B. Continuous synthesis of artificial speech sounds from human cortical surface recordings during silent speech production. *Journal of Neural Engineering*, 20(4):046019, 2023. doi: 10.1088/1741-2552/ace7f6.

Menon, A. P., S, P. S., Sunil, N., Sumitra, S., and BS, M. IIST BCI Dataset-7 for Human Space Missions. Preprint, 2024. doi: 10.36227/techrxiv.172297499.92407232/v1. URL https://doi.org/10.36227/techrxiv.172297499.92407232/v1.

Mesgarani, N., Cheung, C., Johnson, K., and Chang, E. F. Phonetic Feature Encoding in Human Superior Temporal Gyrus. *Science*, 2014. doi: 10.1126/science.1245994. URL https://doi.org/10.1126/science.1245994.

Metwalli, D., Kiroles, A. E., Radwan, Y. A., Mohamed, E. A., Barakat, M., Ahmed, A., Omar, A. M., and Selim, S. Areeg: an Open-Access Arabic inner speech EEG dataset. *Scientific Data*, 12(1):1513, 2025. doi: 10.1038/s41597-025-05387-w.

Metzger, S. L., Liu, J. R., Moses, D. A., Dougherty, M. E., Seaton, M. P., Littlejohn, K. T., Chartier, J., Anumanchipalli, G. K., Tu-Chan, A., Ganguly, K., and Chang, E. F. Generalizable spelling using a speech neuroprosthesis in an individual with severe limb and vocal paralysis. *Nature Communications*, 13(1):6510, 2022. doi: 10.1038/s41467-022-33611-3.

Metzger, S. L., Littlejohn, K. T., Silva, A. B., Moses, D. A., Seaton, M. P., Wang, R., Dougherty, M. E., Liu, J. R., Wu, P., Berger, M. A., Zhuravleva, I., Tu-Chan, A., Ganguly, K., Anumanchipalli, G. K., and Chang, E. F. A high-performance neuroprosthesis for speech decoding and avatar control. *Nature*, 620(7976):1037–1046, 2023. doi: 10.1038/s41586-023-06443-4.

Moreira, J. P. C., Carvalho, V. R., Mendes, E. M. A. M., Fallah, A., Sejnowski, T. J., Lainscsek, C., and Comstock, L. An open-access EEG dataset for speech decoding: Exploring the role of articulation and coarticulation. *Scientific Data*, 12(1):1017, 2025. doi: 10.1038/s41597-025-05187-2.

Morgan, A. M., Devinsky, O., Doyle, W. K., Dugan, P., Friedman, D., and Flinker, A. Decoding words during sentence production with ECoG reveals syntactic role encoding and structure-dependent temporal dynamics. *Communications Psychology*, 3(1):87, 2025. doi: 10.1038/s44271-025-00270-1.

Moses, D. A., Mesgarani, N., Leonard, M. K., and Chang, E. F. Neural speech recognition: continuous phoneme decoding using spatiotemporal representations of human cortical activity. *Journal of Neural Engineering*, 13 (5):056004, 2016. doi: 10.1088/1741-2560/13/5/056004.

Moses, D. A., Leonard, M. K., Makin, J. G., and Chang, E. F. Real-time decoding of question-and-answer speech dialogue using human cortical activity. *Nature Communications*, 10(1):3096, 2019. doi: 10.1038/s41467-019-10994-4.

Moses, D. A., Metzger, S. L., Liu, J. R., Anumanchipalli, G. K., Makin, J. G., Sun, P. F., Chartier, J., Dougherty, M. E., Liu, P. M., Abrams, G. M., Tu-Chan, A., Ganguly, K., and Chang, E. F. Neuroprosthesis for decoding speech in a paralyzed person with anarthria. *New England Journal of Medicine*, 385(3):217–227, 2021. doi: 10.1056/nejmoa2027540.

Motaqi, M., Moallemi, M., Mirani, A., Aboutorabi, Y., and Hatef, B. A Comprehensive Review of Imagined Speech Decoding in Brain-computer Interfaces: Utilizing Electroencephalography and Functional Near-infrared Spectroscopy. *Basic and Clinical Neuroscience Journal*, 17(2):175–190, 2026. doi: 10.32598/bcn.2026.8254.1. URL https://doi.org/10.32598/bcn.2026.8254.1.

Mou, X., He, C., Tan, L., Yu, J., Liang, H., Zhang, J., Tian, Y., Yang, Y.-F., Xu, T., Wang, Q., Cao, M., Chen, Z., Hu, C.-P., Wang, X., Liu, Q., and Wu, H. ChineseEEG: A Chinese Linguistic Corpora EEG Dataset for Semantic Alignment and Neural Decoding. *Scientific Data*, 11(1), 2024. doi: 10.1038/s41597-024-03398-7. URL https://doi.org/10.1038/s41597-024-03398-7.

Mou, X., He, C., Tan, L., Yu, J., Liang, H., Zhang, J., Yan, T., Yang, Y.-F., Xu, T., Wang, Q., Cao, M., Chen, Z., Hu, C.-P., Wang, X., Liu, Q., and Wu, H. ChineseEEG: A Chinese Linguistic Corpora EEG Dataset for Semantic Alignment and Neural Decoding. OpenNeuro data release, version 1.2.2, 2025. doi: 10.18112/openneuro.ds004952.v1.2.2. URL https://openneuro.org/datasets/ds004952/versions/1.2.2.

MSEEG. MSEEG: An EEG-based Dataset for Mandarin Imagined Speech BCI. Zenodo data release, 2024. doi: 10.5281/zenodo.10797879. URL https://zenodo.org/doi/10.5281/zenodo.10797879.

Mugler, E. M., Patton, J. L., Flint, R. D., Wright, Z. A., Schuele, S. U., Rosenow, J., Shih, J. J., Krusienski, D. J., and Slutzky, M. W. Direct classification of all american English phonemes using signals from functional speech motor cortex. *Journal of Neural Engineering*, 11(3):035015, 2014. doi: 10.1088/1741-2560/11/3/035015.

Murad, S. A. and Rahimi, N. Unveiling thoughts: A review of advancements in EEG brain signal decoding into text. *IEEE Transactions on Cognitive and Developmental Systems*, 17(1):61–76, 2025. doi: 10.1109/tcds.2024.3462452.

Murad, S. A., Dahal, A., and Rahimi, N. Eeg-to-text translation: A model for deciphering human brain activity, 2025. doi: 10.48550/ARXIV.2505.13936.

Murhekar, A., Liu, C., Mishra, A., Roychowdhury, S., and Gwizdka, J. Sense: Efficient EEG-to-Text via Privacy-Preserving semantic retrieval, 2026. doi: 10.48550/ARXIV.2603.17109.

Nair, P., S, P. S., Sunil, N., Mukati, A., Chauhan, C., Sumitra, S., and Manoj, B. S. IIST BCI Dataset-1 for Selected Common Malayalam Words. Preprint, 2024. doi: 10.36227/techrxiv.170473894.42689961/v1. URL https://doi.org/10.36227/techrxiv.170473894.42689961/v1.

Nalborczyk, L., Grandchamp, R., Koster, E. H. W., Perrone-Bertolotti, M., and Lœvenbruck, H. Can we decode phonetic features in inner speech using surface electromyography? *PLOS ONE*, 2020. doi: 10.1371/journal.pone.0233282. URL https://doi.org/10.1371/journal.pone.0233282.

Nason-Tomaszewski, S. R., Deevi, P. I., Rabbani, Q., Jacques, B. G., Pritchard, A. L., Wimalasena, L. N., Richards, B. A., Karpowicz, B. M., Bechefsky, P. H., Card, N. S., Deo, D. R., Choi, E. Y., Hochberg, L. R., Stavisky, S. D., Brandman, D. M., AuYong, N., and Pandarinath, C. Restoring brain-to-text communication in a person with dysarthria from pontine stroke using an intracortical brain-computer interface, 2026. doi: 10.64898/2026.02.19.26346583. Preprint.

Nastase, S. A., Liu, Y.-F., Hillman, H., Zadbood, A., Hasenfratz, L., Keshavarzian, N., Chen, J., Honey, C. J., Yeshurun, Y., Regev, M., Nguyen, M., Chang, C. H. C., Baldassano, C., Lositsky, O., Simony, E., Chow, M. A., Leong, Y. C., Brooks, P. P., Micciche, E., Choe, G., Goldstein, A., Vanderwal, T., Halchenko, Y. O., Norman, K. A., and Hasson, U. The "Narratives" fMRI dataset for evaluating models of naturalistic language comprehension. *Scientific Data*, 8(1), 2021. doi: 10.1038/s41597-021-01033-3. URL https://doi.org/10.1038/s41597-021-01033-3.

Nguyen, C. H., Karavas, G. K., and Artemiadis, P. Inferring imagined speech using EEG signals: a new approach using Riemannian manifold features. *Journal of Neural Engineering*, 15(1):016002, 2018. doi: 10.1088/1741-2552/aa8235.

Nguyen, C. H., Karavas, G. K., and Artemiadis, P. Data from: Adaptive multi-degree of freedom Brain Computer Interface using online feedback: Towards novel methods and metrics of mutual adaptation between humans and machines for BCI. Dryad data release, 2019. doi: 10.5061/dryad.609g597. URL https://datadryad.org/dataset/doi:10.5061/dryad.609g597.

Nieto, N., Peterson, V., Rufiner, H. L., Kamienkowski, J. E., and Spies, R. Thinking out loud, an open-access EEG-based BCI dataset for inner speech recognition. *Scientific Data*, 9(1):52, 2022. doi: 10.1038/s41597-022-01147-2.

Norman, S. L., Maresca, D., Christopoulos, V. N., Griggs, W. S., Demene, C., Tanter, M., Shapiro, M. G., and Andersen, R. A. Single-trial decoding of movement intentions using functional ultrasound neuroimaging. *Neuron*, 109(9):1554–1566.e4, 2021. doi: 10.1016/j.neuron.2021.03.003.

Oota, S. R., Chen, Z., Gupta, M., Bapi, R. S., Jobard, G., Alexandre, F., and Hinaut, X. Deep Neural Networks and Brain Alignment: Brain Encoding and Decoding (Survey). *Transactions on Machine Learning Research*, 2024. URL https://arxiv.org/abs/2307.10246. Published December 2024; earlier arXiv version in 2023.

Padfield, N., CAMILLERI, K. P., CAMILLERI, T., BUGEJA, M. K., and FABRI, S. G. Motor and Speech Imagery EEG Dataset. University of Malta data release, 2023. doi: 10.60809/drum.24465871.v1. URL https://drum.um.edu.mt/articles/dataset/Motor_and_Speech_Imagery_EEG_Dataset/24465871/1.

Padfield, N., Türk, S., Mujahid, K., Camilleri, T., Peng, Y., and Camilleri, K. A Spatio-Spectral analysis of decoding imagined speech from the idle state. In *2025 47th Annual International Conference of the IEEE Engineering in Medicine and Biology Society (EMBC)*, pp. 1–7. IEEE, 2025. doi: 10.1109/embc58623.2025.11253510.

Page, M. J., McKenzie, J. E., Bossuyt, P. M., Boutron, I., Hoffmann, T. C., Mulrow, C. D., Shamseer, L., Tetzlaff, J. M., Akl, E. A., Brennan, S. E., Chou, R., Glanville, J., Grimshaw, J. M., Hróbjartsson, A., Lalu, M. M., Li, T., Loder, E. W., Mayo-Wilson, E., McDonald, S., McGuinness, L. A., Stewart, L. A., Thomas, J., Tricco, A. C., Welch, V. A., Whiting, P., and Moher, D. The PRISMA 2020 statement: an updated guideline for reporting systematic reviews. *BMJ*, pp. n71, 2021. doi: 10.1136/bmj.n71.

Panachakel, J. T. and Ramakrishnan, A. G. Decoding covert speech from EEG-A comprehensive review. *Frontiers in Neuroscience*, 15:642251, 2021. doi: 10.3389/fnins.2021.642251.

Papineni, K., Roukos, S., Ward, T., and Zhu, W.-J. Bleu: a method for automatic evaluation of machine translation. In *Proceedings of the 40th Annual Meeting of the Association for Computational Linguistics*, 2002. doi: 10.3115/1073083.1073135. URL https://aclanthology.org/P02-1040/.

Pasley, B. N., David, S. V., Mesgarani, N., Flinker, A., Shamma, S. A., Crone, N. E., Knight, R. T., and Chang, E. F. Reconstructing speech from Human auditory cortex. *PLoS Biology*, 10(1):e1001251, 2012. doi: 10.1371/journal.pbio.1001251.

Peh, W. Y., Thangavel, P., Yao, Y., Thomas, J., Tan, Y. L., and Dauwels, J. Six-center assessment of CNN-Transformer with belief matching loss for patient-independent seizure detection in EEG, 2022. doi: 10.48550/arXiv.2208.00025. URL https://arxiv.org/abs/2208.00025.

Pei, X., Barbour, D. L., Leuthardt, E. C., and Schalk, G. Decoding vowels and consonants in spoken and imagined words using electrocorticographic signals in humans. *Journal of Neural Engineering*, 8(4):046028, 2011. doi: 10.1088/1741-2560/8/4/046028.

Pereira, F., Lou, B., Pritchett, B., Ritter, S., Gershman, S. J., Kanwisher, N., Botvinick, M., and Fedorenko, E. Toward a universal decoder of linguistic meaning from brain activation. *Nature Communications*, 9(1), 2018. doi: 10.1038/s41467-018-03068-4. URL https://doi.org/10.1038/s41467-018-03068-4.

Petrosyan, A., Voskoboinikov, A., Sukhinin, D., Makarova, A., Skalnaya, A., Arkhipova, N., Sinkin, M., and Ossadtchi, A. Speech decoding from a small set of spatially segregated minimally invasive intracranial EEG electrodes with a compact and interpretable neural network. *Journal of Neural Engineering*, 19(6):066016, 2022. doi: 10.1088/1741-2552/aca1e1.

Post, M. A call for clarity in reporting bleu scores. In *Proceedings of the Third Conference on Machine Translation: Research Papers*, 2018. doi: 10.18653/v1/W18-6319. URL https://aclanthology.org/W18-6319/.

Prakash, P. R., Lei, T., Flint, R. D., Hsieh, J. K., Fitzgerald, Z., Mugler, E., Templer, J., Goldrick, M. A., Tate, M. C., Rosenow, J., Glaser, J., and Slutzky, M. W. Decoding speech intent from non-frontal cortical areas. *Journal of Neural Engineering*, 22(1):016024, 2025. doi: 10.1088/1741-2552/adaa20.

Pressel Coretto, G. A., Gareis, I. E., and Rufiner, H. L. Open access database of EEG signals recorded during imagined speech. In Romero, E., Lepore, N., Brieva, J., and Larrabide, I. (eds.), *SPIE Proceedings*, volume 10160, pp. 1016002. SPIE, 2017. doi: 10.1117/12.2255697.

Proix, T., Delgado Saa, J., Christen, A., Martin, S., Pasley, B. N., Knight, R. T., Tian, X., Poeppel, D., Doyle, W. K., Devinsky, O., Arnal, L. H., Mégevand, P., and Giraud, A.-L. Imagined speech can be decoded from low- and cross-frequency intracranial EEG features. *Nature Communications*, 13(1):48, 2022. doi: 10.1038/s41467-021-27725-3.

Qiu, Y., Liu, H., and Zhao, M. A Review of Brain–Computer Interface-Based Language Decoding: From Signal Interpretation to Intelligent Communication. *Applied Sciences*, 15(1):392, 2025. doi: 10.3390/app15010392. URL https://doi.org/10.3390/app15010392.

Rabbani, Q., Shah, S., Milsap, G., Fifer, M. S., Hermansky, H., and Crone, N. E. Iterative alignment discovery of speech-associated neural activity. *Journal of Neural Engineering*, 21(4):046056, 2024. doi: 10.1088/1741-2552/ad663c. URL https://pmc.ncbi.nlm.nih.gov/articles/PMC11351572/.

Rabut, C., Norman, S. L., Griggs, W. S., Russin, J. J., Jann, K., Christopoulos, V., Liu, C., Andersen, R. A., and Shapiro, M. G. Functional ultrasound imaging of human brain activity through an acoustically transparent cranial window. *Science Translational Medicine*, 16(749):eadj3143, 2024. doi: 10.1126/scitranslmed.adj3143.

Rahman, N., Khan, D. M., Masroor, K., Arshad, M., Rafiq, A., and Fahim, S. M. Advances in brain-computer interface for decoding speech imagery from EEG signals: a systematic review. *Cognitive Neurodynamics*, 18(6):3565–3583, 2024. doi: 10.1007/s11571-024-10167-0. URL https://doi.org/10.1007/s11571-024-10167-0.

Rajagopal, G., Chaudhari, A., LaRocco, J., Xue, J., Zachariah, E., Varanasi, S., and Rothman, D. Imagined speech reconstruction with 3d neural metabolism and large language model integration, 2025. doi: 10.1101/2025.07.30.667805. Preprint.

Rastogi, S., Dadwal, H., Modi, K., Bedi, J., and Singh, J. Towards sentence level imagined speech generation from EEG signals. In *Interspeech 2025*, pp. 5558–5562. ISCA, 2025. doi: 10.21437/interspeech.2025-2752.

Rethlefsen, M. L., Kirtley, S., Waffenschmidt, S., Ayala, A. P., Moher, D., Page, M. J., Koffel, J. B., PRISMA-S Group, Blunt, H., Brigham, T., Chang, S., Clark, J., Conway, A., Couban, R., de Kock, S., Farrah, K., Fehrmann, P., Foster, M., Fowler, S. A., Glanville, J., Harris, E., Hoffecker, L., Isojarvi, J., Kaunelis, D., Ket, H., Levay, P., Lyon, J., McGowan, J., Murad, M. H., Nicholson, J., Pannabecker, V., Paynter, R., Pinotti, R., Ross-White, A., Sampson, M., Shields, T., Stevens, A., Sutton, A., Weinfurter, E., Wright, K., and Young, S. Prisma-s: an extension to the PRISMA statement for reporting literature searches in systematic reviews. *Systematic Reviews*, 10(1):39, 2021. doi: 10.1186/s13643-020-01542-z.

Rezazadeh Sereshkeh, A., Yousefi, R., Wong, A. T., and Chau, T. Online classification of imagined speech using functional near-infrared spectroscopy signals. *Journal of Neural Engineering*, 16(1):016005, 2019. doi: 10.1088/1741-2552/aae4b9.

Riegel, J., Schüller, A., and Reichenbach, T. MEG Audiovisual Matrix-Sentence Dataset (using Natural, Avatar, Degraded and Still-Image Version of the Speaker). Zenodo data release, 2026. doi: 10.5281/zenodo.18258659. URL https://zenodo.org/doi/10.5281/zenodo.18258659.

Rotaru, I., Geirnaert, S., Bertrand, A., and Francart, T. KUL-AAD-NFB: Dataset of Auditory Attention Decoding with Neurofeedback, KU Leuven. Zenodo data release, 2026. doi: 10.5281/zenodo.20442638. URL https://zenodo.org/doi/10.5281/zenodo.20442638.

Roussel, P., Le Godais, G., Bocquelet, F., Palma, M., Jiang Hongjie, Zhang, S., Giraud, A.-L., Mégevand, P., Miller, K., Gehrig, J., Kell, C., Kahane, P., Chabardés, S., and Yvert, B. Observation and assessment of acoustic contamination of electrophysiological brain signals during speech production and sound perception. *Journal of Neural Engineering*, 17(5):056028, 2020. doi: 10.1088/1741-2552/abb25e. URL https://pubmed.ncbi.nlm.nih.gov/33055383/.

S, P. S., Sunil, N., Tayade, S., Likhitha, C., Sumitra, S., and Manoj, B. S. IIST BCI Dataset-3 for 100 Malayalam Words. Preprint, 2024. doi: 10.36227/techrxiv.171259992.21826294/v1. URL https://doi.org/10.36227/techrxiv.171259992.21826294/v1.

S., S. M., K., S. D., Sunil, N., S., P. S., Sumitra, S., and S., M. B. Iist BCI dataset-11: Male and female EEG dataset for malayalam vowels and consonants, 2025. doi: 10.36227/techrxiv.174803857.76103011/v1. Preprint.

Sahoo, S., Tayade, S., Likhitha, C., Sumitra, S., and Manoj, B. S. IIST BCI Dataset-6 for Selected Common Odia words. Preprint, 2024. doi: 10.36227/techrxiv.171710270.08933626/v1. URL https://doi.org/10.36227/techrxiv.171710270.08933626/v1.

Samanta, A. K., Mewada, D., Sarma, M., and Samanta, D. Wave2word: A multimodal Transformer framework for joint EEG-Text alignment and Multi-Task representation learning in neurocritical care, 2026. doi: 10.48550/ARXIV.2601.00670.

Sato, M., Kabe, Y., Nobe, S., Yoshida, A., Inoue, M., Shimizu, M., Tomeoka, K., and Sasai, S. Delineating neural contributions to electroencephalogram-based speech decoding, 2024. doi: 10.1101/2024.05.09.591996. Preprint.

Sato, M., Horiguchi, I., Inoue, M., Tomeoka, K., Hatakeyama, E., Kita, Y., Yamamoto, A., Fujisawa, I., and Sasai, S. A 1000-hour EEG-EMG-audio dataset of Japanese speech production, 2026. doi: 10.48550/ARXIV.2606.01264.

Satterlee, N., Zuo, X., Moon, K., Lee, S. Q., Peterson, M., and Kang, J. S. Sentence-level silent speech recognition using a wearable emg/eeg sensor system with AI-Driven sensor fusion and language model. *Sensors*, 25(19):6168, 2025. doi: 10.3390/s25196168.

Sbaih, A., Garcia-Gutierrez, J., Bhushan, M., and Benavides, D. Deep learning methods for EEG-based speech classification and decoding: A PRISMA review. *Computer Speech & Language*, 102:102020, 2026. doi: 10.1016/j.csl.2026.102020. URL https://doi.org/10.1016/j.csl.2026.102020. Available online in 2026; assigned to the February 2027 issue.

Schippers, A., Berezutskaya, J., Vansteensel, M., Freudenburg, Z., Crone, N., and Ramsey, N. The effect of perceived auditory feedback on speech Brain-Computer interface decoding performance. *Clinical Neurophysiology*, 180:2111403, 2025. doi: 10.1016/j.clinph.2025.2111403.

Schneider, F., Kamal, O., Jin, Z., and Schölkopf, B. Moûsai: Text-to-music generation with long-context latent diffusion, 2023. doi: 10.48550/arXiv.2301.11757. URL https://arxiv.org/abs/2301.11757v3.

Schoffelen, J.-M., Oostenveld, R., Lam, N. H. L., Uddén, J., Hultén, A., and Hagoort, P. A 204-subject multimodal neuroimaging dataset to study language processing. *Scientific Data*, 6(1), 2019. doi: 10.1038/s41597-019-0020-y. URL https://doi.org/10.1038/s41597-019-0020-y.

Schroeder, M. L., Sherafati, A., Ulbrich, R. L., Wheelock, M. D., Svoboda, A. M., Klein, E. D., George, T. G., Tripathy, K., Culver, J. P., and Eggebrecht, A. T. Mapping cortical activations underlying covert and overt language production using high-density diffuse optical tomography. *NeuroImage*, 276:120190, 2023. doi: 10.1016/j.neuroimage.2023.120190.

Sereshkeh, A. R., Trott, R., Bricout, A., and Chau, T. Online EEG classification of covert speech for brain–computer interfacing. *International Journal of Neural Systems*, 27(08):1750033, 2017. doi: 10.1142/s0129065717500332.

Sharma, A., Katti, H., Singh, P., Raman, S., and Miyapuram, K. Hierarchic-eeg2text: Assessing EEG-To-Text decoding across hierarchical abstraction levels, 2026. doi: 10.48550/ARXIV.2602.20932.

Shrividya, S., Thundiyil, S., and Picone, J. Fluency in Imagined Speech Decoding Using Non-Invasive Techniques: A Review. In *2025 IEEE Signal Processing in Medicine and Biology Symposium (SPMB)*, pp. 1–3, 2025. doi: 10.1109/SPMB67169.2025.11345383. URL https://doi.org/10.1109/SPMB67169.2025.11345383.

Silva, A. B., Littlejohn, K. T., Liu, J. R., Moses, D. A., and Chang, E. F. The speech neuroprosthesis. *Nature Reviews Neuroscience*, 25(7):473–492, 2024a. doi: 10.1038/s41583-024-00819-9. URL https://pmc.ncbi.nlm.nih.gov/articles/PMC11540306/.

Silva, A. B., Liu, J. R., Metzger, S. L., Bhaya-Grossman, I., Dougherty, M. E., Seaton, M. P., Littlejohn, K. T., Tu-Chan, A., Ganguly, K., Moses, D. A., and Chang, E. F. A bilingual speech neuroprosthesis driven by cortical articulatory representations shared between languages. *Nature Biomedical Engineering*, 8(8):977–991, 2024b. doi: 10.1038/s41551-024-01207-5.

Silversmith, D. B., Abiri, R., Hardy, N. F., Natraj, N., Tu-Chan, A., Chang, E. F., and Ganguly, K. Plug-and-play control of a brain–computer interface through neural map stabilization. *Nature Biotechnology*, 2021. doi: 10.1038/s41587-020-0662-5. URL https://www.nature.com/articles/s41587-020-0662-5.

Simistira Liwicki, F., Gupta, V., Saini, R., De, K., Abid, N., Rakesh, S., Wellington, S., Wilson, H., Liwicki, M., and Eriksson, J. Bimodal electroencephalography-functional magnetic resonance imaging dataset for inner-speech recognition. *Scientific Data*, 10(1):378, 2023. doi: 10.1038/s41597-023-02286-w.

Simistira Liwicki, F., Saini, R., Chakladar, D. D., Rakesh, S., Gupta, V., Liwicki, M., and Eriksson, J. Simultaneous electroencephalography (EEG) and functional magnetic resonance imaging (fMRI) data during an inner speech task. *Data in Brief*, 63:112258, 2025. doi: 10.1016/j.dib.2025.112258.

Singh, A., Thomas, T., Li, J., Hickok, G., Pitkow, X., and Tandon, N. Transfer learning via distributed brain recordings enables reliable speech decoding. *Nature Communications*, 16(1):8749, 2025. doi: 10.1038/s41467-025-63825-0.

Soloukey, S., Vincent, A. J. P. E., Satoer, D. D., Mastik, F., Smits, M., Dirven, C. M. F., Strydis, C., Bosch, J. G., van der Steen, A. F. W., De Zeeuw, C. I., Koekkoek, S. K. E., and Kruizinga, P. Functional ultrasound (fUS) during awake brain surgery: The clinical potential of Intra-Operative functional and vascular brain mapping. *Frontiers in Neuroscience*, 13:1384, 2020. doi: 10.3389/fnins.2019.01384.

Soloukey, S., Collée, E., Verhoef, L., Satoer, D., Dirven, C., Bos, E., Schouten, J., Generowicz, B., Mastik, F., De Zeeuw, C., Koekkoek, S., Vincent, A., Smits, M., and Kruizinga, P. Human brain mapping using co-registered fUS, fMRI and ESM during awake brain surgeries: A proof-of-concept study. *NeuroImage*, 283: 120435, 2023. doi: 10.1016/j.neuroimage.2023.120435.

Soloukey, S., Verhoef, L., Mastik, F., Brown, M., Springeling, G., Generowicz, B. S., Satoer, D. D., Dirven, C. M. F., Smits, M., Hunyadi, B., Koekkoek, S. K. E., Vincent, A. J. P. E., De Zeeuw, C. I., and Kruizinga, P. Mobile human brain imaging using functional ultrasound. *Science Advances*, 11(25):eadu9133, 2025. doi: 10.1126/sciadv.adu9133.

Song, Y., Jia, X., Yang, L., and Xie, L. Transformer-based spatial-temporal feature learning for EEG decoding, 2021. doi: 10.48550/arXiv.2106.11170. URL https://arxiv.org/abs/2106.11170.

Song, Y., Zheng, Q., Liu, B., and Gao, X. EEG Conformer: Convolutional transformer for EEG decoding and visualization. *IEEE Transactions on Neural Systems and Rehabilitation Engineering*, 31:710–719, 2023. doi: 10.1109/TNSRE.2022.3230250.

Soroush, P. Z., Herff, C., Ries, S. K., Shih, J. J., Schultz, T., and Krusienski, D. J. The nested hierarchy of overt, mouthed, and imagined speech activity evident in intracranial recordings. *NeuroImage*, 269:119913, 2023. doi: 10.1016/j.neuroimage.2023.119913.

Spalding, Z., Duraivel, S., Rahimpour, S., Wang, C., Barth, K., Schmitz, C., Lad, S. P., Friedman, A. H., Southwell, D. G., Viventi, J., and Cogan, G. B. Shared latent representations of speech production for cross-patient speech decoding. *Nature Communications*, 17(1):8716, 2026. doi: 10.1038/s41467-026-75455-1.

Speier, W., Arnold, C. W., Deshpande, A., Knall, J., and Pouratian, N. Incorporating advanced language models into the p300 speller using particle filtering. *Journal of Neural Engineering*, 2015. doi: 10.1088/1741-2560/12/4/046018. URL https://pmc.ncbi.nlm.nih.gov/articles/PMC4509796/.

Srinivasan, A., Wairagkar, M., Iacobacci, C., Hou, X., Card, N. S., Jacques, B. G., Pritchard, A. L., Bechefsky, P. H., Hochberg, L. R., AuYong, N., Pandarinath, C., Brandman, D. M., and Stavisky, S. D. Encoding of speech modes and loudness in ventral precentral gyrus. *Nature Communications*, 17(1):5301, 2026. doi: 10.1038/s41467-026-71284-4.

Stavisky, S. D. Restoring Speech Using Brain–Computer Interfaces. *Annual Review of Biomedical Engineering*, 27(1):29–54, 2025. doi: 10.1146/annurev-bioeng-110122-012818. URL https://doi.org/10.1146/annurev-bioeng-110122-012818.

Su, K. and Tian, L. Systematic review: progress in EEG-based speech imagery brain-computer interface decoding and encoding research. *PeerJ Computer Science*, 11:e2938, 2025. doi: 10.7717/peerj-cs.2938.

Sugimoto, Y., Asahara, M., Jeong, H., Kanno, A., Koizumi, M., and Oseki, Y. BCCWJ-fMRI. OpenNeuro dataset release, 2026a. doi: 10.18112/openneuro.ds007752.v1.1.1. URL https://github.com/OpenNeuroDatasets/ds007752.

Sugimoto, Y., Asahara, M., Jeong, H., Kanno, A., Koizumi, M., and Oseki, Y. BCCWJ-MEG. OpenNeuro dataset release, 2026b. doi: 10.18112/openneuro.ds007763.v1.1.1. URL https://github.com/OpenNeuroDatasets/ds007763.

Sugimoto, Y., Asahara, M., Jeong, H., Kanno, A., Koizumi, M., and Oseki, Y. BCCWJ-EEG. OpenNeuro data release, 2026c. doi: 10.18112/openneuro.ds007753.v2.0.0. URL https://openneuro.org/datasets/ds007753/versions/2.0.0.

Sunil, N., S, P. S., Tayade, S., Likhitha, C., Sumitra, S., and S., M. B. IIST BCI Dataset-5 for Malayalam Vowels and Consonants. Preprint, 2024. doi: 10.36227/techrxiv.171527493.34340591/v1. URL https://doi.org/10.36227/techrxiv.171527493.34340591/v1.

Swanson, E., Dohle, E., Bashford, L., Horsfall, H. L., Jovanovic, L., Muirhead, W. R., and Brannigan, J. F. M. Recalibration of implantable brain–computer interfaces to enable long-term independent use–a systematic review. *Journal of Neural Engineering*, 23(3):031004, 2026. doi: 10.1088/1741-2552/ae7694. URL https://doi.org/10.1088/1741-2552/ae7694.

Sümer-Arpak, E., Saini, R., Chakladar, D. D., Varun, S. K., and Simistira Liwicki, F. The current status of foundation models in decoding inner speech from non-invasive brain signals: a mini review. *Frontiers in Human Neuroscience*, 20:1838064, 2026. doi: 10.3389/fnhum.2026.1838064. URL https://doi.org/10.3389/fnhum.2026.1838064.

Taal, C. H., Hendriks, R. C., Heusdens, R., and Jensen, J. An algorithm for intelligibility prediction of time–frequency weighted noisy speech. *IEEE Transactions on Audio, Speech, and Language Processing*, 2011. doi: 10.1109/TASL.2011.2114881. URL https://sps.ewi.tudelft.nl/pubs/Taal2011_1.pdf.

Takahashi, D. Y., El Hady, A., Zhang, Y. S., Liao, D. A., Montaldo, G., Urban, A., and Ghazanfar, A. A. Social-vocal brain networks in a non-human primate, 2021. doi: 10.1101/2021.12.01.470701. Preprint.

Tan, C. and Zhang, Q. Open access dataset integrating behavioral and EEG measures in Chinese spoken word production. *Scientific Data*, 12(1), 2025. doi: 10.1038/s41597-025-05671-9. URL https://doi.org/10.1038/s41597-025-05671-9.

Tang, C., Qi, L., Gao, S., Zhang, Z., Yi, W., Xu, M., Occhipinti, E., Pan, Y., and Occhipinti, L. G. Sensing technologies for silent speech interfaces. *Nature Sensors*, 1(1):16–26, 2026. doi: 10.1038/s44460-025-00010-2. URL https://doi.org/10.1038/s44460-025-00010-2.

Tang, J. and Huth, A. G. Semantic language decoding across participants and stimulus modalities. *Current Biology*, 35(5):1023–1032.e6, 2025. doi: 10.1016/j.cub.2025.01.024.

Tang, J., LeBel, A., Jain, S., and Huth, A. G. Semantic reconstruction of continuous language from non-invasive brain recordings. *Nature Neuroscience*, 26(5):858–866, 2023. doi: 10.1038/s41593-023-01304-9.

Tang, J., Chen, J., Xu, X., Liu, A., and Chen, X. Imagined speech reconstruction from neural signals—an overview of sources and methods. *IEEE Transactions on Instrumentation and Measurement*, 73:1–21, 2024. doi: 10.1109/tim.2024.3472830.

Tankus, A., Stern, E., Klein, G., Kaptzon, N., Nash, L., Marziano, T., Shamia, O., Gurevitch, G., Bergman, L., Goldstein, L., Fahoum, F., and Strauss, I. A speech neuroprosthesis in the frontal lobe and hippocampus: Decoding High-Frequency activity into phonemes. *Neurosurgery*, 96(2):356–364, 2025. doi: 10.1227/neu.0000000000003068.

Tao, Y., Liang, Y., Wang, L., Li, Y., Yang, Q., and Zhang, H. SEE: Semantically aligned EEG-to-text translation. In *ICASSP 2025 - 2025 IEEE International Conference on Acoustics, Speech and Signal Processing (ICASSP)*, pp. 1–5. IEEE, 2025. doi: 10.1109/icassp49660.2025.10889658.

Tates, A., Matran-Fernandez, A., Halder, S., and Daly, I. Speech imagery brain–computer interfaces: a systematic literature review. *Journal of Neural Engineering*, 22(3):031003, 2025. doi: 10.1088/1741-2552/ade28e. URL https://doi.org/10.1088/1741-2552/ade28e.

Tates, A., Matran-Fernandez, A., Halder, S., and Daly, I. Decoding speech imagery or just noise?: a symptom of the replicability crisis. *Journal of Neural Engineering*, 23(5):056018, 2026. doi: 10.1088/1741-2552/aea294.

Tayade, S., S, P. S., Sunil, N., Chauhan, C., Sumitra, S., and Manoj, B. S. IIST BCI Dataset-2 for Selected Common Marathi Words. Preprint, 2024. doi: 10.36227/techrxiv.171043118.80448751/v1. URL https://doi.org/10.36227/techrxiv.171043118.80448751/v1.

Tegon, A., Ingolfsson, T. M., Wang, X., Benini, L., and Li, Y. FEMBA: Efficient and scalable EEG analysis with a bidirectional mamba foundation model. In *2025 47th Annual International Conference of the IEEE Engineering in Medicine and Biology Society (EMBC)*, 2025. URL https://arxiv.org/abs/2502.06438v2.

Thompson, D. E., Blain-Moraes, S., and Huggins, J. E. Performance assessment in brain-computer interface-based augmentative and alternative communication. *BioMedical Engineering OnLine*, 2013. doi: 10.1186/1475-925X-12-43. URL https://pmc.ncbi.nlm.nih.gov/articles/PMC3662584/.

Thompson, D. E., Quitadamo, L. R., Mainardi, L., Laghari, K. u. R., Gao, S., Kindermans, P.-J., Simeral, J. D., Fazel-Rezai, R., Matteucci, M., Falk, T. H., Bianchi, L., Chestek, C. A., and Huggins, J. E. Performance measurement for brain–computer or brain–machine interfaces: a tutorial. *Journal of Neural Engineering*, 2014. doi: 10.1088/1741-2560/11/3/035001. URL https://pmc.ncbi.nlm.nih.gov/articles/PMC4185283/.

Thornton, M., Mandic, D., and Reichenbach, T. Comparison of linear and nonlinear methods for decoding selective attention to speech from ear-EEG recordings. arXiv preprint, 2024. doi: 10.48550/arxiv.2401.05187. URL https://arxiv.org/abs/2401.05187.

Tian, X. and Poeppel, D. Mental imagery of speech and movement implicates the dynamics of internal forward models. *Frontiers in Psychology*, 2010. doi: 10.3389/fpsyg.2010.00166. URL https://doi.org/10.3389/fpsyg.2010.00166.

Tian, X., Zarate, J. M., and Poeppel, D. Mental imagery of speech implicates two mechanisms of perceptual reactivation. *Cortex*, 2016. doi: 10.1016/j.cortex.2016.01.002. URL https://doi.org/10.1016/j.cortex.2016.01.002.

Tripathy, K., Markow, Z. E., Fogarty, M., Schroeder, M. L., Svoboda, A. M., Eggebrecht, A. T., Schlaggar, B. L., Trobaugh, J. W., and Culver, J. P. Multisensory naturalistic decoding with high-density diffuse optical tomography. *Neurophotonics*, 12(01), 2025. doi: 10.1117/1.nph.12.1.015002.

Tuckute, G., Sathe, A., Srikant, S., Taliaferro, M., Wang, M., Schrimpf, M., Kay, K., and Fedorenko, E. Driving and suppressing the human language network using large language models. *Nature Human Behaviour*, 8(3):544–561, 2024. doi: 10.1038/s41562-023-01783-7. URL https://doi.org/10.1038/s41562-023-01783-7.

Türk, S., Padfield, N., Mujahid, K., Camilleri, T., and Camilleri, K. Word-specific properties affect classification performance in brain computer interfaces for decoding imagined speech from EEG [*]. In *2025 47th Annual International Conference of the IEEE Engineering in Medicine and Biology Society (EMBC)*, pp. 1–5. IEEE, 2025. doi: 10.1109/embc58623.2025.11254906.

Vales Cortina, I., Khanday, O. M., Ouellet, M., Pérez-Córdoba, J. L., Rodríguez-San Esteban, P., Miccoli, L., Galdón, A., Olivares Granados, G., and Gonzalez-Lopez, J. A. UGR-MINDVOICE: A multimodal EEG-audio dataset for overt and covert Iberian Spanish speech production. *Computer Speech & Language*, 100:101964, 2026. doi: 10.1016/j.csl.2026.101964. URL https://doi.org/10.1016/j.csl.2026.101964.

van Stuijvenberg, O. C., Broekman, M. L. D., Wolff, S. E. C., Bredenoord, A. L., and Jongsma, K. R. Developer perspectives on the ethics of ai-driven neural implants: a qualitative study. *Scientific Reports*, 2024a. doi: 10.1038/s41598-024-58535-4. URL https://www.nature.com/articles/s41598-024-58535-4.

van Stuijvenberg, O. C., Samlal, D. P. S., Vansteensel, M. J., Broekman, M. L. D., and Jongsma, K. R. The ethical significance of user-control in AI-driven speech-BCIs: a narrative review. *Frontiers in Human Neuroscience*, 18:1420334, 2024b. doi: 10.3389/fnhum.2024.1420334. URL https://doi.org/10.3389/fnhum.2024.1420334.

Vansteensel, M. J., Leinders, S., Branco, M. P., Crone, N. E., Denison, T., Freudenburg, Z. V., Geukes, S. H., Gosselaar, P. H., Raemaekers, M., Schippers, A., Verberne, M., Aarnoutse, E. J., and Ramsey, N. F. Longevity of a brain–computer interface for amyotrophic lateral sclerosis. *New England Journal of Medicine*, 2024. doi: 10.1056/NEJMoa2314598. URL https://pubmed.ncbi.nlm.nih.gov/39141854/.

Varoquaux, G., Raamana, P. R., Engemann, D. A., Hoyos-Idrobo, A., Schwartz, Y., and Thirion, B. Assessing and tuning brain decoders: Cross-validation, caveats, and guidelines. *NeuroImage*, 2017. doi: 10.1016/j.neuroimage.2016.10.038. URL https://pubmed.ncbi.nlm.nih.gov/27989847/.

Verhoef, L., Soloukey, S., Springeling, G., Flikweert, A. J., Lippe, B., de Jong, A. J., Radeljic-Jakic, N., Baas, M., Voorneveld, J., Vincent, A. J., and Kruizinga, P. Miniaturized Four-Dimensional functional ultrasound for mapping Human brain activity, 2025. doi: 10.1101/2025.08.19.25332261. Preprint.

Verwoert, M., Ottenhoff, M. C., Goulis, S., Colon, A. J., Wagner, L., Tousseyn, S., van Dijk, J. P., Kubben, P. L., and Herff, C. Dataset of speech production in intracranial electroencephalography. *Scientific Data*, 9(1):434, 2022. doi: 10.1038/s41597-022-01542-9.

Verwoert, M., Ottenhoff, M. C., Tousseyn, S., van Dijk, J. P., Kubben, P. L., and Herff, C. Moving beyond the motor cortex: A brain-wide evaluation of target locations for intracranial speech neuroprostheses. *Cell Reports*, 44(9):116241, 2025. doi: 10.1016/j.celrep.2025.116241.

Vienneau, E. P., Weeks, A. E., Pan, Y.-C., Shema, P. M., Morgan, V. L., and Byram, B. C. Towards transcranial functional ultrasound imaging through the adult skull. *IEEE Transactions on Biomedical Engineering*, pp. 1–14, 2026. doi: 10.1109/tbme.2026.3680008.

Vitória, M. A., Fernandes, F. G., van den Boom, M., Ramsey, N., and Raemaekers, M. Decoding single and paired phonemes using 7t functional MRI. *Brain Topography*, 37(5):731–747, 2024. doi: 10.1007/s10548-024-01034-6.

Vivek, V., G, J. D., Sumitra, S., and Manoj, B. S. IIST BCI Dataset-12 : A BCI Dataset for Telugu Vocal and Subvocal Commands with Dialect Variation for Wheelchair Control. Preprint, 2025. doi: 10.36227/techrxiv.174953154.47572870/v1. URL https://doi.org/10.36227/techrxiv.174953154.47572870/v1.

Vorontsova, D., Menshikov, I., Zubov, A., Orlov, K., Rikunov, P., Zvereva, E., Flitman, L., Lanikin, A., Sokolova, A., Markov, S., and Bernadotte, A. Silent EEG-Speech recognition using convolutional and recurrent neural network with 85% accuracy of 9 words classification. *Sensors*, 21(20):6744, 2021. doi: 10.3390/s21206744.

Vélez, A., Ru, L., Ahmadi, B., Príncipe, J. C., and Babajani-Feremi, A. Non-invasive Brain-to-Text BCIs: Phoneme-Level sentence reconstruction from MEG, 2026. doi: 10.21203/rs.3.rs-9916752/v1. Preprint.

Wairagkar, M., Card, N. S., Singer-Clark, T., Hou, X., Iacobacci, C., Miller, L. M., Hochberg, L. R., Brandman, D. M., and Stavisky, S. D. An instantaneous voice-synthesis neuroprosthesis. *Nature*, 644(8075):145–152, 2025. doi: 10.1038/s41586-025-09127-3.

Wairagkar, M., Srinivasan, A., Card, N. S., Singer-Clark, T., Hou, X., Iacobacci, C., Miller, L. M., Hochberg, L. R., Brandman, D. M., and Stavisky, S. D. Brain2voice 2.0: High-performance voice synthesis brain-computer interface, 2026. doi: 10.64898/2026.06.30.735633. Preprint.

Wandelt, S. K., Bjånes, D. A., Pejsa, K., Lee, B., Liu, C., and Andersen, R. A. Representation of internal speech by single neurons in human supramarginal gyrus. *Nature Human Behaviour*, 8(6):1136–1149, 2024. doi: 10.1038/s41562-024-01867-y.

Wang, B., Xu, X., Xiao, B., Zheng, L., Wu, X., Cheng, H., and Chen, J. Hierarchical decoding of perceived speech from Non-Invasive brain recordings. *IEEE Transactions on Neural Systems and Rehabilitation Engineering*, 34:2349–2360, 2026a. doi: 10.1109/tnsre.2026.3688564.

Wang, C., Subramaniam, V., Yaari, A. U., Kreiman, G., Katz, B., Cases, I., and Barbu, A. BrainBERT: Self-supervised representation learning for intracranial recordings. In *The Eleventh International Conference on Learning Representations*, 2023. URL https://openreview.net/forum?id=xmcYx_reUn6. Author manuscript: arXiv:2302.14367.

Wang, C., Yaari, A. U., Singh, A. K., Subramaniam, V., Rosenfarb, D., DeWitt, J., Misra, P., Madsen, J. R., Stone, S., Kreiman, G., Katz, B., Cases, I., and Barbu, A. Brain Treebank: Large-scale intracranial recordings from naturalistic language stimuli. arXiv preprint, 2024a. doi: 10.48550/arxiv.2411.08343. URL https://arxiv.org/abs/2411.08343.

Wang, G., Liu, W., He, Y., Xu, C., Ma, L., and Li, H. EEGPT: Pretrained transformer for universal and reliable representation of EEG signals. In *Advances in Neural Information Processing Systems*, volume 37, pp. 39249–39280, 2024b. URL https://proceedings.neurips.cc/paper_files/paper/2024/hash/4540d267eeec4e5dbd9dae9448f0b739-Abstract-Conference.html.

Wang, H., Jia, Z., Shen, Y., Wang, Z., Li, S., Tang, Z., Shu, K., Hu, F., and Wu, D. Sacm: SEEG-Audio contrastive matching for Chinese speech decoding. *IEEE Transactions on Biomedical Engineering*, pp. 1–11, 2026b. doi: 10.1109/tbme.2026.3678858.

Wang, H., Zhang, G., Xie, X., Qin, Y., Zheng, T., Zhou, C., Huang, J., Tian, F., and Wei, S. Decoding Chinese speech across multiple neural conditions via EEG: dataset construction and interpretability driven spatial optimization. *Frontiers in Psychology*, 17:1833448, 2026c. doi: 10.3389/fpsyg.2026.1833448.

Wang, J., Song, Z., Ma, Z., Qiu, X., Zhang, M., and Zhang, Z. Enhancing EEG-to-text decoding through transferable representations from pre-trained contrastive EEG-text masked autoencoder. In *Proceedings of the 62nd Annual Meeting of the Association for Computational Linguistics (Volume 1: Long Papers)*, pp. 7278–7292. Association for Computational Linguistics, 2024c. doi: 10.18653/v1/2024.acl-long.393.

Wang, J., Zhao, S., Luo, Z., Zhou, Y., Jiang, H., Li, S., Li, T., and Pan, G. CBraMod: A criss-cross brain foundation model for EEG decoding. In *The Thirteenth International Conference on Learning Representations*, 2025a. URL https://proceedings.iclr.cc/paper_files/paper/2025/hash/bbbd6d915cb90be21c1254a82d45cedd-Abstract-Conference.html.

Wang, L., Frisson, S., Pan, Y., and Jensen, O. Fast hierarchical processing of orthographic and semantic parafoveal information during natural reading. *Nature Communications*, 16:8893, 2025b. doi: 10.1038/s41467-025-63916-y. URL https://doi.org/10.1038/s41467-025-63916-y.

Wang, S., Zhang, X., Zhang, J., and Zong, C. A synchronized multimodal neuroimaging dataset for studying brain language processing. *Scientific Data*, 9(1), 2022. doi: 10.1038/s41597-022-01708-5. URL https://doi.org/10.1038/s41597-022-01708-5.

Wang, X., Lai, Y.-H., and Chen, F. Intended speech classification with EEG signals based on a temporal attention mechanism: A study of Mandarin vowels. In *2024 46th Annual International Conference of the IEEE Engineering in Medicine and Biology Society (EMBC)*, pp. 1–4. IEEE, 2024d. doi: 10.1109/embc53108.2024.10782383.

Wang, Y., Liu, H., Wang, Y., Xuan, C., Hou, Y., Feng, S., Liu, H., Liao, Y., and Wang, Y. Progress, challenges and future of linguistic neural decoding with deep learning. *Communications Biology*, 8(1):1350, 2025c. doi: 10.1038/s42003-025-08511-z. URL https://www.nature.com/articles/s42003-025-08511-z.

Wang, Y., Wang, S., Cai, W., Ford, G., Cui, Y., Zhang, Y., Du, C., Fan, C., Li, D., Zhou, H., Zhang, H., Li, J., Liu, Q., Huang, W., Lu, Y., Chen, Z., and Sun, J. Representation, Alignment, and Generation: A Comprehensive Survey of Foundation Models for Non-Invasive Brain Decoding. bioRxiv preprint, 2025d. doi: 10.64898/2025.11.30.691403. URL https://doi.org/10.64898/2025.11.30.691403. Preprint; not peer reviewed.

Wang, Y., Wang, H., Guo, Y., Yang, H., and Li, X. Escaping the BLEU trap: A Signal-Grounded framework with decoupled semantic guidance for EEG-to-Text decoding, 2026d. doi: 10.48550/ARXIV.2603.03312.

Wang, Z. and Ji, H. Open vocabulary Electroencephalography-to-Text decoding and Zero-Shot sentiment classification. *Proceedings of the AAAI Conference on Artificial Intelligence*, 36(5):5350–5358, 2022. doi: 10.1609/aaai.v36i5.20472.

Wang, Z., Kou, Z., Zhang, J., Li, J., Gong, C., Lin, C., Wu, J., Oelze, M. L., Zhou, Q., and Yang, Y. Acoustic transparency enabling functional ultrasound imaging through mouse and Human skulls, 2025e. doi: 10.1101/2025.08.22.671878. Preprint.

Wehbe, L., Murphy, B., Talukdar, P., Fyshe, A., Ramdas, A., and Mitchell, T. Simultaneously Uncovering the Patterns of Brain Regions Involved in Different Story Reading Subprocesses. *PLoS ONE*, 9(11):e112575, 2014. doi: 10.1371/journal.pone.0112575. URL https://doi.org/10.1371/journal.pone.0112575.

Wellington, S. and Clayton, J. Fourteen-channel EEG with Imagined Speech (FEIS) dataset. Zenodo data release, 2019. doi: 10.5281/zenodo.3554128. URL https://zenodo.org/record/3554128.

Wellington, S., Wilson, H., Liwicki, F. S., Gupta, V., Saini, R., De, K., Abid, N., Rakesh, S., Eriksson, J., Watts, O., Chen, X., Coyle, D., Golbabaee, M., Proulx, M. J., Liwicki, M., O' Neill, E., and Metcalfe, B. Improving inner speech decoding by hybridisation of bimodal EEG and fMRI data. In *2024 46th Annual International Conference of the IEEE Engineering in Medicine and Biology Society (EMBC)*, pp. 1–5. IEEE, 2024. doi: 10.1109/embc53108.2024.10781692.

Willett, F. R., Kunz, E. M., Fan, C., Avansino, D. T., Wilson, G. H., Choi, E. Y., Kamdar, F., Glasser, M. F., Hochberg, L. R., Druckmann, S., Shenoy, K. V., and Henderson, J. M. A high-performance speech neuroprosthesis. *Nature*, 620(7976):1031–1036, 2023. doi: 10.1038/s41586-023-06377-x.

Willett, F. R., Li, J., Le, T., Fan, C., Chen, M., Shlizerman, E., Chen, Y., Zheng, X., Okubo, T. S., Benster, T., Lee, H. D., Kounga, M., Buchanan, E. K., Zoltowski, D., Linderman, S. W., and Henderson, J. M. Brain-to-Text Benchmark '24: Lessons learned, 2024. doi: 10.48550/arXiv.2412.17227. URL https://arxiv.org/abs/2412.17227v1. Version 1, 23 December 2024. Competition retrospective includes explicitly identified post-competition results.

Wohns, N., Dorfman, N., and Klein, E. Caregivers in implantable brain-computer interface research: a scoping review. *Frontiers in Human Neuroscience*, 18:1490066, 2024. doi: 10.3389/fnhum.2024.1490066. URL https://doi.org/10.3389/fnhum.2024.1490066.

Wolpaw, J. R., Bedlack, R. S., Reda, D. J., Ringer, R. J., Banks, P. G., Vaughan, T. M., Heckman, S. M., McCane, L. M., Carmack, C. S., Winden, S., McFarland, D. J., Sellers, E. W., Shi, H., Paine, T., Higgins, D. S., Lo, A. C., Patwa, H. S., Hill, K. J., Huang, G. D., and Ruff, R. L. Independent home use of a brain-computer interface by people with amyotrophic lateral sclerosis. *Neurology*, 2018. doi: 10.1212/WNL.0000000000005812. URL https://pmc.ncbi.nlm.nih.gov/articles/PMC6059033/.

Wu, H., Cai, C., Ming, W., Chen, W., Zhu, Z., Feng, C., Jiang, H., Zheng, Z., Sawan, M., Wang, T., and Zhu, J. Speech decoding using cortical and subcortical electrophysiological signals. *Frontiers in Neuroscience*, 18: 1345308, 2024a. doi: 10.3389/fnins.2024.1345308.

Wu, S., Bhadra, K., Giraud, A.-L., and Marchesotti, S. Adaptive LDA classifier enhances Real-Time control of an EEG brain–computer interface for decoding imagined syllables. *Brain Sciences*, 14(3):196, 2024b. doi: 10.3390/brainsci14030196.

Wu, X., Wellington, S., Fu, Z., and Zhang, D. Speech decoding from stereo-electroencephalography (sEEG) signals using advanced deep learning methods. *Journal of Neural Engineering*, 21(3):036055, 2024c. doi: 10.1088/1741-2552/ad593a.

Wu, X., Hu, K., Fu, Z., and Zhang, D. Improved evaluation of waveform reconstruction in speech decoding based on invasive brain-computer interfaces. *Imaging Neuroscience*, 3:IMAG.a.146, 2025. doi: 10.1162/imag.a.146.

Xi, N., Zhao, S., Wang, H., Liu, C., Qin, B., and Liu, T. Unicorn: Unified cognitive signal ReconstructioN bridging cognitive signals and human language. In *Proceedings of the 61st Annual Meeting of the Association for Computational Linguistics (Volume 1: Long Papers)*, pp. 13277–13291. Association for Computational Linguistics, 2023. doi: 10.18653/v1/2023.acl-long.741.

Xiao, Q., Cui, Z., Zhang, C., Chen, S., Wu, W., Thwaites, A., Woolgar, A., Zhou, B., and Zhang, C. BrainOmni: A brain foundation model for unified EEG and MEG signals. In *Advances in Neural Information Processing Systems*, volume 38, 2025. URL https://arxiv.org/abs/2505.18185.

Xiong, W., Ma, L., and Li, H. Synthesizing intelligible utterances from EEG of imagined speech. *Frontiers in Neuroscience*, 19:1565848, 2025. doi: 10.3389/fnins.2025.1565848.

Xu, Y., Zhang, Y., Peng, Y., Yan, B., Wu, Z., Ding, M., and Chen, L. A generalizable OPM-MEG framework for time-resolved language decoding during natural speech production. *NeuroImage*, 340:122219, 2026. doi: 10.1016/j.neuroimage.2026.122219.

Yang, B.-h., Gan, A.-a., Guo, W.-b., and Kuang, S. A Review of EEG-Based Speech Imagery Encoding Paradigms and Decoding Algorithms. *Journal of Brain-Computer Interface*, 1(1):58, 2025. doi: 10.58195/bci.2025.1.008. URL https://doi.org/10.58195/bci.2025.1.008.

Yang, C., Westover, M. B., and Sun, J. BIOT: Biosignal transformer for cross-data learning in the wild. In *Advances in Neural Information Processing Systems*, volume 36, pp. 78240–78260, 2023a. URL https://proceedings.neurips.cc/paper_files/paper/2023/hash/f6b30f3e2dd9cb53bbf2024402d02295-Abstract.html.

Yang, C., Xiao, C., Westover, M. B., and Sun, J. Self-supervised electroencephalogram representation learning for automatic sleep staging: Model development and evaluation study. *JMIR AI*, 2:e46769, 2023b. doi: 10.2196/46769.

Yang, X., Tian, H., Li, Y., Zhang, J., Li, S., and Pan, G. Brain-cliplm: semantic compression for EEG-to-text decoding. *Frontiers in Neuroscience*, 20:1899770, 2026a. doi: 10.3389/fnins.2026.1899770.

Yang, Y., Duan, Y., Jo, H., Zhang, Q., Xu, R., Jones, O. P., Hu, X., Lin, C.-t., and Xiong, H. Neugpt: Unified multi-modal neural gpt, 2024a. doi: 10.48550/ARXIV.2410.20916. URL https://arxiv.org/abs/2410.20916.

Yang, Y., Duan, Y., Zhang, Q., Jo, H., Zhou, J., Lee, W. H., Xu, R., and Xiong, H. NeuSpeech: Decode neural signal as speech, 2024b. doi: 10.48550/arXiv.2403.01748. URL https://arxiv.org/abs/2403.01748v3. arXiv:2403.01748v3.

Yang, Y., Jo, H., Duan, Y., Zhang, Q., Zhou, J., Hu, X., Lee, W. H., Xu, R., and Xiong, H. Mad: Multi-alignment meg-to-text decoding, 2024c. doi: 10.48550/ARXIV.2406.01512. URL https://arxiv.org/abs/2406.01512v2. arXiv:2406.01512v2.

Yang, Y., Duan, Y., Zhang, Q., Jo, H., Zhou, J., Lee, W. H., Xu, R., and Xiong, H. Neuspeech: Decode neural signal as speech. In *ICASSP 2026 - 2026 IEEE International Conference on Acoustics, Speech and Signal Processing (ICASSP)*, pp. 6636–6640. IEEE, May 2026b. doi: 10.1109/icassp55912.2026.11463589.

Ye, C., Zhang, Y., Sun, J., Li, C., Zhao, Y., and Wang, S. Decoding the multimodal mind: Generalizable Brain-to-Text translation via multimodal alignment and adaptive routing. In *Findings of the Association for Computational Linguistics: ACL 2026*, pp. 22532–22546. Association for Computational Linguistics, 2026. doi: 10.18653/v1/2026.findings-acl.1131.

Ye, Z., Ai, Q., Liu, Y., de Rijke, M., Zhang, M., Lioma, C., and Ruotsalo, T. Generative language reconstruction from brain recordings. *Communications Biology*, 8(1):346, 2025. doi: 10.1038/s42003-025-07731-7.

Yin, C., Yu, Q., Fang, Z., Peng, C., and Li, P. Rethinking Cross-Subject data splitting for Brain-to-Text decoding. In *Proceedings of the 2025 Conference on Empirical Methods in Natural Language Processing*, pp. 5675–5689. Association for Computational Linguistics, 2025. doi: 10.18653/v1/2025.emnlp-main.289.

Yin, C., Ye, Z., and Li, P. Language reconstruction with brain predictive coding from fMRI data. In *Proceedings of the 64th Annual Meeting of the Association for Computational Linguistics (Volume 1: Long Papers)*, pp. 20720–20743. Association for Computational Linguistics, 2026. doi: 10.18653/v1/2026.acl-long.949. URL https://aclanthology.org/2026.acl-long.949/.

Yoshimura, N., Nishimoto, A., Belkacem, A. N., Shin, D., Kambara, H., Hanakawa, T., and Koike, Y. Decoding of covert vowel articulation using electroencephalography cortical currents. *Frontiers in Neuroscience*, 10, 2016. doi: 10.3389/fnins.2016.00175.

Yu, B., Zhang, S., Zhou, L., Wei, J., Sun, L., and Bu, L. Brain-inspired computing based on deep learning for human-computer interaction: A review. *Neurocomputing*, 650:130928, 2025. doi: 10.1016/j.neucom.2025.130928. URL https://doi.org/10.1016/j.neucom.2025.130928.

Yuan, B. A. and Makin, J. G. Improving speech decoding from ECoG with self-supervised pretraining, 2024. doi: 10.48550/arXiv.2405.18639. URL https://arxiv.org/abs/2405.18639. Preprint; version 1, 28 May 2024.

Zhang, A., Wang, B., Wu, X., Cheng, H., and Chen, J. Cross-subject generalization in decoding perceived speech from Non-Invasive brain recordings, 2026a. doi: 10.48550/ARXIV.2608.22420.

Zhang, D., Wang, Z., Qian, Y., Zhao, Z., Liu, Y., Hao, X., Li, W., Lu, S., Zhu, H., Chen, L., Xu, K., Li, Y., and Lu, J. A brain-to-text framework for decoding natural tonal sentences. *Cell Reports*, 43(11):114924, 2024a. doi: 10.1016/j.celrep.2024.114924.

Zhang, H., Siok, W. T., and Wang, N. Imagined speech brain–computer interface: A Task-Oriented review of neural decoding. *Sensors*, 26(10):3212, 2026b. doi: 10.3390/s26103212.

Zhang, L., Zhou, Y., Gong, P., and Zhang, D. Speech Imagery Decoding Using EEG Signals and Deep Learning: A Survey. *IEEE Transactions on Cognitive and Developmental Systems*, 17(1):22–39, 2025. doi: 10.1109/TCDS.2024.3431224. URL https://doi.org/10.1109/TCDS.2024.3431224.

Zhang, S., Alam, E., Baber, J., Bianco, F., Turner, E., Chamanzar, M., and Dehghani, H. Mindspeech: Continuous imagined speech decoding using high-density fnirs and prompt tuning for advanced human-ai interaction. *arXiv preprint*, 2024b. doi: 10.48550/ARXIV.2408.05362. URL https://arxiv.org/abs/2408.05362.

Zhang, T., Kishore, V., Wu, F., Weinberger, K. Q., and Artzi, Y. Bertscore: Evaluating text generation with bert. In *International Conference on Learning Representations*, 2020. URL https://arxiv.org/abs/1904.09675.

Zhang, X., Liu, S., Lu, R., Woolgar, A., and Wang, L. What are we actually decoding? source attribution for Non-Invasive Brain-to-Language retrieval, 2026c. doi: 10.48550/ARXIV.2605.24524.

Zhang, Y., He, L., Fan, C., Liu, T., Yu, H., Le, T., Li, J., Linderman, S., Duncker, L., Willett, F. R., Mesgarani, N., and Paninski, L. A cross-species neural foundation model for end-to-end speech decoding. In *The Fourteenth International Conference on Learning Representations*, 2026d. URL https://openreview.net/forum?id=Lp1noMpMUG.

Zhang, Z., Ding, X., Bao, Y., Zhao, Y., Liang, X., Qin, B., and Liu, T. Chisco: An EEG-based BCI dataset for decoding of imagined speech. *Scientific Data*, 11(1):1265, 2024c. doi: 10.1038/s41597-024-04114-1.

Zhang, Z., Bao, Y., Ding, X., Jiang, T., and Xiong, K. Is EEG-to-text feasible in real-world scenarios? an in-depth analysis using a neuropsychology-inspired benchmark. In *Proceedings of the 64th Annual Meeting of the Association for Computational Linguistics (Volume 1: Long Papers)*, pp. 1378–1393. Association for Computational Linguistics, 2026e. doi: 10.18653/v1/2026.acl-long.61.

Zhang, Z., Li, S., Sabatini, B. L., Aoi, M. C., and Mishne, G. ALIGN: Adversarial learning for generalizable speech neuroprosthesis. In *Proceedings of the 42nd Conference on Uncertainty in Artificial Intelligence*, volume 337 of *Proceedings of Machine Learning Research*, pp. 8006–8025. PMLR, 2026f. URL https://proceedings.mlr.press/v337/zhang26a.html.

Zhao, S. and Rudzicz, F. Classifying phonological categories in imagined and articulated speech. In *2015 IEEE International Conference on Acoustics, Speech and Signal Processing (ICASSP)*, pp. 992–996. IEEE, 2015. doi: 10.1109/icassp.2015.7178118. URL https://doi.org/10.1109/icassp.2015.7178118.

Zhao, Z., Zhou, J., Jiang, X., Cao, B., Ma, W., Shen, Y., Li, R., Wang, Y.-K., and Lin, C.-t. Brainstack: Neuro-MoE with functionally guided expert routing for EEG-Based language decoding, 2026. doi: 10.48550/ARXIV.2601.21148.

Zheng, H., Wu, Y., Qian, T., Yue, W., and Wang, X. Guiding LLMs to decode text via aligning semantics in EEG signals and language. *Expert Systems with Applications*, 299:130300, 2026. doi: 10.1016/j.eswa.2025.130300. URL https://doi.org/10.1016/j.eswa.2025.130300.

Zhou, J., Duan, Y., Chang, F., Do, T., Wang, Y.-K., and Lin, C.-T. Belt-2: Bootstrapping EEG-to-Language representation alignment for multi-task brain decoding, 2024a. doi: 10.48550/ARXIV.2409.00121.

Zhou, J., Duan, Y., Chang, Y.-C., Wang, Y.-K., and Lin, C.-T. BELT: Bootstrapped EEG-to-language training by natural language supervision. *IEEE Transactions on Neural Systems and Rehabilitation Engineering*, 32: 3278–3288, 2024b. doi: 10.1109/tnsre.2024.3450795.

Zhou, J., Duan, Y., Zhao, Z., Chang, Y.-C., Wang, Y.-K., Do, T., and Lin, C.-T. Towards linguistic neural representation learning and sentence retrieval from electroencephalogram recordings. In *Proceedings of the 1st International Workshop on Brain-Computer Interfaces (BCI) for Multimedia Understanding*, pp. 19–28. ACM, 2024c. doi: 10.1145/3688862.3689109.

Zhou, J., Cao, Z., Duan, Y., Barkley, C., Leong, D., Jiang, X., Nguyen, Q.-T., Zhao, Z., Do, T., Chang, Y.-C., Liang, S.-F., and Lin, C.-t. Pretraining Large Brain Language Model for Active BCI: Silent Speech. arXiv preprint, 2025a. doi: 10.48550/arxiv.2504.21214. URL https://arxiv.org/abs/2504.21214.

Zhou, J., Cao, Z., Duan, Y., Barkley, C., Leong, D., Jiang, X., Nguyen, Q.-T., Zhao, Z., Do, T., Chang, Y.-C., Liang, S.-F., and Lin, C.-T. Pretraining large brain language model for active BCI: Silent speech. In *Proceedings of the 33rd ACM International Conference on Multimedia*, pp. 5883–5892. ACM, 2025b. doi: 10.1145/3746027.3754810.

Zhu, H., Yan, Y., Xu, X., Ge, Z., Tian, P., Wu, X., and Chen, J. ear-EEG dataset for AAD task in Multiple-speaker environment. Zenodo data release, 2024. doi: 10.5281/zenodo.10803261. URL https://zenodo.org/doi/10.5281/zenodo.10803261.

Özdogan, M., Landau, G., Elvers, G., Jayalath, D., Somaiya, P., Mantegna, F., Woolrich, M., and Parker Jones, O. Libribrain: Over 50 hours of Within-Subject MEG to improve speech decoding methods at scale. In *Advances in Neural Information Processing Systems 38*, pp. 17016–17053. Neural Information Processing Systems Foundation, Inc. (NeurIPS), 2025. doi: 10.52202/085713-0511.

A Glossary

Table 14. Terms and abbreviations as used in this survey.

Term	Meaning here
Task group	Articulated, Inner or Perceived, assigned from the actual condition (Table 2)
Task descriptor	content source, elicitation, repetition, cue modality, preparation interval and peripheral monitoring; separate from group and subtype

Term	Meaning here
Source terminology	covert and imagined are mapped to Inner only when instructions meet its definition; silent alone does not determine a group
Articulated	actual articulation: Overt, Mouthed or Limited; Limited requires residual articulation during impaired attempts
Output type	what the decoder produced: candidate selection, text decoding, speech synthesis and facial/body animation (Table 7)
Evidence scope	whether a study decoded content, detected speech state, mapped language, analysed representations, released data or evaluated methods
Validation conditions	test units, controls, uncertainty and verification provenance, recorded separately from output type
Use evidence	condition-specific participants, online evaluation and duration of actual system use
Bridging	training on Overt or clinical attempted speech and transferring to a specified Mouthed or Inner condition
Route	text, voice or meaning pipeline (Figure 9)
iEEG	ECoG and sEEG collectively; μECoG = micro-ECoG
EXG / EMG_aux	peripheral electrodes (EOG, EMG) recorded alongside EEG; systems that use them are flagged
OPM-MEG	MEG with optically pumped magnetometers
HD-DOT	high-density diffuse optical tomography, a dense fNIRS variant
fUSI, tFUS	functional ultrasound imaging (recording; in scope) vs. transcranial focused ultrasound stimulation (out of scope)
ESM	electrical stimulation mapping
PEEK	polyether ether ketone, the polymer of the acoustically transparent cranial window
WER, CER, PER	word, character and phoneme error rate
MOS	mean opinion score from listeners
DTW	dynamic time warping, used to align synthesised and reference audio
RNN-T	recurrent-network transducer, a streaming sequence decoder
LM	language model; LLM = large language model
WFST	weighted finite-state transducer; combines token, lexicon and language-model constraints in decoding
SEM	standard error of the mean
LOSO	leave-one-subject-out evaluation

B Supplementary Signal Mechanisms

The acquisition examples in Table 3 distinguish temporal and spatial sampling from physiological response and functional localisation. The complementary map below explains why faster sampling alone cannot equate their information content. Electrical and magnetic measurements and vascular responses have different physiological origins; decoder windows add another temporal constraint. Recording access also determines which tissue can be sampled. These dependencies support choosing an acquisition configuration for the intended task and operating setting, rather than inferring decoding capability from a nominal resolution value (Section 4).

C Search Strategy Summary

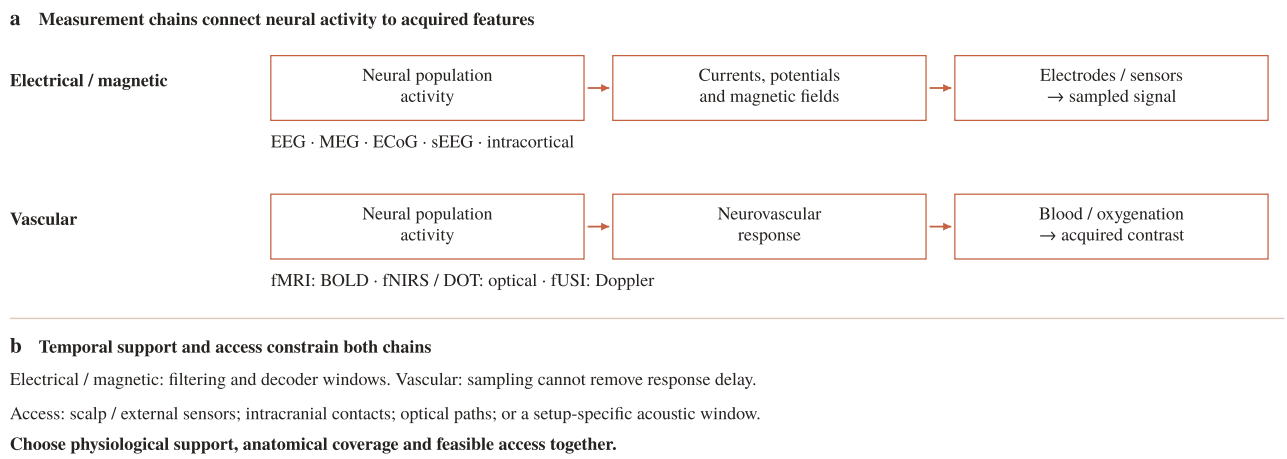


Figure 24. The usable neural measurement depends on its physiological origin, temporal support and recording access. Electrical and magnetic recordings and vascular measurements observe different consequences of neural activity. Acquisition speed does not remove vascular response delay, while filtering and decoder windows also constrain electrical or magnetic information. The access map is schematic, not a ranking of spatial resolution, latency or decoding accuracy. fUSI depends on the acoustic window and preparation; its placement does not imply established word- or sentence-level speech decoding.

Table 15. Selected human-relevant fUSI reports examined here. The listed studies do not demonstrate word- or sentence-level speech-content decoding; adjacent feasibility and motor tasks are kept distinct.

Study	Access, task	Reported evidence scope
(Soloukey et al., 2020)	intra-op; aloud and source-labelled covert repetition	language mapping; covert instructions require task-level interpretation
(Soloukey et al., 2023)	intra-op; language task	mapping, fUS–fMRI–ESM overlap
(Imbault et al., 2017)	intra-op; motor task	feasibility of intra-operative fUS
(Rabut et al., 2024)	cranial window; motor and guitar	non-linguistic decoding
(Lin et al., 2026)	cranial window; effectors, fingers	single-trial motor decoding
(Soloukey et al., 2025)	polymer (PEEK) window; walking, imagined lip licking	mapping; motor imagery
(Verhoef et al., 2025)	window/defect; finger task	4-D imaging feasibility
(Vienneau et al., 2026)	intact skull; breath hold	vascular reactivity
(Chen et al., 2025d)	skull defect; clicks	non-speech auditory mapping

Table 16. Search sources, procedures and coverage dates. Detailed queries and version links are available in the accompanying search materials.

Step	Search procedure	Coverage / interpretation
Broad database search	Europe PMC: 12 query groups; OpenAlex: 4 query groups; full pagination without a lower year limit	First publication through 15 September 2026
Keyword coverage	Signal synonyms combined with speech, phoneme, vowel, word or language and decoding, recognition, classification, synthesis or reconstruction	Separate unspoken, attempted, watched and functional-ultrasound queries
Citation tracking	Forward citations of 16 reviews and key papers; backward references of surveys and fUSI reports; Crossref metadata completion	Seed-based follow-up; not an estimate of field-wide recall
Recall check	All 44 entries in the earlier seed survey recovered	Tests this predefined seed set

Step	Search procedure	Coverage / interpretation
Author and reading supplements	Author tracing added three records; reading-route searches added 36 stable IDs	16 September; original publication cut-off retained
Recent-review search	Europe PMC, Crossref, publisher and repository discovery, and reference tracking for reviews from 2024 onwards	18 September; separate review inventory (Appendix D)
Thematic follow-up	Subsection-specific primary-source searches and recent comparative-result tables	19–21 September; eligible reports/resources added to the updated registry
Version consolidation	DOI, normalised title and explicit preprint–publication links; aliases retain source provenance	938 retained IDs; 920 canonical report/resource entries
Screening and extraction	Condition-level task, signal, target and evaluation fields; cohort links recorded separately	246 entries with selected structured extraction; depth varies by claim
Companion resources	Dataset releases linked to corresponding articles; follow-up studies retained when they report new evidence	Entries are not independent participant cohorts

The accompanying thematic-search records retain the subsection queries and source checks; the manuscript repository provides the registry-derived counts and figure scripts. Example query structure:

```
(speech OR phonem* OR vowel* OR word* OR language OR verbal)
AND (decod* OR recogn* OR classif* OR synthes* OR reconstruct* OR neuroprosthe*)
AND (EEG OR electroencephalog* [or other signal synonyms])

Silent paradigms:  ("imagined speech" OR "inner speech" OR "covert speech"
                    OR "internal speech" OR "speech imagery" OR "silent speech")
Ultrasound:        "functional ultrasound" OR fUSI
                   OR "functional ultrasonography"
```

D Recent Reviews and Their Scope

The targeted review supplement searched 2024–2026 publications through 18 September 2026. The first part of Table 17 lists 30 directly relevant reviews; the second lists 16 contextual reviews or perspectives used in the synthesis. These are reports with different scopes, not independent replications of the studies they cite. Characterisations identify a reported focus rather than score completeness or methodological quality. A denotes abstract-level scope checking; P denotes targeted article-section checking, not complete full-text appraisal; T denotes title/metadata only. Source descriptions are retained without importing their task terminology into this survey's operational definitions.

Table 17. Recent reviews informing the survey. Preprints, short reviews, proceedings and online/issue-year differences are explicitly identified.

Reference	Date	Scope and publication qualification	Check
Directly relevant reviews			
(Silva et al., 2024a)	2024	Speech neuroprostheses: cortical representations, output forms and clinical performance.	A
(Rahman et al., 2024)	2024	EEG speech imagery: neural basis, signal processing and learning methods.	A
(Alzahrani et al., 2024)	2024	EEG imagined-speech classification: paradigms, features, classifiers and datasets.	A

Reference	Date	Scope and publication qualification	Check
(Zhang et al., 2025)	2025	EEG speech imagery: datasets, input representations, deep models and evaluation. 2024 online; 2025 issue.	A
(Tang et al., 2024)	2024	Imagined-speech reconstruction across neural sources and methodological routes.	A
(Murad & Rahimi, 2025)	2025	EEG-to-text: acquisition, signal processing and text-generation pipelines. 2024 preprint/online; 2025 issue.	A
(Stavisky, 2025)	2025	Clinical need, discrete and continuous speech decoding, closed-loop systems and metrics.	A
(Qiu et al., 2025)	2025	Language decoding from signal interpretation to intelligent communication.	A
(Wang et al., 2025c)	2025	Linguistic decoding across perception and production, signals and deep-learning methods.	A
(Su & Tian, 2025)	2025	EEG speech imagery: encoding paradigms, neural connectivity and decoding algorithms.	P
(Tates et al., 2025)	2025	Speech-imagery pipelines across modalities; task instructions, transfer rates and online use.	A
(Jin et al., 2025)	2025	EEG imagined speech: theory, data, features and learning methods.	A
(Almufareh et al., 2025)	2025	Inner-speech signals, models, calibration and ethical or translational constraints.	A
(Chowdhury et al., 2025a)	2025	Inner-speech recognition: datasets, preprocessing and machine-learning approaches.	P
(Jhilal et al., 2025)	2025	Implantable speech decoders: patient selection, recording targets and training. 2025 online; 2026 issue.	A
(Doda et al., 2025)	2025	Speech BCI models, communication rehabilitation and ethical challenges.	A
(Yu et al., 2025)	2025	Deep-learning approaches to brain-to-text and brain-to-speech interaction.	A
(Duhair et al., 2026)	2026	EEG imagined-speech decoding methods and challenges.	A
(Estrella-Ibarra et al., 2026)	2026	Imagined-speech EEG pipelines with linguistic, neural and computational perspectives.	A
(Zhang et al., 2026b)	2026	Task granularity, constrained output spaces and output pathways.	P
(Belfrouh et al., 2026)	2026	Brain-to-speech for paralysis: acquisition, AI methods and clinical evidence appraisal.	P
(Sümer-Arpak et al., 2026)	2026	Non-invasive inner speech and foundation models; direct evidence and transfer prospects. Mini review.	P
(He et al., 2026)	2026	Intracranial language BCI mechanisms, hardware, algorithms, evaluation and clinical pathways. Preprint, v2; not peer reviewed.	P
(Divya Keerthana et al., 2026)	2026	EEG imagined-speech techniques, applications and challenges.	A
(Sbaih et al., 2026)	2026	Deep learning for speech classification and decoding; PRISMA-organised synthesis. 2026 availability; 2027 issue.	A
(Geetha et al., 2025)	2025	Brain-to-text technologies and communication aids (title-level scope only). 2025 conference; indexed 2026.	T
(Gao, 2026)	2026	Brain-to-text, speech and image interfaces; visual reconstruction extends beyond our scope. Conference proceedings.	A
(Shrividya et al., 2025)	2025	Fluency in non-invasive imagined-speech decoding; short conference review. 2025 conference; indexed 2026.	A
(Yang et al., 2025)	2025	Chinese-language review of EEG speech-imagery encoding paradigms and decoding algorithms.	A
(Motaqi et al., 2026)	2026	EEG, fNIRS and hybrid imagined-speech decoding.	A
Contextual reviews and perspectives			

Reference	Date	Scope and publication qualification	Check
(Wang et al., 2025d)	2025	Non-invasive foundation models: representation, alignment and generation. Preprint; not peer reviewed.	A
(Mai et al., 2025)	2025	Brain-conditional multimodal synthesis and its taxonomy. 2024 online; 2025 issue.	A
(Kuruppu et al., 2026)	2026	EEG foundation models: progress, evaluation and open challenges.	A
(Li et al., 2025e)	2025	Domain adaptation for neural signal decoding.	A
(Khan et al., 2025)	2025	Invasive BCI communication, including channels other than speech.	P
(Dohle et al., 2025)	2025	Implantable BCI translation and decoder, task and clinical outcome measures.	P
(Swanson et al., 2026)	2026	Recalibration frequency, duration, assistance and setting for long-term use.	A
(Wohns et al., 2024)	2024	Caregiver participation in implantable BCI research and operation.	P
(Kreiner & Eviatar, 2024)	2024	The form and prosody of inner speech.	A
(Dahò & Monzani, 2025)	2025	Inner-speech phenomenology, neural correlates and clinical implications.	A
(Li et al., 2026b)	2026	A perspective on moving from speech to language BCIs. Perspective.	A
(Hong et al., 2024)	2024	Stimulation-induced speech perception and prospective neural return channels.	A
(Tang et al., 2026)	2026	Silent-speech sensing across neural and peripheral modalities.	A
(van Stuijvenberg et al., 2024b)	2024	Executory and guidance control in AI-assisted speech BCIs.	P
(Oota et al., 2024)	2024	Language, visual and auditory brain encoding/decoding with deep neural networks. 2024 journal; 2023 preprint.	A
(Alexander & Stark, 2024)	2024	Multidimensional inner speech and interdisciplinary clinical evidence.	A

E Additional Study Coverage

E.1 Coverage beyond the selected performance examples

The performance examples below are a selective synthesis, whereas the accompanying study registry contains every workbook entry. This separation matters because bibliographic coverage, task coding and result verification are different stages. The companion coverage table retains original registry labels; these are provenance fields, not the three-group classification. Pending entries are retained with source links and stable IDs; their presence establishes what remains to be checked, not a positive decoding result. The following map brings additional directions already recorded in the workbook into the scope of the narrative. Author–year citations identify the reports discussed here; the accompanying registry records the extraction status of each entry. Descriptions of pending work are limited to its indexed topic or existing task note, without adding unverified accuracies.

Articulated: Overt and Mouthed methods. The index extends from phoneme localisation and classification (Blakely et al., 2008; Mugler et al., 2014) and cortical-surface spoken-word classification (Kellis et al., 2010) to continuous phoneme decoding (Moses et al., 2016) and direct ECoG synthesis (Herff et al., 2016; Angrick et al., 2019). More recent entries address sparse depth electrodes (Petrosyan et al., 2022), surface/depth Transformer models (Chen et al., 2025a), syntactic roles during sentence production (Morgan et al., 2025), EEG continuous versus discrete outputs (Craik et al., 2025), speech envelopes (Ivucic et al., 2025), and neural–audio matching (Wang et al., 2026b). They motivate separate comparisons of classification, waveform reconstruction and retrieval. Acoustic–linguistic dual-pathway models (Li et al., 2026a) and evaluation-specific work (Wu et al., 2025) also belong in that comparison once their protocols are checked. A reported architectural improvement is

not automatically evidence of transfer to a new speaker or an unseen sentence.

Limited and clinical attempted-speech boundaries. Limited membership requires documented residual articulation; the broader clinical comparison also retains source-labelled attempts outside that boundary. The index includes attempted-speech spelling (Metzger et al., 2022), bilingual neuroprostheses (Silva et al., 2024b), stable control without recalibration (Luo et al., 2023), and newer reports concerning cross-session or cross-participant generalisation (Fogg et al., 2026) and pontine-stroke dysarthria (Nason-Tomaszewski et al., 2026). These directions are relevant to usability, language coverage and clinical heterogeneity even when they do not furnish a directly comparable word error rate. Their task-level inclusion here does not promote pending records to verified clinical milestones.

Cross-condition transfer and peripheral contributions. Original covert or imagined labels do not themselves establish an Inner strategy. The broader index contains EEG cortical-current vowel decoding (Yoshimura et al., 2016), online internal-speech classification (Sereshkeh et al., 2017), and fNIRS Overt/Inner comparisons (Kamavuako et al., 2018). Cross-mode studies include overt-trained ECoG Transformers (Komeiji et al., 2024), nested Overt/Mouthed/Inner activity (Soroush et al., 2023), and speech-event detection transferred between modes (de Borman et al., 2024). The latter is about event timing rather than word identity. Sentence-level wearable EEG–EMG systems (Satterlee et al., 2025) and large-model pretraining described as active silent-speech BCI (Zhou et al., 2025b) require explicit inspection of instructions, peripheral inputs and splits. The term "silent" in an indexed title alone does not establish motionless neural decoding.

Inner: datasets and multimodal measurement. Beyond the selected intracortical and EEG/MEG results, the registry includes bimodal EEG–fMRI datasets (Simistira Liwicki et al., 2023; 2025), hybrid decoding (Wellington et al., 2024), inter-trial-coherence features (Lopez-Bernal et al., 2024), and Arabic inner-speech data (Metwalli et al., 2025). These entries broaden language and recording coverage. Dataset availability does not itself validate open-vocabulary decoding, and features computed across trials require checking that test information is not shared with training. Possible shared cohorts and dataset versions remain explicit verification tasks rather than assumed independent replications.

Inner: methods, control and imagery design. The index spans common spatial patterns (DaSalla et al., 2009), syllable-rhythm features (Deng et al., 2010), Overt/Inner phonetic components (Pei et al., 2011), deep metric learning (Lee et al., 2021), and multiscale temporal convolution (Li et al., 2021). Rhythm or state classification should not be pooled with content recognition. Online fNIRS (Rezazadeh Sereshkeh et al., 2019), ear-EEG device control (Kaongoen et al., 2022), and adaptive LDA feedback (Wu et al., 2024b) add interaction settings that offline classification alone misses. Tonal imagery (Guo & Chen, 2022), delayed dynamical features (Carvalho et al., 2024), Chinese word models (Liu et al., 2025b), and Chisco (Zhang et al., 2024c) broaden the tasks. Additional indexed questions concern articulation and coarticulation in datasets (Moreira et al., 2025), Overt-to-Inner training (Alonso-Vázquez et al., 2025), idle-state detection (Padfield et al., 2025), learning to operate a BCI (Bhadra et al., 2025), imagery rate (Guo et al., 2025), and word-specific difficulty (Türk et al., 2025). EEG-to-EEG translation and neural simulation represent different uses of generative models. EEG-Translator maps imagined-speech EEG towards the overt-speech domain and reports a 6.2% improvement in class decoding accuracy over the original imagined signals (Lee et al., 2025b). Rajagopal et al. instead use language-model-generated text to drive phoneme-linked EEG synthesis and neurometabolic simulation (Rajagopal et al., 2025). The former evaluates reconstructed signals for classification; the latter simulates electrical and metabolic patterns rather than recovering text from measured brain activity. A Mandarin vowel classifier reports 49.47% four-class accuracy and 69.83% mean binary accuracy across ten participants under its original "intended speech" label (Wang et al., 2024d). Multimodal feedback in real-time synthesis (Brumberg et al., 2018) adds another interaction question. Non-speech visual imagery comparisons (Lee et al., 2020) are controls outside Perceived–Visual speech.

Perceived: Auditory, Visual and Audiovisual conditions. Perceived–Auditory decoding also includes Chinese MEG (Jia et al., 2025), EEG acoustics beyond the amplitude envelope (MacIntyre et al., 2026), cross-subject generalisability (Zhang et al., 2026a), and phoneme-sequence auxiliary prediction (Lee et al., 2025a). Listening to a question and speaking an answer (Moses et al., 2019) is a mixed task: question context can constrain the response. Perceived feedback in a production BCI (Schippers et al., 2025) likewise does not make the whole experiment a passive listening study. Non-human-primate auditory recordings (Heelan et al., 2019) and audiovisual representational studies (Li et al., 2026c) belong to different evidence strata. An Inner-to-Perceived–Auditory mapping proposal (Maghsoudi & Shamma, 2026) requires checking both the training paradigm and the tested target. The preprint and formal versions of the lip-reading report (Bourguignon et al., 2020) count as one report.

Functional ultrasound: adjacent evidence remains adjacent. The full registry retains auditory-hierarchy mapping (Bimbard et al., 2018), activity propagation in behaving primates (Dizeux et al., 2019), motor-plan decoding (Griggs et al., 2024), human cranial windows (Rabut et al., 2024), four-dimensional imaging (Verhoef et al., 2025), crow auditory responses (Liao et al., 2025), and spatiotemporal-resolution work (Bian et al., 2026). These records inform measurement feasibility and experimental design; they are not additional human speech-content decoders. EEG neural-versus-nonneural contribution analysis (Sato et al., 2024) is similarly retained as methodological evidence rather than a communication milestone.

Reading-route evidence and remaining protocol checks. GLIM (Liu et al., 2025a) and Brain-CLIPLM (Yang et al., 2026a) have selected result and protocol checks supporting their use in the main synthesis (Table 25); they are no longer merely unchecked bibliographic leads. The GLIM values in the main comparison come from SemKey's shared unique-text benchmark (Wang et al., 2026d), whereas Brain-CLIPLM's comparison quotes earlier literature values and uses a task-specific sentence corpus. Multimodal alignment and routing (Ye et al., 2026) likewise contributes a selected fMRI comparison in Methods. These claim-level checks do not imply a complete audit of every experiment in those reports.

The reading supplement also retains diffusion, retrieval-augmented, hierarchical and privacy-related leads (Lamprou & Moshfeghi, 2025; Jeon & Kim, 2025; Gedawy et al., 2025; Masry et al., 2025; Murad et al., 2025; Murhekar et al., 2026; Collautti et al., 2026; Sharma et al., 2026; Samanta et al., 2026; Khushiyant, 2025; Lamprou et al., 2025; McGuire & Moshfeghi, 2025) for further protocol assessment. Their inclusion alone does not add verified systems to the main comparison. Study-wide registry status and the depth of a selected claim check are distinct; version aliases do not add independent studies.

E.2 Additional published benchmark conditions

Complementary decoding conditions and uncertainty clarify how benchmark results depend on training data, temporal context and adaptation. Parentheses indicate the source-reported SD or SEM specified in each caption.

Table 18. LibriBrain word retrieval: top-10 balanced accuracy (%), with the standard error of the mean (SEM) over three seeds in parentheses. The candidate set contains 50 words. Source: Jayalath & Parker Jones (2026), Table 1. Model references appear in Figure 10.

Method	13% training data	All training data
BioCodec	19.9 (0.1)	41.9 (1.0)
EEGPT	20.3 (0.4)	22.9 (0.3)
BIOT	20.6 (0.3)	45.6 (0.4)
BBL	32.1 (1.2)	49.9 (0.3)
BrainOmni	29.7 (9.3)	63.0 (0.1)
LaBraM	40.3 (0.1)	47.7 (0.3)
MEG-XL	57.3 (0.4)	63.0 (0.4)

Table 19. LibriBrain sentence generation and matched noise inputs. All metrics use a 0–100 scale; parentheses show source-reported SD. The paper describes seven-seed training for the proposed model but does not enumerate Table 3 repeat counts for each baseline; differences are descriptive. All methods receive sentence boundaries; the d'Ascoli implementation also receives word timing. Source: Landau et al. (2026), Table 3.

Method	WER ↓	BLEU-1 ↑	ROUGE-1 ↑	BERTScore ↑
Brain2Semantics2Text	192.5 (10.0)	10.0 (0.8)	13.2 (0.3)	83.0 (0.1)
Brain2Semantics2Text (noise)	264.8 (41.5)	8.6 (0.9)	11.3 (0.4)	81.9 (0.6)
BrainECHO	101.8 (3.0)	6.1 (0.8)	9.1 (0.7)	82.8 (0.2)
BrainECHO (noise)	101.2 (0.5)	5.6 (0.6)	8.5 (0.8)	82.5 (0.2)
d'Ascoli word-aligned	87.1 (0.2)	19.0 (0.4)	17.2 (0.4)	82.0 (0.1)
d'Ascoli word-aligned (noise)	99.4 (0.3)	7.2 (2.4)	5.7 (2.1)	79.4 (0.4)

Table 20. Narratives text reconstruction across 20, 40 and 60 repetition-time (TR) windows. All metrics use the source 0–100 scale; higher is better. Source: Lu et al. (2025b), Table 1. Model references appear in Figure 15.

Method	TR	BLEU-1	BLEU-4	ROUGE-1 F	BERTScore F
UniCoRN	20	22.9	0.0	20.3	43.9
EEG-Text	20	24.6	1.9	21.9	44.6
BP-GPT	20	21.6	1.7	21.6	44.1
PREDFT	20	24.3	0.1	20.1	45.9
CogReader	20	25.4	2.6	23.4	46.3
UniCoRN	40	19.1	0.1	17.8	43.8
EEG-Text	40	20.1	1.3	24.4	45.4
BP-GPT	40	19.9	1.5	21.1	42.6
PREDFT	40	25.9	0.4	21.1	46.3
CogReader	40	31.2	8.2	29.6	50.0
UniCoRN	60	18.0	0.4	16.5	43.2
EEG-Text	60	22.1	1.6	28.1	47.7
BP-GPT	60	19.3	0.6	19.4	41.6
PREDFT	60	26.4	0.6	28.1	48.1
CogReader	60	36.2	12.1	36.2	53.5

Table 21. Huth reconstruction with a supplied text prompt, kept separate from the no-prompt main comparison. Source: Ye et al. (2026), Table 2. Model references appear in Figure 15.

Method	BLEU-1 ↑	ROUGE-1 ↑	ROUGE-L ↑	WER (%) ↓
Tang decoder	14.95	13.39	13.26	93.34
BrainLLM	16.91	15.81	15.03	92.16
Multimodal routing	17.35	15.89	15.28	91.35

F Selected Conditions and Source Checks

The condition overview and consolidated source-check table provide the detailed protocols behind the main comparisons. Shared participant identifiers, including T15 across Inner and long-term-use reports, indicate repeated evidence rather than additional independent recruitment. Source-verification labels describe the inspected material, not experimental quality.

Table 22. BCIC2020-3 imagined-speech classification: means and source SDs. The first eleven rows follow El Ouahidi et al. (2025), Table 11; the last three follow Ma et al. (2026a), Table 2. All use the official trial split, with paper-specific downstream tuning. All metrics are higher-is-better. Method references appear in Figure 18.

Method	Balanced accuracy (%)	Cohen's κ	Weighted F1
EEGNet	44.13 (0.96)	0.302 (0.012)	0.441 (0.010)
EEGConformer	45.06 (1.33)	0.313 (0.018)	0.449 (0.015)
SPaRCNet	44.26 (1.56)	0.303 (0.023)	0.442 (0.011)
ContraWR	42.57 (1.62)	0.308 (0.022)	0.441 (0.018)
CNN-Transformer	45.33 (0.92)	0.317 (0.012)	0.451 (0.013)
FFCL	46.78 (1.97)	0.330 (0.036)	0.469 (0.021)
ST-Transformer	41.26 (1.22)	0.294 (0.016)	0.425 (0.014)
BIOT	49.20 (0.86)	0.365 (0.018)	0.492 (0.008)
LaBraM-Base	50.60 (1.55)	0.380 (0.024)	0.505 (0.021)
CBraMod	53.73 (1.08)	0.422 (0.016)	0.538 (0.010)
REVE-Base	56.35 (1.23)	0.454 (0.015)	0.563 (0.012)
BENDR	24.85 (0.75)	0.061 (0.009)	0.238 (0.017)
EEGPT	24.53 (1.31)	0.057 (0.016)	0.244 (0.011)
CodeBrain	61.01 (0.52)	0.513 (0.006)	0.610 (0.005)

Table 23. BCI-Speech subject-disjoint balanced accuracy (%); parentheses show SD across three runs. Source: Lu et al. (2026), Supplementary Table 5. Frozen probing and full fine-tuning use different adaptation procedures. Model references appear in Figure 18.

Method	Linear probe	Full fine-tuning
BrainOmni	22.5 (1.0)	19.9 (0.7)
CBraMod	28.9 (3.3)	26.2 (1.0)
REVE	22.3 (0.9)	20.8 (1.2)
FEMBA	21.0 (1.3)	24.9 (0.3)
BIOT	20.4 (1.4)	26.7 (2.5)
LaBraM	20.3 (1.1)	22.5 (0.3)
NeuroLM	21.1 (0.4)	20.7 (0.5)
Neuro-GPT	21.2 (0.8)	21.0 (2.2)
EEGMamba	19.7 (1.2)	20.0 (0.8)
BENDR	20.0 (0.0)	20.0 (0.0)

Table 24. Selected reported outputs, validation boundaries and use evidence. Rows are illustrative, not exhaustive maxima. N is attached to a named study or condition; study totals, test-condition participants and independent clinical cohorts are not interchangeable. Source provenance for selected conclusions is in Table 25.

Group / condition	Reported outputs / examples	Validation boundary	Participant and use boundary
Articulated: Overt	text and sentence synthesis (ECoG, sEEG)	3% WER in a closed-set repetition condition (Makin et al., 2020); listener choice differs from free transcription	Makin study N=4; Chen study N=48 (Chen et al., 2024b); different studies and conditions
Articulated: Mouthed	transfer of Overt-trained synthesis to unvoiced articulation	actual movement remains; Mouthed and Inner results differ (Anumanchipalli et al., 2019; Meng et al., 2023)	source-specific participant and listener-test conditions; no motionless-decoding inference

Group / condition	Reported outputs / examples	Validation boundary	Participant and use boundary
Articulated: Limited	clinical decoding with residual articulation	residual execution must be documented; speech attempts cannot be assigned from a diagnostic label alone (Willett et al., 2023; Angrick et al., 2024)	report residual movement and voicing for each evaluated condition
Inner	cued text, word classification, acoustic and semantic generation	strategy, content source, bridging and model priors require separate controls (Kunz et al., 2025; Lee et al., 2023; Zhang et al., 2024b; Rastogi et al., 2025)	Kunz study N=4; large-vocabulary condition N=2; unspecified imagery strategy is not Mixed
Perceived: Auditory	retrieval, generated text and semantic gist	candidate sets, repeated stimuli and unseen stories define different tests (Défossez et al., 2023; Yang et al., 2024c; Tang et al., 2023)	pooled retrieval datasets and small generation cohorts do not establish self-generated communication
Perceived: Visual / Audiovisual	Reading text, lip-reading categories and audiovisual representations	Reading protocols are detailed in Table 11; Lip-reading and Audiovisual use different targets (Karthik et al., 2024; Li et al., 2026c)	N=64 fMRI and N=14 iEEG belong to the lip-reading study, not a common audiovisual-generation cohort
Attempted boundary	clinical attempted-speech results without established group membership	actual motor intention does not establish residual articulation (Kunz et al., 2025; Jude et al., 2026)	retained for clinical comparison; not pooled into Limited or reassigned to Inner

Table 25. Selected result conditions and inference boundaries. F denotes inspected full-text sections, not a complete study-wide audit. Dataset size and the retained sample for a particular result are distinguished; an unreported field remains unreported. Version-specific locators identify the evidence actually checked. These targeted checks do not upgrade the registry's study-wide verification status.

Study / check	Condition	Source locator / permitted statement	Inference boundary
(Willett et al., 2023) F	Clinical attempted speech (source task); intracortical; N=1; evaluation sentences	Results: Real-time speech decoding; Table 1. T12: large-vocabulary online text in a prompted task.	No aggregate claim about home use or other participants.
(Kunz et al., 2025) F	Cued inner speech; intracortical; N=2 in large-vocabulary condition; 4 in whole study; non-overlapping evaluation sentences; online retraining	Results: Real-time decoding of inner speech; Figure 3D; STAR Methods: Online inner speech decoder (Figure 3); Vocabulary and Sentence Selection. T15/T16: 125,000-word inner-speech decoding, WER 26-54%; study-wide N=4 must not replace condition N=2.	Online adaptation and instructed strategies limit generalization; no spontaneous private-thought claim.

Study / check	Condition	Source locator / permitted statement	Inference boundary
(Card et al., 2026) F	Clinical attempted speech (source task); intracortical; N=1; longitudinal use; prompted-copy assessment	Results: Overview and Speech decoding; Methods: Continuous fine-tuning, Speech decoding latency, BCI system software. T15: over 3,800 h home BCI use including idle time; 99.2% word accuracy belongs to prompted copy.	Caregiver setup remains; the 92% conversational rating includes user-corrected sentences and is not uncorrected decoder accuracy.
(Yang et al., 2024b) F	Perceived–Auditory speech; MEG; dataset N=27; retained result N not separately reported; sentence-recording pairs 8:1:1	arXiv v3, Sections 3.1–3.2, 3.5.1 and Appendix A; Table 4: Gwilliams BLEU-1 60.30 without test-time teacher forcing.	Recording-pair holdout does not establish unseen-text generation. Table 1's 57.68 is a separate entry; v3 does not explain the difference.
(Yang et al., 2024c) F	Perceived–Auditory speech; MEG; dataset N=27; held-out story: cable spool fort	arXiv v2 (26 December 2025), Sections 4.1–4.3, Tables 1–2. Without test-time teacher forcing, BLEU-1 is 6.86 vs noise 3.87 and random sentence 5.86.	CER is 89.82 vs random-sentence CER 87.30; superiority is metric-specific. NeuGPT quotes an earlier MAD BLEU-1 of 6.94.
(Yang et al., 2024a) F	Perceived–Auditory speech; MEG-MASC; dataset N=27; held-out story: cable spool fort	arXiv v1, Sections 2.3.4, 3.1, 3.4.2; Table 3 reports BLEU-1 12.92 and CER 99.8.	Test-time prefix policy is not stated in the inspected methods. Table 3 has a random-sentence baseline, not a neural-input noise control; Table 2 WER 10.35 is audio ASR.
(Jo et al., 2026) F	Reading audit; word-aligned ZuCo EEG; retained participant N not separately reported for Table 1; unique sentences; 80:10:10 split	Version of record, Methods: ZuCo datasets and EEG-to-text decoding; Figure 1; Tables 1 and 5. Tested BART/Pegasus/T5 implementations showed similar EEG/noise performance.	Table 5 gives sample counts, not the retained participant denominator. The audit does not directly evaluate every successor, COFETT, or MEG decoder.
(Liu et al., 2025a) F	Reading; word-aligned ZuCo EEG; unique-text split; autoregressive generation	arXiv v1, Section 4.1 and Appendix A.4 explicitly describe generation without teacher forcing and text-disjoint partitions. Original Table 1 separates original-reference and multiple-variant scores.	The main survey's BLEU-1 7.84 and identification 10.74% are SemKey's shared-benchmark results (Wang et al., 2026d), not GLIM's original Table 1.
(Yang et al., 2026a) F	Reading; fixation-aligned ZuCo EEG; fixed keyword bank; task-specific sentence corpus; descriptive retrieval N=30	Version of record, Sections 3.1–3.4 and 4.3–4.4; Tables 2–4. Retrieval summaries use participant-level SD; matched-material inferential analyses use N=12.	Table 3 quotes earlier literature baselines rather than rerunning every method. The retrieval pool is the full task sentence set; this is corpus-assisted reconstruction, not unrestricted unseen-text generation.

(Zhang et al., 2026e) F	COFETT corpus: cued recall after reading; 128-channel EEG; N=2 completing the full experiment; session holdout with repeated sentences	ACL version, Sections 3.1–3.2, 4.1–4.2 and Appendix A; Tables 1–2 separate ZuCo reruns from COFETT's embedding-correlation endpoint.	The Methods generation comparison uses the ZuCo reruns, not the N=2 COFETT corpus. Correlation under repeated-content session holdout does not establish generation of novel sentences.

Table 26. Ten reporting questions connect a measured result to its intended interpretation. Answering them makes task, output, generalisation and operating conditions explicit.

Field	Question answered
Task group/subtype, actual articulation, cue type	Which linguistic process and information source are being decoded?
Output type and class / candidate / vocabulary count	What output space is available, and what counts as success?
Train / validation / test unit	Does the test introduce new observations, new content or both?
Cross-participant, cross-session, cross-day	How well does performance transfer across recording conditions?
LM-only, shuffled-signal, cue-removed, noise-matched controls	What does aligned neural input add beyond cues and model priors?
EMG, eye, head and acoustic cross-talk (EEG/MEG); instrument cross-talk (invasive)	How much information is carried by neural and peripheral channels?
All participants, successful subset, best individual	How are outcomes distributed across the evaluated participants?
Truly online, pseudo-online, offline replay	Does evaluation include live initiation, causal feedback and user adaptation?
Update step, algorithm latency, haemodynamic delay, end-to-end latency	When does useful feedback arrive, and how long does a corrected exchange take?
Independent cohort, repeated cohort, public-data reuse	Which results add new participants, and which reuse earlier recordings?

G Dataset and Resource Inventory

Neural-language resources span controlled production and imagery, attempted communication, listening, reading and naturalistic interaction. The 110 resource/version entries below distinguish recruited, released and analysed cohorts where these differ. Continuous recording hours include within-run pauses; task-window hours describe only the stated epochs or stimulus intervals. Trials, runs and linguistic items provide complementary measures of scale. Derived files, simultaneous modalities and successive releases can share recordings or participants and are not independent additions. Access descriptions were checked on 20–21 September 2026; public annotations or model responses do not imply public raw neural signals.

Table 27. Neural-language data resources and versions. Each amount retains its denominator: participants, continuous recordings, task epochs, trials or stimulus items. Approximate and protocol-derived durations are identified explicitly. Resource citations identify the report or deposit; the access and scope column distinguishes raw signals, derived releases and shared acquisitions.

Resource and citation	Signal; participants	Task	Recording amount	Access, scope and relationships
KARA ONE (Zhao & Rudzicz, 2015)	EEG + face/ audio N=14	Imagined and overt prompts	Nominal 5-s imagery trials	**Academic/nonprofit use** Typically 132 trials; MM08 has 131, while P02 provides 165 retained feature entries.
UNL-CONICET /Coretto (Pressel Coretto et al., 2017)	EEG N=15	Imagined/overt vowels and commands	9,314 epochs; 10.35 h	**Author Drive; sign-in** Four-second task epochs; excludes visit/setup time.
ASU /Nguyen (Nguyen et al., 2018)	EEG N=15	Cued speech imagery	6,600 planned trials	**Author release; MOABB mirror** Condition subsets contain 8/6/6/6 overlapping participants.
Broderick (Broderick et al., 2018)	EEG N=19	Narrative listening	$\approx$ 19 h listening	**Public; CC0** Forward-speech subset; other Dryad conditions excluded.

Dataset and resource inventory (continued)

Resource and citation	Signal; participants	Task	Recording amount	Access, scope and relationships
DTU auditory attention (Fuglsang et al., 2018)	EEG N=18 released; 19 recorded	Selective listening to competing Danish speech	Approximately 18 h continuous EEG; 1,080 trials	**Public raw + processed EEG** The 50-s task segments alone total 15 h.
ZuCo 1.0 (Hollenstein et al., 2018)	EEG + eye tracking N=12	Natural/task-specific reading	22.16 h; 273 raw blocks	**Public; CC BY** Summed original EEG samples; excludes setup time.
ASU online adaptive MI/SI (Nguyen et al., 2019)	EEG N=8	Speech and motor imagery with adaptive online feedback	56 runs; 2,240 trials	**Public release; CC0** Half the four classes are speech imagery. Each trial includes 2 s preparation and 8 s imagery; overlapping analysis windows are not extra trials.
Brennan–Hale Alice EEG (Brennan & Hale, 2019)	EEG N=49 released; 52 recruited; 33 analyzed	Listening to Alice in Wonderland	10.13 h story-aligned support; 49 recordings	**Public raw + preprocessing metadata** The 42 preprocessed datasets and 33-case analysis are subsets of the 49-case release.
FEIS (Wellington & Clayton, 2019)	EEG N=23	Phoneme cue, imagery and overt speech	21.28 h retained EEG	**Public; ODC-BY** 21 English plus two Chinese participants; phase duplicates excluded.
KUL auditory attention (Das et al., 2019)	EEG N=16	Selective listening to two Dutch speakers	Approximately 19.2 h; 20 trials per participant	**Public processed EEG; raw by request** Protocol-based duration includes repeated excerpts.
ZuCo 2.0 (Hollenstein et al., 2020)	EEG + eye tracking N=18	Natural/task-specific reading	21.05 h; 252 raw blocks	**Public; CC BY** One of 19 recruits excluded; fourteen blocks per released participant.
ERP CORE: N400 language task (Kappenman et al., 2021)	EEG N=40 released; 39 N400 analysis	Visual word-pair relatedness judgments	40 N400 task recordings	**Public release and processing code** The other five ERP tasks are outside the language subset; excluded participants remain in the public files.
Russian silent commands (Vorontsova et al., 2021)	EEG N=268 in Methods demographic table	Silent and aloud Russian command reading	5–14 sessions per participant; 10 trials per session	**Study corpus; no raw repository identified** Eight commands plus pseudoword control; abstract lists 270 participants.
BCI Competition 2020 Track 3 (Jeong et al., 2022)	EEG N=15 released	Five-class imagined command speech	6,000 epochs; 3.33 h of imagery windows	**Public MATLAB datasets; OSF** Each 3.1-s epoch contains a 2-s imagery task.
Thinking Out Loud /Nieto (Nieto et al., 2022)	EEG + EOG/ EMG N=10	Overt/inner speech and visualization	5,640 trials; 30 recordings	**Public OpenNeuro** Visualization is a separate control condition.
DAIS (Dekker et al., 2023)	EEG N=20	Reading, covert and overt speech	24,370 epochs; 13.54 h	**DANS; request required** Two-second epochs including rest; validation uses 15 participants.
Padfield motor/speech imagery (Padfield et al., 2023)	EEG N=5	Four imagined direction words; separate motor imagery and idle conditions	800 speech trials; 0.89 h	**Public release; CC BY 4.0** Speech trials last 4 s. Motor imagery, idle trials and intertrial fixation are excluded from the speech amount.
ArEEG_Chars (Almalah et al., 2024; Darwish et al., 2024b)	EEG N=30 reported	Arabic character imagery	929 CSVs; 2.80 h raw file coverage	**Public; CC BY** Raw trial-file coverage; inconsistent clock labels; 31 characters.
ArEEG_Words (Darwish et al., 2024a;c)	EEG N=22 reported	Arabic word imagery	359 CSVs; 1.08 h raw file coverage	**Public; CC BY** Raw trial-file coverage; includes distinct repeated word recordings.
Chisco (Zhang et al., 2024c)	EEG N=3	Sentence reading and imagery	20,043 trials; >45 h	**Public; CC0** Three released participants selected from eleven screened.
EEGIS (Lara et al., 2024)	EEG N=10	Eight imagined Spanish words and rest	4,044 one-second windows	**Public release; CC BY 4.0** Windows overlap by 48 of 128 samples; raw and five filtered bands describe the same recordings.
IIST BCI 1: Common Malayalam words (Nair et al., 2024)	EEG N=1	26 Malayalam words: overt and imagined; overt English equivalents	780 word trials	**IEEE DataPort subscription** Variable-length, manually bounded trials; visit duration is not summed EEG time.
IIST BCI 2: Common Marathi words (Tayade et al., 2024)	EEG N=1	100 Marathi words, overt and subvocal; overt English equivalents	3,000 word trials	**IEEE DataPort subscription** Variable-length, manually bounded trials; visit duration is not summed EEG time.

Dataset and resource inventory (continued)

Resource and citation	Signal; participants	Task	Recording amount	Access, scope and relationships
IIST BCI 3: 100 Malayalam words (S et al., 2024)	EEG N=1	100 Malayalam words, vocal/ subvocal; vocal English translations	3,000 word trials	**IEEE DataPort subscription** Variable-length, manually bounded trials; visit duration is not summed EEG time.
IIST BCI 4: 100 Telugu words (Likhitha et al., 2024)	EEG N=1	100 Telugu words and English equivalents, vocal and subvocal	4,000 word trials	**IEEE DataPort subscription** Four language/production conditions; manually bounded, variable-length word records.
IIST BCI 5: Malayalam vowels/consonants (Sunil et al., 2024)	EEG N=1	Malayalam letters, vocal and subvocal	1,120 letter trials	**IEEE DataPort subscription** Variable-length, manually bounded trials; visit duration is not summed EEG time.
IIST BCI 6: Common Odia words (Sahoo et al., 2024)	EEG N=1	100 Odia words and English translations, each vocal and subvocal	4,000 word trials	**IEEE DataPort subscription** Variable-length, manually bounded trials; visit duration is not summed EEG time.
IIST BCI 7: Human space missions (Menon et al., 2024)	EEG (8 channels) N=1	Vocal and subvocal English/Malayalam words	20,000 reported trials; 100 words per language	**IEEE DataPort subscription** 50 trials per word and mode. Subvocal is described as silent thought; no fixed trial duration or total hours are reported.
IIST BCI 8: Common Telugu words (Boddapu et al., 2024)	EEG N=2	100 Telugu words and English translations, vocal and subvocal in both languages	8,000 word trials	**IEEE DataPort subscription** Variable-length, manually bounded trials; visit duration is not summed EEG time.
Imperial ear-EEG AAD (Thornton et al., 2024)	In-ear EEG N=18	Auditory attention in competing-speech scenes	Approximately 12 h; 288 trials	**Public EEG** Duration uses the reported mean of 150 s per trial.
MSEEG (MSEEG, 2024)	EEG N=10	Imagined, intended and spoken syllables	16.98 h retained EEG	**Public; CC BY** Continuous files contain preprocessing; mode archives overlap.
Peking University ear/scalp EEG (Zhu et al., 2024)	Scalp + around-ear EEG N=16	Spatial auditory attention to Mandarin speech	Approximately 10.67 h per simultaneous montage	**Public EEG; original audio by request** Peking University dataset; scalp and ear signals share acquisition time.
Proposed EEG Vowel Dataset (Iqbal et al., 2024)	EEG N=5 recorded	Five-vowel imagery	2,125 one-minute blocks; 35.42 h of imagery	**Data available on reasonable request** One-second feature windows are subdivisions of the same recordings.
SparrKULee (Accou et al., 2024)	EEG N=85	Clean/noisy story listening	168 h	**Public + restricted; CC BY-NC** Continuous Dutch speech; final 2024 release.
UBA natural dialogue EEG (Gonzalez et al., 2024)	EEG hyperscanning N=20 released (10 dyads); 18 analyzed	Unscripted cooperative Spanish dialogue	249 paired trials; 10.69 participant-h of EEG	**Public artifact-corrected EEG, audio and annotations** 5.35 pair-h; 512 Hz trial files with inter-trial gaps removed. Release includes the excluded dyad.
Aguilera paradigm comparison (Aguilera-Rodríguez et al., 2025)	EEG N=15	Paced and gamified speech imagery	3,600 imagery instances; nominal 1.4 h	**Public; CC BY** Same participants; three paced instances are nested within each long trial.
ArEEG (five commands) (Metwalli et al., 2025)	EEG N=12	Arabic command imagery	4,650 trials; 186 sessions	**Public OpenNeuro** One participant completes 21 sessions; others complete 15.
CIRE (He et al., 2025a)	EEG N=38 released; 40 recruited	Mandarin sentences with contrasting prosody	51.26 h; 188 raw blocks	**Public raw + derivatives** Two of 190 planned blocks absent; 5-s analysis epochs are a different duration basis.
Chinese spoken-word production (Tan & Zhang, 2025)	EEG N=87: 27 /23 / 19 /18	Overt picture naming with priming/ interference	87 raw recordings across four experiments	**Public raw + derivatives** Independent cohorts; raw, epoched and averaged data reuse the same recordings.
ChineseEEG (Mou et al., 2025; 2024)	EEG + eye tracking N=10 released; 15 recruited	Silent reading of two Chinese books	121.74 h; 245 raw EEG runs	**Public raw + derivatives** Five of 250 planned runs absent from the current release.
ChineseEEG-2 (Chen et al., 2025b)	EEG N=12: 4 reading, 8 listening	Reading aloud; passive listening	32.4 h: 10.8 reading + 21.6 listening	**Public EEG + embeddings** Disjoint task cohorts; original participant audio withheld.
Cueless imagined speech (Derakhshesh et al., 2025)	EEG N=11; 55 sessions	Self-selected imagined Persian commands	14.82 h; 55 raw FIF recordings	**Public raw + derivatives** A timing cue is present, but it does not specify the imagined word.
ETS /Xiong (Xiong et al., 2025)	EEG N=16 recruited; 13 analyzed	Four-word Chinese reading and imagery	1,560 EEG segments; 120 per retained participant	**Author inquiry; no linked raw repository** Reading and imagery segments are paired within trials.

Dataset and resource inventory (continued)

Resource and citation	Signal; participants	Task	Recording amount	Access, scope and relationships
Ear-SAAD (Geirnaert et al., 2025a)	Scalp + around-ear + in-ear EEG N=15	Auditory attention with concurrent ear/ scalp recording	15 h per simultaneous montage; 90 trials	**Public raw BIDS + processed data** Three montages observe the same 15 participant-hours.
IIST BCI 10: Telugu vowels/consonants (Boddapu et al., 2025)	EEG N=3	Telugu vowels and consonants, vocal and subvocal	52 character classes; two modes	**IEEE DataPort subscription** Vowels and consonants recorded on separate days.
IIST BCI 11: Malayalam letters (S. et al., 2025)	EEG N=6	Malayalam character vocalization and imagery	6,120 recordings; 51 characters	**IEEE DataPort subscription** Ten trials per character and mode per participant; raw and processed files overlap.
IIST BCI 12: Telugu dialect commands (Vivek et al., 2025)	EEG N=2	87 Telugu command variants in six classes, spoken and imagined without lip/tongue movement	2,610 word trials	**IEEE DataPort subscription** Variable-length, manually bounded trials; visit duration is not summed EEG time.
IIST BCI 9: Malayalam dialect commands (K et al., 2025)	EEG N=10	Malayalam navigation commands, vocal and subvocal; 15 dialect sets, seven commands per set	2,100 word trials	**IEEE DataPort subscription** Variable-length, manually bounded trials; visit duration is not summed EEG time.
Matin/Faraji imagined speech (matin et al., 2025)	EEG N=9	Imagined words with visual, auditory, combined or self-generated cues	9 subject collections; 2.5-s epochs	**Public release; CC BY 4.0** Continuous EDF, processed epochs and event logs represent the same sessions; processed copies are not extra recordings.
Moreira articulation corpus (Moreira et al., 2025)	EEG (TMS) N=8 + 16 released	Phoneme/word discrimination and repetition	3,742 + 10,888 released trials	**Public OpenNeuro** 2019/2021 cohorts; single-phoneme listening and repetition share trials.
Native Arabic Silent Speech /SSDC (Chowdhury et al., 2025b)	EEG N=10 recorded	Inner and overt Arabic commands	8,994 study-wide trials; 6.25 h of speech-task windows	**Registered teams; signed agreement; registration closed** Challenge shares inner speech only; overt speech was not shared. Separate public tutorial sample.
SS-EEG (Zhou et al., 2025a)	EEG N=12	Silent articulation	72,000 reported trials	**Author EULA; teaser available** Attempted articulatory movement without sound.
3M-CPSEED (Ma et al., 2026b)	EEG N=20	Overt, silently articulated and imagined Pinyin	29.39 h; 80 raw recordings	**Public; release CC0, paper CC BY 4.0** Hours count original EDF recordings only; processed files are also released.
Arabic–Hindi L2 word reading (Aldhaheri et al., 2025; 2026a;b)	EEG N=20 released IDs; 20 analyzed in 2026 report	Arabic/Hindi word learning with visually cued vocalization	296 EDF files; 4.60 h after overlap removal	**Public EDF, samplewise and feature CSVs; CC BY 4.0** Release description reports 300 files; 12 s of repeated coverage removed.
COFETT /Chisco-2.0 (Zhang et al., 2026e)	EEG N=7 screened; 2 released	Chinese sentence reading and cued recall	64 runs; 62.12 h continuous EEG; 17,056 trials	**Public raw and processed data; OpenNeuro** Reading, recall and rest phases belong to each trial.
Directional words: Russian/Spanish (Kostulin et al., 2026)	EEG; EMG subset N=22: 12 Russian, 10 Spanish	Overt and covert directional words	24.39 h; 22 raw EDF recordings	**Public raw + derivatives** Four Russian participants have series markers for multiple utterances.
EMA–EEG speech production (Friedrichs et al., 2026)	EEG + EMA + audio N=29; 25 complete tri-modal cases	Habitual and rapid syllable production	8,700 DDK trials; 300 per participant	**SWISSUbase; CC BY 4.0** The reported 17 h covers EMA/audio; additional reading and anatomy tasks do not imply EEG.
Japanese speech (Sato et al., 2026)	EEG + EMG N=3	Overt, listening and covert speech	1,020 h continuous	**Public; CC0** Overt event support is 457.5 h; shared listening/covert runs counted once.
KUL-AAD-NFB (Rotaru et al., 2026)	EEG N=11 released; 19 recorded; 12 released sessions	Auditory attention with neurofeedback/ calibration	15.52 h; 122 raw BDF files	**Public raw + metadata** One participant contributes two sessions; total includes calibration.
Mandarin multi-condition / Wang (Wang et al., 2026c)	EEG N=1 recorded	Overt, noisy overt, silent articulation and imagined Chinese speech	720 vowel and 480 word trials reported	**Raw data on request** Four task conditions; publication hours do not reconcile with trial timing.

Dataset and resource inventory (continued)

Resource and citation	Signal; participants	Task	Recording amount	Access, scope and relationships
TESSCCo (Lobo-Alonso et al., 2026)	EEG N=24 released (21 native, 3 non-native Spanish)	Overt and silent articulation of bilingual TV commands	7,936 epochs; 11.02 h of cue-plus-production segments	**Public raw and processed data; CC BY 4.0** 45 sessions; silent articulation includes mouth movement.
UGR-MINDVOICE (Vales Cortina et al., 2026)	EEG + audio N=15; 22 sessions	Overt/covert Spanish syllables, words and pseudowords	38.04 h; 22 raw EDF recordings	**Public raw + derivatives** Overt and covert trials alternate within sessions; repeated visits are not new participants.
Armeni (Armeni et al., 2022)	MEG N=3	Audiobook listening	≈ 30 h	**Donders data-use agreement** Ten stories over ten days per participant.
MEG-MASC (Gwilliams et al., 2023)	MEG N=27	Story and word-list listening	≈ 49 h; 49 sessions	**Public; CC0** Five participants have one session; 22 have two.
LibriBrain (Özdogan et al., 2025)	MEG N=1	Audiobook listening	52.32 h listening; 93 public sessions	**Public; CC BY-NC** Original release; included in LibriBrain100.
Chen vocoded audiobook MEG (Chen et al., 2026; 2023)	MEG N=24	Audiobook listening at six intelligibility levels	175 runs; 22.30 h	**Public release; ANC data-use agreement** The 2026 release accompanies a 2023 article. Run coverage differs across participants; recorded time includes within-run pauses.
LPP MEG listening (Bel et al., 2026b)	MEG N=58	Listening to Le Petit Prince	94.81 h; 521 raw runs	**Public raw + annotations** One participant has eight rather than nine released runs.
LPP MEG reading (Bel et al., 2026a)	MEG N=50	Rapid serial visual reading of Le Petit Prince	63.99 h; 450 raw runs	**Public raw + annotations** Separate reading collection; no assumed cohort overlap with the listening release.
LibriBrain100 (Mantegna et al., 2026b)	MEG N=33	Audiobook/sentence listening	104.2 h	**Public; CC BY-NC** 80.5 h deep subject plus 23.7 h broad cohort; includes LibriBrain.
MegNIST (Kwon et al., 2026)	MEG N=1 released	Covert digit production	12 runs; 12,000 trials; 5.20 h continuous MEG	**Public BIDS data; CC BY-NC 4.0** Digit presentation windows total 2.5 h.
Riegel audiovisual matrix sentences (Riegel et al., 2026)	MEG N=32	Audiovisual and visual-only sentence perception	13,359 sentence segments	**Public release; CC BY 4.0** Two acquisition sessions per participant; archive omits 81 planned trials listed in the README. Audio-only calibration is separate.
StudyForrest audio movie 7T (Hanke et al., 2014)	fMRI N=20	Forrest Gump audio-description listening	160 runs; 39.99 h	**Public release** 7 T, partial-brain coverage. Includes all acquired story-run volumes; audiovisual follow-up reuses 15 participants.
Wehbe Harry Potter (Wehbe et al., 2014)	fMRI N=9 recruited; 8 retained	Word-paced Harry Potter reading	4 runs per participant; about 6 h retained	**Public author-hosted data** About 45 min per participant; excluded subject is not added.
Huth semantic maps (Huth et al., 2016)	fMRI N=7	Natural narrative listening	84 story runs	**Public maps; tutorial subset** Study has 12 story runs per person. Map viewer and tutorial subset do not represent the entire raw cohort.
StudyForrest audiovisual 3T (Hanke et al., 2016)	fMRI N=15	Audiovisual Forrest Gump viewing with eye tracking	120 runs; 29.99 h	**Public release; PDDL** New 3 T recordings from 15 participants in the original 20-person audio cohort; shared recruitment, different acquisitions.
Narrative Brain Dataset (Lopopolo et al., 2018)	fMRI N=24	Three Dutch stories and reversed versions	16.02 h; 65,540 released volumes in 144 runs	**Public processed fMRI + annotations** First four volumes per run removed; this is processed support, not raw acquisition.
Pereira linguistic meaning (Pereira et al., 2018)	fMRI N=20 recruited; 16 retained	Concept presentation and sentence reading	180 concepts; 384- and 243-sentence experiments	**Author activation-data release: MIT/ Dropbox; materials: OSF** Sentence experiments contain overlapping participant subsets.
Naturalistic Neuroimaging Database (Aliko et al., 2020)	fMRI N=86	Ten full-length audiovisual films	264 raw BOLD runs; 161.20 h	**Public release** One film per participant. Raw acquisition support is distinct from the 160.59 h of participant-weighted movie exposure.
Narratives (Nastase et al., 2021)	fMRI N=345	Narrative listening	153.96 h story-aligned BOLD	**Public; CC0** 369,496 story TRs; 4.6 h unique stimuli.
LeBel (LeBel et al., 2023)	fMRI N=8	Narrative listening	81 h BOLD	**Public OpenNeuro** Published eight-person release includes three extended participants.
Tang semantic reconstruction (Tang et al., 2023)	fMRI N=7 studied; 3 in public decoding release	Heard and imagined narratives, movies and attention	3 imagined-story runs, 14 min each; other decoding runs	**Public data and code; resistance data on request** Earlier story-training data overlap the UT Austin release.

Dataset and resource inventory (continued)

Resource and citation	Signal; participants	Task	Recording amount	Access, scope and relationships
Tuckute drive/suppress language (Tuckute et al., 2024)	fMRI N=14	Reading sentences selected to drive or suppress language responses	274 main-task runs	**Public derived data** Five training, five new evaluation and four additional blocked-design participants. Public responses are processed sentence-level data.
LPPC multilingual fMRI (Li et al., 2025a; 2022b)	fMRI N=112: 49 English, 35 Chinese, 28 French	Listening to Le Petit Prince	181.93 h; 1,011 acquisition runs	**Public raw + derivatives** Three simultaneous echoes count once; three short interrupted runs are included.
Fedorenko sentence meaning (Fedorenko et al., 2016)	ECoG N=6 original participants; 5 in benchmark derivative	Sentence and control-string reading	52 sentences; 416 word responses at 97 electrodes	**Public processed Brain-Score benchmark** Benchmark derivative differs from the full original cohort and conditions.
SingleWordProduction Dutch-iBIDS (Verwoert et al., 2022)	sEEG + audio N=10 patients	Overt production of 100 Dutch words	0.83 h task support; 1,000 trials	**Public iBIDS + aligned audio** Task support uses 2-s word display + 1-s fixation per trial.
T12 speechBCI /B2T-24 (Willett et al., 2023)	Intracortical N=1 released (T12)	Attempted sentence production	12,100 sentence trials reported; 10,850 used for training	**Public neural features; Dryad** Competition splits and subsequent corrections share the same acquisition.
Brain Treebank (Wang et al., 2024a)	sEEG N=10	Audiovisual movie viewing	43 h	**Public; CC BY** Clinical monitoring cohort; includes visual context.
Jamali single-cell semantics (Jamali et al., 2024)	Single units N=13	Listening to sentences, word lists and narrative controls	21 sessions; 287 units	**Public derived data; CC BY 4.0** Ten microarray participants and three Neuropixels participants; word-aligned responses do not specify continuous recording hours.
T15 rapidly calibrating BCI (Card et al., 2024)	Intracortical N=1 participant (T15)	Attempted text communication and conversation	1,718 copy-evaluation and 22,126 conversation records	**Public evaluation records; Dryad** 2024 evaluation release; the 2025 neural expansion uses the same cohort.
Kunz inner-speech motor cortex (Kunz et al., 2025)	Intracortical N=4 studied; 2 in large-vocabulary inner-speech condition	Attempted, cued inner and other controlled speech tasks	22 participant-dates; 11 task archives	**Public neural features and code** Condition-specific cohorts overlap T12 and T15 resources.
T15 /Brain-to-Text 2025 (Card et al., 2025)	Intracortical N=1 released (T15)	Attempted speech to text	45 sessions; 10,948 trials; 53.92 h of feature windows	**Public neural features; Dryad and competition** 512 features at 20 ms: threshold crossings and spike-band power; same T15 release family.
VocalMind (He et al., 2025b)	sEEG N=1	Overt, mimed and imagined speech	67.85 min task epochs	**Public; CC BY** 110 retained contacts; three modes share one cohort.
Cai natural language production (Cai et al., 2026)	Single units; LFP N=8	Natural conversational speech production	14 sessions; 17.51 h	**Public derived data; CC BY 4.0** Continuous firing-rate time includes conversation pauses and listening. Private utterance transcripts are withheld; word timing and model embeddings are released.
MOUS (Schoffelen et al., 2019)	MEG + fMRI N=204: 102 auditory, 102 visual	Sentence and word-list comprehension	240 planned MEG + 120 fMRI trials per participant	**Registration + Data Use Agreement** Three MEG cases are incomplete; separate rest recordings also have documented omissions.
Cooney bimodal speech (Cooney et al., 2022)	EEG + fNIRS N=19 recorded; 15 performed imagined speech	Words and word pairs with multimodal cues	55 original EEG sessions; 49 paired sessions analyzed	**Public code; raw release not provided by repository** Six fNIRS sessions excluded; further artifact rejection reduces trial counts.
Pippi audiovisual iEEG–fMRI (Berezutskaya et al., 2022)	ECoG/sEEG + fMRI N=63 unique: 51 iEEG, 30 fMRI, 18 shared	Watching speech/ music film; iEEG rest	6.00 h main iEEG film; 3.25 h fMRI film	**Public neural data; film by request** Three supplemental HD streams include simultaneous channels and a repeated acquisition.
SMN4Lang (Wang et al., 2022)	MEG + fMRI N=12 in both modalities	Listening to 60 Mandarin stories	68.09 h MEG; 66.76 h task fMRI	**Public raw + annotations** Separate modality visits; rest scans excluded from the task amounts.
Bimodal Inner Speech (Simistira Liwicki et al., 2023)	EEG + fMRI N=4 released; 5 recruited	Cued inner speech in separate recording sessions	1.51 h EEG; 5.03 h fMRI	**Public raw + derivatives** One participant excluded for poor EEG quality; modality durations differ.

Dataset and resource inventory (continued)

Resource and citation	Signal; participants	Task	Recording amount	Access, scope and relationships
BABA (Li et al., 2025d)	OPM-MEG + fMRI N=60: separate cohorts of 30	Watching a dialogue-rich social-interaction film	12.66 h MEG film; 12.67 h fMRI film	**Public raw + task material** Questions, replay and fMRI rest are additional tasks, excluded from film totals.
LPP Multi-talker (Ma et al., 2025)	EEG + 7 T fMRI N=26 in both modalities	Single/competing Mandarin audiobook speech	19.98 h EEG; 17.56 h task fMRI	**Public raw + derivatives** One EEG file has an incomplete final sample frame; fMRI rest excluded.
MEG-SCANS (Habersetzer & Meyer, 2025; Habersetzer et al., 2025)	MEG; pilot EEG N=24; 22 under final protocol	Audiobook listening and speech-in-noise sentences	18.89 h task MEG; 118 runs	**Public raw + metadata** Chirps remain inside audiobook runs; 2.846 h empty-room noise excluded.
Simultaneous Inner Speech (Simistira Liwicki et al., 2025)	EEG + fMRI N=3	Simultaneous cued English inner speech	2.19 h EEG; 2.39 h fMRI	**Public corrected EEG + fMRI; raw EEG by request** Five EEG sessions versus six fMRI runs; dummy volumes and interruption affect duration.
BCCWJ-Brain (Sugimoto et al., 2026c;a;b)	fMRI /EEG / MEG N=36 /41 /35 released; separate cohorts	Japanese newspaper word-paced reading	23.12 /25.34 /21.87 h of continuous recordings	**Public neural data; OpenNeuro** Licensed BCCWJ text is separate; modalities use different participants. fMRI events accompany 134 of 144 runs.
Hons hybrid phonemes (Hons et al., 2026)	EEG + fNIRS N=27 recruited; 22 analyzed	Four perceived and imagined phonemes	12,709 retained trials; 17.65 h of task windows per modality	**Public EEG/fNIRS recording files, code and results; OSF** Retained task windows; simultaneous modalities. Public EEG deposit includes 24 ID prefixes; 22 participants were analyzed.
Defenderfer vocoded/noisy speech (Defenderfer, 2019; Defenderfer et al., 2021)	fNIRS N=39 recruited; 38 analyzed; 38 released IDs	Listen and repeat sentences in vocoding/noise conditions	23.24 h continuous release; 6,421 study trials	**Public data; Mendeley** Healthy listeners; paper-derived listening-plus-repetition windows total 10.70 h.
Guo tonal monosyllables (Guo & Chen, 2022)	fNIRS (44 channels; 7.41 Hz) N=20	Imagined Mandarin vowels with four lexical tones	1,600 trials; 4.44 h of protocol-derived imagery windows	**Data on reasonable request** 80 trials/person; 16 combinations, five repetitions each. Imagery lasts 10 s within 34-s trials. Raw data are not public for legal/ethical reasons; the supplementary channel map is public.
Kolisnyk fNIRS narratives (Kolisnyk et al., 2024)	fNIRS N=30 recruited; 26 analyzed	Intact and scrambled audiovisual/audio narratives	11.23 h of stimulus windows across retained participants	**Data on request with ethics agreement; public code** Four stimulus conditions; acquisition failures and quality exclusions omitted.
MindSpeech (Zhang et al., 2024b)	HD-fNIRS N=4 analyzed	Cued sentence imagination with typed reports	2,646 sentence trials; 5.15 h of imagery windows	**Study corpus; public raw release not identified** Seven-second imagery excludes untimed sentence typing.
CI/NH multimodal speech fNIRS (Bálint et al., 2025a;b)	fNIRS N=72 recorded (46 cochlear implant, 26 normal hearing)	Speech in quiet/noise, audiovisual speech and lipreading	72 recordings; 10.40 h of stimulus windows	**Public raw SNIRF archive; Dryad** 40 stimulus windows per participant; appointment time excluded.
Natural conversations fNIRS (Hu et al., 2025)	fNIRS N=31 released	Fat talk and control conversations	31 recordings; 13.87 h continuous fNIRS	**Public raw and processed signals; OSF** Conversation windows total 7.75 h; only one partner wore fNIRS.